NOVA ACTA LEOPOLDINA
NEUE FOLGE, BAND 96, NUMMER 357

Imaging and Integrating Heterogeneity of Plant Functions: Functional Biodiversity from Cells to the Biosphere

International Leopoldina Meeting
Forschungszentrum Jülich, July 29 to 31, 2007

Ulrich Schurr, Barry Osmond, Ulrich Lüttge, Uwe Rascher, Susanne von Caemmerer and Achim Walter (Eds.)

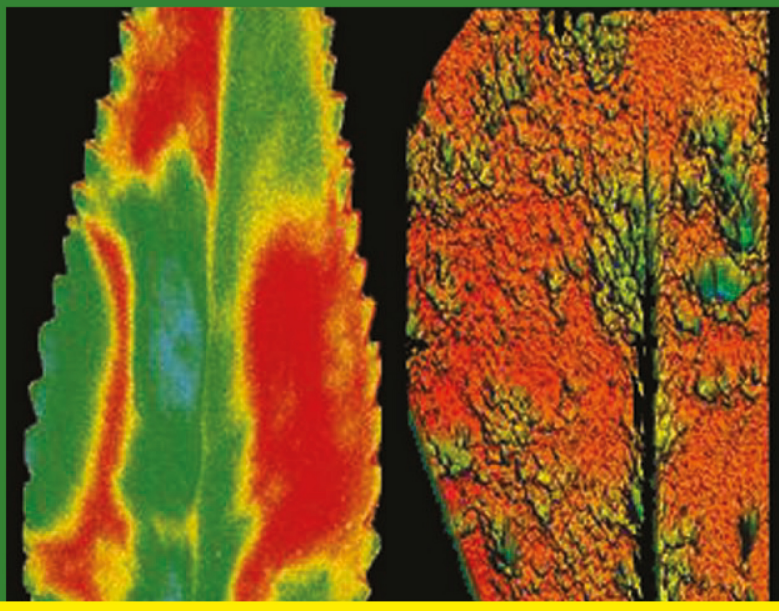

Deutsche Akademie der Naturforscher Leopoldina –
Nationale Akademie der Wissenschaften, Halle (Saale) 2009
Wissenschaftliche Verlagsgesellschaft mbH Stuttgart

Imaging and Integrating Heterogeneity of Plant Function: Functional Biodiversity from Cells to the Biosphere

NOVA ACTA LEOPOLDINA

Abhandlungen der Deutschen Akademie der Naturforscher Leopoldina

Im Auftrage des Präsidiums herausgegeben von
HARALD ZUR HAUSEN
Vizepräsident der Akademie

NEUE FOLGE NUMMER 357 BAND 96

Imaging and Integrating Heterogeneity of Plant Functions: Functional Biodiversity from Cells to the Biosphere

International Leopoldina Meeting

Forschungszentrum Jülich, Germany
July 29 to 31, 2007

Editors:

Ulrich SCHURR (Jülich)

Barry OSMOND (Canberra City)
Member of the Academy

Ulrich LÜTTGE (Darmstadt)
Member of the Academy

Uwe RASCHER (Jülich)

Susanne VON CAEMMERER (Canberra City)
Member of the Academy

Achim WALTER (Jülich)

With 60 Figures and 5 Tables

Deutsche Akademie der Naturforscher Leopoldina –
Nationale Akademie der Wissenschaften, Halle (Saale) 2009
Wissenschaftliche Verlagsgesellschaft mbH Stuttgart

Redaktion: Dr. Michael KAASCH und Dr. Joachim KAASCH

Die Schriftenreihe Nova Acta Leopoldina erscheint bei der Wissenschaftlichen Verlagsgesellschaft mbH, Stuttgart, Birkenwaldstraße 44, 70191 Stuttgart, Bundesrepublik Deutschland.
Jedes Heft ist einzeln käuflich!

Die Schriftenreihe wird gefördert durch das Bundesministerium für Bildung und Forschung sowie das Kultusministerium des Landes Sachsen-Anhalt.

Cover image:
Examples of chlorophyll fluorescence imaging. *Left*: Leaf of *Kalanchoë daigremontiana* performing Crassulacean acid metabolism (CAM). *Right*: Leaf of *Clusia minor* performing C_3-photosynthesis (see LÜTTGE in this Volume p. 65).

Bibliografische Information Der Deutschen Nationalbibliothek
Die Deutsche Nationalbibliothek verzeichnet diese Publikation in der Deutschen Nationalbibliografie; detaillierte bibliografische Daten sind im Internet über http//dnb.ddb.de abrufbar.

Die Abkürzung ML hinter dem Namen der Autoren steht für Mitglied der Deutschen Akademie der Naturforscher Leopoldina.

06019 Halle (Saale), Postfach 11 05 43, Tel. + 49 345 4723934
Hausadresse: 06108 Halle (Saale), Emil-Abderhalden-Straße 37
Herausgeber: Prof. Dr. Dr. h. c. mult. Harald ZUR HAUSEN, Vizepräsident der Akademie
Printed in Germany 2009
Gesamtherstellung: Druck-Zuck GmbH Halle (Saale)
ISBN: 978-3-8047-2603-1
ISSN: 0369-5034
Gedruckt auf chlorfrei gebleichtem Papier.

Contents

Modelling and Theory of Spatial Heterogeneity

Nova Acta Leopoldina NF *96*, Nr. 357, 7–13 (2009)

Imaging and Integrating Heterogeneity of Plant Functions: Functional Biodiversity from Cells to Biosphere – A Synopsis

Ulrich Schurr (Jülich)

With 1 Table

Abstract

Spatial heterogeneity and temporal dynamics of structures and functions are essential to understand plants and their interaction with soils and atmospheric processes. Quantitative analysis plays an essential role for the generation of basic knowledge as well as for the development of innovative applications in plant production. Thus, novel imaging methods and quantitative image (sequence) analysis that are presently developed provide the basis for an entirely new understanding of the role of heterogeneity and dynamic in plants and their environment on all scales from the cell to the ecosystem. It is only now that we can see the real dynamic nature of growth, photosynthesis and transport and the relevance of spatial and temporal patterns for plants. Research on these topics has only just begun; it requires a very high degree of interdisciplinarity and communication between technology developers, researchers in plant and environmental sciences, modeling and theory. The Leopoldina workshop "***Imaging and Integrating Heterogeneity of Plant Functions: Functional Biodiversity from Cells to Biosphere***" has clearly indicated that the integration of modern methods, innovative experiments and theory will revolutionize our understanding of plants in their ever changing environment.

Zusammenfassung

Räumliche Heterogenitäten und zeitliche Dynamik von Strukturen und Funktionen sind essentiell, um das Verhalten von Pflanzen und ihre Wechselwirkung mit Böden und der Atmosphäre verstehen zu können. Ihrer quantitativen Analyse kommt deshalb eine Schlüsselrolle zu – sowohl für die Erforschung der Grundlagen pflanzlichen Verhaltens als auch für die Entwicklung innovativer Anwendungen in der Pflanzenproduktion. Neue Methoden der Bildaufnahme und die quantitative Bild(sequenz)analyse schaffen derzeit die Grundlage für ein völlig neues Verständnis der Bedeutung von Heterogenität und Dynamik in Pflanzen und Umwelt auf allen Skalen von der Zelle bis zum Ökosystem. Erst jetzt wird deutlich, wie dynamisch Wachstum, Photosynthese und Transport wirklich sind und welche Bedeutung räumliche und zeitliche Muster für Pflanzen haben. Die Forschung hierzu hat erst angefangen; sie benötigt ein hohes Maß an Interdisziplinarität und Kommunikation zwischen Entwicklern von Verfahren, Anwendern aus den Pflanzen- und Umweltwissenschaften sowie Modellierern und Theoretikern. Der Leopoldina-Workshop „***Imaging and Integrating Heterogeneity of Plant Functions: Functional Biodiversity from Cells to Biosphere***" hat gezeigt, dass die Integration von modernen Methoden, innovativen experimentellen Ansätzen und Theoriebildung unser Verständnis von Pflanzen und von ihrem Verhalten in ihrer sich ständig verändernden Umwelt grundlegend wandeln wird.

1. Heterogeneity and Dynamics in Plants and their Environment

Heterogeneity and dynamic changes are the normal case and certainly not the exception for plants growing in natural ecosystems and even in managed agricultural environments. With their sessile mode of life, plants are exposed to ever changing weather conditions during all seasons. They are exposed to fluctuating biotic and abiotic stressors, as they simultaneously cope with greatly contrasting environmental conditions belowground and aboveground

(Tab. 1). Having no central control unit ("brain"), the organization of plants makes heterogeneous and distributed signal perception and processing a fundamental strategy. However, it is not only a matter of survival in a dynamically changing environment: proper mechanisms for utilization and acquisition of heterogeneously available resources from the environment are of central importance for the efficiency of plants and an important determinant of their fitness (SCHURR et al. 2006). Thus, heterogeneity in space and time is a key to understanding plant structure and function (WALTER et al. 2009).

Tab. 1 Characteristic features of leaf and root environment

	Leaf environment	Root environment
Resources	Light, CO_2, O_2	Nutrients, water
Physical characteristics	Low density Mechanical conditions mainly determined by plant characteristics	High density (often strong mechanical impedance) Strong external mechanical constraints
Chemical characteristics	Gas phase, thus well mixed phases; colloidal conditions	Mixture of gas, aqueous and solid
Biological conditions (biological interaction)	Exchange between biota over long distances possible	Biotic interactions often confined in externally determined spaces
Characteristics of dynamic and heterogeneity	No simple, predictable spatial structure of resources CO_2, O_2: well mixed Light: often highly fluctuating in time and space within natural canopies (e.g. light flecks)	Patchy, determined by soil characteristics Strong spatial heterogeneity of major resources is common

Up to now experiments have often aimed to maintain environmental conditions as constant as possible in space and time. However, novel experimental approaches and theoretical concepts are required in plant sciences to identify and observe heterogeneity and dynamics of structure and functions at the cell, tissue, organism and ecosystem levels, and to integrate and interpret these functions in the complex interaction with the spatial and temporal heterogeneity of the environment (WALTER and SCHURR 2006). Only if this is achieved, it is possible to understand and predict the feedbacks of living plant biota on the Earth system and to use the potential of plants for sustained production of the food, fuel and fiber needed by humankind in an optimal and efficient manner. Eventually, we will have to incorporate these insights into the design of plants through breeding or transgenic routes to obtain plant varieties better suited to the changed climate and shifting economic realities.

2. Imaging Technologies Promote Research on Heterogeneity and Dynamics of Plants

The general character of an image is that quantitative information of a specific physical parameter is assigned to a specific spatial position. Image sequences demonstrate the change of such assignments with time. Thus imaging and especially image sequences are tools of choice to evaluate heterogeneity, dynamic processes and patterns. Images can either be taken by arrays of sensors (e.g. the light sensitive elements of a CCD chip) or can be built up through a sequence

of analyzing processes, if the structure or function that is determined is changing slower than the measurement process. Development of imaging techniques has a proven record of accelerating progress in botany and plant sciences from early times on, when plant images were used to illustrate plant structures, e.g. for purposes of plant systematic or for the analysis of cellular and subcellular processes associated with the various jumps in microscopy techniques from light and electron microscopy to confocal laser scanning and analytical microscopy. Historically, there have been many examples of image sequences that have become critically important for functional analysis in the plant sciences. However, the outburst of imaging technologies in recent years that have originated from the medical field and from monitoring of the environment, e.g. in remote sensing from satellites and airplanes (Pieruschka et al.: Optical Remote Sensing and Laser Induced Fluorescence Transients [LIFT] to Quantify the Spatio-Temporal Functionality of Plant Canopies) has inspired the development of novel imaging systems in plant sciences, opening new routes for insight into plant characteristics and their dynamic responses.

For example, **tomographic imaging** using differences in magnetic resonance (mainly of protons) to give contrast and thus deliver non-invasive 3D images and -sequences has only recently been assimilated in the plant sciences and promises a wide range of applications in the future. The paper by Blümler et al. (Magnetic Resonance of Plants) provides a sound basis for understanding opportunities and limitations of this technology as well as some impressive examples of what can already be achieved. At a different scale, **quantitative 3D imaging** provides a tool to measure plant and stand geometrical characteristics (Biskup et al.: Quantification of Plant Surface Structures from Small Baseline Stereo Images to Measure the Three-Dimensional Surface from the Leaf to the Canopy Scale) and illustrates the approach that quantitative image analysis goes beyond providing "nice pictures". Given that the correct mathematical tools are combined with proper image acquisition and analysis in measuring devices, it becomes possible to span a wide range of scales in space and time.

Recording chlorophyll fluorescence has become one of the most powerful tools in studying heterogeneity and dynamics of photosynthesis. Most interestingly in the context of this issue of *Nova Acta Leopoldina* the greatest information content is gained from analyzing the change of chlorophyll fluorescence over time – an approach, which became generally feasible with the development of the Pulse Amplitude Modulated Fluorometry as a non-invasive quantitative measure that has been extended into an imaging technology (Schreiber et al. 1995, Siebke and Weis 1995). Further developments extending the application of chlorophyll fluorescence to the scales of canopies and beyond are on their way (Pieruschka et al.: Optical Remote Sensing and Laser Induced Fluorescence Transients [LIFT] to Quantify the Spatio-Temporal Functionality of Plant Canopies). These technological developments push for the analysis of photosynthesis dynamics and heterogeneity under field conditions and at the stand level. Here additional mechanisms come into play and determine light use efficiency of canopy photosynthesis. Moreover through the technological approach of analyzing chlorophyll fluorescence from above even previously not accessible locations (and thus functions) can be explored.

3. Heterogeneity of Photosynthesis – a Prototypic Example of the Role of Spatial and Temporal Organization in Plants

Photosynthesis is one of the most central processes for all life on earth and one of the most well studied plant functions. Characteristically the three known modes of photosynthesis are

different in their spatial and temporal organization. The most common C_3 photosynthesis is located in all cells of the palisade and spongy parenchyma of the plants expressing this form of photosynthesis. In contrast, plants running CAM photosynthesis are characterized by the defined temporal sequence of storage and release of carbon intermediates throughout the diel cycle. However, heterogeneity of CAM photosynthesis also has a whole plant aspect that is dependent on the developmental stage and linked all the way back to the evolutionary position of the species. Thus, CAM photosynthesis has been developed in recent years into one of the most prominent examples, in which the combination of chlorophyll fluorescence imaging, and theoretical modeling guided by destructive sampling leads to a mechanistic understanding of the role of functional heterogeneity in these plants (LÜTTGE: Crassulacean Acid Metabolism a Natural Tool to Study Photosynthetic Heterogeneity in Leaves).

The biochemical heterogeneity and spatial separation of the components of the CO_2-concentrating mechanisms of C_4 photosynthesis has long challenged our ability to offer tight interpretations of the evolution of this functional biodiversity in the face of selective pressures in different environments. Imaging in combination with growth of plants in controlled environmental conditions has offered yet another scale of opportunities for analysis of photosynthetic heterogeneity at the cellular and biochemical level in relation to optimization of light and nitrogen use efficiency (VON CAEMMERER and OSMOND: Testing the Functional Implications of Photosynthetic Heterogeneity in Leaves of C_4 plants: Reductionism during Scale Expansion). These studies confirm that anatomical and biochemical heterogeneity among C_4 types seem to deliver an array of compensating responses that confer a similar and robust, leaf-level advantage with respect to water and nutrient economy. The heterogeneity presumably reflects the independent origins of the C_4 pathway in different plant taxa. Other processes, unrelated to the pathway itself, may be responsible for distinctive patterns of distribution of the differing biochemical C_4 type grasses in relation to precipitation. Thus heterogeneity of biochemical characteristics in plants can deliver common outcomes that contribute to evolutionary fitness in broad terms, whereas other "higher order" structural and developmental properties might determine plant distribution and abundance in vegetation.

Homogenization of spatially distinct responses of photosynthesis could happen through the lateral diffusion of carbon dioxide within open gas spaces inside of leaves. However, such lateral transport may be strongly restricted and has most prominent effects, when stomata are closed and thus internal transport in leaves can play a significant role over the exchange through stomata (JAHNKE and PIERUSCHKA: Lateral Gas Diffusion inside Leaves: a Long Neglected Topic in Plant Physiology). Nevertheless, in homobaric leaves local differences in photosynthesis and respiratory activity due to localized metabolic action driven by environmental (e.g. light gradients) or plant-internal heterogeneity can cause carbon dioxide fluxes that may contribute to fitness under transitory drought or variable light regimes.

In nature biological fitness is undoubtedly related to the ability of plants to defend them against biotic attack. While plants defense has a local character to restrict negative impact to as little area as possible, other mechanisms alert other regions to prepare for potential attack (CONRAD et al. 2002). This example illustrates that communication between heterogeneously responding parts of tissues and plants is essential to optimize plant performance when challenged by spatially and temporally variable environmental cues.

4. Dynamics and Heterogeneity of Plant Growth and Transport

Sensing of heterogeneous environmental conditions requires highly responsive sensory elements. Within the highly spatially organized soil environment (Tab. 1) the root apex can be shown to be very receptive to environmental variation. The root apex hairs can be used as a model system to understand the interaction between plant polarity, cell-cell communication, and sensory plant biology (Baluška et al.: Intracellular Domains and Polarity in Root Apices: from Synaptic Domains to Plant Neurobiology). Clearly the polarity and the dynamics of elements of the cytoskeleton in the root apex – as integral parts of the sensory system of cells – are linked to identifying and communicating environmental changes to the plant. Different parts of the root growth zone show distinct sensitivity to environmental impact and these functions correlate with the cellular and tissue configuration and also resemble their exchange activity with the surrounding soil. It is tempting to compare these sensory functions of the different parts of growing tissues with sensory elements in animals, even though the basic mechanisms are quite distinct and include oriented transport of plant signaling substances.

Finely tuned signaling is also required for the integration of various environmental factors and resource availability with the plant-internal organization of the dynamic of growth. Growth itself is a highly dynamic process and is organized in characteristic spatial and temporal modi (Walter et al. 2009). As growth is the endpoint of a sequence of processes and dependent on the availability of many resources it integrates external impact as well as internal mechanisms (Walter: Leaf Growth Dynamics). The results clearly identify endogenously triggered temporal changes – so-called "endogenous rhythms" – as important nominators of aboveground growth control in dicots to override fast changes in aboveground environmental cues. Externally triggered alterations of growth, e.g. via changing light intensity, show a characteristic, non-linear relation between effector and reaction. This is contrasted by the root growth control, which is governed strongly by long-distance transport of carbon and which is linked more directly to environmental patterns. Such progress has only been possible through the development of suitable imaging tools to analyze growth of leaves and roots with high spatial and temporal accuracy. The heterogeneity of resource availability to growing tissues can even be traced back months after growth has ceased (Gloser et al.: Shoot Heterogeneity in Trees: Consequences of Patchy N Availability and Vascular Transport). It is obvious that even long-lived trees do not have mechanisms to homogenize imbalances of nitrogen distributions that have been laid down during growth. This links the patchy distribution of nutrients in the soil with the heterogeneity of aboveground composition.

5. Modeling and Theory – Towards Understanding of the Role of Spatial and Temporal Heterogeneity

The role of heterogeneities at various levels has been a major focus and challenge of the workshop covered by this issue of *Nova Acta Leopoldina*. Aspects of non-linearities and scaling problems gain a special importance in the context of heterogeneities. Here significant input from theory is required in order to allow adequate up- and downscaling of heterogeneous processes and structures. This will be crucial for understanding the role of heterogeneity at larger scales (upscaling) and the composition of effective quantities at larger scales from local and temporally variable parameters.

Multilevel and integrated modeling is necessary to obtain a set of conclusive interpretations of ecophysiological data and interpretative models (Bohn: Integrative Computational Approaches to Complex Ecophysiological Systems). Adequate interaction between experimentalists and modelers – as illustrated in the successful analysis of CAM photosynthesis as well as of heterogeneity in biofilms – is the basis for rapid and consistent progress on sound experimental basis and on valid models. This challenge goes beyond interpretation of heterogeneity and dynamics in plants, but is a general requirement for systems biology, in which complex and huge datasets need to be extracted to gain relevant information.

The many examples of heterogeneity in plant structure and function demonstrated in the workshop and this issue of *Nova Acta Leopoldina* indicates patterns rather than stochastic fluctuations. Self-organization and decentralized signal perception and processing are crucial mechanisms in plants. Local neighborhood relations and regulatory loops play an important role in establishing such patterns. Through advancements in the theory of pattern recognition and the integration of self-organization spatio-temporal patterns in biological systems in general can be approached by pattern analysis (Geberth et al.: Systematics of Spatiotemporal Heterogeneity – Regulation of Large-scale Patterns by Biological Variability). Biological mechanism form deterministic structures that distinguish pattern formation in plants from pure physical processes – a feature that can be exploited to collect additional information about the biological system.

While heterogeneity is a common feature from the molecular to the ecosystem level, the individual structural and functional elements are often not randomly organized but rather in patterns. Lüttge and Hütt (Talking Patterns: Communication of Organisms at Different Levels of Organization – an Alternative View on Systems Biology) feature the role of communication and signaling at all scales for the development of such patterns. The identification of universal rules integrating heterogeneity across many scales is one of the most outstanding roles of theory for the biological sciences, as it identifies common principles in living systems and (eco-)systems shaped by them.

6. Future Prospects of Imaging and Integrating Heterogeneity of Plant Structure and Function

Already in May 2002 the Leopoldina had addressed this important topic in a workshop at Darmstadt on „Nonlinear Dynamics and the Spatiotemporal Principles of Biology“ (*Nova Acta Leopoldina* NF *88*, No. 332). The Jülich workshop (July 2007) has indicated the significant development that this field has taken already within this relatively short period of time. This workshop, as illustrated by the diverse contributions to this issue of *Nova Acta Leopoldina*, made clear that different communities have used different approaches to analyze and gain new insight from imaging approaches. Still there are major gaps in communication between disciplines like remote sensing and plant physiology, but concepts and approaches from each discipline will proof to be valuable in the future in other field and scales. A major challenge remains the lack of communication and common language between disciplines. Here the workshop provided a first step and a strong need was seen to continue trans disciplinary approaches in research but also in education. On such a basis significant progress will be made in the future in the quantification of a large variety of key processes in plant sciences at various scales and temporal frequencies – illustrating the importance of spatial and temporal

heterogeneity for plant performance in a changing environment as well as being an important characteristic of the strategy of plants to establish efficient mechanisms due to their sessile life form. The increasingly available technologies and the development of proper concepts will allow taking the next steps – namely the linking of processes and scales to understand plant behavior at a holistic level. This will allow better understanding of plants in the environment for urgent problems in general and for processes that explicitly are characterized by environmental cues changing in space and time like climate change. In addition this will help open new routes for application in breeding (phenotyping) as well as in agricultural practice and land management (precision agriculture and remote sensing).

References

Conrad, U., Pieterse, C. M. J., and Mauch-Mani, B.: Priming in plant-pathogen interactions. Trends Plant Sci. *7*, 210–216 (2002)

Schreiber, U., Bilger, W., and Neubauer, C.: Chlorophyll fluorescence as a nonintrusive indicator for rapid assessment of in vivo photosynthesis. In: Schulze, E.-D., and Cadwell, M. M. (Eds.): Ecophysiology of Photosynthesis; pp. 49–70. Berlin, Heidelberg, New York: Springer 1995

Schurr, U., Walter, A., and Rascher, U.: Functional dynamics of plant growth and photosynthesis – from steady-state to dynamics – from homogeneity to heterogeneity. Plant Cell Environ. *29*, 340–352 (2006)

Siebke, K., and Weis, E.: 'Assimilation images' of leaves of *Glechoma hederacea*; analysis of non-synchronous stomata related oscillations. Planta *196*, 155–165 (1995)

Walter, A., Silk, W. K., and Schurr, U.: Environmental effects on spatial and temporal patterns of leaf and root growth. Annu. Rev. Plant Biol. *60*, 279–304 (2009)

Walter, A., and Schurr, U.: Botanical Briefing: Dynamics of leaf and root growth: endogenous control versus environmental impact. Ann. Bot. *95*, 891–900 (2005)

Prof. Dr. Ulrich Schurr
Institute of Chemistry and Dynamics
of the Geosphere ICG-3: Phytosphere
Research Center Juelich GmbH
52425 Juelich
Germany
Phone: +49 2461 613073
Fax: +49 2461 612492
E-Mail: u.schurr@fz-juelich.de

Novel Techniques in Plant Imaging

Nova Acta Leopoldina NF *96*, Nr. 357, 17–30 (2009)

Magnetic Resonance of Plants

Peter Blümler, Carel W. Windt, and Dagmar van Dusschoten (Jülich)

With 6 Figures

Abstract

This paper aims to give interested biologists a short (albeit incomplete) introduction to magnetic resonance imaging (MRI) and its potential for research on plants and soils. Hence, the first section addresses the basic principles of nuclear magnetic resonance (NMR), its spatially resolved variant (MRI) and how the contrast of images acquired with MRI differs from other methods.

A second chapter shows a few examples of the application of MRI to plants and describes the possibilities as well as the difficulties for MRI in plant research. One difficulty that is almost irrelevant in clinical MRI is the fact that shape and size of plants vary from compact fruits to branched trees, which requires special and problem specific hardware solutions which very often need to be developed first. Therefore, the last chapter focuses on a few strategies to solve this problem and introduces dedicated devices for plant investigations.

Zusammenfassung

In diesem Artikel wird versucht, interessierten Biologen eine kurze, vereinfachte und deshalb natürlich unvollständige Einführung in Magnetresonanztomographie (MRI) zu geben und ihr Potential für Pflanzenforschung und Bodenkunde darzustellen. Der erste Abschnitt erläutert deshalb die grundlegenden Prinzipien der kernmagnetischen Resonanz, ihrer ortsaufgelösten Variante (MRI) und welche Bildkontraste im Unterschied zu anderen bildgebenden Verfahren möglich sind.

Der zweite Abschnitt zeigt exemplarische MRI-Anwendungen an Pflanzen und geht auch auf Möglichkeiten und Schwierigkeiten der Methode speziell in der Pflanzenforschung ein. Eine solche Schwierigkeit, welche für klinische MRI irrelevant ist, ist die extreme Variabilität von Pflanzen in Form und Größe, z. B. von kompakten Früchten zu verzweigten Bäumen, wofür jeweils spezielle und problemspezifische Geräte eingesetzt und meistens zuerst auch noch entwickelt werden müssen. Deshalb widmet sich der letzte Abschnitt einigen Strategien, wie dieses Problem gelöst werden kann, und stellt speziell für MRI an Pflanzen entwickelte Geräte vor.

1. Introduction to NMR and MRI

Magnetic resonance is a physical phenomenon using the quantum mechanical magnetic properties of electrons and atomic nuclei to gather information about the local magnetic fields as they are altered by the atomic environment (e.g. chemical structure) or dynamics (e.g. lattice movements). The electrons or nuclei are excited by radio waves in external magnetic fields. Due to the low energies associated with the excitation the method is non-invasive, i.e. the sample stays intact and most organic materials are transparent for the applied magnetic fields and waves.

This paper will focus on magnetic resonance on nuclei, only. Therefore, the method is called NMR (nuclear magnetic resonance) with the most prominent application being named

MRI (magnetic resonance imaging), which is spatially resolved NMR. It is not the intention of this paper to explain NMR or MRI in depth, but only to give the minimal background to understand its potential use for plant physiology. Hence, more physical details should be looked up in the following textbooks (Hashemi and Bradley 2003, Westbrook et al. 2005) or on the web http://www.cis.rit.edu/htbooks/mri/inside.htm.

1.1 Physical and Technical Principles

Nuclear magnetic resonance (NMR) uses the magnetic properties of atomic nuclei which possess an intrinsic angular momentum (i.e. a nuclear spin). There are many isotopes which are of interest (e.g. ^{10}B, ^{11}B, ^{13}C, ^{14}N, ^{15}N, ^{19}F, ^{23}Na, ^{31}P, ^{39}K, ^{35}Cl, etc.) but this paper will mainly talk about the ^{1}H-nuclei in water (that is, protons). The spins of the nuclei cause a very weak magnetic field, but the axes of the spins are normally randomly oriented, so that they all cancel. An external magnetic field is needed to align them. Hence, when a sample of water is placed in a static magnetic field the spins of the ^{1}H-nuclei in the water molecules start to realign relative to the direction of that field. The sum of these oriented atomic magnets generates a macroscopic magnetization vector. The orientation of the spins, however, is not simply parallel to the magnetic field, but also antiparallel. This quantum mechanical effect creates two energy states separated by a quantum of energy. If this energy is irradiated via the alternating electric field of an electromagnetic wave, transitions between these two states are induced and the system is perturbed. This resonance effect uses an electromagnetic wave with a frequency that is directly proportional (e.g. 42 MHz at 1 T field strength for protons) to the strength of the applied magnetic field, resulting in an alternating magnetic field of orthogonal direction. This corresponds to a radio wave, which is typically applied in the form of a short burst (pulse) to excite the system. As soon as this pulse is switched off, the transverse (to the magnetic field) magnetization vector component produces an oscillating magnetic field which induces a small current in the receiver coil. This free induction decay (FID) is the measured signal which may last for a period between 10 µs and a few seconds before the thermal equilibrium of the spins is restored. The information on the local magnetic field as experienced by the protons is best visualized after Fourier transformation of the signal.

Although ^{1}H is very abundant (e.g. plants consists of ca. 90 % water and in each drop of water there are about 10^{21} ^{1}H-nuclei) NMR is not a very sensitive method, because the energy of the transitions are very small. Therefore, macroscopic samples are needed to gather sufficient signals. On the other hand, the used energies are so small that the samples are not disturbed and a wealth of information can be obtained this way. This is why NMR is not only used for the elucidation of chemical structures but also for the study of porous media, medical diagnostics or even neurological studies of the brain.

1.2 Spatial Resolution

The frequency of the nuclear spins is directly proportional to the strength of the magnetic field that they experience locally. To resolve NMR spatially, it is only necessary to superimpose a spatially varying magnetic field. Ideally this field will depend linearly on a spatial coordinate, hence have a constant gradient (first spatial derivative). This is the reason why these additional fields are called “gradients”. Their influence on the NMR-signal is schematically explained in Figure 1. These gradient fields can be utilized in such a way that they result in 2D or 3D images or slices along arbitrary directions.

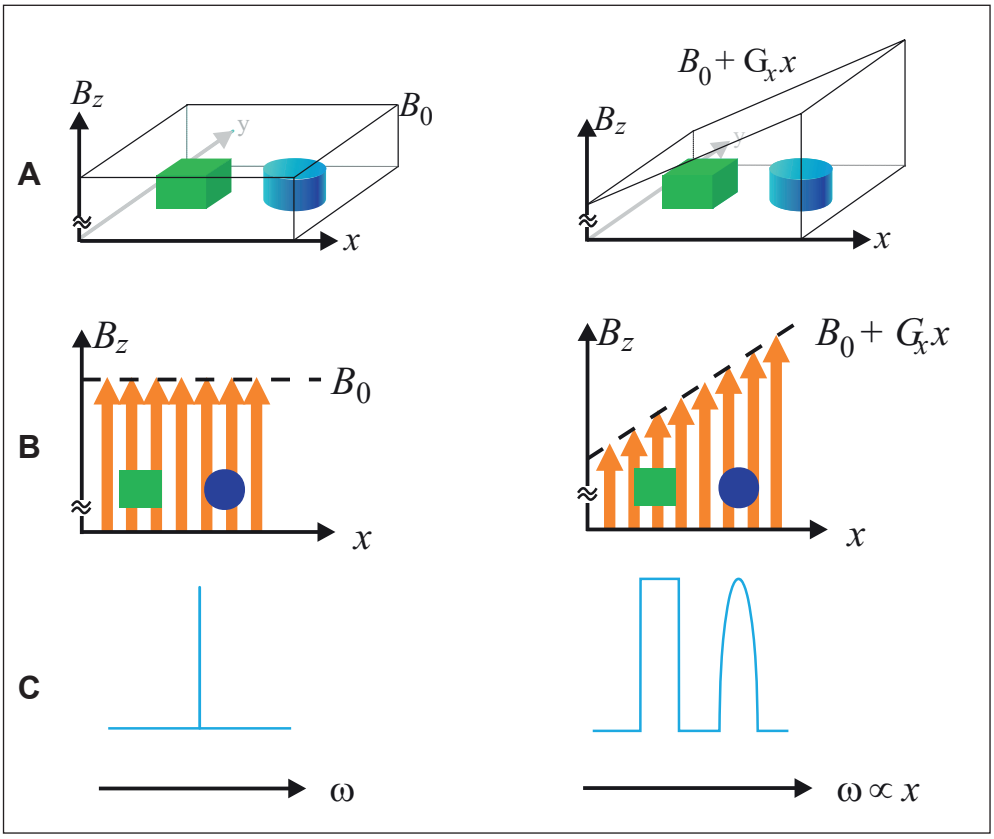

Fig. 1 Schematic representation of the principle of spatial resolution in NMR using gradient fields. Shown is the signal from two samples of different shape and location but with same chemical content (green box and blue cylinder). *Left*: NMR spectroscopy in a homogeneous magnetic field, B_0. *Right*: MRI in the same field but with superimposed gradient, G_x. (*A*) Field and sample geometry in 3D, (*B*) field dependence along the direction of the gradient, (*C*) resulting NMR signal (after Fourier transformation). The signal on the right then corresponds to a spatial projection of the object along the *x*-axis, i.e. displaying the spin concentration along the *x*-axis while it is integrated over the other dimensions.

The spatial resolution in such images then depends on the way they are acquired. Generally it is the ratio of the line width without gradients and the line broadening due to the gradient. The spatial resolution also greatly depends on the strength of the NMR-signal from the sample under investigation. If it is too weak to be measured in a single scan, several scans have to be co-added. For a given density of nuclei the signal strength is directly proportional to the volume it originates from, hence when this volume is reduced due to increased spatial resolution, more scans have to be acquired. Unfortunately, the signal-to-noise ratio only increases with the square-root of scans, which means that for twice the resolution along one dimension four times more scans have to be acquired and for twice the resolution in 3D already a 64 times (4^3) longer acquisition time results.

So usually the spatial resolution is optimized to be as high as necessary and as low as possible for each dimension. The dimensions of a MRI experiment are not necessarily all spatial

dimensions, but could also include time (e.g. a snapshot of a short event consisting of a few subsequent images of the same scene) or other NMR information (e.g. spectroscopy, diffusion, etc.). These considerations also greatly depend on what one expects to be encoded in the image intensities and how much one can contrast the sample properties of interest.

1.3 Contrast

While in clinical MRI images contrast can be used to distinguish healthy from unhealthy tissues, NMR spectroscopy is able to elucidate complex chemical structures, even for proteins in solution. Information about chemical bonds originates mainly from two effects which can readily be used as contrasting mechanisms. The first is the so-called "chemical shift", which describes an individual shielding of nuclei in a molecule due to the specific distribution of the electrons (i.e. the chemical bonding = molecular structure). This local field shields the nucleus from the external field and is characteristic for the local structure and the neighboring atoms and hence can be used for structural analysis. The other mechanism is "dipolar coupling". All atomic magnets act like magnetic dipoles which not only interact with the external magnetic field but also mutually. Since the strength of this interaction is known and the observed effect mainly depends on the distance and the orientation of the dipoles, interatomic distances, angles and local orientations can be determined very accurately even in complex molecules.

Chemical shift can be used to contrast different chemical substances within a sample by selecting a range of characteristic frequencies (e.g. separation of fat and water or aliphatic and aromatic structures) (Rumpel and Pope 1992). Dipolar couplings on the other hand can distinguish tissues due to molecular dynamics which reduces dipolar couplings and sometimes also due to different orientations, e.g. of fibers.

In MRI the most important contrast mechanism, however, is caused by relaxation of the nuclear magnetization, which has a longitudinal and a transverse component. The longitudinal component is due to an excess of protons in the lower energy state. This gives a net polarization parallel to the external field. Excitation generates transverse magnetization perpendicular to the external field. The recovery after a radio frequency (r. f.) pulse of longitudinal magnetization is called T_1 relaxation, and the loss of phase coherence in the transverse plane is called T_2 relaxation.

Relaxation is a change in the magnetization with time which is typically caused by very fast variations of local fields (e.g. fluctuations of the dipoles of neighboring spins). This allows investigation of molecular dynamics over wide frequency ranges. In soils paramagnetic or ferromagnetic centers (e.g. iron oxides) can also greatly influence the relaxation times of surrounding protons. Exactly this mechanism is used for most clinical contrast agents.

Finally, the magnetic field gradients applied to obtain spatial encoding of the nuclear spins can also be used to detect transport phenomena. The fact that spatial encoding can be performed during an NMR sequence for a limited time and that it can be decoded or compared with a new spatial situation later on, allows to determine coherent and incoherent motion of the spins. Coherent motion of the spins is typically referred to as flow or convection while incoherent motion is referred to as diffusion or perfusion. Both processes can be distinguished and studied over a wide range, which makes it possible to acquire interesting insights into mass transport in plants and soils. Very small velocities, however, normally require the use of contrast agents.

2. MRI of Plants

When compared to imaging of people or animals, MRI of plants would appear to be much simpler. Plants barely move during measurements, the internal structure is rather symmetric and predictable in large parts of the plant (like stems which have essentially a cylindrical symmetry), and internal transport tends to be slow and is not pulsatile. In many cases there is plenty of time to acquire signal, which should yield high quality images with high resolution. For this reason NMR images of harvested fruits are abundant and have been used as demo objects for MRI since its inception. Another advantage is that many safety regulations and constraints, necessary in clinical MRI, do not apply when working with plants. This allows, for instance, the application of many, intense and very short excitation pulses. Thus MRI on plants can be performed in a much more direct and quantitative way than in humans.

However, living plants do not have a "closed" (hence compact) body layout, where internal surfaces separate organs which are connected by vessels. They rather show a so-called "open" body plan, as they have to expose relatively large surfaces to the environment for maximal light interception, water and nutrient uptake. In order to fulfil this aim a branched structure is much more advantageous, but when considering them as MRI samples this leaves a lot of empty spaces between the ramified plant parts, resulting in a poor filling factor. Ideally, however, the r. f. and gradient coils should be very close to the interesting regions to achieve best noise figures and spatial resolution.

Furthermore, plants have a "second half" that is hidden in a completely different environment – the soil. MRI of roots can be even more challenging than that of the parts above ground, because delicate plant structures here are surrounded by water filled pores and often abundantly present para- or ferromagnetic impurities, which can result in image distortion. Even in terms of filling factors this scenario is typically worse than above ground, because healthy plants require big pots to grow. In those pots a lot of water is not associated with the plant, and this water has to be distinguished from signal arising from plant roots by utilizing suitable MRI contrast. Taken together the general shape of plants and its biodiversity make MRI on living plants particularly demanding in terms of suitable hardware.

Another factor that complicates matters is that most plant tissues contain air. Air conducts the magnetic field slightly different than water, which causes a local variation in the magnetic field. Therefore, an air bubble causes a local magnetic field gradient, which will compete with the gradients used for the MRI experiment. The result is a loss of signal, mainly caused by diffusion in the local gradient and a dislocation of the water signal in the image. In order to overcome some of the above problems, strong gradient coils are required in combination with high r. f. power, which is useful to shorten the time for signal detection and therewith the time that diffusion can take place. This again is quite demanding on the equipment.

A well equipped MRI lab for the investigation of plants therefore needs a variety of hardware solutions to match the various regions of interest. Additionally, a vertical bore magnet, high power gradient- and r.f.-coils are required, driven by strong amplifiers. Finally, for many plant experiments one should be able to control the environmental conditions inside the magnet with regard to light, temperature and humidity.

2.1 Contrast, Spatial Resolution and Dynamic Information

A stated in section 1.2 MRI has a limited spatial resolution, which is often debated to be too low for microscopic applications. For very small objects (diameter on the order of a few

millimeters), the highest in-plane resolution for plant parts can be close to 10×10 µm^2, with a so-called slice thickness of roughly 100 µm. When studying larger parts of living plants, like buds or stems, the in plane resolution will typically be around 50×50 µm^2 within a slice of 200 µm. This is roughly at the cellular level or above, and it is often argued that MRI can thus not be used to gather information on a cellular or even sub-cellular level. However, this is an over-simplification. In many plant regions cell groups exist that exhibit roughly identical features, like overall size, relative compartment size, membrane permeability or sugar concentration. These cells can be taken together and viewed as an assembly. When special MRI sequences are then applied to such an assembly, averaged information can be acquired (like T_2, T_1, flow or translation diffusion, the four most commonly measured parameters). These MRI parameters can be translated on a pixel-by-pixel basis into morphological or physiological information which originates from the (sub-)cellular level, for instance:

– vacuole size (van Dusschoten et al. 1995);
– plasmalemma permeability (van der Weerd et al. 2002);
– relative sugar concentrations (Köckenberger et al. 2004);
– flow velocity, flow conducting area and volume flow in xylem and phloem (Scheenen et al. 2000, Windt et al. 2006).

In a time series of experiments one can thus follow the dynamical response of plant characteristics to varying environmental conditions by monitoring these or equally relevant, physiological parameters.

Albeit not a dynamical response of singular cells, the averaged response is often more than sufficient for plant physiological and biochemical studies. Such studies are therefore often restricted to two spatial coordinates, because generating 3D maps of NMR parameters is time consuming, and the focus of interest can typically be limited to one or a few slices through the plant. Still it is a nice feature of MRI that internal and external features of the sample can easily be recorded in 3D. If we limit ourselves to obtaining an appropriate contrast between tissues, as is common for MRI studies in the medical field, the duration of such 3D measurements does not become too excessive (e.g. 30 min) and can be used to study the development of morphological features. Figure 2 shows an example of a maize plant with its roots in normal sand not fully saturated with water. The roots sit in a plastic pipe with 3 reference tubes attached to it to allow for concatenation. This image shows a $256 \times 192 \times 216$ data matrix corresponding to a field of view of $68 \times 68 \times 120$ mm, based on two 3D MRI measurements that were concatenated using MeVisLab (MeVis Research GmbH, Bremen, Germany). In this case it was possible to zoom in on the water within the roots alone, disregarding the water in between the sand due to the good contrast that can sometimes to be obtained between plant water and soil water. This type of 3D image can be used to follow the root structure over time, thereby enabling the measurement of the relative root growth rate in 3D within a natural soil. Studies like these can be performed in half an hour such that even moderate changes of the growth rate during the day, or the effect of changes in the environment can be monitored and quantified.

The internal structure of plants or plant parts can also easily be visualized. As an example, Figure 3 shows four images of (virtual) slices through a sugar beet. The image at the top left (Fig. 3*A*) is a slice through the lower parts of the stems. The vascular bundles are easily recognized as brighter zones. This is normally caused by the large size of the xylem vessels, which results in longer T_1 and T_2 values. Because the images are T_2 weighted, a longer T_2 results in

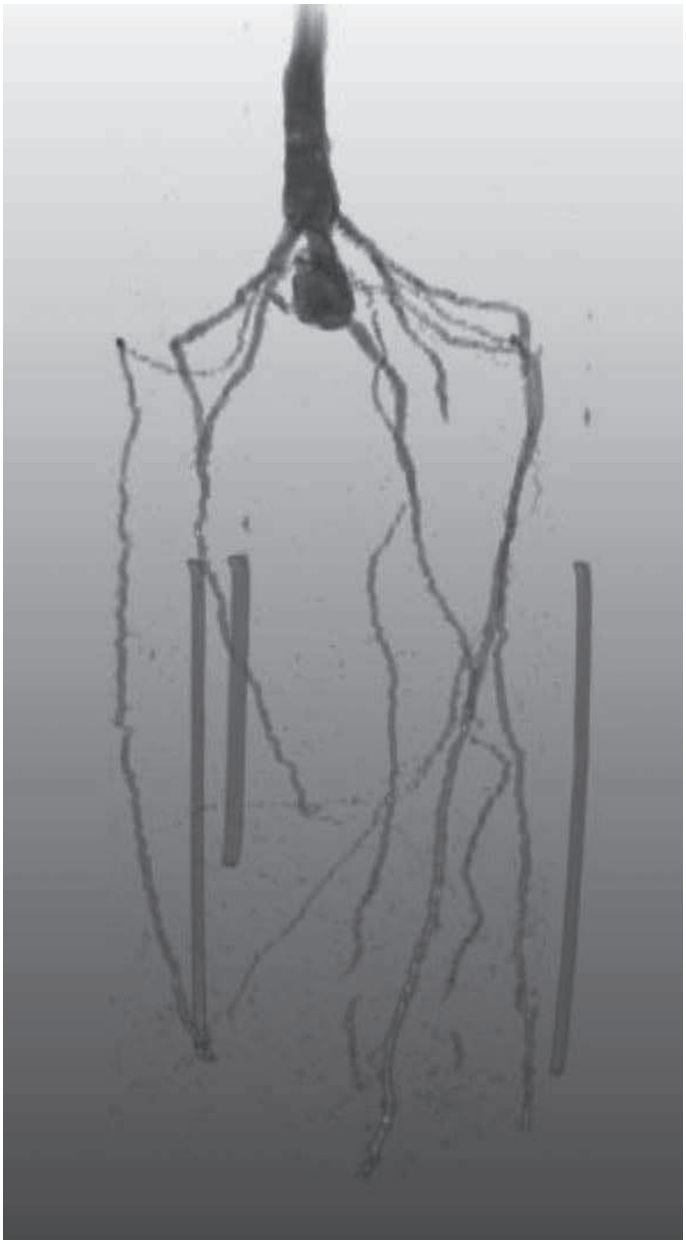

Fig 2 3D reconstruction of a maize root system in a 58 mm wide pot. Three reference tubes were fixed to the outside allowing for concatenation of two 3D data sets. Field of view (FOV) is 68×68×130 mm, corresponding to 256×192×216 pixels. Time between excitation and echo detection, TE = 12 ms, recovery time between two succeeding experiments, TR = 3.5 s, slice thickness = 0.6 mm

a brighter pixel color. The effect of T_1 relaxation could be excluded in these images by allowing for full relaxation before new excitation. The upper part of the sugar beet is shown in the two lower slices (Fig. 3*C* and *D*). The brighter pixels correspond with transport tissue. The outer layer of the beet appears to have a higher water density, which was quantified by using another MRI sequence which also determines the T_1 values. These T_1 values turned out to be uncommonly short, often less than 100 ms, which is a clear indication that a lot of sugar was accumulated in this beet in a period of just over a month. Only in the center of the pith, which is known to have lower sugar content, higher T_1 relation times were determined.

In case one wants to obtain more than just plain morphological information over time it can be beneficial to measure intrinsic NMR parameters like T_1, T_2 and water density, which requires the use of slightly more complicated pulse sequences. In Figure 4 we present a demonstration of this type of measurement on an excised rhubarb stalk. Using a so-called

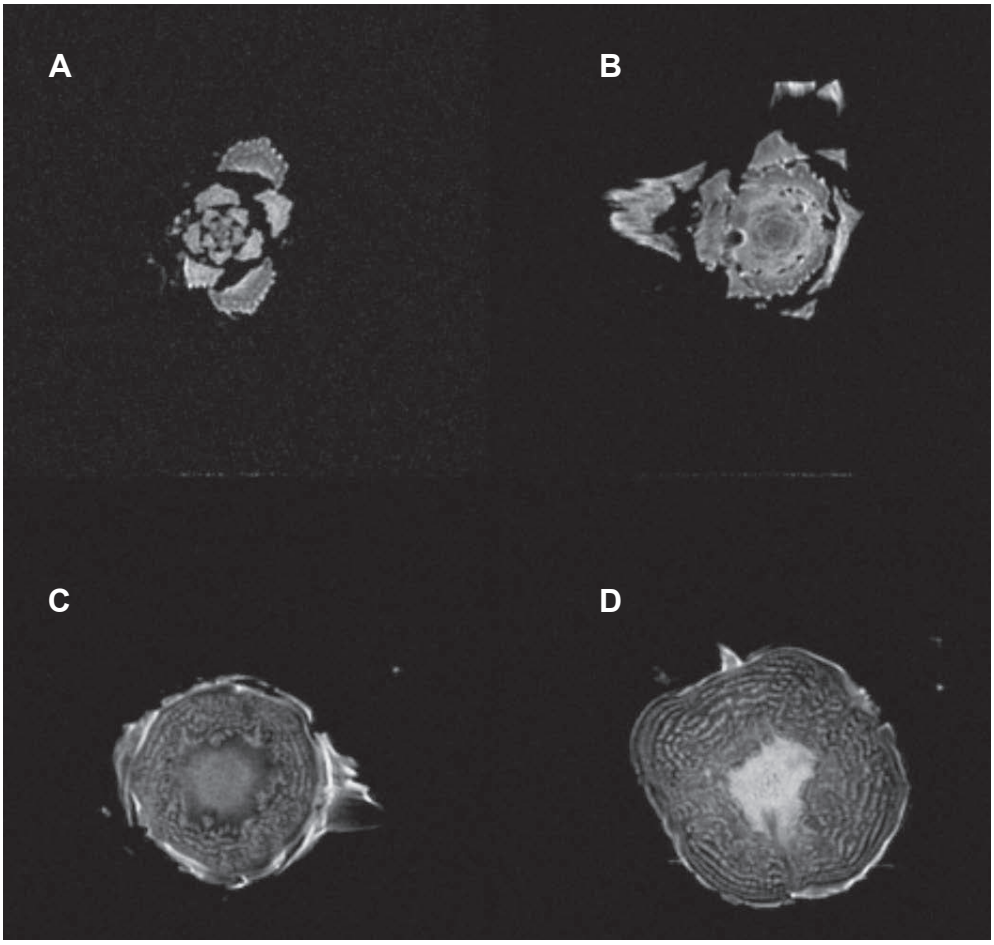

Fig. 3 A series of 4 slices through a sugar beet starting at the leaf stems just above the sugar beet (*A*) and descending into the upper part of the beet (*D*). MRI details: Spin Echo, TE = 12 ms, TR = 3 s, FOV = 68×68 mm, slice thickness = 0.6 mm.

saturation recovery multi echo sequence a 4D data set (two spatial dimensions and two time dimensions of characteristic changes of magnetization) was acquired. Using a 2D fit routine water density, T_2 and T_1 maps are calculated for each pixel (Fig. 4*A*, *B*, *C* respectively). Additionally, the ratios of the T_1's and T_2's can be displayed (Figs. 4*D* and *E*). One can clearly distinguish structures like the vascular bundles, with phloem (T_1 and T_2 shorter than in pith), xylem (larger xylem vessels have emptied) and sclerenchyma cells (shorter T_2, long T_1). Furthermore, the cortex (both T_1 and T_2 are long, 2 s and 0.4 s, respectively) and an outer layer of more densely packed cells (short T_1, long T_2) can be recognized. The long T_1 for cells in the cortex in combination with a long T_2 indicate the presence of large vacuoles with a low organic content. The cells within the outer layers that have a T_1 of roughly 1 s and a T_2 of about 300 ms, most probably exhibit an increased concentration of smaller organic compounds within the vacuole. Since the duration of the experiment is about half an hour, changes of water and e.g. sugar content within the stem or phloem can be measured on a physiologically relevant time-scale.

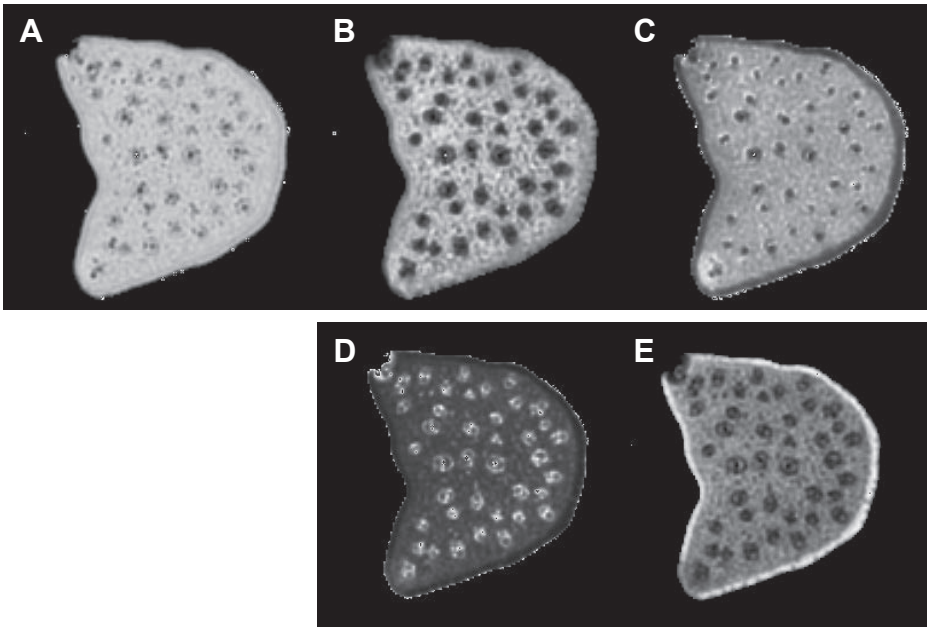

Fig. 4 Maps of the (*A*) water density, (*B*) T_2 and (*C*) T_1 as obtained from a saturation recovery multi echo experiment on an excised Rhubarb stalk after 2D fitting. Additionally the ratio-maps T_1/T_2 and T_2/T_1 are presented as a visual tool to identify plant structures. Grayscales: (*B*) 0.05 to 0.5 s; (*C*) 0.3 to 2 s. TR= 0.06 to 3.2 s, TE = n*0.008 s (n = 1,..,30). FOV = 15 × 15 mm, slice thickness = 1 mm

2.2 MRI Velocimetry

An example that illustrates how MRI can be used to obtain information from structures smaller than the spatial resolution is MRI flow imaging. MRI generally does not allow the visualization of vessels or conduits: they are just too small. In practice this means that pixels with flow do not only contain a flow conducting conduit, but also a sizeable amount of stationary water located in tissue surrounding that conduit. However, by using a pulsed field gradient (PFG) type flow measurement technique the contributions of both water fractions, stationary and flowing, can be separated.

In a typical flow measurement the velocity spectrum is measured for every pixel in an image. In such a spectrum the amplitude of the signal is a measure for the amount of water, while the velocity spectrum reveals what velocities are present. Stationary but randomly diffusing water will become visible as a Gaussian shape centered at velocity zero. Water that exhibits a net directional flow will appear left or right from the stationary water, depending on the direction of flow. Unfortunately, the velocity spectrum itself is not yet enough to separate the flowing from the stationary water. The contributions of the stationary and the flowing water still appear in a convoluted fashion. However, it is known that the signal of the stationary water must be symmetrical around velocity zero and has a Gaussian shape. This knowledge can be employed to separate the stationary from the flowing water, thus giving access to displacement information on a sub-pixel level (Scheenen et al. 2000). The results can subsequently be quantified both in terms of amount of water, linear flow velocity, flow conducting area, and volume flow (cf. Fig. 5*A* and *B*).

What makes MRI velocimetry especially well suited for the study of long distance transport is the fact that it is completely non-invasive. Both xylem and phloem transport rely on fragile pressure gradients that are easily disrupted. The xylem easily becomes embolized when punctured, and the phloem (which consists of living cells) shows a range of defense reactions whenever it is touched or cut. MRI velocimetry does not have these drawbacks, making it possible to monitor transport in plants for days (Fig. 5*C*) or even weeks.

3. Specialized Hardware

In order to detect an NMR signal, the region of interest in a sample must experience a magnetic field for the duration of the experiment. Furthermore, the spins in this volume must be excited by a strong burst of a suitable radio frequency and a spatial detection also requires additional magnetic field gradients. Typically the magnetic field is provided by a strong electro magnet, into which the sample is placed. To achieve strong fields over large volumes very high currents are necessary, and the best way to provide them is to use superconducting magnets, which do no longer possess electrical resistance but must be cooled by liquid helium. The sample must then be surrounded by gradient coils and radio frequency coils which further reduce the accessible volume, so that for a sample of 15 cm diameter, a magnet with an inner bore of 30 cm is needed. Such equipment is expensive and of course stationary.

Another problem that easily arises when investigating plants by NMR is the fact, that while the entire plant has to be placed inside the magnet only a small part (e.g. branch, fruit) is of actual interest. The principal non-invasive nature of NMR experiments is therefore often waived for the sake of achieving better fill factors or investigating larger plants. From an extremely puristic view even cultivating and observing a plant in a flower pot could be called

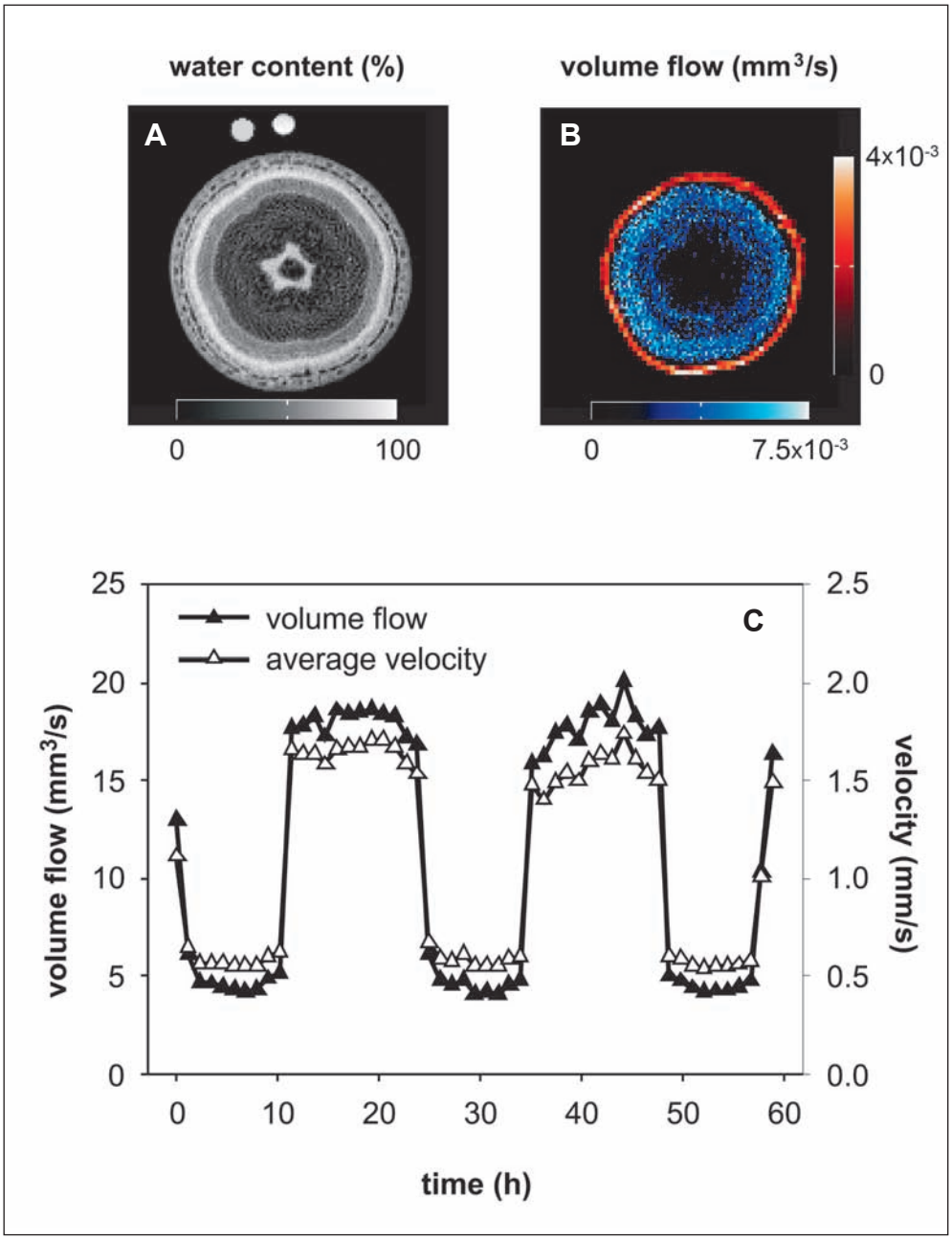

Fig. 5 Water content and long distance transport in poplar. (*A*) Water content. (*B*) Volume flow per pixel. The xylem and phloem flow images originate from different measurements and have been superimposed. Xylem transport is shown in blue and occurs in an upward direction. Phloem transport is shown in red and is directed downward. (*C*) Xylem flow in poplar during a period of two and a half days. Shown are total volume flow in the stem (closed symbols, left axis) and average linear velocity (open symbols, right axis). MRI details: PFG-SE-TSE, TR = 2.5 s, FOV = 12.5 × 12.5 mm, slice thickness = 3 mm. (WINDT et al. 2006)

an "invasive" procedure, but definitely the study of intact plants in the field by NMR requires other hardware solutions.

Recently great improvements in light-weight, portable magnet systems and spectrometers have been made (Goodson 2006). This development was triggered by an increasing need of "outdoor" applications of NMR (e.g. in veterinary medicine or geophysical oil well inspections) and has become technically feasible due to the development of stronger permanent magnets, suitable assembly of such magnets and systematic methodological research in NMR experiments. This trend started with mobile single-sided equipment (Blümich et al. 2008), where a small magnet is placed on the surface of an arbitrarily large object and measures the NMR-signal from a small spot close to the surface. While this technique is very useful for material testing, its use in plant research is limited due to the fact that signal is difficult to quantify and the penetration depth is typically too low (a few millimeters).

Quantitative measurements of water content in entire plant segments and detailed studies of plant physiology therefore require relatively homogeneous magnetic fields over the entire volume of interest; at least the variation of the magnetic field must be smaller than the bandwidth of the applied radiofrequency pulse in order to excite all the contained spins.

One possible solution for all these requests is a hinged magnet system, which opens and closes without noteworthy force and is therefore called the NMR-CUFF (**Cu**t-open **F**orce **F**ree). The principle and a working prototype are shown in Figure 6. The magnets in the NMR-CUFF generate a very homogeneous and strong field (see Fig. 6*A*) (Raich and Blümler 2004), that when opened along a diagonal generates attracting and repelling forces of almost equal strength: See flux lines in Figure 6*B*, where in the center of the device a local maximum of the magnetic field lies in between two local minima (white circles). Due to this design idea the NMR-CUFF is the first magnet which can be opened almost without force. (The measured force associated with opening and closing is smaller than 20 N.) The prototype in Figure 6 *A*'/*B*' generates a field of 0.57 T (which corresponds to a ^{1}H resonance frequency of 24 MHz) with a homogeneity of 400 ppm over a spherical volume with 5 mm diameter. This versatile instrument only weights 4 kg and can for instance be clamped around a tree, branch or stem of a plant and will allow quantitative measurements of relaxation or diffusion in the entire enclosed volume. Mobile equipment like the NMR-CUFF allow studies of plants or plant parts which cannot be investigated *in vivo* by stationary MRI scanners either because the plants are too big or have to be studied in the field. High resolution imaging and spectroscopy, however, will be challenging to realize with such devices (Blümich et al. 2008, and references therein), but one might bear in mind that their field strength and homogeneity is already comparable to commercial stationary MRI equipment 20 years ago.

The principle design of the NMR-CUFF can be scaled up. However, for the sake of mobility one should consider, that doubling the dimensions (e.g. inner diameter), by simply scaling the design up, increases the mass by a factor of $2^3 = 8$!

4. Conclusion and Outlook

MRI of plants is no simple task. It can only be realized by innovative refinement of technological solutions from medical imaging to special requirements of plants as living systems: Illumination, climate control and, ideally, even the hardware has to be optimized to produce meaningful data. Yet, the wealth of dynamical, physiological information that is accessible

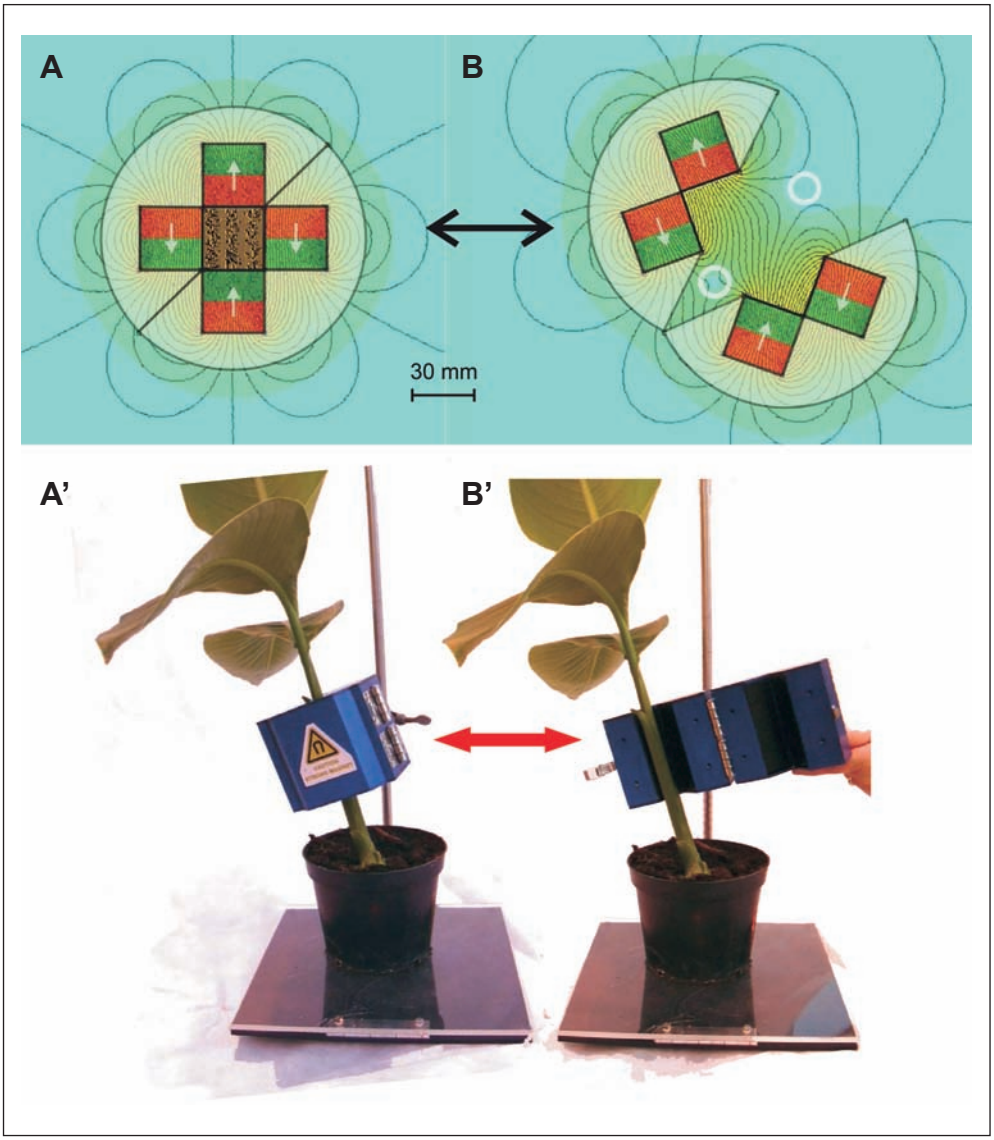

Fig. 6 The NMR-CUFF – a hinged magnet which opens without force. (*A*) closed and (*B*) opened system. Magnets and supporting material are superimposed a calculated plot of the generated flux lines of each arrangement. Local minima in the flux in (*B*) are marked by white circles. Top row: Principle arrangement of the permanent magnets overlaying a simulation of the resulting magnetic field. Bottom row: Prototype applied to a plant stem. This prototype has a field strength of 0.57 T and weighs ca. 4 kg. The central opening is 30 mm.

via *in-situ* and *in-vivo* MRI experiments definitely justifies the effort. Morphology, chemical and physical composition, water status and transport and maybe even uptake of other nuclei can be followed non-invasively with sub-millimeter resolution. Therefore, MRI has the potential to become an indispensible tool for plant physiology and biophysical research.

References

Blümich, B., Perlo, J., and Casanova, F.: Mobile single sided NMR. Prog. Nucl. Magn. Reson. Spectrosc. *52*/4, 197–269 (2008)

Goodson, B.: Mobilizing magnetic resonance. Physics World *5*, 28–33 (2006)

Hashemi, R. H., and Bradley, W. G.: MRI the Basics. Philadelphia: Lippincott Williams and Wilki 2003

Köckenberger, W., Panfilis, C. de, Santoro, D., Dahiya, P., and Rawsthorne, S.: High resolution NMR microscopy of plants and fungi. J. Microscopy *214*, 182–189 (2004)

Raich, H., and Blümler, P.: Design and construction of a dipolar Halbach array with an homogeneous field from identical bar-magnets – NMR-mandhalas –. Conc. Magn. Reson. B: Magn. Reson. Eng. *23*B/1, 16–25 (2004)

Rumpel, H., and Pope, J. M.: The application of 3D chemical shift microscopy to noninvasive histochemistry. Magn. Reson. Imag. *10*/2, 187–194 (1992)

Scheenen, T. W. J., van Dusschoten, D., Jager, P. A. de, and Van As, H.: Quantification of water transport in plants with NMR imaging. J. Exp. Bot. *51*/351, 1751–1759 (2000)

van Dusschoten, D., Jager, P. A. de, and Van As, H.: Extracting diffusion constants from echo-time-dependent PFG NMR data using relaxation-time information. J. Magn. Reson. A *116*, 22–28 (1995)

van der Weerd, L., Claessens M. M. A. E., Efdé, C., and Van As, H.: NMR imaging of membrane permeability changes in plants during osmotic stress. Plant Cell Environ. *25*/11, 1539–1549 (2002)

Westbrook, C., Roth, C. K., and Talbot, J.: MRI in Practice. Wiley-Blackwell 2005

Windt, C. W., Gerkema, E., Oosterkamp, J., and Van As, H.: MRI of long-distance water transport: a comparison of the phloem and xylem flow characteristics and dynamics in poplar, castor bean, tomato and tobacco. Plant Cell Environ. *29*/9, 1715–1729 (2006)

Dr. Peter Blümler
Forschungszentrum Jülich GmbH
Institut für Chemie und Dynamik der Geosphäre
ICG-3: Phytosphäre, Geb. 06.2 (E5)
52425 Jülich
Germany
Phone: +49 2461 613263
Fax: +49 2461 612492
E-Mail: p.bluemler@fz-juelich.de

Nova Acta Leopoldina NF *96*, Nr. 357, 31–47 (2009)

Quantification of Plant Surface Structures from Small Baseline Stereo Images to Measure the Three-dimensional Surface from the Leaf to the Canopy Scale

Bernhard Biskup[1], Ralf Küsters[1], Hanno Scharr[1], Achim Walter[1], and Uwe Rascher[1,2]

With 6 Figures

Abstract

Structural changes are one key feature of plant life and determine performance of plants in their natural environment. Shape and structure of single organs (e.g. leaves) and whole canopies constantly adjust to environmental factors. Currently only a limited number of methods are available to directly measure these structural changes under natural conditions. Here, we present and review the potential of small baseline stereo for mapping the surface of plant organs and canopies in 3 dimensions. To avoid occlusion, we suggest using a small baseline stereo approach, where images from different camera positions differ only slightly. Scaling this approach to the canopy is possible, and we mapped extended canopies of several meters diameter. On the ecosystem scale, a robotic arm was used to take mosaics of stereo images of the 40×40 m² canopy of the tropical rainforest mesocosm of Columbia University's Biosphere 2 Laboratory, an enclosed artificial ecological model system. This revealed a map of the outer canopy demonstrating the potential to give better insight into light penetration within the canopy and to provide quantitative data about the structure of the outer canopy of plant ecosystems.

Zusammenfassung

Strukturänderungen sind ein charakteristisches Merkmal pflanzlichen Lebens und haben einen maßgeblichen Einfluss auf die Leistungsfähigkeit von Pflanzen. Form und Struktur einzelner Organe (z. B. Blätter) und ganzer Kronendächer passen sich permanent ihren Umweltbedingungen an. Zurzeit existiert nur eine begrenzte Zahl von Verfahren zur Messung der Oberflächenstruktur von Pflanzen unter natürlichen Bedingungen. In dieser Arbeit stellen wir das Potential von *Small-Baseline*-Stereoverfahren zur Vermessung pflanzlicher Oberflächen und Kronendächer dar, d. h., Einzelbilder wurden von nah beieinander liegenden Positionen aufgenommen und daraus eine Tiefenkarte errechnet. Das Verfahren ist auch für größere Kronendächer geeignet; es wurden 3D-Modelle von Kronendächern mit mehreren Metern Durchmesser erzeugt. Auf Ökosystemskala wurden mittels eines Roboterarmes zahlreiche Stereobilder eines 40×40 m² Kronendachs des tropischen Mesokosmos im Biosphere-2-Labor (einem abgeschlossenen, künstlichen ökologischen Modellsystem der *Columbia University*) aufgenommen und fusioniert. Das resultierende 3D-Modell ist von großem Nutzen für die Untersuchung der Lichtdurchdringung und die Gewinnung quantitativer Daten über die Struktur des äußeren Kronendachs pflanzlicher Ökosysteme.

1. Introduction

Plants constantly adjust to changing environmental conditions. Being sessile organisms, a wealth of acclimation mechanisms affect plant structure by altering the distribution of growth

1 Institute of Chemistry and Dynamics of the Geosphere ICG-III: Phytosphere, Forschungszentrum Jülich, Stetternicher Forst.

2 Corresponding author.

of single organs such as leaves or the interplay and arrangement of their modules, which e.g. changes foliage orientation. Thus, the structure of plant canopies is highly dynamic, changing on various time scales, from minutes to seasons (for recent review see SCHURR et al. 2006). Structural changes in plants have been studied for decades and different approaches to quantify the structural parameters of plant canopies have been developed in the past (e.g. CAMPBELL and NORMAN 1989, SINOQUET and RIVET 1997, SINOQUET et al. 1998, RAKOCEVIC et al. 2000). However, most of these methods require the plant being fixed in the lab or are too time consuming (such as laser scanning methods) to account for fast changes in natural conditions (RAKOCEVIC et al. 2000 reported a time of 3–7 h needed for a 10 cm × 10 cm canopy of white clover).

On the microscopic scale, stereo microscopes are usually used together with correlation based reconstruction approaches (see e.g. LIAO et al. 1997, OMASA 2000). On the large scale, photogrammetry has established a variety of approaches to map the surface of earth in three dimensions: digital elevation models have been elaborated with enormous precision by methods such as relief displacement, shadow length analysis and aerial stereoscopic photography (see e.g. HIRSCHMÜLLER et al. 2005).

Considering this background, there is surprisingly little information available on the three-dimensional structure of plant canopies and ecosystems, which pose the specific challenge of changing their shape and structure frequently. To our knowledge, there is currently no reliable field method available for reconstructing plant structure on a medium scale, i.e. from the level of single leaves (cm resolution) to canopies (a few meters). Stereo imaging methods are often hampered by the limited contrast of plant leaves and the cleft structure of plant canopies, which consist of almost two-dimensional leaves parted by great discontinuities. These structural properties make it difficult to use standard stereo algorithms on plant canopies. Thus alternative methods were used to get information about plant ecosystems, with active radar and light detection and ranging (LIDAR) methods currently being the most frequently used.

LIDAR is used to quantify biomass and to retrieve structural information about whole forest stands for forest management (MALTAMO et al. 2005). LIDAR devices emit light onto a target, and the travel time from the device to the target and back to the device is used to determine the height of an object. Because return signals are received from structures at different heights (such as canopy stories), LIDAR is capable of determining the vertical distribution of foliage. However, the top of the canopy may be hard to detect if insufficient leaf material is present (LEFSKY et al. 2002). By turning the LIDAR device or by moving it across an area, height distributions of complex surfaces, such as forest canopies being reconstructed from airplane measurements, can be obtained. In general, LIDAR provides a sparser sampling than optical approaches (BALTSAVIAS 1999). Results from LIDAR allow understanding dynamic vegetation changes which helps to improve forest management. Moreover, LIDAR vegetation data is discussed as a measure of carbon stocks in the frame of the Kyoto protocol (TURNER et al. 2003, PATENAUDE et al. 2005). Recently on the smaller spatial scale, scanning LIDAR techniques have successfully been employed to create three-dimensional (3-D) reconstructions of single broad-leaved plants (OMASA et al. 2006). Despite great technical advantages high spatial resolution results in long scanning times, which to date limits the applicability of high resolution LIDAR to laboratory experiments

During the past years it became obvious that processes well understood on the single leaf level cannot linearly be scaled up to the canopy level to understand ecosystem processes. Hence, the need was emphasized to:

– Monitor growth and phenotype of crops to facilitate improved management practices there. Analysis of plant reaction towards environmental stresses would allow rapid screening for optimized crop lines.
– Better understand and model foliage changes and light interception in canopies. These input parameters are necessary to increase precision of carbon models. Micrometeorological parameters have to be validated and parameterized for turbulences within plant canopies and to correctly parameterize plant mediated exchange processes in soil-vegetation-atmosphere-transfer and mechanistic ecosystem models.
– Get first insight into structural changes of the outer canopy as a response to environmental factors. Structural changes are an inherent feature of plants to adjust to different environments and the importance of structural changes as a trait of physiological acclimation and hence survival probability is just about to be realized (Niinemets et al. 2005).
– Remote sensing will help to better understand the radiative transfer processes within a canopy with the help of 3-D structural information, which will allow retrieving and correcting for effects related to bidirectional reflectance distribution functions (BRDF): due to their complex structure, leaf reflectance commonly depends both on the incidence angle of the sun and the viewing angle (Barton and North 2001).

With this communication we address this gap in knowledge and present a proof-of-concept evaluation on 3-D imaging of plant surfaces from the single leaf to the canopy. We use a small baseline stereo approach, meaning a stereo reconstruction approach where the camera positions differ only little in comparison with the distance to the object. The method can be established with comparably small financial investment. Texture of plant surfaces is often sufficient for this approach, and images of leaves and small canopies can often directly be used for 3-D reconstruction. However, it has to be pointed out that some plant organs, such as leaves of certain species, may have to be pretreated for texture enhancement (e.g. by applying spray markers or illuminating with structured light). On the canopy scale, however, single leaves provide enough texture to calculate distance as long as the camera system provides sufficient spatial resolution.

2. Small Baseline Approach to Quantify Three-Dimensional Surfaces

2.1 Background

Stereo imaging is a way to measure 3-D surface structure non-destructively. There is a wide variety of two-camera stereo image reconstruction schemes (see Scharstein and Szeliski 2002 for a recent overview and performance comparison; also see Brown et al. 2003). The basic idea of stereo reconstruction is to find positions in the acquired images corresponding to the same surface point (the so-called correspondence problem) and triangulate its depth using the known camera geometry. Camera geometry can be determined using freely available calibration tools (see e.g. http://www.vision.caltech.edu/bouguetj/calib_doc/index.html). Due to this work it is rather straightforward to calibrate single cameras for their intrinsic parameters as well as two cameras with respect to their relative positions and orientations (extrinsic parameters). The major remaining problem is to solve the correspondence problem for as many points as possible. Point or feature based approaches look for distinct image structures like corners or junctions that can be detected reliably in both images. Dis-

criminative features (see e.g. Shi and Tomasi 1994) can be matched even if their positions are far apart from each other in the two images. While these features deliver highly accurate depth estimates there are only few of them in an image and the reconstruction is usually too sparse for a full surface reconstruction. Area or correlation based approaches search for similar patches in both images. As for features their positions are also allowed to be separated considerably. Thus, large position changes due to large distances between the two cameras, i.e. wide baseline stereo, can be handled. Unfortunately, using correlation, patch positions can only be determined with pixel accuracy (i.e. discrete depth steps) leading to staircase-like depth reconstructions unless additional subpixel estimations are performed. Among the most promising approaches, even though not yet listed on the Middlebury web page (experimental comparison of stereo algorithms, http://cat.middlebury.edu/stereo/; see Scharstein and Szeliski 2002), are optical flow based methods (Slesareva et al. 2005). They benefit from the tremendous accuracy increases in optical flow estimation achieved in the last decade (Papenberg et al. 2006). Originally designed to measure motion in temporal image sequences, they also solve the correspondence problem. Using optimized numerical differentiation schemes, even higher accuracy can be achieved when more than 2 images are used (Scharr 2005) due to lower systematic errors. As explained in more detail below, the approach proposed in the current paper uses the optical flow assumption on usually 3–5 images acquired by a single camera shifted via a moving stage, together with a local total least squares estimation scheme. This approach thus benefits from the high accuracy of multiple-image optical flow without the need for elaborate camera calibration: internal parameters are fixed, and external parameters are known from the motion of the moving stage ('hardware calibration').

2.2 Experimental Set-up

Generally, the experimental set-up is an advancement of the 2-D growth set-up (see Walter and Schurr 2005), adding the additional dimension with the moving stage. Multi-camera images were acquired using a standard 640 × 480, black/white CCD video camera (XC-75, Sony, Tokyo, Japan). The relative spectral response of the camera ranged from 400 nm (0.5) to 1000 nm, reaching its maximum (1) at 500 nm (Sony). Images were acquired according to the near-baseline approach (see e.g. Hartley and Zisserman 2004) with a small parallel shift (the so-called stereo baseline) of the camera position to the distance of the object (parallel shift: distance to object = 1 : 100). For small objects such as leaves, this resulted in a parallel shift of a few millimeters only, prohibiting the use of separate cameras. We thus used a computer controlled moving stage (VTM80, OWIS, Stauffen, Germany) allowing high accuracy camera movements (repetition error < 1 μm) via a step motor. Images could be acquired within a few seconds, which is necessary to ensure that the object does not move during the measurement. If fast motions e.g. due to wind are an issue, multiple synchronized cameras should be used instead of a single one on a moving stage (Biskup et al. 2007). However, with two cameras, a near-baseline setup can only be achieved when the working distance is sufficiently high, depending on the size of the camera bodies. To compensate for noise of the CCD chip, 5–20 images were averaged with a frame rate of 25Hz.

Physiological performance and structure of plants adapt to environmental conditions and e.g. leaves move according to direction and intensity of light. Thus, measurements of plant surfaces and structure often involve natural conditions with day/night changes of light or fluc-

tuating light conditions that are common in the field (Rascher and Nedbal 2006). This may pose special challenge for time series of optical flow estimates for which measuring light conditions have to be kept constant. For laboratory measurements (Fig. 1 and 2) we illuminated the plants with two light sources, (*i*) photosynthetic active light ($\lambda < 800$ nm) and (*ii*) infrared (IR) LED panel ($\lambda = 940$ nm; Conrad Elektronik, Hirschau, Germany). An IR long-pass filter ($\lambda > 940$ nm; Schott, Mainz, Germany) was used with the camera lens. This set-up allows separation of surface measurements under constant illumination in the near infrared, which is physiologically not effective for plants, and changes in photosynthetically active illumination, which is necessary to apply e.g. day/night cycles.

By restricting the imaged spectrum to a narrow band and by applying artificial illumination, the influence of variations in brightness of natural illumination was reduced. This is especially important when acquiring image sequences for growth measurements (Walter and Schurr 2005). However, natural intensity variations during acquisition of one image set was consistently low and thus did not cause problems with optical flow estimation. Long-term intensity variations can be allowed for by explicit modeling (Haussecker and Fleet 2001, Schuchert and Scharr 2007).

2.3 Algorithm

Optical flow is a concept for measuring motion in image sequences. The assumption used to do this is that intensity values of surface elements projected onto the camera sensor do not change (much) from one image to the next – the so-called brightness constancy assumption. Temporal brightness changes at a given pixel position are assumed to arise from motion of imaged objects, or from camera motion. Interpreting the acquired image sequence as a continuous spatio-temporal volume, allows for the calculation of derivatives in this data set. For each point, the spatio-temporal direction in which intensities change least is the direction where the intensity point is assumed to have moved. Such a moving intensity point produces a linear structure of constant brightness in the spatio-temporal volume if moving at constant velocity, or a bent structure if it accelerates or decelerates. Fulfilling the brightness constancy assumption formally means that the total derivative of the acquired intensity I has to be zero or $\mathrm{d}I(x,y,t)/\mathrm{d}t = 0$, where x, y, and t denote the spatial and temporal image (pixel) coordinates. Applying the chain rule we get:

$$\frac{\partial I}{\partial x}\frac{dx}{dt} + \frac{\partial I}{\partial y}\frac{dy}{dt} + \frac{\partial I}{\partial t} = 0 \qquad [1]$$

The partial derivatives of intensity I are calculated directly from the image data using suitable convolution kernels (derivative filters; comp. Scharr 2005). The remaining total derivatives of the spatial coordinates are the sought-for components of the displacement vector $\mathbf{u} = (u_x, u_y) = (\mathrm{d}x/\mathrm{d}t, \mathrm{d}y/\mathrm{d}t)$. They are calculated via the so-called structure tensor technique (Bigün and Granlund 1987, Haussecker and Fleet 2001), a local total least squares (TLS) estimator. The TLS data modeling technique (also termed orthogonal regression) bears the advantage over ordinary least squares in that it assumes observational errors in both the dependent and the independent variables, which is more appropriate.

In order to relate multi-image optical flow with surface reconstruction, we need to know how a surface point is projected into an image and how this projected position changes with

time, i.e. camera position, in the acquired sequence. Using a high-quality, low-distortion lens, or assuming an internally calibrated camera, we can correct for optical distortions, and are allowed to use a simple pinhole camera model. The only parameter varied from image to image is the horizontal camera position $X_c = V_x\, t$ where t is the time in the image sequence or, better, the image index and V_x is the image to image camera position distance. A 3-D surface point $(X, Y, Z)^T$ is projected to an image point $(x, y)^T$ using a pinhole at $(X_c, 0, 0)^T$ and focal length f (i.e. distance between image sensor and pinhole) by

$$\begin{pmatrix} x \\ y \end{pmatrix} = \frac{f}{Z} \begin{pmatrix} X - V_x t \\ Y \end{pmatrix}. \qquad [2]$$

Consequently, the image to image position change of an image point $(x,y)^T$ due to the camera shift is the derivative with respect to t or

$$\frac{dx}{dt} = -\frac{f}{Z} V_x \quad \text{and} \quad \frac{dy}{dt} = 0\,. \qquad [3]$$

We see that the y component u_y of the optical flow vanishes, and we can calculate depth Z from its x-component u_x via $Z = -f\, V_x / u_x$.

2.4 Accuracy

The accuracy of the proposed method has been investigated in Scharr (2006). Tests using data with available ground truth showed that *systematic* errors of optical flow estimation, i. e. in u_x and therefore also for depth Z, using 5 camera positions are well below 0.03 % (0.85 % for 3 positions) when no noise is present. This error can be further decreased when more images are used. This shows that the method gives very accurate results under optimal conditions. However, for less optimal conditions (e.g. noise, reflections, poorly structured surfaces), the error increases. For a signal-to-noise ratio of 0.025, which one usually gets with consumer grade cameras under challenging but still realistic light conditions, the error rises to 0.2 % (1 % for 3 cameras). This accuracy is achieved as long as the working depth interval and camera shifts are chosen such that the x-component u_x of the optical flow is in the range of 0.2 to 1 pixel, and sufficient structure is present in the data. If structure information is not sufficient (so-called "aperture problem"), or the optical flow assumption is not well fulfilled, the estimation breaks down. Fortunately, using TLS estimation, this break-down can be detected. When the aperture problem occurs, the error in the estimated disparity becomes very large. It can be calculated e.g. via local estimation of the Cramer-Rao lower bound (Kay 1993) on the error covariance matrix (Nestares et al. 2000). When the optical flow assumption does not hold, the so-called model error becomes large. It is calculated via the residual of the numerical estimation process (Hartley and Zisserman, 2004). The model error, as well as the lower bound on the variance of the estimated parameters, is directly linked to the variance of the noise in the data. Rejecting high error areas by thresholding model error and covariance estimate suppresses outliers reliably.

2.5 Performance

Optical-flow-based techniques tend to be more demanding in terms of computing power compared to correlation-based stereo algorithms. However, optical-flow-based techniques lend themselves to parallelization on computer clusters (e.g. KOHLBERGER et al. 2003) or massive parallelization on graphics cards, allowing real-time computation (e.g. STRZODKA and GARBE 2004). In practice, computing time is not limiting for most applications, and all the case studies in this communication were processed on standard desktop computers without parallelization.

3. Surface Reconstruction of Single Leaves and Small Plants

Figure 1 shows 3-D reconstructions of *Arabidopsis thaliana* (L.) Heynh. obtained with different pre-treatments of the plant. The 3-D reconstruction of the untreated plant (Fig. 1*A*, *B*) shows notable depth variations and holes due to insufficient scene contrast (see also cross-section). Enhancing contrast by either spray marking the plant (Fig. 1*C*, *D*) or illuminating it with structured light (Fig. 1*E*, *F*) profoundly enhances the quality of reconstruction (compare height profiles in Fig. 1). Depending on the illumination angle used for the structured light projector, shadowed regions may occur in which no reconstruction is possible. To avoid interference with light signaling, an IR light source should be used. Another way to improve reconstruction quality is to operate at higher resolutions, at which, e.g., hairs and wrinkles in the cuticle may provide additional contrast.

For practical reasons, spray marking may be the easiest method to enhance contrast, and thus we tested this straight forward method on a variety of different plant organs (Fig. 2). With all leaves and the cactus cladode tested, spray marking provided sufficient contrast for reliable 3-D surface reconstruction. Even small surface structures such as the spines on the *Opuntia* cladode were reconstructed with high accuracy (Fig. 2*A*, *B*). 3-D reconstruction was best when size of the marks (color dots) were comparably small, providing fine contrast on the leaf surface (see better 3-D reconstruction in Fig. 2*E*, *F*; small dots versus Fig. 2*C*, *D*; large dots).

4. Surface Reconstruction of a Rainforest Canopy

4.1 Test Case: Biosphere 2 Laboratory

Encouraged by the success on the leaf and small plant level, the small baseline approach was applied to reconstruct the three-dimensional surface of the tropical rainforest of Biosphere 2 Laboratory. The enclosed and controllable tropical rainforest mesocosm of Columbia University's Biosphere 2 Laboratory is an experimental model system which is encased in a glass and metal shell controlled for temperature, humidity, atmospheric gas composition, and precipitation (for details see LIN et al. 1999, RASCHER et al. 2004, WALTER and LAMBRECHT 2004). It was used to test the potential of the small baseline approach to reconstruct the outer surface of an extended canopy. The tropical rainforest mesocosm within Biosphere 2 Laboratory was not intended to represent any particular natural rainforest. However, its plant species composition, leaf area index (LAI: 4–5), canopy height (15 m), and other factors (LEIGH 1999, LEIGH et al. 1999) are similar to natural rainforests. The mesocosm has a total projected

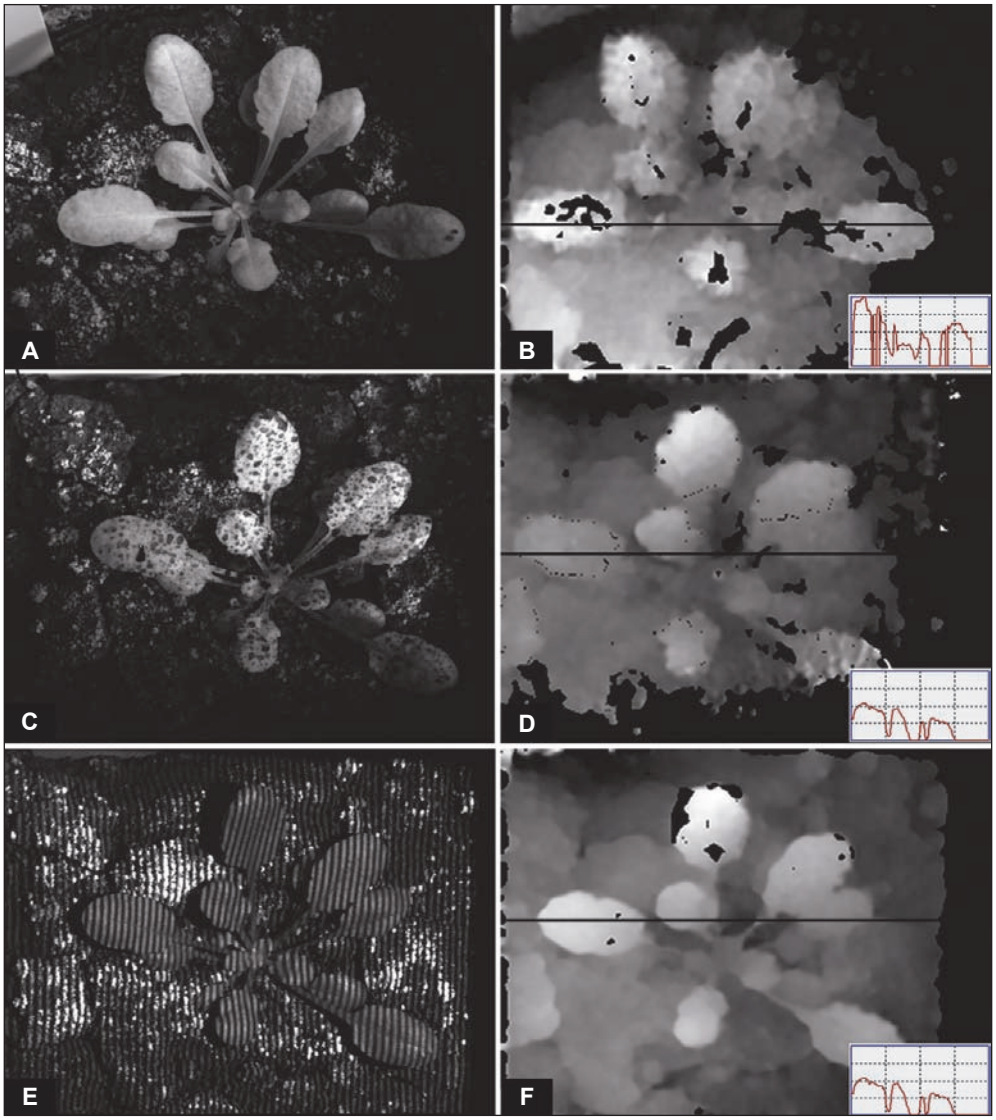

Fig. 1 3-D reconstruction of Arabidopsis thaliana (l.) Heinh. achieved with different pretreatments of the plant. (*A*, *B*) No pre-treatment. (*C*, *D*) Spray-marked. (*E*, *F*) Illuminated with structured light. Left column: input image; right column: disparity map, grey values code for depth and areas of insufficient reconstruction were masked out (black patches). Insets: height profiles along the line shown in right column.

area of 1940 m^2 and an atmospheric volume of 26,700 m^3. The rainforest was planted with a mixture of some 410 species from humid rainforests from the old world and neotropics (Leigh 1999, Leigh et al. 1999). At the time of the measurements 110 species were remaining, composing an enclosed canopy of 15 m height, with the highest tree (*Ceiba pentandra* L.) reaching 25 m.

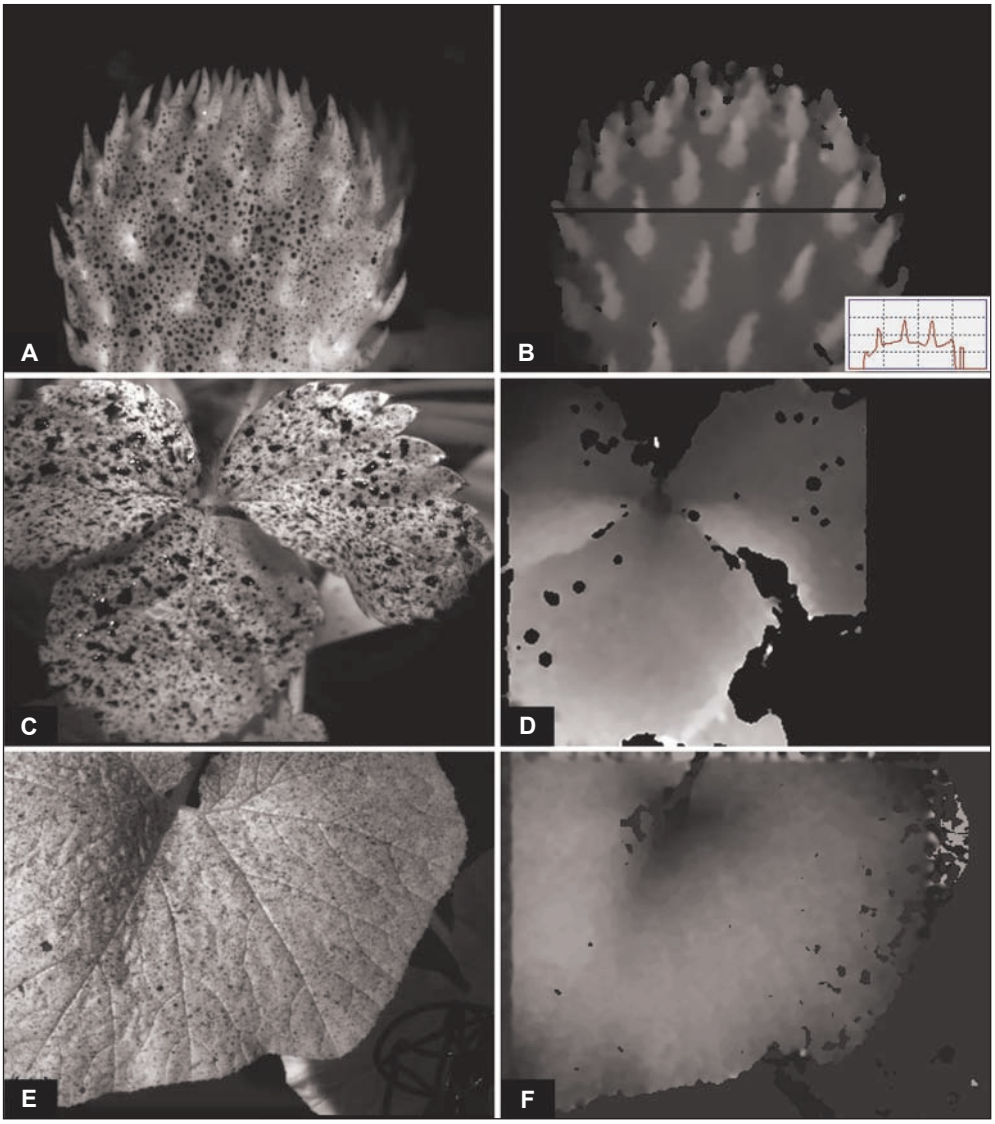

Fig. 2 Examples of 3-D reconstructions of plant organs pre-treated by spray marking. (*A*, *B*) *Opuntia phaeacantha* Engelm. cladodes; (*C*, *D*) *Fragaria* x *ananassa* Duch. leaf with comparably large spray dots. (*E*, *F*) *Cucurbita pepo* L. leaf with comparably fine dots. From left to right: column 1: input image; column 2: disparity map. Insets: height profile along the line shown in (*B*).

Stereo images of canopy elements of 0.4 and 2 m diameter were acquired from the space frame of Biosphere 2 Laboratory under natural illumination (Fig. 3, Fig. 4*A*, *B*). Single leaves and illumination differences resulted in small scale contrast, which was further increased by a high pass Gaussian filter. The small baseline algorithm yielded good depth information for canopy patches, which were well illuminated (Fig. 3 for two representative examples). Insuf-

ficient stability was detected in dark areas, which corresponded to canopy leaves of lower canopy layers. Those dark areas were readily masked out in the depth images of the canopy (Fig. 3*B*, *D*).

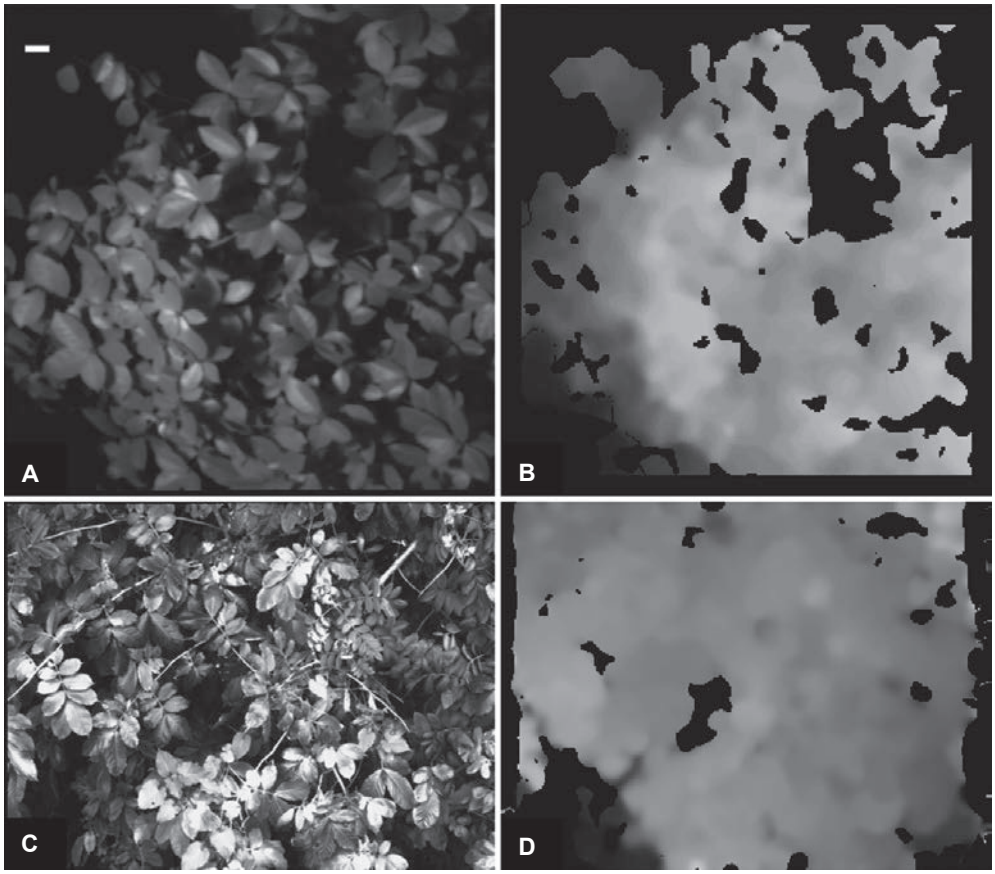

Fig. 3 Surface reconstruction of two medium sized canopy elements. Upper panels: *Ficus benjamini* L., lower panels: *Inga* cf. *sapindoides* Willd. (*A*, *B*): original 2-D image of the canopies imaged from a distance of 2–8 meters. White bar indicates 0.1 m. (*B*, *D*): distances to the camera as encoded in gray values. Pixels which did not yield a satisfying reconstruction were masked out (black patches).

Different distances between canopy and camera resulted in different spatial resolution for each image. Moreover, various shading effects occurred induced by the encasing steel structure or shading branches above the scene resulting in a realistic forest-plot situation in which light conditions are likely to be non homogeneous and patchy. Error classification of canopy element depth reconstruction is shown in the bottom row of Figure 4, where the black and white areas indicate patches for which depth could not be calculated, while the grey areas indicate that satisfying information was available for surface reconstruction. Overall, good results were obtained in most image regions for the three-dimensional surface reconstruction – regardless of the size and shape of leaves within the image (see e.g. the star like leaves

in Fig. 4*C*). Insufficient information for depth reconstruction was primarily obtained in image regions that were characterized by great brightness heterogeneity, induced by e.g. shading (see e.g. diagonal shades in Fig. 4*A* and *D*).

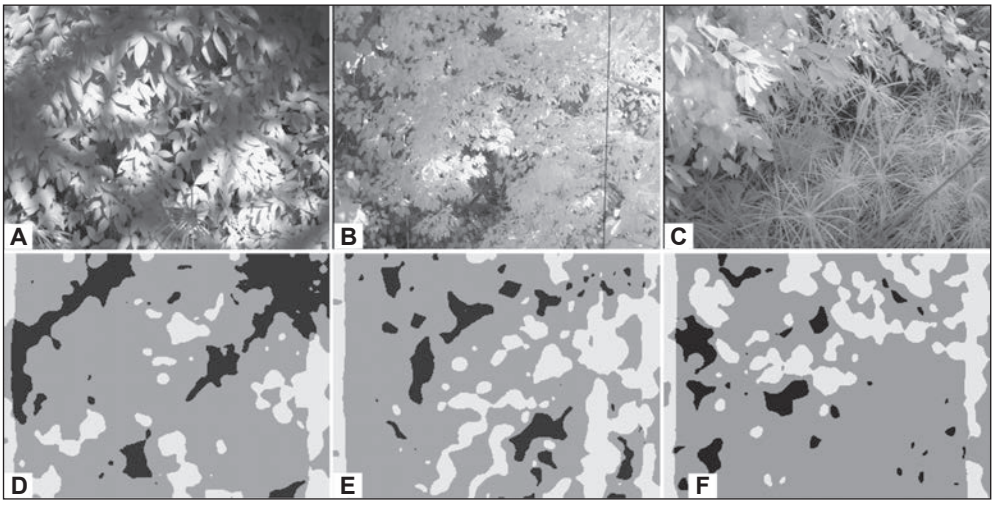

Fig. 4 Quality of 3-D information on canopy elements of the tropical mesocosm in Biosphere 2. Upper row: images of different canopy types, which were found in different distance to the camera set-up, resulting in different spatial resolution. Lower row: Images encoding outlier classification of the depth reconstruction. In black areas, the lower bound on the variance is too high and white areas indicate patches where the model error is too high. In the grey areas, sufficient information was available for surface reconstruction.

4.2 Assembly of Single Canopy Elements to Full Canopy Reconstruction

For surface reconstruction of the full rainforest canopy of Biosphere 2 Laboratory, the moving stage was mounted on a two-axis, computer controllable robot arm (model HS-310P, Vinten TSM Inc., New York, USA). This rigid computer arm allowed for precise pointing of the camera along the horizontal and vertical axis, i.e. for panning and tilting of the camera (Fig. 5*B*). The whole set-up, including a control computer, was mounted at the east wall within the space frame of the tropical rainforest mesocosm of Biosphere 2 Laboratory, 15 m above ground, providing a good view on the major part of the rainforest canopy (Fig. 5*A*). The stereo camera set-up itself was mounted on a 1 m pole reaching into the free air space enabling a 180° view in horizontal and vertical direction. The camera position was about at mean height of the canopy with the big *Ceiba pentandra* tree and some vegetation at a nearby hill reaching higher. The center of the rainforest canopy is bowl-shaped and thus was clearly lower than the camera stand. Because of the highly varying distance between canopy surface and camera (3–40 m), single images varied from showing a few leaves only to showing canopy elements of several meters dimension.

We used 3 parallel camera positions, each with a 5 cm parallel shift for stereo reconstruction. At all scales stereo reconstruction yielded good results. The whole canopy was imaged using 140 stereo images, taken at viewing directions with equidistant pan- and tilt-angles. Images were captured without overlap in the horizontal plane (Fig. 5*C*). With moving the

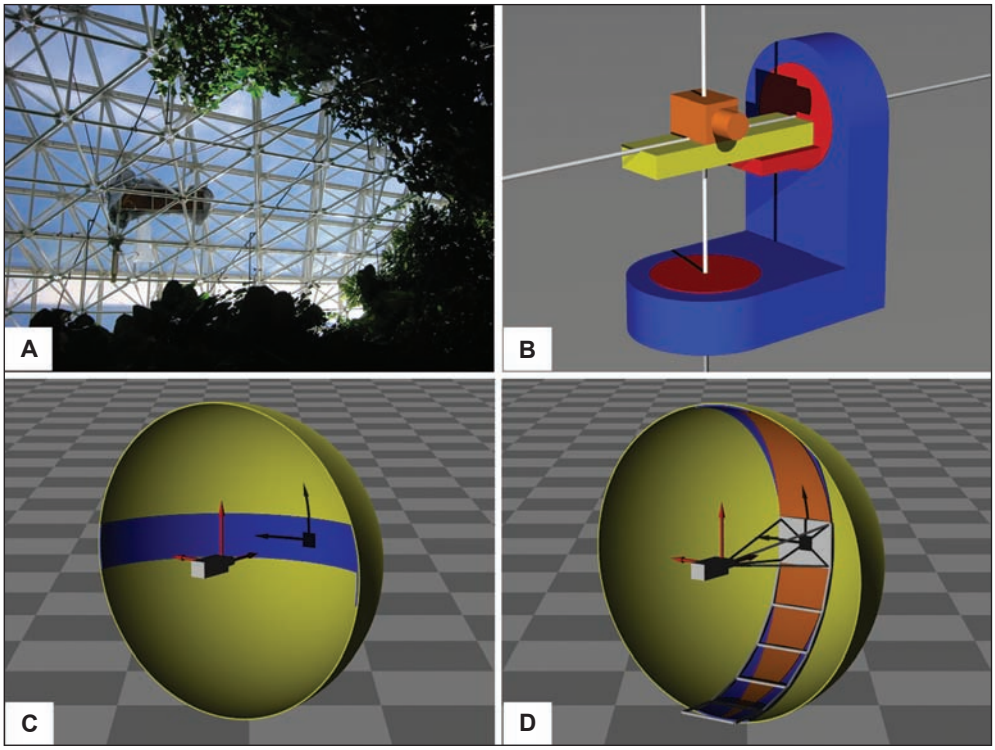

Fig. 5 Set-up and procedure for the assembly of single 3-D canopy elements the rainforest canopy of Biosphere 2 Center. (*A*): Picture of the stereo camera setup, mounted in the space frame of Biosphere 2 rainforest. (*B*): Schematic drawing of the controllable robot head, allowing horizontal and vertical scanning. (*C*, *D*): Schematic representation of horizontal and vertical camera movements that allow scanning the whole rainforest canopy using several adjacent images. Overlaps (see *D*) were eliminated in post-processing.

camera off the horizontal plane single, images increasingly overlapped and had to be cut to their non-overlapping regions (Fig. 5*C*). 122 stereo images were finally used to reconstruct the full canopy of the tropical mesocosm.

3-D points calculated by the proposed approach were first obtained in the coordinate frame of the respective camera, i.e. a coordinate frame with its origin at the camera projection center and depth direction being the viewing direction. The 3-D point coordinates were transformed into a common world coordinate frame (with the central camera at the origin, its x and y axis aligned with the world X and Y axes) using external camera parameters (rotation and translation) known from the robot position, forming the reconstructed canopy. World coordinates were calculated for pixels with high confidence values only (grey regions in Fig. 4, lower row) and used for further processing. In our case study 3.5 Million pixels yielded reliable information to calculate world coordinates. From there on two alternative procedures were pursued. (*i*) All available pixels were combined to a single map, representing the three-dimensional surface of the tropical mesocosm of Biosphere 2 Laboratory with a resolution of few centimeters, where points closer to the camera were reconstructed more accurately (Fig. 6*D*). This resulted in a very dense surface mesh, which, however, still did not yield single leaf

orientation and which had the disadvantage of different spacing between the single points. (*ii*) Every reconstructed depth image was divided in 4 quadrants (any other division may be used for different spatial resolution), and the average world coordinate for each quadrant was calculated. This resulted in a lower number of surface points (in our case 488) which was easier to handle and display. Since points were spaced by constant angles from each other, single points could be used to easily calculate a surface mesh (Fig. 6*E*).

5. Discussion

The results presented here show that it is possible to reconstruct three-dimensional surfaces of a wide range of plant structures from single leaves to extended plant canopies with a small baseline, stereoscopic approach. This approach may prove less costly, faster and more flexible than LIDAR approaches. Compared to other methods, such as manual, semi-automatic three-dimensional digitizing (Sonohat et al. 2002, Sinoquet et al. 2005), it provides a high degree of automation, thereby allowing higher experimental throughput. Hence, it is ideally suited to monitor temporal changes of structural canopy characteristics and to improve e.g. models of canopy light interception. Light interception models are an important requirement to understand the vegetation response in the context of agriculture or global climate change. The accuracy of light interception models is determined by the accuracy of three-dimensional measurements of vegetation canopies that have to be investigated at scales relevant for the model. The three-dimensional structure of a plant canopy, which greatly affects light intensity within the canopy as well as other microclimatic conditions is currently recognized as a crucial and long neglected variable, which greatly affects the performance of plants in their natural environment and in ecosystem exchange processes and which produces substantial uncertainties in scaling leaf-level knowledge to the canopy and ecosystem (Rascher et al. 2004).

This paves the way to apply this approach to airborne platforms where the movement of the aircraft can provide the different baselines of adjacent images. Thus far, structure of plant ecosystems cannot sufficiently be quantified and information such as leaf angle distribution, fraction cover or canopy roughness are products that greatly would contribute to link remote sensing data to vegetation models. Additionally information about canopy structure can greatly benefit optical remote sensing. The Photochemical Reflectance Index (PRI) for example is greatly influenced by BRDF effects of varying leaf orientation (Barton and North 2001). Leaves of natural canopies greatly depend on species, are influenced by diurnal changes and environmental factors (Biskup et al. 2007) and currently hamper estimates of photosynthetic efficiency using the PRI and other optical approaches.

Rapid and flexible analysis of the three-dimensional shape of a vegetation canopy might also provide a novel tool for growth analyses of crops or natural vegetation. The increase in height and compactness of a canopy can be extracted from two successive maps, to allow monitoring the effect of altered ecofactors determining growth (temperature, salt stress, etc.) and allowing to rapidly selecting plants for agricultural breeding purposes.

We thus argue that this stereo approach has the potential to serve as a serious alternative or complement (Baltsavias 1999) to LIDAR methods, especially when sub-leaf resolution is needed, e.g. to determine leaf angle distribution. Our approach, being an optical technique, can provide instantaneous snapshots of moving objects such as canopies, facilitates object

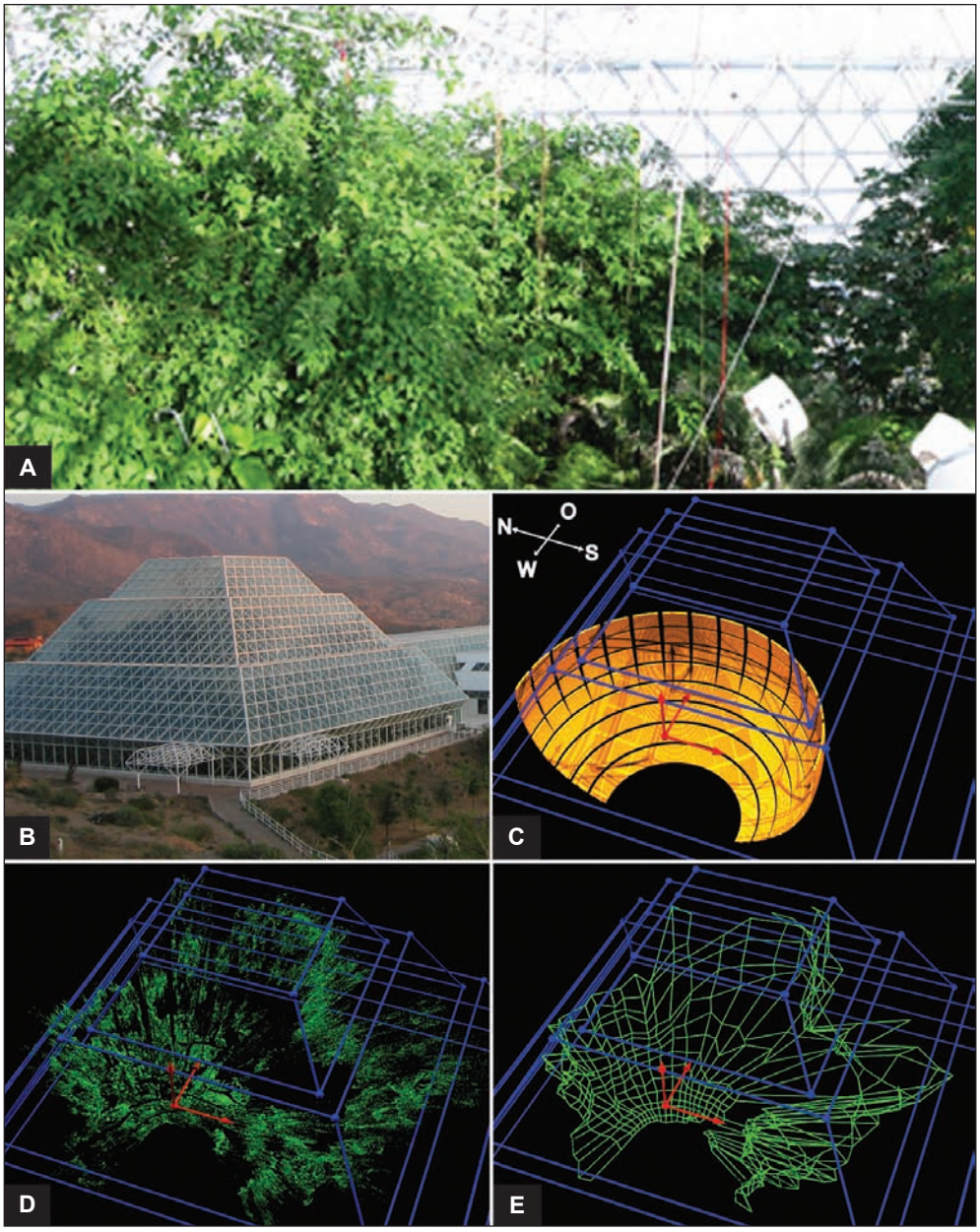

Fig. 6 Reconstruction of the surface structure of tropical rainforest mesocosm from the single images of the canopy element. (*A*): View of the tropical canopy of Biosphere 2 mesocosm, showing the complex three-dimensional structure and heterogeneity of different species having different morphology. (*B*) Outside view of Biosphere 2 mesocosm. (*C*): Scheme of how 122 single canopy elements were arranged to represent the whole canopy. (*D*): 3-D surface information of the canopy using all successfully reconstructed points (3.5 Million Pixels resulting from 122 single images were successfully reconstructed; for this presentation only 350 000 are plotted). (*E*): Reduction of the raw-data to a manageable resolution. In this example each canopy element was used to reconstruct 4 points. Averaging yielded a conceivable mesh representing the outer surface of the canopy.

recognition and allows segmentation of individual leaves or plant organs (Biskup et al. 2007) and thus also has potential to be beneficially combined with LIDAR approaches. The specific strength of our approach may be in long term ecological monitoring set-ups, where continuous measurements can provide data about structural changes in plant ecosystems. Yet, on the longer perspective also airborne approaches may be feasible to provide additional and crucial information for optical sensors. The algorithms used in this communication are freely available and parameters can easily be adjusted to fit the special needs.

Acknowledgements

B. Biskup acknowledges support of his PhD work by the Heinrich-Heine University of Düsseldorf, Germany. H. Scharr and R. Küsters were supported by the Deutsche Forschungsgemeinschaft (SPP1114, LOCOMOTOR). We greatly thank Barry Osmond, whose support as director of Biosphere 2 Laboratory made this work possible. We also thank the maintenance crew of Biosphere 2 Laboratory, especially Allen Wright and Robert Arrington for climbing support.

References

Baltsavias, E. P.: A comparison between photogrammetry and laser scanning. ISPRS J. Photogramm. Remote Sens. *54*, 83–94 (1999)

Barton, C. V. M., and North, P. R. J.: Remote sensing of canopy light use efficiency using the photochemical reflectance index – Model and sensitivity analysis. Remote Sens. Environ. *78*, 264–273 (2001)

Bigün, J., and Granlund, G.: Optimal orientation detection of linear symmetry. In: Proceedings of the First International Conference on Computer Vision ICCV'87; pp. 433–438. London: IEEE 1987

Biskup, B., Scharr, H., Schurr, U., and Rascher, U.: A stereo imaging system for measuring structural parameters of plant canopies. Plant Cell Environ. *30*, 1299–1308 (2007)

Brown, M. Z., Burschka, D., and Hager, G. D.: Advances in computational stereo. IEEE Trans. Pattern Anal. Mach. Intell. *25*, 993–1008 (2003)

Campbell, G. S., and Norman, J. M.: The description and measurement of plant canopy structure. In: Russell, G., Marshall, B., and Jarvis, P. (Eds.): Plant Canopies: Their Growth, Form, and Function; pp. 1–19. Cambridge: University Press 1989

Hartley, R., and Zisserman, A.: Multiple View Geometry in Computer Vision. Cambridge: University Press 2004

Haussecker, H., and Fleet, D. J.: Computing optical flow with physical models of brightness variation. IEEE Trans. Pattern Anal. Mach. Intell. *23*, 661–673 (2001)

Hirschmüller, H., Scholten, F., and Hirzinger, G.: Stereo vision based reconstruction of huge urban areas from an airborne pushbroom camera (HRSC). In: Lecture Notes in Computer Science: Pattern Recognition, Proceedings of the 27th DAGM Symposium, 30 August – 2 September 2005, Vienna, Austria, *3663*, 58–66. Heidelberg: Springer 2005

Kay, S. M.: Fundamentals of Statistical Signal Processing. Vol. 1: Estimation Theory. New Jersey: Prentice-Hall 1993

Kohlberger, T., Schnörr, C., Bruhn, A., and Weickert, J.: Domain decomposition for parallel variational optic flow computation. In: Michaelis, B., and Krell, G. (Eds.): Proceedings of DAGM Symposium 2003, Lecture Notes in Computer Science; pp. 196–202. Berlin: Springer 2003

Leigh, L. S.: The Basis for Rainforest Diversity and Biosphere 2. PhD dissertation. University of Florida, Gainsville, FL, USA 1999

Leigh, L. S., Burgess, T., Marino, B. D. V., and Wei, Y. D.: Tropical rainforest biome of Biosphere 2: structure, composition and results of first two years of operation. Ecol. Eng. *13*, 65–94 (1999)

Lefsky, M. A., Cohen, W. A., Parker, G. G., and Harding, D. J.: Lidar remote sensing for ecosystem studies. BioScience *52*, 19–30 (2002)

Liao, W. H., Aggarwal, S. J., and Aggarwal, J. K.: The reconstruction of dynamic 3-D structure of biological objects using stereo microscope images. Mach. Vision Appl. *9*, 166–178 (1997)

Lin, G. H., Adams, J., Farnsworth, B., Wei, Y. D., Marino, B. D. V., and Berry, J. A.: Ecosystem carbon exchange in two terrestrial ecosystem mesocosms under different atmospheric CO_2 concentrations. Oecologia *119*, 97–108 (1999)

Maltamo, M., Packalen, P., Yu, X., Eerikainen, K., Hyyppa, J., and Pitkanen, J.: Identifying and quantifying structural characteristics of heterogeneous boreal forests using laser scanner data. Forest Ecol. Manag. *216*, 41–50 (2005)

Nestares, O., Fleet, D., and Heeger, D.: Likelihood functions and confidence bounds or total-least-squares problems. IEEE Conference on Computer Vision and Pattern Recognition *3*, 523–530 (2000)

Niinemets, Ü., Lukjanova, A., Sparrow, A. D., and Turnbull, M. H.: Light-acclimation of cladode photosynthetic potentials in *Casuarina glauca*: trade-offs between physiological and structural investments. Funct. Plant Biol. *32*, 571–582 (2005)

Omasa, K.: 3-D color video microscopy. In: Häder, D. P. (Ed.): Image Analysis: Methods and Applications. 2nd edn.; pp. 257–273. Boca Raton, FL: CRC Press 2000

Omasa, K., Hosoi, F., and Konishi, A.: 3d lidar imaging for detecting and understanding plant responses and canopy structure. J. Exp. Bot. *58*, 881–898 (2007)

Papenberg, N., Bruhn, A., Brox, A., Didas, S., and Weickert, S.: Highly accurate optic flow computation with theoretically justified warping. Int. J. Comput. Vision *67*, 141–158 (2006)

Patenaude, G., Milne, R., and Dawson, T. P.: Synthesis of remote sensing approaches for forest carbon estimation: reporting to the Kyoto Protocol. Environ. Sci. Policy *8*, 161–178 (2005)

Rakocevic, M., Sinoquet, H., Christophe, A., and Varlet-Grancher, C.: Assessing the geometric structure of a white clover (*Trifolium repens* L.) canopy using 3-D digitising. Ann. Bot. *86*, 519–526 (2000)

Rascher, U., Bobich, E. G., Lin, G. H., Walter, A., Morris, T., Naumann, M., Nichol, C. J., Pierce, D., Bil, K., Kudeyarov, V., and Berry, J. A.: Functional diversity of photosynthesis during drought in a model tropical rainforest – the contributions of leaf area, photosynthetic electron transport and stomatal conductance to reduction in net ecosystem carbon exchange. Plant Cell Environ. *27*, 1239–1256 (2004)

Rascher, U., and Nedbal, L.: Dynamics of photosynthesis in fluctuating light. Curr. Opin. Plant Biol. *9*, 671–678 (2006)

Scharr, H.: Optimal filters for extended optical flow. In: Complex Motion, 1. Int. Workshop, Günzburg, Oct. 2004, Lecture Notes in Computer Science *3417*. Berlin: Springer 2005

Scharr, H.: Towards a multi-camera generalization of brightness constancy. In: Complex Motion, 1. Int. Workshop, Günzburg, Oct. 2004, Lect. Notes Computer Science *3417*. Berlin: Springer 2006

Scharstein, D., and Szeliski, R.: A taxonomy and evaluation of dense two-frame stereo correspondence algorithms. Int. J. Comput. Vision *47*, 7–42 (2002)

Schuchert, T., and Scharr, H.: Simultaneous estimation of surface motion, depth and slopes under changing illumination. In: Pattern Recognition: Proceedings of the 29th DAGM Symposium, Heidelberg, Germany, Lecture Notes in Computer Science *4713*. Berlin: Springer 2007

Schurr, U., Walter, A., and Rascher, U.: Functional dynamics of plant growth and photosynthesis – from steady-state to dynamics – from homogeneity to heterogeneity. Plant Cell Environ. *29*, 340–352 (2006)

Shi, J., and Tomasi, C.: Good features to track. In: IEEE Computer Society Conference on Computer Vision and Pattern Recognition (CVPR'94); pp. 593–600. Seattle: IEEE Computer Society 1994

Sinoquet, H., and Rivet, P.: Measurement and visualisation of the architecture of an adult tree based on a three-dimensional digitising device. Trees-Struct. Funct. *11*, 265–270 (1997)

Sinoquet, H., Sonohat, G., Phattaralerphong, J., and Godin, C.: Foliage randomness and light interception in 3-D digitized trees: an analysis from multiscale discretization of the canopy. Plant Cell Environ. *28*, 1158–1170 (2005)

Sinoquet, H., Thanisawanyangkura, S., Mabrouk, H., and Kasemsap, P.: Characterization of the light environment in canopies using 3D digitising and image processing. Ann. Bot. *82*, 203–212 (1998)

Slesareva, N., Bruhn, A., and Weickert, J.: Optic flow goes stereo: a variational method for estimating discontinuity-preserving dense disparity maps. In: Kropatsch, W., Sablatnig, R., and Hanbury, A. (Eds.): Pattern Recognition. 27th DAGM Symposium, Proceedings 33–40. Berlin: Springer 2005

Sonohat, G., Sinoquet, H. C., Varlet-Grancher, C., Rakocevic, M., Jacquet, A., Simon, J. C., and Adam, B.: Leaf dispersion and light partitioning in three-dimensionally digitized tall fescue-white clover mixtures. Plant Cell Environ. *25*, 529–538 (2002)

Strzodka, R., and Garbe, C.: Real-time motion estimation and visualization on graphics cards. In: Proceedings IEEE Visualization 2004. Washington: IEEE Computer Society 2004

Turner, W., Spector, S., Gardiner, N., Fladeland, M., Sterling, E., and Steininger, M.: Remote sensing for biodiversity science and conservation. Trends Ecol. Evol. *18*, 306–314 (2003)

Walter, A., and Lambrecht, S. C.: Biosphere 2 Center as a unique tool for environmental studies. J. Environ. Monitor. *6*, 267–277 (2004)

Walter, A., and Schurr, U.: Dynamics of leaf and root growth – endogenous control versus environmental impact. Ann. Bot. *95*, 891–900 (2005)

Dr. Uwe Rascher
Institute of Chemistry and Dynamics
of the Geosphere ICG-III: Phytosphere
Forschungszentrum Jülich
52425 Jülich
Germany
Phone: +49 2461 612638
Fax: +49 2461 612492
E-Mail: u.rascher@fz-juelich.de

Natur und Migration

Vorträge anlässlich der Jahresversammlung vom 5. bis 7. Oktober 2007
zu Halle (Saale)

Nova Acta Leopoldina N. F., Bd. *97*, Nr. 358
Herausgegeben von Harald ZUR HAUSEN (Heidelberg)
(2008, 225 Seiten, 81 Abbildungen, 2 Tabellen, 29,95 Euro,
ISBN: 978-3-8047-2500-3)

„Natur und Migration" – assoziiert sehr verschiedenartige Phänomene, die sich durch Wanderungsprozesse auszeichnen. In diesem Band wurden besonders interessante Gebiete ausgewählt, u. a. Migration und Seuchen, Reisen und Epidemien in einer globalisierten Welt, der Vogelzug, aber auch die Migration geologischer Fluide, die Elektronenmigration in Halbleitern, die Migration als treibende Kraft in der Organogenese, die Biophysik der Zellbewegungen, die Migration von Tumorzellen, Migration als Phänomen in der Neurobiologie oder die Migration wissenschaftlicher Ideen. Besondere Akzente setzen die Themen „Diversität als neues Paradigma für Integration?" und „Vorspiel der Globalisierung. Die Emigration deutscher Wissenschaftler 1933 bis 1945".
Die Beiträge sind von herausragenden Experten der jeweiligen Gebiete, u. a. durch die Leopoldina-Mitglieder Markus AFFOLTER, Lorraine DASTON, Wolfgang FRÜHWALD, Michael FROTSCHER, Jörg HACKER, Hans KEPPLER und Otmar WIESTLER, in anspruchsvoller, aber durchaus gut verständlicher Form verfasst.

Wissenschaftliche Verlagsgesellschaft mbH Stuttgart

Nova Acta Leopoldina NF *96*, Nr. 357, 49 – 62 (2009)

Optical Remote Sensing and Laser Induced Fluorescence Transients (LIFT) to Quantify the Spatio-Temporal Functionality of Plant Canopies

Roland Pieruschka[1, 2, 3], Uwe Rascher[2, 3], Denis Klimov[4], Zbigniew S. Kolber[4], and Joseph A. Berry[1]

With 5 Figures

Abstract

Photosynthetic light use efficiency dynamically adapts to environmental factors which leads to complex spatio-temporal variations from the leaf to the canopy level and presents many challenges for determination of photosynthesis. Here we review the results from selected remote sensing projects for their potential to quantify light use efficiency using: (*i*) the passively detected photochemical reflectance index (PRI), (*ii*) the recently developed Laser Induced Fluorescence Transient (LIFT) technique capable of remote measurement of light use efficiency in inaccessible canopies from a distance up to 50 m, and (*iii*) detection of steady state fluorescence in the Fraunhofer lines suitable for remote sensing of extended areas. This approach was recently promoted by the selection of the FLuorescence EXplorer (FLEX) mission that proposed to launch a satellite for the global monitoring of steady-state chlorophyll fluorescence in terrestrial vegetation.

Zusammenfassung

Photosynthetische Lichtausnutzung ist sehr dynamisch an die herrschenden Umweltbedingungen angepasst, was die Bestimmung der Photosynthese unter natürlichen Bedingungen zu einer Herausforderung macht. Wir präsentieren einen Überblick über ausgewählte Fernerkundungsmethoden, die das Potential haben, die photosynthetische Lichtausnutzung zu quantifizieren: (*a.*) passive Bestimmung des Photochemischen Reflexions-Indexes (PRI), (*b.*) Laser-Induzierte-Fluoreszenz-Transient (LIFT)-Technik für die Messung von Lichtausnutzungskoeffizienten in unzugänglichen Baumkronen aus einer Entfernung von bis zu 50 m und (*c.*) passive Bestimmung der Grundfluoreszenz in den Fraunhofer-Linien als eine Methode zur Messung ausgedehnter Vegetationsflächen. Diese Methode wurde im Rahmen der Fluoreszenz-EXplorer (FLEX)-Mission in die nähere Auswahl für ein satellitenunterstütztes Monitoring der Grundfluoreszenz terrestrischer Vegetation genommen.

1. Introduction

Photosynthesis Dynamically Adapts to Environmental Constrains

Photosynthesis harvests light from an often quite variable stream of photons and converts this energy to carbohydrates that ultimately fuel all plant processes and, life on earth. The

1 Carnegie Institution of Washington, Department of Global Ecology, 260 Panama Street, Stanford, CA 94305, USA.
2 Institute of Chemistry and Dynamics of the Geosphere, ICG-3: Phytosphere, Forschungszentrum Jülich GmbH, 52425 Jülich, Germany.
3 These authors contributed equally to this work.
4 Monterey Bay Aquarium Research Institute, 7700 Sandholdt Road, Moss Landing, CA 95039, USA.

efficiency of the utilization of photons used for photosynthetic electron transport and carbon fixation is highly regulated. Plants have to solve a most challenging problem in the naturally occurring fluctuating light environments: On the one hand they need to optimize their energy gain for carbon fixation; on the other hand the sensitivity of the photosystem to over-energetization requires protecting the light harvesting systems from photo-damage at high irradiances (Ort 2001). Thus, plants have evolved a variety of photochemical and non-photochemical regulation mechanisms that are either constitutively active or are activated on demand to optimize the distribution of energy to photosynthesis and to avoid over-energetization damage of metabolism (see e.g. book edited by Schulze and Caldwell 1995) as a comprehensive summary of the eco-physiological regulation of photosynthesis). The balance between photochemical charge separation and non-photochemical protection is crucial for plant survival and also greatly determines plant carbon gain and biomass production in natural ecosystems as well as in managed crops (Rascher and Nedbal 2006, Schurr et al. 2006).

Plant performance under controlled laboratory conditions is well studied and many aspects are well understood. However, the transition of this finding into natural heterogeneous environment proves difficult but is essential for carbon and climate models. Leaf level chlorophyll fluorescence measurements are widely used to quantify photosynthesis, and the pulse amplitude modulated (PAM) approach is the most common technique deployed under natural conditions (Maxwell and Johnson 2000, Schreiber et al. 1995). However, limited accessibility of many canopies and application of saturating pulses over the extended canopy remains impractical. To overcome these constraints a Laser Induced Fluorescence Transient (LIFT) technique for remote measurement of chlorophyll fluorescence has been developed and successfully applied in Biosphere 2 Laboratories (Ananyev et al. 2005, Kolber et al. 2005). Here we present an extensive test of this technique under laboratory conditions and compare the results with gas exchange as a gold standard. Two case studies also represent the applicability of the LIFT approach to monitor spatial and temporal heterogeneity.

The Photochemical Reflectance Index (PRI) was developed to serve as an estimate of photosynthetic light use efficiency. This normalized difference reflectance index uses two wavebands: 531 nm, which is correlated with the degree of non-photochemical energy dissipation, and 570 nm, which serves as a reference waveband (Gamon et al. 1992). PRI has been used in a variety of case studies and positively correlates with photosynthetic efficiency and has been successfully used to detect changes in photosynthetic efficiency at the leaf level (see Rascher et al. 2007 for an overview of the literature). However, PRI values vary considerably between species with the same photosynthetic capacity (Guo and Trotter 2004). Additionally, the PRI is significantly affected by the direction of incoming sunlight as well as by the geometry of the leaf and the detector (Barton and North 2001). As natural canopies are an assembly of differently oriented leaves which variably change their orientation during plant development and as a response to environmental conditions, canopy measurements of PRI often failed to quantify photosynthetic efficiency (Methy 2000) or were extensively affected by seasonal changes in canopy structure (Filella et al. 2004).

2. Material and Methods

2.1 SoyFACE Facility

The hyperspectral reflectance measurements were conducted in 2004 in a 16 ha soybean (*Glycine max*) field at the Soybean Free Air Concentration Enrichment (SoyFACE) facility in Champaign, Illinois, USA (40°02' N, 88°14' W, 228 m a. s. l.). The facility operation procedures and crop management practices have been described in detail previously (Rogers et al. 2004). The experiment contained four blocks, each containing one control plot (ambient [CO_2] of 378 ppm) and one elevated [CO_2] treatment plot (550 ppm), one elevated [O_3] (50 % above ambient), and one elevated [CO_2] and [O_3]. The CO_2 and O_3 enrichment systems were installed immediately after planting. Fumigation began end of May 2004. The crop was fumigated until plants were fully mature and leaves had senesced (October 2004). Half of each 20 m diameter plot was planted with variety Pioneer 93B15, and the other half of the plot was planted with 11 different varieties in ~9 m^2 sub-plots (Fig. 2*A*).

2.2 Hyperspectral Imaging of SoyFACE

Hyperspectral image cubes of reflectance were acquired in July 2004 with the SOC-700 (Surface Optics Corp, San Diego, CA, USA). The instrument is a line scanner that can be operated from a wide range of distances and acquires 12 bit reflectance images between 440 and 880 nm with about 4 nm spectral resolutions (for detailed description of the instrument see Rascher et al. 2007). Images from the SoyFACE experiment (Fig. 2*A*) were taken from a height of about 20 m with an angle of about 45° using a cherry picker (Fig. 2*B*). About 10 single images were taken to cover the full ring. Within each single image a reflectance standard (50 % Spectralon, Labsphere, North Sutton, NH, USA) was placed, and relative reflectances were calculated for each image individually. Later single images were registered to a full image of the ring.

Reflectance images were filtered using the filtering procedure in Principal Component Space as described in detail in Rascher et al. (2007).

2.3 Plant Material for LIFT Studies

Plants of *Helianthus annuus* and *Phaseolus vulgaris* were gown from seeds at the growth facilities at the Carnegie Institution at Stanford University in 10 l pots. The plants were watered periodically with tap water, and a nutrient solution was added every two weeks. *Citrus* spec. tree grew next to the Carnegie Institution, and a branch was cut under water and kept under water for the duration of the experiment. A grass community dominated by *Avina barbata*, *Lolium multiflorum*, and *Bromus diandrus* grew outside the building of Carnegie's Department of Global Ecology under natural conditions.

2.4 The LIFT Approach

The LIFT approach is based on the principle of the Fast Repetition Rate Fluorescence (FRRF) (Kolber et al. 1998). The system uses a collimated laser excitation beam (10 cm in diameter) with peak emission at 665 nm (peak optical power of 125 W m^{-2}, 684 µM photons m^{-2} s^{-1}) to

induce fluorescence of a target leaf at a distance of 5–50 m. The re-emitted fluorescence signal is collected at 690 nm by a Cassegrian telescope and detected by an avalanche photodiode. The apparatus has a motorized pan and tilt that allows targeting the leaves within a canopy automatically, and a web camera to monitor the instrument from any terminal connected to the internet. The technique applies laser pulses to both manipulate the level of photosynthetic activity and to measure the corresponding changes in the chlorophyll fluorescence yield by working with variable duty cycles. The fluorescence yield increases at high duty cycle as the rate of charge separation in PS II reaction center exceeds the rate of photosynthetic electron transport, and Q_A, the first stable electron acceptor in PS II, becomes progressively reduced, and the fluorescence yield increases. At low duty cycle the rate of charge separation is lower than the rate of photosynthetic electron transport, Q_A re-oxidizes, and the fluorescence yield decreases (Fig. 1). The resulting fluorescence transient is fitted with a model described earlier and renders minimum (F) and maximum (F_m) fluorescence among other parameters (Ananyev et al. 2005, Kolber et al. 2005). In order to increase the signal to noise ratio one pulse train contained 12 consecutively repeated sequences of low and high duty cycles (Fig. 1, 2 sequences are present) within a single pulse train that were averaged. Additionally 50 pulse trains were also averaged so that fluorescence transients could be reliably detected under high light intensity.

2.5 Gas Exchange and Chlorophyll Fluorescence Measurements

Gas exchange was measured by an open gas exchange system LI-6400 (LI-COR Biosciences, Lincoln NE, USA) and fluorescence by a bench top FRR fluorometer (FRRF) (Kolber et al. 1998, 2000) and by commercial PAM fluorometry (PAM 2000, Walz GmbH, Effeltrich, Germany). The FRRF was modified with an external LED light unit (Lightspeed Technologies, Campbell, CA, USA) with a blue LED (455 nm) for excitation of the leaves enclosed in LI-6400. The re-emitted fluorescence was transferred by fiber optics to the FRRF detector. The measurements were performed under non-photorespiratory conditions (2 % O_2) with 250 and 400 µmol mol^{-1} CO_2 and photosynthetic photon flux density (PPFD) between 50–1000 µmol m^{-2} s^{-1}.

LIFT fluorometry was combined with measurement of gas exchange in a standard, open system with a large leaf cuvette with an area of 7.8 × 11.5 cm (MPH 1000, Campbell Scientific Inc., Logan, Utah, USA) and PAM fluorometry. The leaf cuvette was arranged in a vertical position, and LIFT fluorescence transients of the enclosed leaves were measured from 8 m distance. The measurements were performed under non-photorespiratory conditions (2 % O_2) and ambient O_2 concentration, [CO_2] was kept constant at 400 µmol CO_2 mol^{-1} and PPFD ranged between 50–1500 µmol m^{-2} s^{-1}. The quantum yield ($\Delta F/F_m'$) was calculated as follows: $\Delta F/F_m' = (F_m' - F)/F_m'$ with F as the steady state and F_m' as the maximum fluorescence of the light-adapted leaf for the FRRF, LIFT and PAM approach, respectively. The electron transport rate (ETR) was than assessed as: $ETR = \Delta F/F_m' \cdot PPFD \cdot 0.85 \cdot 0.5$ with 0.85 as an estimate of absorbed light and 0.5 assumes equal excitation of PSI and PSII (Genty et al. 1989). The electron transport rates based on gas exchange were calculated according to Laisk and Loreto (1996), Peterson and Havir (2004) with a liquid phase diffusion resistance of $r_m = 0.02$ s mm^{-1}, respiration in light of $R_d = 1$ µmol m^{-2} s^{-1}, and a Rubisco specifity of $\tau = 100$.

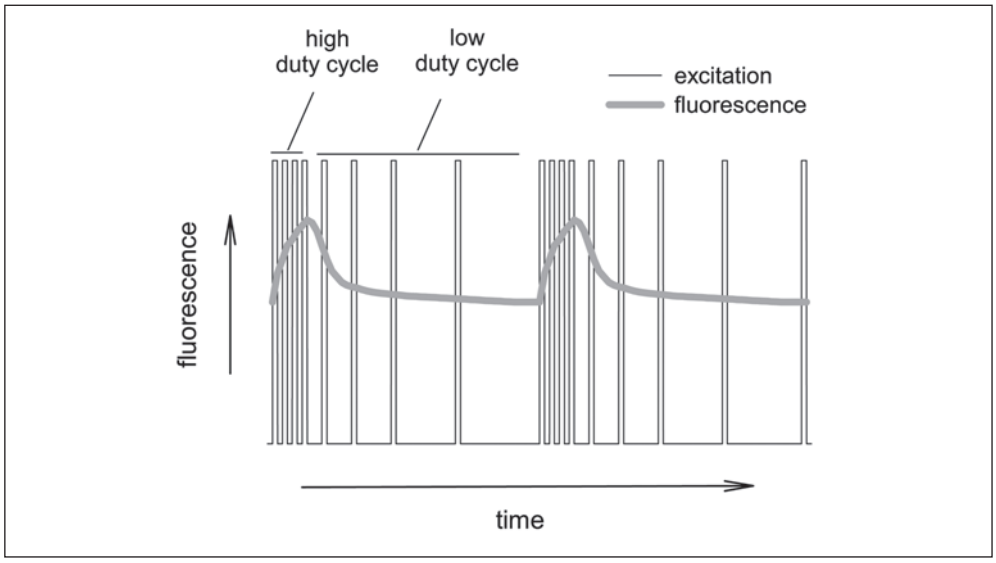

Fig. 1 Schematic diagram of the excitation protocols used in the LIFT method which consists of a series of pulses applied at varied intervals. The amplitude of each pulse is constant, while the pulse width and the interval between pulses are varied to modulate the excitation energy. When the excitation energy exceeds the rates of the photosynthetic electron transport, the fluorescence signal transiently increases, and if it is lower, the signal decreases.

3. Results and Discussion

3.1 Assessing Photosynthetic Efficiency Using the Photochemical Reflectance Index (PRI) from Hyperspectral Reflectance

Taking advantage of the controlled elevated [CO_2] and [O_3] enrichment facility of SoyFACE, we investigated the potential of PRI to detect photosynthetic efficiency in a crop system. The SoyFACE facility of the University of Illinois provides an ideal test case to study the effects of elevated CO_2 enrichment in the field (Rogers et al. 2004). Elevated CO_2 inside the treatment rings results in elevated photosynthetic electron transport of the soy beans (Rascher et al. submitted) and concomitant increase in biomass and crop yield (Long et al. 2006). Soy beans grown under elevated [O_3] have a decreased photosynthetic efficiency and yield (Morgan et al. 2003). We thus expected PRI being in average higher within the elevated [CO_2] treatment plots and lower within the elevated [O_3] plots.

We used the SOC-700 high performance imager (Rascher et al. 2007) to map reflectance of the soy bean canopy in the elevated [CO_2] (Fig. 2*C*) and in the elevated [O_3] treatments (Fig. 2*D*). Images were taken around midday approx. 1 h apart for the [CO_2] and [O_3] treatments. It is obvious that there was no clear difference between PRI of the fumigated plants within the treatment plots and the surrounding area where plants experienced ambient atmospheric conditions (Fig 2*C* and *D*). PRI within the rings, however, showed clear variations with different cultivars. These differences result from a different canopy structure of the soy bean cultivars which was clearly larger than the potential differences of PRI that might be related to different photosynthetic efficiency.

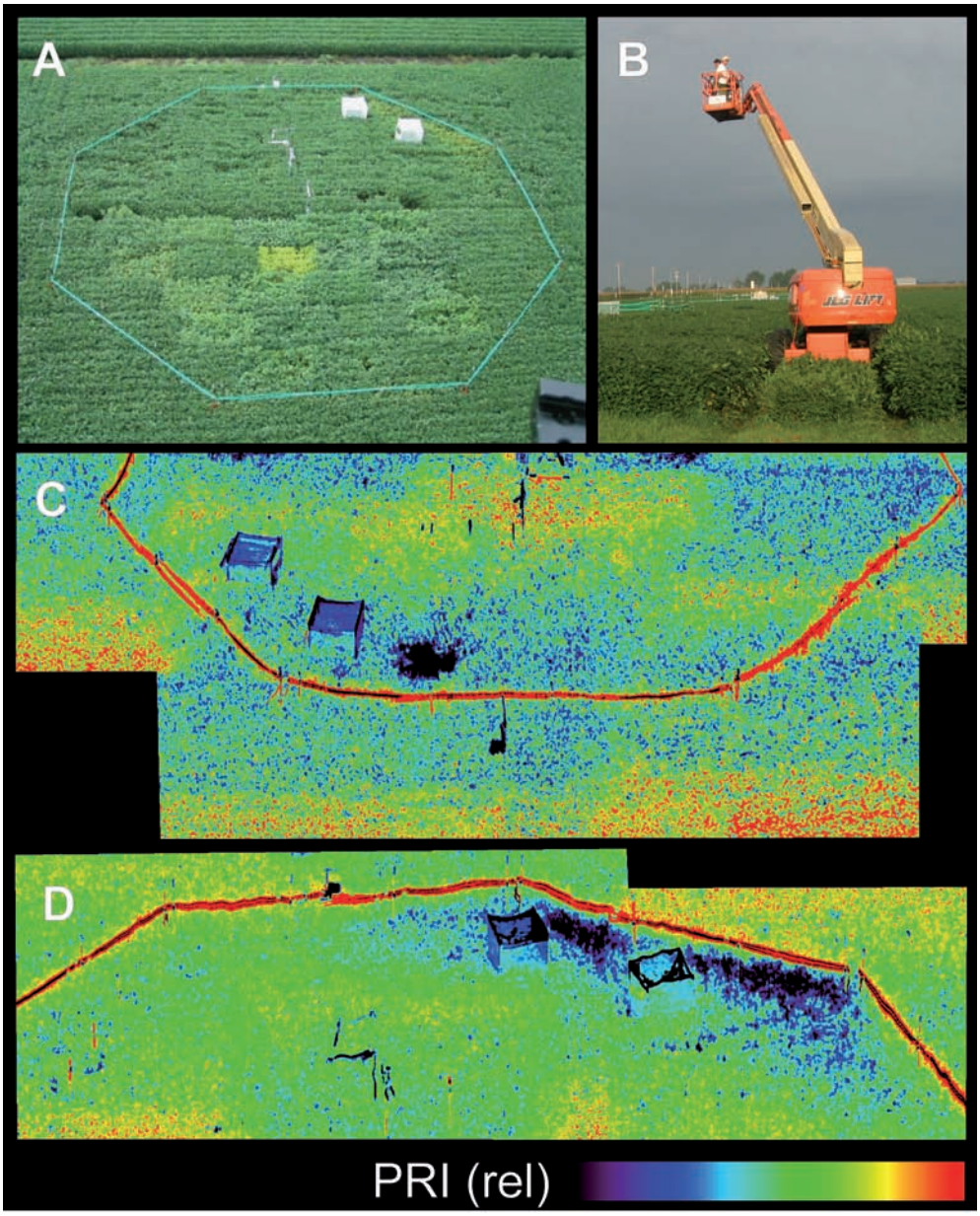

Fig. 2 PRI images of the SoyFACE facility of the University of Urbana-Champaign, Illinois, IL, USA. (*A*) View of one plot of the facility. Free air [CO_2] and [O_3] fumigation were provided using computer controlled tubes in 20 m circles. Within each plot several varieties of soy bean are planted, the white boxes are part of an insect exclusion experiment. (*B*) View of the cherry picker on which the SOC-700 hyperspectral imager was mounted; pictures were taken from about 20 m height and an angle of about 45°. (*C*) PRI images of a part of the ring with elevated [CO_2]. PRI values are scaled between –0.026 and 0.063 color code see bottom right. (*D*) PRI images of a part of the ring with elevated [O_3]. PRI values are scaled between 0.021 and 0.078, color code see bottom right.

3.2 Quantifying Photosynthetic Efficiency Using Active Chlorophyll Fluorescence Measurements on the Leaf Level with the Saturating Light Pulse Method

One of the most powerful tools to measure leaf photosynthetic efficiency, electron transport, and non-photochemical energy dissipation processes is the non-invasive quantification of the fluorescence signal of chlorophyll a of photosystem II (SCHREIBER and BILGER 1993, SCHREIBER et al. 1995). Quantum yield of photosystem II, either measured in the dark adapted state (potential quantum yield: F_v/F_m) or in the light adapted state (effective quantum yield: $\Delta F/F_m'$), as well as non-photochemical quenching (NPQ), which accounts for the sum of all non-photochemical energy dissipating processes, have proven to be robust parameters for quantifying leaf photosynthesis (MAXWELL and JOHNSON 2000). $\Delta F/F_m'$ and NPQ values dynamically adapt primarily to changes in light intensity, however, if irradiance is kept constant those parameters reflect the underlying mechanisms, such as light stress induced activation of the xanthophyll cycle or drought stress (RASCHER et al. 2004).

In general light within the canopy changes rapidly and shows patches of varying intensity. $\Delta F/F_m'$, ETR and NPQ values adapt to these changes in light intensity. Additional parameters, such as maximum apparent electron transport rate (ETR_{max}) and the capacity of the non-photochemical energy dissipation (NPQ) can be quantified from fluorescence light response curves. In order to obtain light response characteristics, several and representative spot measurements within the canopy are grouped and plotted against PPFD. Light dependency data plotted in such way can be mathematically fitted using simple photosynthesis model assumptions in order to quantify the characteristic cardinal points of photosynthesis (RASCHER et al. 2000). These cardinal points reflect the physiological plasticity of a species and are a powerful tool to quantify differences in ontogeny of the plant, to monitor environmental constraints, and to finally scale leaf level processes to the canopy.

However, in order to obtain these fluorescence parameters, photosynthesis has to be excited actively by a saturating light pulse, which still limits this method for remote ecosystem monitoring. It will remain impractical to deliver saturating flashes at the canopy scale. Laser-induced spot- or scanning-methods (ANANYEV et al. 2005, KOLBER et al. 1998, 2005) or sun-induced fluorescence measured in the Fraunhofer or Oxygen bands (PLASCYK and GABRIEL 1975) may overcome this methodological difficulty and are discussed in the next chapters.

3.3 Quantifying Photosynthetic Efficiency using Active Chlorophyll Fluorescence Measurements with Laser Induced Fluorescence Transients (LIFT)

The FRRF and LIFT approaches were extensively tested under laboratory conditions against gas exchange measurements as the gold standard. In agreement with literature (cf. GENTY et al. 1989) PAM based electron transport rate (ETR_{PAM}) correlated very well with the ETR based on CO_2 uptake (ETR_{CO_2}) under non-photorespiratory conditions and closely matched the 1:1 line (Fig. 3*A*, gray symbols). The ETR_{FRR} also compared well with ETR_{CO_2} for two different CO_2 environments but the slope of the linear regressions of ETR_{FRR} versus ETR_{CO_2} ranged between 0.6–0.7 (Fig. 3*A*). The ETR_{LIFT} also correlated well with ETR_{CO_2} and the linear regression revealed a slope similar to the FRR experiment with 0.65 as obtained for three different species (Fig. 3*B*). Under ambient oxygen the ETR_{PAM} versus ETR_{CO_2} slope reached 1.33 whereas ETR_{LIFT} versus ETR_{CO_2} reached 0.95 (Fig. 3*C*). Under ambient conditions electrons are utilized for the carboxylation and oxygenation reaction of the RubisCO,

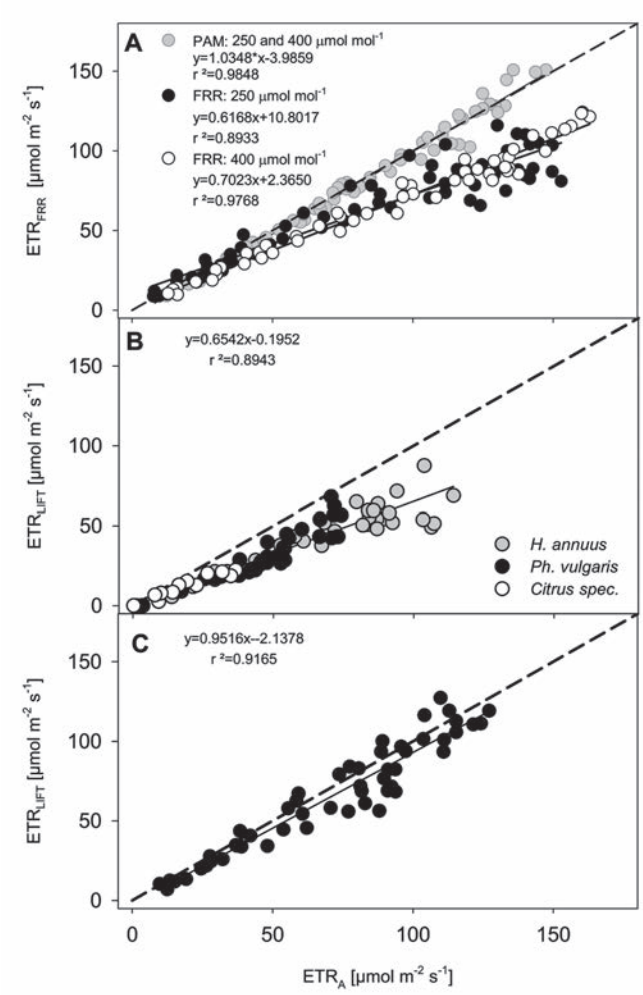

Fig. 3 Correlation between electron transport rates based on assimilation (ETR_{CO_2}) with (*A*) electron transport rates based on FRR (ETR_{FRR}) and PAM (ETR_{PAM}) fluorometry measured under non-photorespiratory conditions (2 % O_2) with *H. annuus*, (*B*) electron transport rates based on LIFT (ETR_{LIFT}) fluorometry measured for three different species measured under non-photorespiratory conditions (2 % O_2) and 250 and 400 µmol CO_2 mol, and (*C*) LIFT based ETR (ETR_{LIFT}) measured under photorespiratory conditions (21 % O_2) with *H. annuus.*

and therefore the ETR_{PAM} versus ETR_{CO_2} relation indicates that approximately one third of the electrons was used for photorespiration.

The difference between the PAM and FRR/LIFT approaches is based on the intensity and duration of the excitation beams. The PAM method uses modulated light with low intensity to derive steady-state fluorescence and saturating pulses with a 0.8 – 1.0 s duration in order to completely reduce the PSII reaction center and the electron transport chain compounds in particular the plastoquinone pool and, to induce F_m (Schreiber et al. 1986). The FRR/LIFT

approach uses sub-saturating pulses in microsecond intervals which continuously reduce the PSII reaction centers and induce a fluorescence transient which is numerically fitted to derive F and F_m (Kolber et al. 1998). The variable chlorophyll a fluorescence ($\Delta F=F_m' - F$) is considered to reflect a photochemical reaction in photosystem II (Genty et al. 1989, Harbinson et al. 2003, Schreiber et al. 1995). Whether fluorescence yield and thus variable fluorescence may also be quenched by other processes as oxidized plastoquinon (PQ) pool and to what extend these processes may influence the measurement and interpretation of chlorophyll fluorescence is still under debate (Koblizek et al. 2001, Samson et al. 1999, Vernotte et al. 1978). However, both systems are apparently capable of characterizing photochemistry (Fig. 3), and further studies are required to elucidate the differences between these approaches. Yet, since PAM depends on saturating pulses and since their application is only possible in close proximity to the leaf, PAM is not practical in ecosystem studies with inaccessible canopies. Even the newly developed Monitoring-PAM (Porcar-Castel et al. 2008) may not prove practical when a leaf is permanently fixed in a leaf holder for an extended time period. The LIFT approach, however, can remotely monitor photosynthetic efficiency of selected leaves each in its own environment making up the canopy.

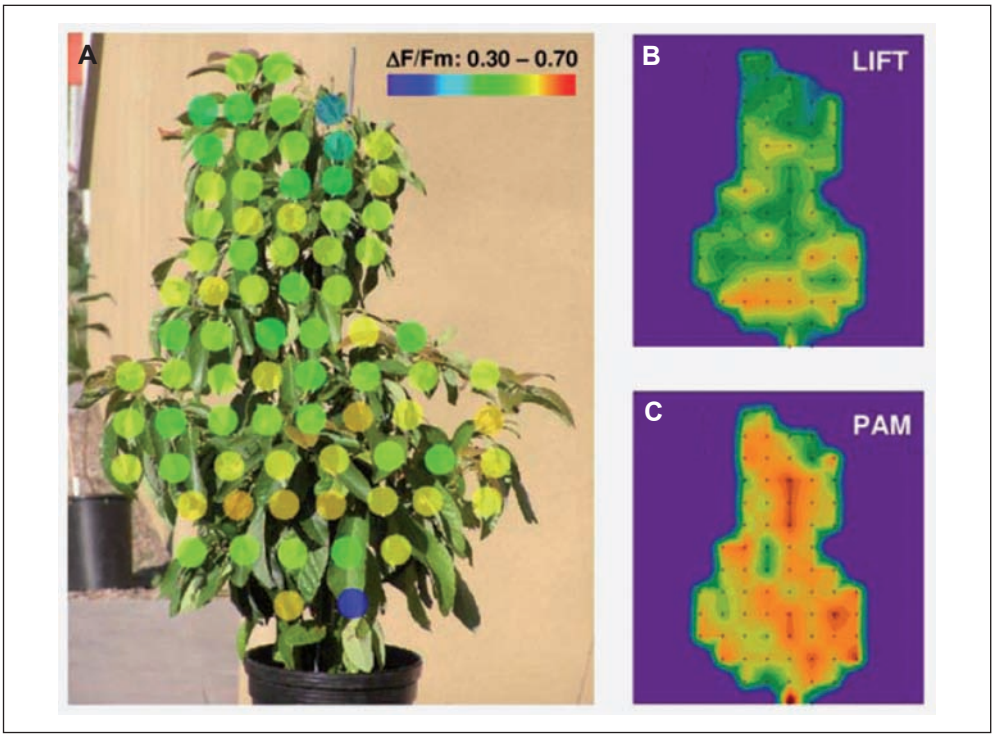

Fig. 4 Map of photosynthetic efficiency ($\Delta F/F_m'$) measured with the LIFT apparatus and PAM on the outer canopy of a cold stressed avocado tree (*Persea americana*) which was exposed to full sun. (*A*) The $\Delta F/F_m'$ values of the outer canopy obtained by the LIFT were scanned spot by spot as indicated by the semi-transparent circles. The $\Delta F/F_m'$ scan was performed with the LIFT and PAM measuring alternately the same canopy sections. Areas with the same $\Delta F/F_m'$ values were encircled by $\Delta F/F_m'$-isolines providing regions with similar photosynthetic efficiency within a canopy which is indicated by different colours for (*B*) LIFT and (*C*) PAM.

Light within the canopy changes rapidly and photosynthesis dynamically adapts to this ever changing mosaic. It is a challenge to precisely detect the changes in photosynthesis in natural and fluctuating conditions. Yet, measurement of actual photosynthetic efficiency is highly desirable to improve the canopy integration scheme (Collatz et al. 1991, Sellers et al. 1992) which is implemented in large scale models (Baker et al. 2003, Sellers et al. 1996). First spatially explicit measurements with the LIFT apparatus proved to have the potential to deliver spatially explicit maps of photosynthetic efficiency (Fig. 4). The LIFT measurements may even more realistically reflect spatial heterogeneity within the canopy than the PAM and clearly displayed lowered $\Delta F/F_m'$ values in the upper-most, high light exposed region of the canopy (Fig. 4*B* and *C*). The LIFT apparatus has also proved successful in monitoring temporal variation in $\Delta F/F_m'$ of a grass community in the winter in California (Fig. 5). The grass was exposed to high illumination with a radiation load up to 500 W m^{-2} (approximately 1500 µmol m^{-2} s^{-1}) during the day and low temperatures at night with minima of –3 °C (Fig. 5*A*). The quantum yield ($\Delta F/F_m'$), however, was only slightly influenced with small differences between the days (Fig. 5*B*). Several different grass patches were monitored, and no difference between these monitored areas was found (data not shown).

The LIFT apparatus has already been successfully used in previous studies to quantify electron transport and dissipation of excess light in *Populus deltoides* stands under ambient and elevated CO_2 concentrations, and in a tropical forest canopy (Ananyev et al. 2005), to detect differences in time constant of genetically modified *Arabidopsis thaliana* strains (Kolber et al. 2005), and to monitor cold stress under field conditions (Pieruschka et al. 2007a, b).

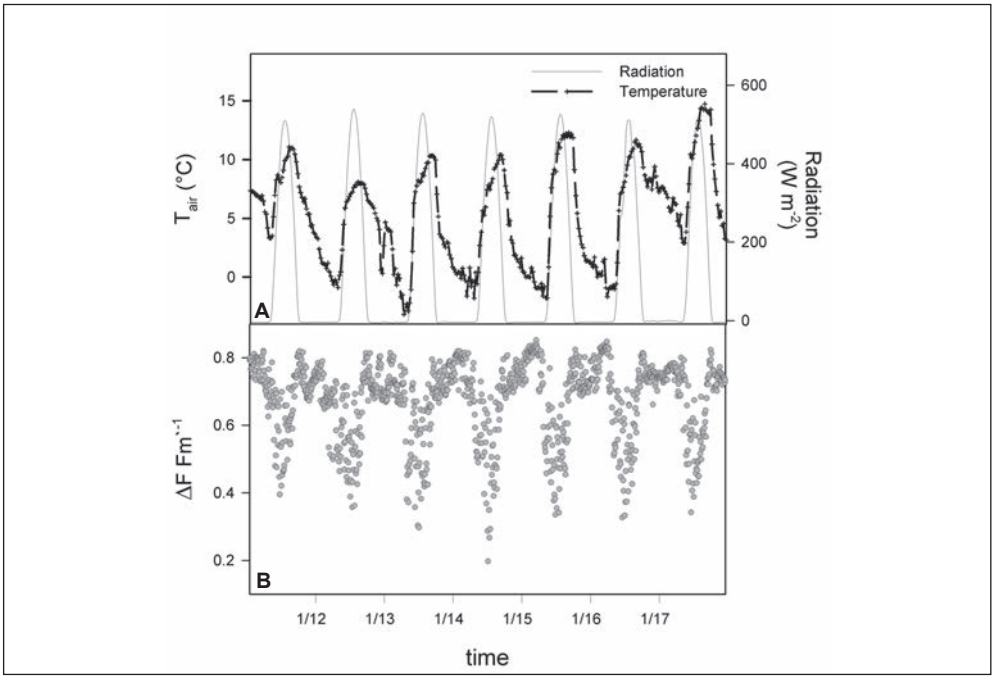

Fig. 5 Diel courses of (*A*) radiation and air temperature (T_{air}) and (*B*) the resulting quantum yield ($\Delta F/F_m'$) pattern of a grass community measured by LIFT.

It will remain a challenge to really measure the distribution of photosynthesis in natural and fluctuating conditions. Data of actual photosynthetic efficiency on the other hand would be highly desirable to better scale leaf level processes to the canopy level. First spatially explicit measurements with a prototype of the LIFT apparatus proved to have the potential to deliver spatially explicit maps of photosynthetic efficiency.

3.4 Passive Chlorophyll Fluorescence using the Fraunhofer Line Principle (FLD)

Especially approaches to quantify sun-induced fluorescence (F_s) under the prevailing light conditions were greatly supported by the selection of the FLEX mission as one of ESA's candidate missions for a future Earth Explorer (Rascher 2007). It has been shown that sun-induced fluorescence can be obtained from remote sensing platforms, and there is experimental and theoretical evidence that sun-induced fluorescence can be correlated with photosynthetic efficiency and stress induced limitation of photosynthetic electron transport. Sun-induced fluorescence thus may serve as a proxy to quantify $\Delta F/F_m$' and photosynthetic efficiency see e.g. Flexas et al. (2000, 2002).

The amount of chlorophyll fluorescence emitted by a leaf under natural sunlight is only 1–5 % of the total light that is reflected, which makes it difficult to quantitatively extract the fluorescence signal for remote sensing. However, at certain wavelengths the solar spectrum is absorbed in the solar or earth atmosphere (so called Fraunhofer lines, Fraunhofer 1817) and thus there is no or greatly reduced incoming radiation on earth surface in these wavebands. Solar irradiance exhibits three main absorption bands in the red and near infrared part: the H_α line at 656.3 nm is due to the hydrogen absorption by the solar atmosphere whereas two bands at 687 (O_2–A) and 760 nm (O_2–B) are due to the molecular oxygen absorption by the terrestrial atmosphere. As the fluorescence signal is always shifted to longer wavelengths, it also occurs in the otherwise 'black' absorption bands and can be selectively quantified. Especially the O_2-A and O_2-B bands overlap with the chlorophyll fluorescence emission spectrum and are wide enough to have the potential to be retrieved from air and space borne platforms. Thus, they can potentially be used to monitor the chlorophyll fluorescence emission under daylight excitation by the method of the Fraunhofer lines in-filling (Moya et al. 2004). Measurements within the center of the absorption bands in comparison to both flanks next to the absorption bands can be used (Plascyk and Gabriel 1975). Currently, several campaigns are under way to evaluate the accuracy with which sun-induced fluorescence can be used to quantify photosynthetic efficiency and stresses (see e.g. http://www.esa.int/esaLP/SEMQACHYX3F_index_0.html). The Fluorescence Explorer (FLEX) mission, which was proposed to ESA, is currently being studied as one out of six candidates Earth Explorer missions in the assessment phase. FLEX has the objective to observe and monitor photosynthetic efficiency from space by measuring all needed components including solar induced vegetation fluorescence at oxygen lines of the solar spectrum (Rascher 2007).

4. Conclusions

It is still a challenge to measure the actual physiological status of photosynthesis using non-invasive remote sensing techniques. The presented approaches show high potential to reach this goal in the near future. Nevertheless, we do not underestimate the challenges that derive

especially from scaling leaf level methods to the canopy. The plant canopy is a complex three-dimensional structure that changes due to environmental factors and structural adaptation of the plants. Explicit methods that aim to map the structure of the outer canopy in the field are currently developed and first results are promising (Biskup et al. 2007).

Acknowledgements

We thank Elisabeth Ainsworth, Andrew Leakey and Steve Long (University of Urbana-Champaign) for supporting our measurements at SoyFACE. SoyFACE was supported by the Illinois Council for Food and Agricultural Research, Archer Daniels Midland Company, the U. S. Department of Agricultural, and the Illinois Agricultural Experiment Station. RP has been supported by Marie Curie Outgoing International Fellowship (Nr: 041060 – LIFT).

References

Ananyev, G., Kolber, Z. S., Klimov, D., Falkowski, P. G., Berry, J. A., Rascher, U., Martin, R., and Osmond, C. B.: Remote sensing of heterogeneity in photosynthetic efficiency, electron transport and dissipation of excess light in *Populus deltoides* stands under ambient and elevated CO_2 concentrations, and in a tropical forest canopy, using a new laser-induced fluorescence transient device. Global Change Biol. *11*, 1195–1206 (2005)

Baker, I., Denning, A. S., Hanan, N., Prihodko, L., Uliasz, M., Vidale, P.-L., Davis, K., and Bakwin, P.: Simulated and observed fluxes of sensible and latent heat and CO_2 at the WLEF-TV tower using SiB2.5. Global Change Biol. *9*, 1262–1277 (2003)

Barton, C. V. M., and North, P. R. J.: Remote sensing of canopy light use efficiency using the photochemical reflectance index. Model and sensitivity analysis. Remote Sens. Environ. *78*, 264–273 (2001)

Biskup, B., Scharr, H., Schurr, U., and Rascher, U.: A stereo imaging system for measuring structural parameters of plant canopies. Plant Cell Environ. *30*, 1299–1308 (2007)

Collatz, G. J., Ball, J. T., Grivet, C., and Berry, J. A.: Physiological and environmental regulation of stomatal conductance, photosynthesis and transpiration – A model that includes a laminar boundary layer. Agricult. Forest Meteorol. *54*, 107–136 (1991)

Filella, I., Penuelas, J., Llorens, L., and Estiarte, M.: Reflectance assessment of seasonal and annual changes in biomass and CO_2 uptake of a Mediterranean shrubland submitted to experimental warming and drought. Remote Sens. Environ. *90*, 308–318 (2004)

Flexas, J., Briantais, J.-M., Cerovic, Z., Medrano, H., and Moya, I.: Steady-state and maximum chlorophyll fluorescence response to water stress in grapevine leaves: a new remote sensing system. Remote Sens. Environ. *73*, 283–297 (2000)

Flexas, J., Escalona, J. M., Evain, S., Gulías, J., Moya, I., Osmond, C. B., and Medrano, H.: Steady-state chlorophyll fluorescence (Fs) measurements as a tool to follow variations of net CO_2 assimilation and stomatal conductance during water-stress in C-3 plants. Physiologia Plantarum *114*, 231–240 (2002)

Fraunhofer, J.: Bestimmung des Brechungs- und Farbenzerstreuungs-Vermoegens verschiedener Glasarten, in Bezug auf die Vervollkommnung achromatischer Fernroehre. Denkschriften der koeniglichen Akademie der Wissenschaften zu Muenchen *5*, 193–226 (1817)

Gamon, J. A., Penuelas, J., and Field C. B.: A narrow-waveband spectral index that tracks diurnal changes in photosynthetic efficiency. Remote Sens. Environ. *41*, 35–44 (1992)

Genty, B., Briantais, J. M., and Baker N. R.: The relationship between the quantum yield of photosynthetic electron transport and quenching of chlorophyll fluorescence. Biochim. Biophys. Acta *990*, 87–92 (1989)

Guo, J., and Trotter, C. M.: Estimating photosynthetic light-use efficiency using the photochemical reflectance index: variations among species. Funct. Plant Biol. *31*, 255–265 (2004)

Harbinson, J., Genty, B., and Baker, N. R.: The relationship between CO_2 assimilation and electron transport in leaves. Photosynthesis Res. *25*, 213–224 (2003)

Koblizek, M., Kaftan, D., and Nedbal, L.: On the relationship between the non-photochemical quenching of the chlorophyll fluorescence and the Photosystem II light harvesting efficiency. A repetitive flash fluorescence induction study. Photosynthesis Res. *68*, 141–152 (2001)

Kolber, Z., Klimov, D., Ananyev, G., Rascher, U., Berry, J., and Osmond, B.: Measuring photosynthetic parameters at a distance: laser induced fluorescence transient (LIFT) method for remote measurement of photosynthesis in terrestrial vegetation. Photosynthesis Res. *84*, 121–129 (2005)

Kolber, Z., Prasil, O., and Falkowski, P. G.: Measurements of variable chlorophyll fluorescence using fast repetition rate techniques: defining methodology and experimental protocols. Biochim. Biophys. Acta (BBA) – Bioenergetics *1367*, 88–106 (1998)

Kolber, Z. S., Van Dover, C. L., Niederman, R. A., and Falkowski, P. G.: Bacterial photosynthesis in surface waters of the open ocean. Nature *407*, 177–179 (2000)

Laisk, A., and Loreto, F.: Determining photosynthetic parameters from leaf CO_2 exchange and chlorophyll fluorescence. Plant Physiol. *110*, 903–912 (1996)

Long, S. P., Ainsworth, E. A., Leakey, A. D. B., Nösberger, J., and Ort, D. R.: Food for thought: Lower-than-expected crop yield stimulation with rising CO_2 concentrations. Science *312*, 1918–1921 (2006)

Maxwell, K., and Johnson, G. N.: Chlorophyll fluorescence – a practical guide. J. Exp. Bot. *51*, 659–668 (2000)

Methy, M.: Analysis of photosynthetic activity at the leaf and canopy levels from reflectance measurements: a case study. Photosynthetica *38*, 505–512 (2000)

Morgan, P. B., Ainsworth, E. A., and Long, S. P.: How does elevated ozone impact soybean? A meta-analysis of photosynthesis, growth and yield. Plant Cell Environ. *26*, 1317–1328 (2003)

Moya, I., Camenen, L., Evain, S., Goulas, Y., Cerovic, Z. G., Latouche, G., Flexas, J., and Ounis, A.: A new instrument for passive remote sensing. 1. Measurements of sunlight-induced chlorophyll fluorescence. Remote Sens. Environ. *91*, 197 (2004)

Ort, D. R.: When there is too much light. Plant Physiol. *125*, 29–32 (2001)

Peterson, R. B., and Havir, E. A.: The multiphasic nature of nonphotochemical quenching: Implications for assessment of photosynthetic electron transport based on chlorophyll fluorescence. Photosynthesis Res. *82*, 95–107 (2004)

Pieruschka, R., Klimov, D., Rascher, U., Kolber, Z., and Berry, J.: Remote monitoring of cold and light stress induced effects on photosynthesis using laser induced fluorescence transient (LIFT) technique. Photosynthesis Res. *91*, 318–319 (2007a)

Pieruschka, R., et al.: Laser Induced Fluorescence Transient (LIFT): remote measurement of light use efficiency in ecosystems. 3rd FLEX Workshop, Florence 2007 (2007b)

Plascyk, J. A., and Gabriel, F. C.: The Fraunhofer line discriminator MKII – an airborne instrument for precise and standardized ecological luminescence measurements. IEEE Transactions on Instrumentation and Measurement *24*, 313 (1975)

Porcar-Castel, A., Pfündel, E., Korhonen, J. F. J., and Juurola, E.: A new monitoring PAM fluorometer (MONI-PAM) to study the short- and long-term acclimation of photosystem II in field conditions. Photosynthesis Res. *96*, 173–179 (DOI: 10.1007/s11120-008-9292-3) (2008)

Rascher, U.: FLEX – FLuorescence EXplorer: a remote sensing approach to quantify spatio-temporal variations of photosynthetic efficiency from space. Photosynthesis Res. *91*, 293–294 (2007)

Rascher, U., Bobich, E. G., Lin, G. H., Walter, A., Morris, T., Naumann, M., Nichol, C. J., Pierce, D., Bil, K., Kudeyarov, V., and Berry, J. A.: Functional diversity of photosynthesis during drought in a model tropical rainforest – the contributions of leaf area, photosynthetic electron transport and stomatal conductance to reduction in net ecosystem carbon exchange. Plant Cell Environ. *27*, 1239–1256 (2004)

Rascher, U., Liebig, M., and Lüttge, U.: Evaluation of instant light-response curves of chlorophyll fluorescence parameters obtained with a portable chlorophyll fluorometer on site in the field. Plant Cell Environ. *23*, 1397–1405 (2000)

Rascher, U., and Nedbal, L.: Dynamics of photosynthesis in fluctuating light. Curr. Opin. Plant Biol. *9*, 671–678 (2006)

Rascher, U., Nichol, C. J., Small, C., and Hendricks, L.: Monitoring spatio-temporal dynamics of photosynthesis with a portable hyperspectral imaging system. Photogrammetric Engineering and Remote Sensing *73*, 45–56 (2007)

Rogers, A., Allen, D. J., Davey, P. A., Morgan, P. B., Ainsworth, E. A., Bernacchi, C. J., Cornic, G., Dermody, O., Dohleman, F. G., Heaton, E. A., Mahoney, J., Zhu, X.-G., Delucia, E. H., Ort, D. R., and Long, S. P.: Leaf photosynthesis and carbohydrate dynamics of soybeans grown throughout their life-cycle under free-air carbon dioxide enrichment. Plant Cell Environ. *27*, 449–458 (2004)

Samson, G., Prasil, O., and Yaakoubd, B.: Photochemical and thermal phases of chlorophyll a fluorescence. Photosynthetica *37*, 163–182 (1999)

Schreiber, U., and Bilger, W.: Progress in chlorophyll fluorescence research: major developments during the past years in retrospect. Prog. Bot. *54*, 151–173 (1993)

Schreiber, U., Bilger, W., and Neubauer, C.: Chlorophyll fluorescence as a nonintrusive indicator for rapid assessment of in vivo photosynthesis. In: Schulze, E.-D., and Cadwell, M. M. (Eds.): Ecophysiology of Photosynthesis; pp. 49–70. Berlin, Heidelberg, New York: Springer 1995

Schreiber, U., Schliwa, U., and Bilger, W.: Continious recording of photochemical and non-photochemical chlorophyll fluorescence quenching with a new type of modulation fluorometer. Photosynthesis Res. *10*, 51–62 (1986)

Schulze, E.-D., and Caldwell, M. M.: Ecophysiology of Photosynthesis. Ecological Studies Vol. *100*. Berlin, Heidelberg: Springer 1995

Schurr, U., Walter, A., and Rascher, U.: Functional dynamics of plant growth and photosynthesis – from steady-state to dynamics – from homogeneity to heterogeneity. Plant Cell Environ. *29*, 340–352 (2006)

Sellers, P. J., Berry, J. A., Collatz, G. J., Field, C. B., and Hall, F. G.: Canopy reflectance, photosynthesis, and transpiration. III. A reanalysis using improved leaf models and a new canopy integration scheme. Remote Sens. Environ. *42*, 187–216 (1992)

Sellers, P. J., Randall, D. A., Collatz, G. J., Berry, J. A., Field, C. B., Dazlich, D. A., Zhang, C., Collelo, G. D., and Bounoua, L.: A revised land surface parameterization (SiB2) for atmospheric GCMS. Part I: Model formulation. J. Climate *9*, 676–705 (1996)

Vernotte, C., Etienne, A. L., and Briantais, J. M.: Quenching of the system II chlorophyll fluorescence by the plasroquinone pool. Biochim. Biophys. Acta *545*, 519–527 (1978)

Dr. Uwe Rascher
Institute of Chemistry and Dynamics
of the Geosphere ICG-III: Phytosphere
Forschungszentrum Jülich
52425 Jülich
Germany
Phone: +49 2461 612638
Fax: +49 2461 612492
E-Mail: u.rascher@fz-juelich.de
http://www.fz-juelich.de/icg/icg-3/Research/
Research_Areas/Ecosystem_Dynamics/Ecophysiology_of_Photosynthesis

Dynamics and Heterogeneity of Photosynthesis

Nova Acta Leopoldina NF *96*, Nr. 357, 65–72 (2009)

Crassulacean Acid Metabolism a Natural Tool to Study Photosynthetic Heterogeneity in Leaves

Ulrich Lüttge ML (Darmstadt)

With 2 Figures and 2 Tables

Abstract

Carbon dioxide is a signaling molecule synchronizing photosynthetic activities over entire leaves. During the cycle of Crassulacean acid metabolism (CAM) strong non-linear dynamics of CO_2 concentration in the leaves cause internal CO_2 gradients driving lateral diffusion of CO_2. This makes CAM a useful natural tool for the study of photosynthetic heterogeneity in leaves. At the whole plant level heterogeneity is given by an ontogenetically increasing expression of CAM from developing to mature leaves along the axis of shoots in the obligate CAM plant *Kalanchoë daigremontiana* Hamet et Perrier de la Bâthie and by performance of C_3 photosynthesis and CAM, respectively, at the same time by two opposite leaves at one node in the C_3/CAM intermediate plant *Clusia minor* L. At the leaf level heterogeneity is given by patchy expression of photosynthetic activity, e.g. in natural dark-light rhythms due to internal CO_2 gradients building up during the transitions between the different phases of CAM and in endogenous circadian rhythms due to desynchronization of the individual oscillators in the leaf cells. Lateral diffusion of CO_2 and the high energy demand of photorespiration reduce heterogeneity and synchronize photosynthetic activity over the leaves.

Zusammenfassung

Kohlendioxid ist ein Signalmolekül für die Synchronisation der photosynthetischen Aktivität in ganzen Blättern. Während des Zyklus' des Crassulaceen-Säurestoffwechsels (CAM) bauen sich durch die ausgeprägte nichtlineare Dynamik der internen CO_2-Konzentration der Blätter CO_2-Gradienten auf, die die laterale CO_2-Diffusion in den Blättern antreiben. Dadurch wird der CAM zu einem sehr brauchbaren natürlichen Werkzeug für das Studium der photosynthetischen Heterogenität in Blättern. Auf dem Niveau der ganzen Pflanze ergibt sich Heterogenität entlang der Sprossachse in der obligaten CAM-Pflanze *Kalanchoë daigremontiana* Hamet et Perrier de la Bâthie dadurch, dass der CAM in voll entwickelten Blättern stärker ausgeprägt ist als in jungen, sich noch entwickelnden Blättern. Bei der C_3/CAM-intermediären Pflanze *Clusia minor* L. kann Heterogenität dadurch entstehen, dass zwei benachbarte Blätter am selben Knoten zur gleichen Zeit C_3-Photosynthese bzw. CAM betreiben. Auf dem Niveau einzelner Blätter entsteht Heterogenität durch die fleckige Ausbildung der photosynthetischen Aktivität, z. B. unter natürlichen äußeren Dunkel-Licht-Rhythmen wegen der internen CO_2-Gradienten, die sich in den Übergängen zwischen den CAM-Phasen aufbauen, oder während endogener circadianer Rhythmen wegen der Desynchronisation der individuellen Oszillatoren der einzelnen Blattzellen. Die laterale CO_2-Diffusion und der hohe Energiebedarf der Photorespiration erniedrigen die Heterogenität und synchronisieren die photosynthetische Aktivität in den Blättern.

1. Properties of Crassulacean Acid Metabolism (CAM) Making it Suitable as a Tool for the Study of Photosynthetic Heterogeneity in Leaves

Physiology and biochemistry of the day/night cycle of CAM is organized in four separate phases during which large differences in internal CO_2 concentrations ($p^i_{CO_2}$) are established. Phase I is the dark period, when stomata are open and atmospheric CO_2 is fixed via phos-

pho*enol*pyruvate carboxylase (PEPC) and stored in the form of malic acid in the central cell sap vacuoles. $p^i_{CO_2}$ tends to be low in phase I. Phase II is a transition in the early morning when PEPC begins to be down regulated and ribulose-bis-phosphate carboxylase/oxygenase (RubisCO) is up regulated. Both carboxylating enzymes are active for a while, $p^i_{CO_2}$ tends to be low but then starts to increase rapidly as stomata begin to close and CO_2 is enriched internally as malic acid is remobilized from the vacuoles and decarboxylated. In phase III during the day stomata are closed and $p^i_{CO_2}$ rises to high levels due to malate decarboxylation behind closed stomata (Lüttge 2002). Internal CO_2 is fixed via RubisCO. In the two species discussed in this review, i.e. *Kalanchoë daigremontiana* Hamet et Perrier de la Bâthie and *Clusia minor* L., $p^i_{CO_2}$ in phase III may be up to 0.5 % (Lüttge 2002, 2007b). In phase IV in the later light period stomata open again and CO_2 is taken up from the atmosphere. $p^i_{CO_2}$ tends to decrease in late phase III and early phase IV and is low again during phase IV.

Hence, the CAM cycle involves rather strong nonlinear dynamics of $p^i_{CO_2}$ and this also causes internal CO_2 gradients especially in the transitions between phases driving lateral diffusion of CO_2 in the leaves. This makes CAM a natural tool for studying heterogeneity because internal CO_2 is considered as one of the most important signals in desynchronization/synchronization events of photosynthesis over entire leaves (Lüttge 2007a).

2. Complement of Methods for the Collection of Data Sets

The present review mainly dwells on experiments reported in Rascher et al. (2001), Rascher and Lüttge (2002), Duarte (2006), Duarte and Lüttge (2007a, b) and Lüttge (2007b, 2008). In these studies a leaf remaining at the intact plant was enclosed in a gas exchange cuvette set up in a growth chamber with controlled climate in a phytotron. A complement of methods was developed which allowed continuous on line determinations of

- CO_2 and H_2O vapour gas exchange by infrared gas analysis;
- calculation of $p^i_{CO_2}$ from the gas exchange data;
- photorespiration by on line applications of pulses of air with only 1 % O_2, where the rate of photorespiration is given by the difference of net CO_2-exchange under non photorespiratory conditions at 1 % O_2 (total activity of RubisCO) and under photorespiratory conditions at 21 % O_2 (carboxylation minus oxygenation activity of RubisCO);
- activity of photosystem II integrated over the entire leaves ($\int\Phi$PSII) using chlorophyll fluorescence images of the leaves;
- heterogeneity (*H*) of $\int\Phi$PSII over the leaves calculated from the chlorophyll fluorescence images.

The chlorophyll fluorescence images are the essential basis for the assessment of heterogeneity. Examples for the two species surveyed here, *K. daigremontiana* and *C. minor*, are given in Figure 1. The extent of heterogeneity is quantified by using methods from cellular automata theory and nearest neighbor algorithms, where *H* is defined as the average difference between states of nearest neighbors (Hütt and Neff 2001, Rascher et al. 2001).

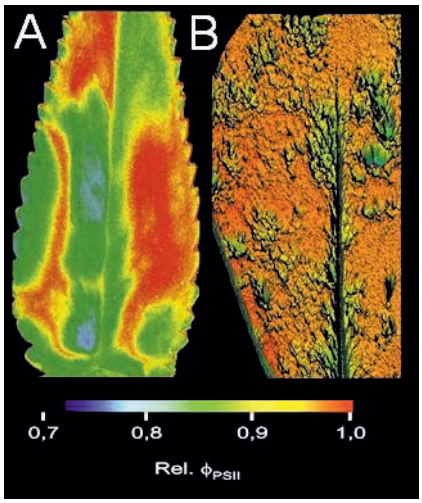

Fig. 1 Examples of chlorophyll fluorescence imaging. (*A*) Leaf of *Kalanchoë daigremontiana* performing CAM. (*B*) Leaf of *Clusia minor* performing C_3 photosynthesis.

3. Heterogeneity due to CAM Flexibility at the Whole Plant Level

Flexibility of CAM results from plasticity in the expression of the four phases in response to environmental cues. Flexibility is also given by the potential to switch between the C_3- and the CAM mode of photosynthesis. In most CAM plants developmental ontogenetic programmes modulate the capacity of CAM expression. In the obligate CAM plant *K. daigremontiana* CAM expression gets increasingly established as the leaves mature (Winter et al. 1982), so that we have heterogeneity along the shoot axis. *C. minor* is a truly C_3/CAM intermediate species which in response to environmental factors can reversibly switch between the two modes of photosynthesis (Lüttge 2007b). Experimentally one can cause the two opposite leaves at one node of the shoot to perform C_3 photosynthesis and CAM, respectively, when the two leaves are subject to different conditions of illumination or water vapor difference of the atmosphere where a dry atmosphere as compared to a moist atmosphere elicits the performance of CAM while the effects of light are more complicated and related to the availability of water to the plant (Lüttge 2007b).

4. Heterogeneity at the Leaf Level

4.1 Leaf Lamina and Major Leaf Vein

Chlorophyll fluorescence images allow separate assessment of ∫ΦPSII for the major vein and the interveinal lamina tissue of the leaves. It is seen that in plants of *C. minor* acclimated to perform C_3 photosynthesis by well watering the root medium the green photosynthesizing tissue above the major veins shows clear features of CAM comparable to plants acclimated by drought stress to perform CAM (Duarte 2006, Duarte and Lüttge 2007a,b, Lüttge 2007b). This photosynthetic heterogeneity is due to the anatomical heterogeneity of the pho-

tosynthetically active tissue in lamina and vein. An interesting thought brought up during the discussions in the Leopoldina Meeting (Rowan Sage) was that also the adaxial palisade parenchyma and the abaxial spongy parenchyma (for the anatomy see Lüttge and Duarte 2007) might show heterogeneity of modes of photosynthesis. However, by contrast to the comparison of vein and lamina this would involve similarly large volumes of photosynthesizing tissue and should have been seen in the analyses of malate levels and measurements of gas exchange of the authors cited above, which was not the case.

4.2 CAM in Leaves of K. daigremontiana

As expected from Section 1 in the obligate CAM species *K. daigremontiana* in the normal external dark-light rhythm the degree of heterogeneity is strongly related to the timing of the CAM phases. Table 1 shows that *H* is rather low in phase III when internal $p^i_{CO_2}$ is high and stomata are closed as indicated by zero net CO_2 exchange (J_{CO_2}). *H* is highest at the beginning of phase IV while the leaves switch from high $p^i_{CO_2}$ due to malate decarboxylation to stomatal opening and uptake of atmospheric CO_2. *H* then declines again as the leaves operate with CO_2 uptake from the atmosphere and open stomata. In the peak of phase II, when both PEPC and RubisCO are active and stomata are still open, *H* has intermediate values. At times one can note that even waves of ΦPSII activity are running laterally along the leaves in opposite directions and extinguish each other when they meet (Rascher and Lüttge 2002), a phenomenon that is consistent with the assumption that a diffusion mechanism is involved in regulation.

Tab. 1 Heterogeneity (*H*) of photosystem II activity (ΦPSII) and net CO_2 exchange (J_{CO_2}) at critical stages during the CAM rhythm of *K. daigremontiana*. Extracted from the data of Rascher et al. 2001 and Rascher and Lüttge 2002.

	Peak of phase II	Phase III	Start of phase IV	Peak of phase IV
H (rel. units)	0.4	0.2	1.0	0.3
J_{CO_2} (μmol m^{-2} s^{-1})	3.5	0.0	0.4	3.7

The development of heterogeneity of ΦPSII was also studied during the free running endogenous circadian rhythm of CAM in *K. daigremontiana* under constant environmental conditions (Rascher et al. 2001). It is known that during ongoing oscillations of net CO_2 exchange (J_{CO_2}) the circadian CAM rhythm in the leaves changes from operation of a biophysical/biochemical oscillator based on the C_4-like turnover of malate (Δmalate) and its compartmentation in the first few endogenous periods to a more C_3-like oscillator in subsequent periods (Wyka and Lüttge 2003, Wyka et al. 2004, Lüttge 2008). This is also depicted in Figure 2 by the strong dampening of malate oscillations while overt J_{CO_2} remains unperturbed. In this context it is an intriguing enigma that heterogeneity is building up as J_{CO_2} pertains and Δmalate is lost. This seems to indicate a stronger synchronization effective in the malate rhythm with high $p^i_{CO_2}$ during malate remobilization than during more C_3-like oscillations.

Varying *H* during the circadian cycle of CAM indicates that the individual oscillators contained in all leaf cells are subject to desynchronization/synchronization events during the rhythm. In the circadian rhythm *H* is always higher in the subjective dark periods (corre-

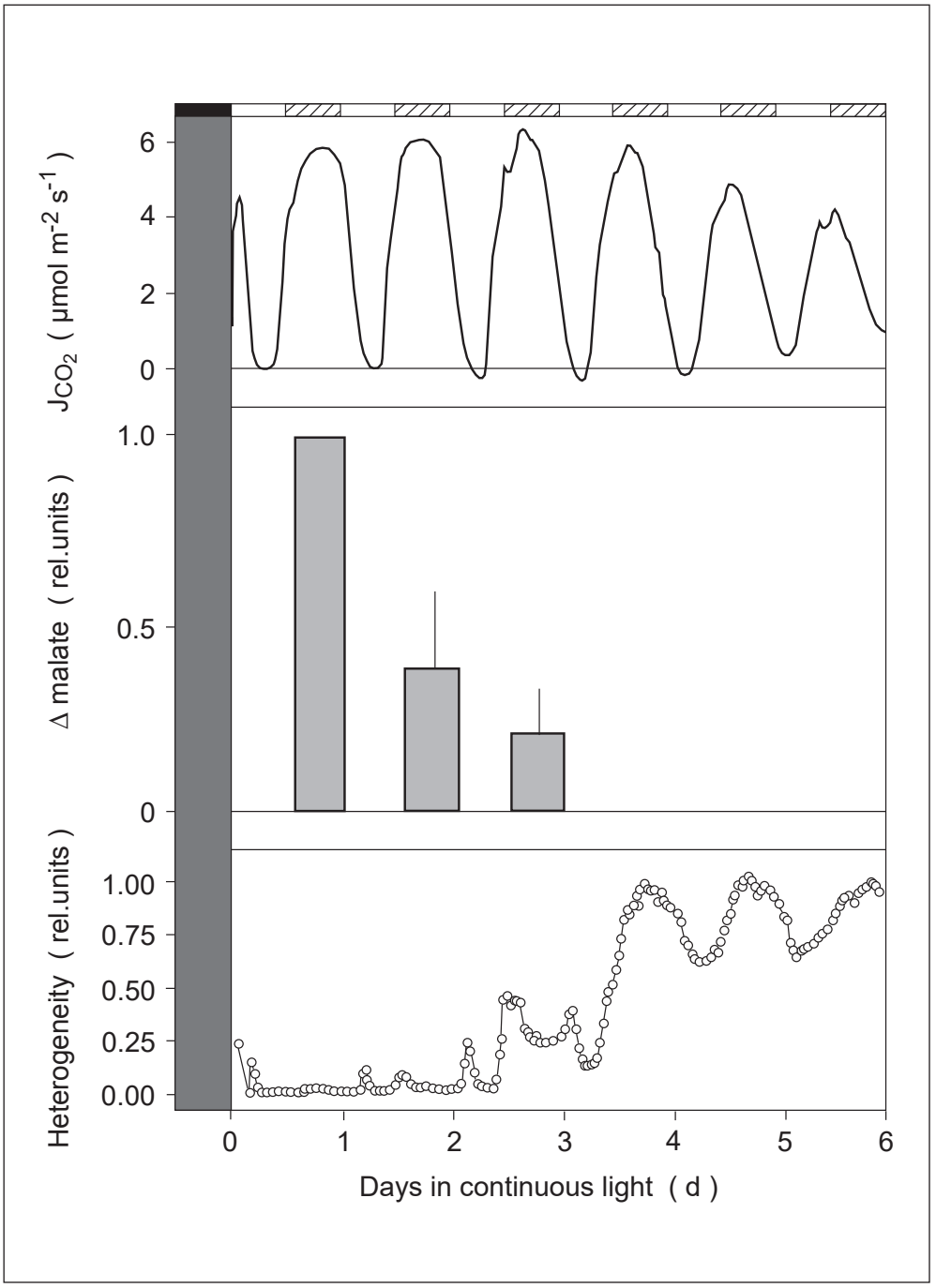

Fig. 2 Circadian rhythmicity of net CO_2 exchange (J_{CO_2}) and heterogeneity of photosystem II-activity (ΦPSII) in *K. daigremontiana* (Rascher et al. 2001) related to rhythmic changes of malate levels (Δmalate) (Wyka and Lüttge 2003).

sponding to phase I when atmospheric CO_2 is taken up) than in the subjective light periods (corresponding to phase III when stomata are closed and CO_2 is remobilized internally from malate). This is, of course, consistent with the prospects developed in Section 1 and the observations made under a natural dark-light rhythm in Table 1.

5. Synchronization by Lateral Diffusion of CO_2 in the Leaves: The Carboxylase Activity of RubisCO

CO_2 in the leaves is thought to be the synchronizing signal reducing heterogeneity of ΦPSII mediated by lateral diffusion within the leaves (Lüttge 2007a). Duarte et al. (2005) have caused artificial patchiness in leaves of *K. daigremontiana* by partially blocking stomatal gas exchange using transparent silicon grease. As shown by low ΦPSII in chlorophyll fluorescence imaging this prevented photosynthesis due to stomatal CO_2 uptake and, of course, it also suppressed malate accumulation due to CO_2 fixation via PEPC in the greased patches. However, when stomata closed during the circadian CAM rhythm in the non-greased parts of the leaves, indicating that the internal CO_2-concentrating mechanism of malate decarboxylation (Lüttge 2002) began to operate, ΦPSII abruptly rose in the greased parts to values close to those of the non-greased parts. This is a direct indication of the role of lateral CO_2 diffusion because it can only be explained by some export of CO_2 for fixation via RubisCO from the non-greased into the greased parts as the greased parts did not have malate of their own to decarboxylate.

6. Synchronization by the high Energy Demand of Photorespiration: The Oxygenase Function of RubisCO

Chlorophyll fluorescence imaging during measurements with regular application of 20 min pulses of air with 1 % O_2 causing non photorespiratory conditions suggests that the particularly high energy demand of photorespiration (Osmond and Grace 1995, Heber 2002, Heber et al. 2001) also exerts a strong synchronization effect on ΦPSII activity over the leaves. ΦPSII is a measure of photosynthetic energy use. Table 2 summarizes experiments under normal dark-light regimes with plants of *C. minor* acclimatized to perform C_3 photosynthesis and CAM, respectively. The particular energy demand of photorespiration is documented by the observation that ∫ΦPSII of the entire leaves is always much higher under photorespiratory than under non-photorespiratory conditions, i.e in the C_3 mode and in phases II and IV in the CAM mode. (Note that in phase III of CAM the impact of 1 % O_2 in the external atmosphere on photosynthetic activity in the leaves cannot be tested because stomata are closed.) In the C_3 mode heterogeneity is much lower under photorespiratory conditions showing the synchronizing effect of photorespiration. In the CAM mode the effects of the CAM phases as detailed in Section 4 overrule those of photorespiration.

The work of Duarte (Duarte 2006, Duarte and Lüttge 2007a, Lüttge 2008) with *C. minor* for the first time in any plant shows circadian oscillations of photorespiration under constant environmental conditions. Photorespiration oscillates in phase with net CO_2 exchange. Under photorespiratory conditions heterogeneity of ΦPSII was constantly low throughout at about 0.12 relative units in the C_3 mode and 0.07 units in the CAM mode, which confirms

Tab. 2 Activity of photosystem II integrated over the whole leaves (∫ΦPSII) and heterogeneity (*H*), both in relative units, under photorespiratory (+) and non-photorespiratory (−) conditions in leaves of *C. minor* in the C_3 mode and in different phases of the CAM mode (with phase IV separated into its early and later part, subscripts 1 and 2, respectively). n. d. = not determined; non-photorespiratory conditions could not be checked in phase III because due to stomatal closure external air with only 1 % O_2 had no access to inside the leaves. Extracted from data of Duarte 2006, Duarte and Lüttge 2007b, Lüttge 2007b, 2008.

	∫ ΦPSII		*H*	
	+	−	+	−
C3	94	22	17	98
CAM-II	68	36	72	33
CAM-III	87	n. d.	1	n. d.
CAM-IV_1	84	35	1	40
CAM-IV_2	72	22	31	20

the synchronizing effect of photorespiration on leaf energy use. Under non-photorespiratory conditions *H* was much higher and oscillated between values of 0.27 and 1.00 relative units in the C_3 mode and 0.08 and 0.93 in the CAM mode. Particularly in the CAM mode *H* appeared to be inversely correlated to J_{CO_2} supporting the synchronizing effect of higher internal CO_2 concentrations building up during malate remobilization behind closing stomata as in the case of *K. daigremontiana* (Section 4.2, Fig. 2).

The signaling mechanism in the synchronizing effect of photorespiration on leaf ΦPSII is not clear to date. It remains an open question if energy demand per se can exert such a function and how that might be mediated at the level of the molecules involved in PSII. Or is it signaling by diffusion of both substrates of RubisCO, i.e. O_2 in addition to CO_2?

References

Duarte, H. M.: Chronobiologie von *Clusia minor*: circadianer Rhythmus in einer Pflanze mit C_3/CAM-intermediärem photosynthetischen Verhalten. Dissertation, Darmstadt, Germany 2006

Duarte, H. M., and Lüttge, U.: Circadian rhythmicity. In: Lüttge, U. (Ed.): Clusia. A Woody Neotropical Genus of Remarkable Plasticity and Diversity. Ecological Studies Vol. *194*, pp. 245–256. Berlin, Heidelberg, New York: Springer 2007a

Duarte, H. M., and Lüttge, U.: Correlation between photorespiration, CO_2-assimilation and spatiotemporal dynamics of photosynthesis in leaves of the C_3-photosynthesis/crassulacean acid metabolism-intermediate species *Clusia minor* L. (Clusiaceae). Trees *21*, 531–540 (2007b)

Duarte, H. M., Jakovljevic, I., Kaiser, F., and Lüttge, U.: Lateral diffusion of CO_2 in leaves of the crassulacean acid metabolism plant *Kalanchoë daigremontiana* Hamet et Perrier. Planta *220*, 809–816 (2005)

Heber, U.: Irrungen, Wirrungen? The Mehler reaction in relation to cyclic electron transport in C_3 plants. Photosynthesis Res. *73,* 223–231 (2002)

Heber, U., Bukhof, N. G., Shuvalov, V. A., Kobayashi, Y., and Lange, O. L.: Protection of the photosynthetic apparatus against damage by excessive illumination in homoiohydric leaves and poikilohydric mosses and lichens. J. Exp. Bot. *52*, 1999–2006 (2001)

Hütt, M.-T., and Neff, R.: Quantification of spatiotemporal phenomena by means of cellular automata techniques. Physica A *289*, 498–516 (2001)

Lüttge, U.: CO_2-concentrating: consequences in crassulacean acid metabolism. J. Exp. Bot. *53*, 2131–2142 (2002)

Lüttge, U.: Carbon dioxide signalling in plant leaves. Comptes Rendus Biologies Paris *330*, 375–381 (2007a)

LÜTTGE, U.: Photosynthesis. In: LÜTTGE, U. (Ed.): Clusia. A Woody Neotropical Genus of Remarkable Plasticity and Diversity. Ecological Studies Vol. *194*, pp. 135–186. Berlin, Heidelberg, New York: Springer 2007b

LÜTTGE, U.: Clusia: Holy Grail and Enigma. J. Exp. Bot. *59*, 1503–1514 (2008)

LÜTTGE, U., and DUARTE, H. M.: Morphology, anatomy, life forms and hydraulic architecture. In: LÜTTGE, U. (Ed.): Clusia. A Woody Neotropical Genus of Remarkable Plasticity and Diversity. Ecological Studies Vol. *194*, pp. 17–30. Berlin, Heidelberg, New York: Springer 2007

OSMOND, C. B., and GRACE, C. E.: Perspectives on photoinhibition and photorespiration in the field: quintessential inefficiencies of the light and dark reactions of photosynthesis? J. Exp. Bot. *46*, 1351–1362 (1995)

RASCHER, U., HÜTT, M.-T., SIEBKE, K., OSMOND, B., BECK, F., and LÜTTGE, U.: Spatiotemporal variation of metabolism in a plant circadian rhythm: the biological clock as an assembly of coupled individual oscillators. Proc. Natl. Acad. Sci. USA *98*, 11801–11805 (2001)

RASCHER, U., and LÜTTGE, U.: High-resolution chlorophyll fluorescence imaging serves as a non-invasive indicator to monitor the spatio-temporal variations of metabolism during the day-night cycle and during the endogenous rhythm in continuous light in the CAM plant *Kalanchoë daigremontiana*. Plant Biol. *4*, 671–681 (2002)

WINTER, K., FOSTER, J. G., SCHMITT, M. R., and EDWARDS, G. E.: Activity and quantity of ribulose bisphosphate carboxylase- and phosphoenolpyruvate carboxylase-protein in two Crassulacean acid metabolism plants in relation to leaf age, nitrogen nutrition, and point in time during a day/night cycle. Planta *154*, 309–317 (1982)

WYKA, T. P., and LÜTTGE, U.: Contribution of C_3 carboxylation to the circadian rhythm of carbon dioxide uptake in a Crassulacean acid metabolism plant *Kalanchoë daigremontiana.* J. Exp. Bot. *54*, 1471–1479 (2003)

WYKA, T. P., BOHN, A., DUARTE, H. M., KAISER, F., and LÜTTGE, U.: Perturbations of malate accumulation and the endogenous rhythm of gas exchange in the Crassulacean acid metabolism plant *Kalanchoë daigremontiana*: testing the tonoplast-as-oscillator model. Planta *219*, 705–713 (2004)

Prof. Dr. Ulrich LÜTTGE
Institut für Botanik
Technische Universität Darmstadt
Schnittspahnstraße 3–5
64287 Darmstadt
Germany
Phone: +49 6151 163700
Fax: +49 6151 164630
E-Mail: luettge@bio.tu-darmstadt.de

Nova Acta Leopoldina NF *96*, Nr. 357, 73 – 91 (2009)

Testing the Functional Implications of Photosynthetic Heterogeneity in Leaves of C_4 Plants: "Reductionism during Scale Expansion"

Susanne von Caemmerer[1] ML and Barry Osmond[2] ML

With 8 Figures

Abstract

This chapter illustrates how experimental studies of the remarkable heterogeneity of photosynthetic properties in C_4 plants can determine if and when heterogeneity and diversity in complex systems matter. The studies reviewed here confirm that anatomical and biochemical heterogeneity among C_4 types seem to deliver an array of compensating responses that confer a similar and robust, leaf-level advantage with respect to water and nutrient economy of CO_2 assimilation at high light and temperature in a low CO_2, high O_2 atmosphere. The heterogeneity presumably reflects the independent origins of the C_4 pathway in different plant taxa, and other processes, unrelated to the pathway itself, may be responsible for distinctive patterns such as, for example, the differing distribution of NADP- and NAD-ME C_4 type grasses in relation to precipitation.

Zusammenfassung

Dieser Beitrag veranschaulicht, wie experimentelle Untersuchungen die bemerkenswert heterogenen Photosyntheseeigenschaften von C_4-Pflanzen bestimmen können, ob und wann Heterogenität und Vielfalt in komplexen Systemen von ausschlaggebender Bedeutung sind. Die hier dargestellten Untersuchungen bestätigen, dass die anatomische und biochemische Heterogenität innerhalb der unterschiedlichen C_4-Arten scheinbar eine große Anzahl von gegenseitig kompensierend wirkenden Eigenschaften und Reaktionswegen darstellt, welche, auf dem Niveau des Blattes, vergleichbare und robuste Vorteile bezüglich des Wasser- und Nährstoffhaushaltes für die CO_2-Assimilation unter hohen Lichtintensitäten und Temperaturen in einer Atmosphäre mit geringem CO_2- und hohem O_2-Gehalt verleihen. Vermutlich spiegelt diese Heterogenität die unabhängigen Ursprünge der C_4-Photosynthesewege in den unterschiedlichen Taxa der Pflanzen wider. Andere Prozesse, die nicht mit dem C_4-Weg selbst in Verbindung stehen, sind möglicherweise für distinkte Muster, wie, zum Beispiel, die unterschiedliche Verbreitung der NADP- und NAD-ME C_4-Grassarten in Verbindung mit dem Niederschlag, verantwortlich.

1. Introduction

"Photosynthesis and other natural phenomena, especially evolved, biological phenomena, are very complex and difficult to comprehend. It is useful to formally organize our knowledge in hierarchical levels, knowing of the upscale and downscale effects that one hierarchical level has on the other" (Smith et al. 2004). These authors offered a comprehensive attempt

1 Molecular Plant Physiology Group, Research School of Biological Sciences, Australian National University, Box 475 Canberra ACT 2601, Australia.

2 School of Biochemistry and Molecular Biology, Australian National University, Canberra ACT 0200, Australia.

to scale our understanding of photosynthetic processes from the molecule to the biosphere. An earlier focus on the still to be explained nexus between scale in size and relaxation times of key processes (Osmond et al. 1980) suggested that although the whole is clearly the sum of its parts (at any scale), for practical purposes in scaling up, the whole may become a good deal less than this. Reductionism thus takes on two meanings in relation to scaling; the commonly expressed (but semantically incorrect) fascination with ever increasing detail down scale, and the need to selectively discard much of this detail if one is to evaluate the "bigger picture" up scale.

There may be few general rules but with presently available technologies, the leaf is probably the most appropriate scale for experimental evaluation of the importance of photosynthetic heterogeneity. Speculations about the function of heterogeneity in cells of leaves, their specialization with respect to metabolism, their arrangement with respect to light absorption and to export of the products of CO_2 assimilation, date from the earliest microscopic studies. In this chapter we deal with one of the most striking and now possibly best understood cases of heterogeneity in the photosynthetic apparatus in leaves of plants that assimilate CO_2 by the C_4 pathway of photosynthesis. Most clearly anticipated by Haberlandt (1909) when he speculated "*ob eine noch unbekannte Arbeitsteilung zwischen den Chloroplasten der Kranz- und jenen der Scheidenzellen dabei im Spiele ist*", we now know that this "division of labor" involves tight coordination of the partial reactions (both light and dark) to function as an internal CO_2-concentrating mechanism (Hatch and Osmond 1976, Edwards et al. 2001).

Until recently, it was thought that the CO_2-concentrating mechanisms of the C_4-photosynthetic pathway were distinctive in that they involve close collaboration of two adjacent highly differentiated photosynthetic cell types, the mesophyll (M) and bundle sheath (BS) cells (Edwards et al. 2001). However, now C_4 Chenopodiaceae have been discovered in central Asia in which all the components of the CO_2-concentrating mechanisms were found in spatially separated, clearly differentiated chloroplasts in the same cells. The biochemistry of the CO_2-concentrating mechanisms in these C_4 plants seems similar to those of the two-cell systems, but the symplastic connections sustaining the metabolite transfers are based on fascinating forms of intracellular compartmentation (Edwards et al. 2004).

Most common among plants well adapted to dry and hot environments, the biochemical heterogeneity of C_4 metabolism is thought to confer robust advantages of more efficient CO_2 assimilation, water use and nitrogen use, and productivity at high temperature, at the cost of less efficient light use in the prevailing low CO_2 and high O_2 atmosphere (Sage 2004). In focusing attention on this particular form of heterogeneity we will briefly review its role in molecular through physiological processes and describe experiments that explore whether it makes a difference to environmental responses at the leaf and larger scales.

The issues that bedevil efforts to deal with scaling and to bring accountability to plant sciences research were elegantly expounded by Passioura (1979) in a brief but no longer easily accessible article. Passioura's "parable" of scaling, based on the dots in a screened image taken from Piaget (1971), is especially relevant to the Jülich symposium theme, and can be re-told using images of chlorophyll fluorescence from a shade leaf exposed to full sunlight through a photographic negative. The rather stable images stored in the leaf as differential chlorophyll fluorescence emission from active and inactive photosystem II centers in grana of chloroplast thylakoids are readily captured using a digital camera fitted with appropriate excitation and filters (Osmond et al. 1999). It is a simple matter to expand the image size to the extent that, although we can differentiate every pixel and its intensity on a scale of 1–256,

it remains a meaningless landscape of light and shade. One can only begin to make sense of the image by reducing it so that mind's eye no longer resolves the fine structure and instead reveals the big picture as the ear of a distinguished plant biologist (Fig. 1).

Thus we can imagine our purpose to be the experimental evaluation of "operational structuralism" in which PIAGET ascribed primary importance to understanding the natural structures that comprise the whole, rather than the detail in the components that make up the natural structures, or the emergent properties of the whole itself. We ask whether heterogeneous biochemical components that underlie the natural structures in C_4 plants (including CO_2-concentrating mechanisms, water use and nutrient use efficiency, and thermal responses) significantly influence the whole, as reflected in the ecological distribution of C_4 plants along environmental gradients.

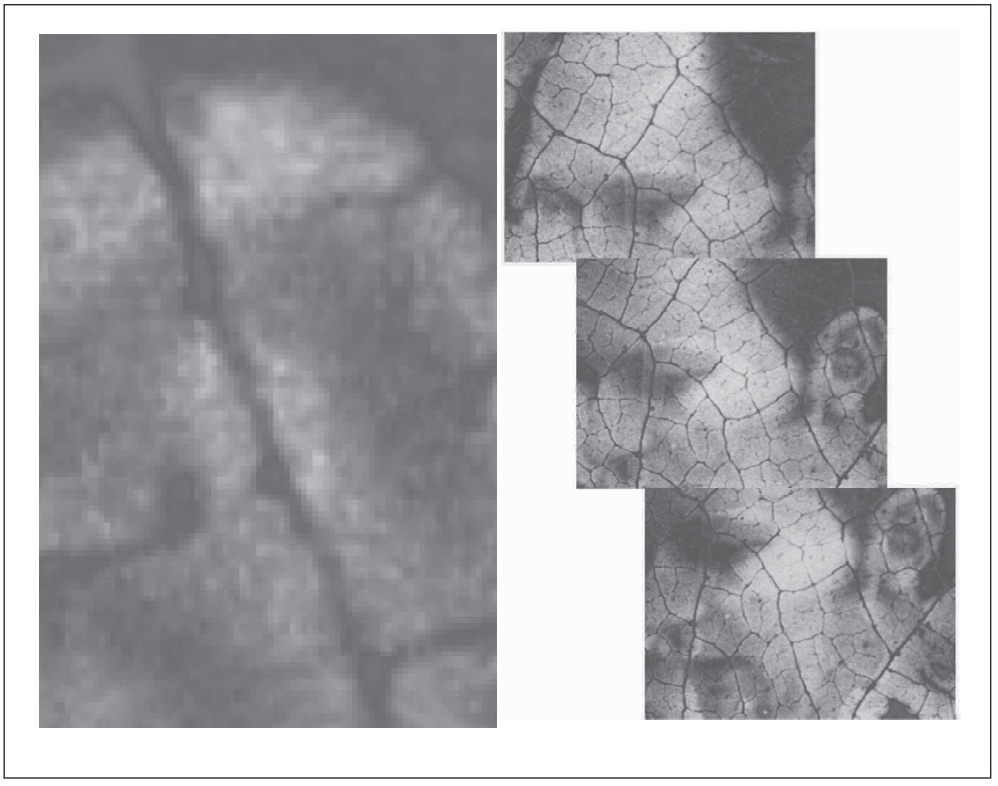

Fig. 1 A photoinactivation portrait of a well known plant biologist made on a shaded bramble leaf and imaged by chlorophyll fluorescence (OSMOND et al. 1999). The enlarged pixilated image on the left is precisely representative of the heterogeneity of information in one of the images on the right. The left image is perhaps analogous to our detailed molecular understanding of C_4 photosynthesis. At a larger scale it becomes recognizable as a "natural structure", the left ear in the central image on the right. These are perhaps analogous to our broad understanding of C_4 plant ecophysiology; of the whole in different contexts. Photos prepared by Barry OSMOND at the Botanical Institute, Technical University Darmstadt, July 1999.

2. Dimensions of Heterogeneity in the Photosynthetic Apparatus of C_4 Plants

Rubisco, the primary CO_2-fixing enzyme of photosynthesis, is a poor catalyst (Andrews et al. 1971, Andrews and Lorimer 1981, Tcherkez et al. 2006). Many species, including unicellular algae (Badger and Price 1992) and crassulacean acid metabolism plants and C_4 plants (Leegood et al. 1997), have evolved CO_2-concentrating mechanisms that deliver high CO_2 at the site of carboxylation and enhance Rubisco catalysis. This reduces Rubisco oxygenation and photorespiration and allows Rubisco to operate close to its maximal activity.

Photosynthetic heterogeneity in the multicellular C_4 types is most commonly illustrated and analyzed in transverse leaf sections (Fig. 2*A*) showing the "Kranz" (wreath-like) radial arrangement (Haberlandt 1909, Hattersley and Watson 1975) to highlight the path-length for metabolite exchange (Hatch and Osmond 1976, von Caemmerer and Furbank 2003) between chloroplasts in mesophyll and bundle sheath cells. However, Figure 2*B* also shows a median paradermal section that emphasizes the large air spaces between loosely arranged mesophyll cells in which CO_2 is initially fixed into C_4 acids by phosphoenol pyruvate carboxylase (PEPC). These and other metabolites are then exchanged with bundle sheath cells tightly appressed to veins, and are decarboxylated there by three distinctly compartmented and different biochemical pathways that generate elevated [CO_2]. The structure of the bundle sheath wall (which has a low permeability to CO_2), the relative biochemical capacities of the C_3 cycle in the bundle sheath, and metabolite exchange across the mesophyll-bundle sheath interface, all contribute to achievement of elevated [CO_2] for Rubisco in the bundle sheath (von Caemmerer and Furbank 2003).

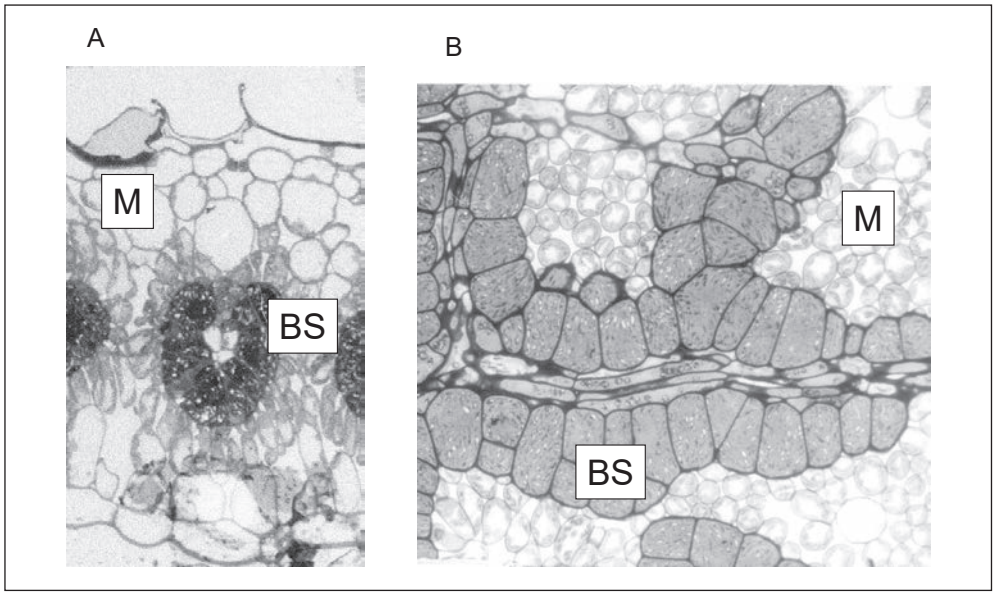

Fig. 2 Transverse (*A*) and (*B*) paradermal sections of the "Kranz" anatomy in *Atriplex vesicaria* leaves grown under warm conditions (28 °C day/20 °C night), showing marked differences in the size and vacuolation of mesophyll cells (M) and bundle sheath cells (BS). Light micrographs × 100 of thin sections prepared for transmission electron microscopy; for details see Caldwell et al. (1977).

The C_4 photosynthetic pathway has evolved a number of times in a large number of both dicot and monocot genera (Sage 2004). Three major biochemical subgroups of C_4 plants have been characterized, that use different C_4-acid decarboxylases in different bundle sheath cell compartments to generate elevated [CO_2]; NADP-ME type in chloroplasts, NAD-ME type in mitochondria and PCK types primarily in the cytosol (Downton 1971, Hatch et al. 1975). These biochemical variations are accompanied by a suite of anatomical features, such as the presence or absence of a suberized lamella in the cell wall between bundle sheath and mesophyll cells, and the centripetal and centrifugal orientation of chloroplasts in the bundle sheath. They are also accompanied by suites of complementary alterations in the light harvesting and photosynthetic electron transport capacities of chloroplasts in the two cell types (Hatch and Osmond 1976, Hatch 1987).

Deficiency of PSII activity in the bundle sheath of sorghum and other NADP-ME types is one of the best documented examples of heterogeneity in thylakoid composition in chloroplasts of C_4 species (Woo et al. 1970, Mayne et al. 1974, Edwards et al. 1976, Ghirardi and Melis 1984). Agranal bundle sheath chloroplasts of sorghum have very limited PSII activity and CO_2 reduction is driven by complementary metabolite shuttles, not by PSII electron transport. The remarkably different PSII fluorescence emission of mesophyll and bundle-sheath cells of sorghum *in vivo* is clearly displayed by confocal microscopy (Fig. 3) which even resolves the strong point sources of PSII fluorescence in grana of mesophyll chloroplasts, and the weak diffuse fluorescence of agranal bundle-sheath chloroplasts (Edwards et al. 2001, Gunning 2007). It is not yet entirely clear how the tight coupling between demands of CO_2 reduction and the bioenergetic capabilities of light reactions in chloroplasts in the adjacent cells is co-ordinated (Meierhoff and Westhoff 1993).

Here we confine ourselves to recent studies of the extent to which functional heterogeneity in the CO_2 assimilation machineries of bundle sheath and mesophyll cells, and the light reactions of their chloroplasts, is reflected in photosynthesis measured by leaf level gas exchange and chlorophyll fluorescence in different C_4 plants. We also examine whether heterogeneity in these attributes helps improve our understanding of the distribution of these plants in relation to gradients in temperature and water availability, nitrogen nutrition and light environments.

3. Heterogeneity of CO_2 Diffusion within Leaves and its Implications for Water Use Efficiency of C_4 Plants

Heterogeneity of photosynthesis in C_3 leaves arises from patchy stomatal closure that denies CO_2 supply to sectors in leaves isolated by vein extensions which prevent lateral diffusion of gases (heterobaric leaves; Terashima et al. 1988), as well as from slow lateral diffusion of CO_2 between mesophyll cells in homobaric leaves (Pieruschka et al. 2005, Morison et al. 2005). Heterogeneity of photosynthesis is also evident at high internal CO_2 concentrations in CAM plants with very large, uniform mesophyll cells because these cells are tightly packed and have little intercellular air space for CO_2 diffusion which is much slower when confined to wet cell walls (Rascher et al. 2001, Nelson et al. 2005, Duarte et al. 2005).

The functional cooperation between mesophyll and bundle sheath cells puts quite different constraints on CO_2 diffusion in C_4 leaves. A prerequisite for high photosynthetic rates of C_4 photosynthesis is a high rate of CO_2 diffusion from intercellular airspace to the mesophyll cytosol. Since PEPC is located in the mesophyll cytosol, CO_2 has to diffuse through the cell

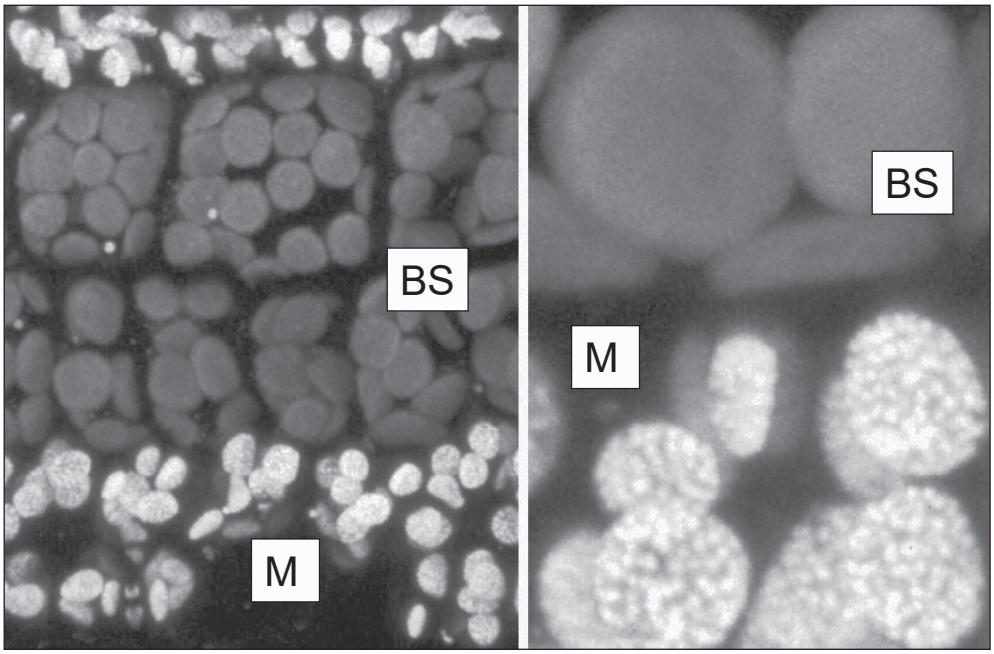

Fig. 3 Confocal microscope image of chlorophyll auto-fluorescence from mesophyll and bundle sheath cells of *Sorghum bicolor* in longitudinal view. Mesophyll cell chloroplasts (M, outer rows, *left*) have thylakoids with high activity of both photosystems show strong fluorescence from PSII in grana (resolved in lower chloroplasts, *right*). Adjacent bundle sheath cells contain larger chloroplasts (BS, inner rows, left) with PSII deficient thylakoids, lack grana and show diffuse fluorescence from PSI alone (upper chloroplasts, right). Photographs courtesy of B. E. S. Gunning; modified after Edwards et al. 2001.

wall and the plasma membrane and cytosol, and the path length in the cytosol is difficult to estimate (Evans and von Caemmerer 1996). The mean value for mesophyll cell surface area to leaf area is 11.6 ± 1.1 for C_4 monocots and 15.6 ± 1.4 for C_4 dicots (von Caemmerer et al. 2007). These values are slightly lower than those reported for C_3 species but similar to values of chloroplast surface areas adjacent to intercellular airspaces in leaves of C_3 species (von Caemmerer et al. 2007). Given the need for rapid CO_2 diffusion across this interface one wonders whether the lower mesophyll cell surface areas in C_4 leaves are an anatomical constraint imposed by the need to stay connected with the bundle sheath cells. There are no studies we know of that have examined lateral photosynthetic heterogeneity in C_4 species which we suspect may be less pronounced than in C_3 leaves. It might be interesting to repeat the fluorescence imaging experiments of Morison et al. (2005) who occluded stomata with spots of grease to examine CO_2 diffusion within the mesophyll of C_3 species.

The requirement of high conductance for CO_2 diffusion, from intercellular airspace to the mesophyll, contrasts with the requirement of low CO_2 permeability across the mesophyll bundle sheath interface needed to achieve elevated [CO_2] for the CO_2-concentrating mechanism. In part this is achieved by low bundle sheath to leaf surface area ratios (1.8 ± 0.1) that vary little amongst species (von Caemmerer et al. 2007). One of the measures of the success of the cooperation between mesophyll and bundle sheath cells in C_4 photosynthetic CO_2 concentra-

tion mechanism is the CO_2 leakiness of the bundle sheath, defined as the rate of CO_2 leakage out of the bundle sheath relative to the rate of CO_2 supply of the C_4 cycle (Farquhar 1983). It has been suggested that NADP-ME grasses may be less leaky than NAD-ME grasses since they posses a suberized lamella in the bundle sheath cell wall which could increase the gas tightness of the bundle sheath. This hypothesis fits with the differences in the carbon isotope composition of leaf dry matter observed between NAD-ME and NADP-ME species (Hattersley 1982, Farquhar 1983, Ghannoum et al. 2002). However, short term measurements of photosynthetic carbon isotope discrimination made concurrently with gas exchange revealed no evidence for differences between the biochemical subtypes (Henderson et al. 1992, Cousins et al. 2007). Perhaps differences in dry matter carbon isotope discrimination are related to differences in respiratory metabolism, but this has yet to be explored.

The near constancy of the estimated leakiness in C_4 species from a range of evolutionary origins seems quite remarkable. It complements the convergence found in other gas exchange characteristics despite anatomical and biochemical heterogeneity observed in these species. For example, when grown under standard conditions there was a surprising similarity in photosynthetic rate per leaf area although NAD-ME species had slightly greater whole plant water used efficiency under drought (Ghannoum et al. 2002). It turned out that the key factor contributing to this difference was a higher catalytic turnover rate of Rubisco carboxylation in NADP-ME compared to NAD-ME species (Ghannoum et al. 2005). The geographic distribution of the different C_4 types with rainfall shows dramatically different correlations; species of the NADP-ME subtype are more abundant in high rainfall areas whereas the NAD-ME subtype is more abundant in drier habitats (Ellis et al. 1980, Hattersley 1983). Clearly, there is more to ecological success than water efficient CO_2 assimilation.

In most temperature transects examined, whether latitudinal or altitudinal, the frequency of C_4 plants in grass floras is positively correlated with growing season minimum temperature (Teeri and Stowe 1976, Vogel et al. 1978, Hattersley 1983, Taub, 2000). Since Ehleringer and Björkman (1977), this correlation has been attributed to the temperature insensitivity of quantum yield in C_4 plants, and the higher quantum yield of C_3 photosynthesis at about 10 °C. However, we need to remember that the quantum yield advantage is only likely to be selected in low light environments. The canopy of tall tropical grasslands may be light limited, but it is clear that the development of the photosynthetic apparatus in tropical C_4 grasses is impaired at low temperatures (Taylor and Craig 1971, Slack et al. 1974). Moreover, species with the same C_4 type (NADP-ME), but from different genetic lineages, show remarkably different responses to low temperature. Cold-tolerance in *Miscanthus* × *giganteus* is associated with maintenance of high levels of Rubisco and some C_4 enzymes, compared with cold-sensitive *Zea mays* (Naidu et al. 2003). Low temperature tolerance is widely known among NAD-ME type C_4 dicotyledons such as *Atriplex* spp. (Osmond et al. 1980), and the yet to be explained starch accumulation in both mesophyll and bundle sheath cells at low temperature (Caldwell et al. 1977) seems common across both pathway types and between species.

4. Heterogeneity, Nitrogen use Efficiency and Light Environment

The higher gross leaf nitrogen use efficiency of the C_4 pathway compared to the C_3 pathway is well known (Seemann et al. 1984, Hatch 1987, Long 1999). Recent detailed comparisons

of photosynthetic N allocation in C_3 and C_4 plants (Makino et al. 2003) have been refined to show that the higher efficiency in the latter arises from both reduced Rubisco content (less carboxylase is needed to sustain the same rate of CO_2 fixation at elevated [CO_2]) and improved catalytic turnover rates of Rubisco in C_4 species (Ghannoum et al. 2005). The partitioning of leaf chlorophyll and nitrogen to the bundle sheath in four C_4 grasses examined by Ghannoum et al. (2005) is shown in Figure 4. The NAD-ME grasses had a lower photosynthetic nitrogen use efficiency than NADP-ME grasses because they contained more leaf N per area (Ghannoum et al. 2005). In the NAD-ME species 65 % of both leaf N and chlorophyll is found in the PSII-rich bundle sheath, whereas only 35 % of both chlorophyll and nitrogen is found the PSII-depleted bundle sheath of NADP-ME species. Despite containing 65 % of leaf chlorophyll less than 40 % of leaf functional PSII and PSI centers are located in the bundle sheath of the two NAD-ME species. Bundle sheath cells of the two NADP-ME species contain a similar amount of PSI activity but PSII activity is almost negligible.

There are few studies of the plasticity of chloroplast thylakoid organization in mesophyll and bundle sheath in C_4 species in relation to N nutrition and light environment. Henderson

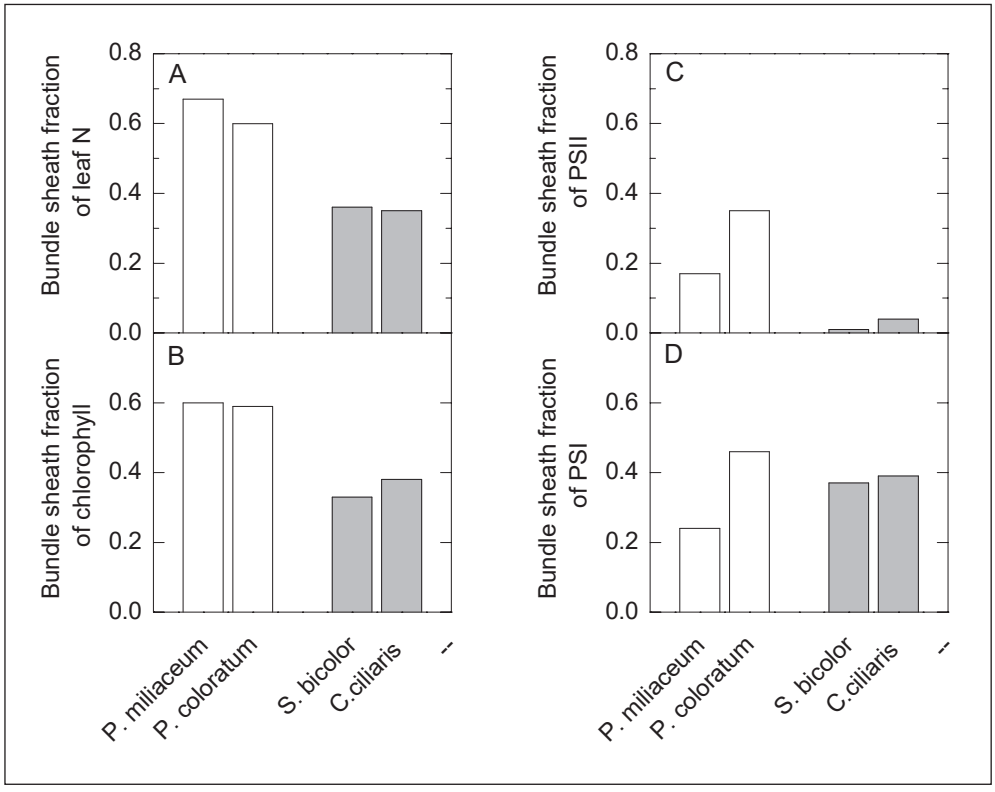

Fig. 4 Bundle sheath nitrogen as fraction of leaf nitrogen content (*A*), bundle sheath chlorophyll as a fraction of leaf chlorophyll (*B*), bundle sheath PSII activity as a fraction of leaf PSII activity (*C*) and bundle sheath PSI activity as a fraction of leaf PSI activity (*D*). Measurements were made on two NAD-ME grasses (*Panicum mileacium* and *Panicum coloratum*) and two NADP-ME grasses (*Sorghum bicolor* and *Cenchris ciliaris*). Data have been collated from Table V of Ghannoum et al. (2005). Two replicate measurements were made for each species.

et al. (1992) observed increased leakiness in NADP- and NAD-ME types at low light, and Wong and Osmond (1991) noted an increase in $\delta^{13}C$ composition of *Echinochloa frumentacea* (NADP-ME type) and stimulation of growth by elevated [CO_2], indirectly indicating a partial failure of the CO_2-concentrating mechanism at low N. In the C_4 dicot *Amaranthus cruentus* (NAD-ME) low N and low light increased the investment of N in light harvesting systems and surprisingly, sustained a higher quantum yield of photosynthesis at low light, in spite of increased leakiness (Tazoe et al. 2006). In maize, Drozak and Romanowska (2006) reported that low light increased the ratio of PSII electron transport activity of bundle sheath chloroplasts relative to mesophyll from 0.15 to 0.20 and decreased the ratio of PSI electron transport from 1.94 to 1.70. Larger increases in the PSII-associated light harvesting components of mesophyll and bundle sheath cells were observed, with little change in PSI antennae. The range of photosystem plasticity seems limited, but seems to compensate the bioenergetics of CO_2 assimilation.

5. Distribution of Light Absorption in C_4 Leaves

Terashima and Saeki (1983) first showed that monochromatic light was attenuated in direct proportion to the cumulative chlorophyll content of a C_3 leaf. Careful paradermal sectioning of spinach leaves demonstrated that chloroplasts differed vertically through the leaf, both biochemically and ultrastructurally (Terashima and Inoue 1985a, b). Evans and Vogelmann (2003) measured profiles of light absorption more directly by quantifying chlorophyll fluorescence images of transversely cut faces obtained when blue or green or blue light was applied to the abaxial or adaxial surface of spinach leaves.

However, the anatomy of C_4 leaves means that bundle sheath chlorophyll is generally shielded by the surrounding mesophyll cells. Therefore, one would expect that relatively less light would be absorbed per chlorophyll in the bundle sheath compared with the mesophyll. To investigate this, Evans et al. (2007) used the above techniques to image chlorophyll fluorescence emitted from the cut transverse face of leaves *F. bidentis*. Three images are shown in Figure 5*A*. Under epi-illumination, light is directed onto the transverse face through the microscope lens, which also captures the fluorescence. The distribution of fluorescence represents that of chlorophyll. Bright fluorescence can be seen throughout the mesophyll. The fluorescence is less in the bundle sheath because of reduced PSII content (cf. Fig. 3). By applying light to the adaxial surface, the fluorescence image reveals the gradient in light absorption through the leaf. Blue light is strongly absorbed by chlorophyll and is rapidly scattered on entry into the leaf. This results in intense fluorescence near the adaxial surface, but little fluorescence from the lower half of the leaf. In contrast, green light penetrates further into the leaf and some fluorescence is still emitted from chloroplasts near the lower surface.

The profile of fluorescence across the leaf was quantified from *F. bidentis* images by sampling transects through mesophyll or vascular tissue (Fig. 5*B*). Depth was measured from the boundary between the epidermis and mesophyll. Under blue light, fluorescence declines rapidly, falling below 20 % within 40 µm through the mesophyll. In contrast, it takes about 300 µm for blue light absorption to decline by a similar amount in leaves of *Spinacia oleracea* (Fig. 4*B*; Evans and Vogelmann 2003). Thus a C_4 leaf like *F. bidentis* absorbs light very efficiently over a short distance in comparison to the much thicker spinach leaves (Fig. 5).

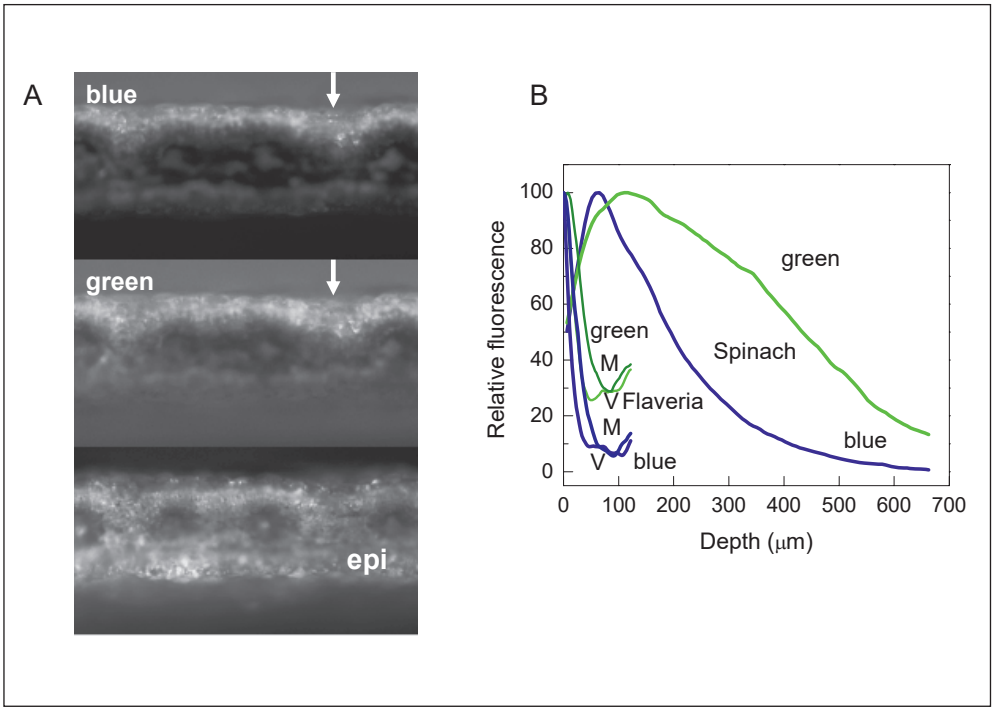

Fig. 5 Fluorescence (680 nm) images of the transverse face of *Flaveria bidentis*. (*A*) The adaxial surface of the leaf was irradiated with monochromatic blue or green light while fluorescence exiting from the transversely cut face of the leaf was imaged. Then light perpendicular to the transverse face was applied to capture the epi-illumination fluorescence image. (*B*) Quantitative analysis of the fluorescence images in (*A*). Chlorophyll fluorescence profiles through *Flaveria bidentis* leaves with sampling through veins (V) or mesophyll regions between veins (M) when blue or green light was applied to the adaxial surface. Data redrawn form (Evans et al. 2007). For comparison, similar fluorescence gradients through a spinach leaf are shown. Data were redrawn from Evans and Vogelmann 2003.

Green light penetrated further and significant amounts of green light reached the bundle sheath chloroplasts compared with relatively little blue light. The differential penetration of blue and green light into *F. bidentis* leaves led us to investigate the consequent effect on photosynthesis. We compared steady-state rates of CO_2 assimilation and photochemical efficiency under white, green, or blue light with equivalent incident photon fluxes (Fig. 6). Despite giving the same incident photon irradiance for each colour, the rates of CO_2 assimilation were lower under blue light by about 25 % for *Spinacia* (data not shown) and 50 % for *F. bidentis* (Evans et al. 2007). This was not reflected in the photochemical efficiency signal, which decreased by only 15 % (Fig. 5). This illustrates the fact that gas exchange integrates the flux through the depth of the leaf over a given area, while fluorescence records from a layer of chloroplasts near the adaxial surface. The results presented in Figure 6 suggest that the poor penetration of blue light into the bundle sheath cells did not allow for sufficient ATP formation in the bundle sheath to match the rate of CO_2 pumping. One would predict that leakiness should be greater under blue light than under green light and this prediction remains to be investigated. Our results highlight that bundle sheath and mesophyll experience very different light environments.

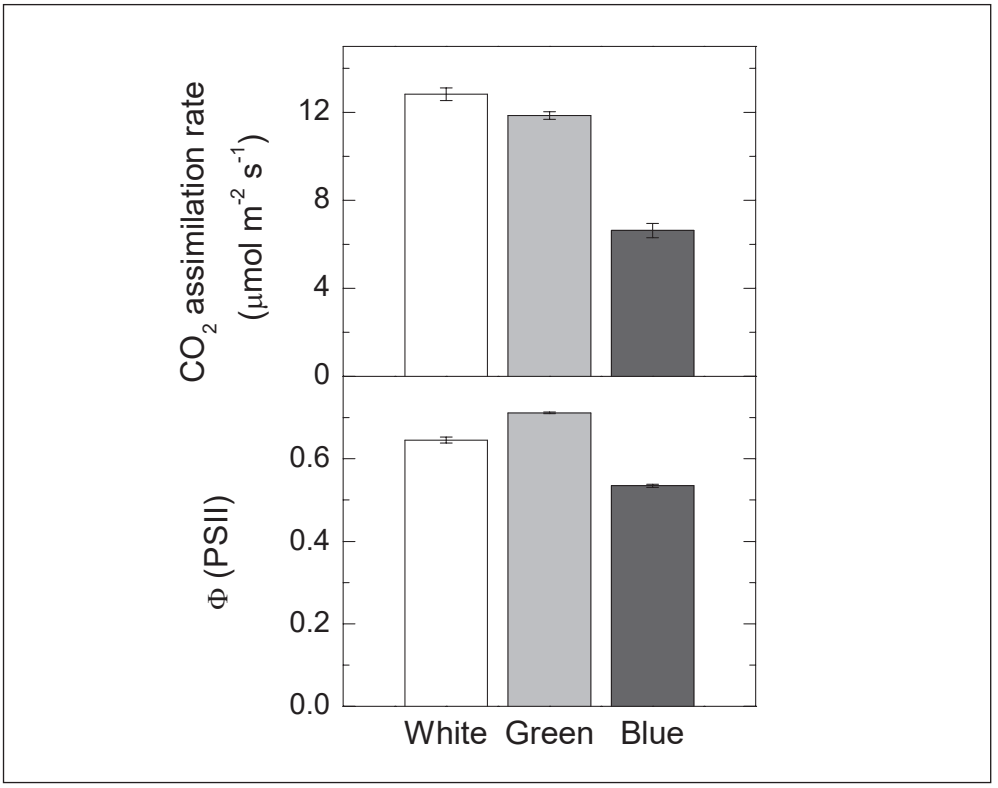

Fig. 6 Rates of CO_2 assimilation (μmol m^{-2} s^{-1}), and photochemical efficiency, φPSII, for leaves of *Flaveria bidentis* measured under different-coloured light (mean ± s. e., n = 3). Measurement conditions were 370 μmol CO_2 mol^{-1}, 12 – 15 mbar leaf to air vapour pressure difference, and a leaf temperature of 25 ºC. Photochemical efficiency was measured with a PAM fluorometer using a blue modulated light. Data redrawn from Evans et al. 2007.

6. Whole Leaf Chlorophyll Fluorescence, What Do We See?

A close relationship between chloroplast electron transport estimated from chlorophyll fluorescence and CO_2 assimilation rate was first demonstrated for *Zea mays* by Genty et al. 1992 and Edwards and Baker 1993. Surprisingly, the differences in chlorophyll and PSII distribution between mesophyll and bundle sheath cells amongst the different biochemical subtypes is not apparent when rates of chloroplast electron transport estimated from chlorophyll fluorescence are correlated with measurements of CO_2 assimilation rates (Krall and Edwards 1990). Likewise, the changes in PSII and PSI light harvesting and electron transport activity in *Z. mays* grown at different light intensities had little impact on light dependence of PSII efficiency estimated by fluorescence, although low light grown leaves had about 30 % lower capacity for nonphotochemical quenching at high light (Drozak and Romanowska 2006).

Comparison of mass spectrometric measurements of gross O_2 evolution (originating form PSII) with measurements of chloroplast electron transport by chlorophyll fluorescence shows an almost one to one relationship (Fig. 7*A*; Siebke et al. 2003), whereas chloroplast electron transport measured with chlorophyll fluorescence overestimates gross CO_2 uptake slightly

(Fig. 7*B*). This can probably be explained by the significant amount of light dependent O_2 uptake via the Mehler reaction which was 18 % of gross O_2 evolution (Fig. 8). Leaf discs of a number of C_4 grasses of either the NAD-ME or NADP-ME biochemical subtypes showed a linear dependence of ^{18}O uptake on light intensity, and no differences between subtypes was observed (Siebke et al. 2003). These studies confirm earlier indications of uniformly lower quantum yield of O_2 evolution in different C_4 types compared with C_3 plants (Demmig and Björkman 1987).

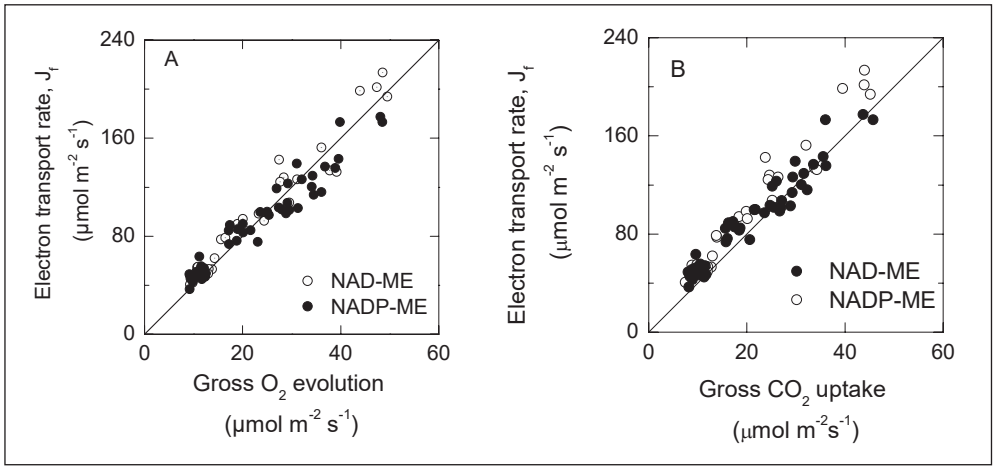

Fig. 7 Electron transport rate, J_f, calculated from fluorescence measurements as a function of gross O_2 evolution (*A*) or gross CO_2 uptake (*B*). Measurements were made on leaf discs at high CO_2 at different irradiances and with different species. NAD-ME species (open circles) used were*: Astrebla lappacea*, *Eleusine coracana*, *Eragrostis superba*, *Leptochloa dubia*, *Panicum coloratum*; (*B*) NADP-ME species (closed circles) used were: *Bothriochloa biloba*, *Bothriochloa bladhii*, *Cenchrus ciliaris*, *Dichanthium sericeum*, *Panicum antidotale*, *Paspalum notatum*, *Pennisetum alopecuroides*, *Sorghum bicolor*. Lines show the four to one relationships. Data are taken from Siebke et al. 2003.

7. Heterogeneity and the Ecology and Evolution of C_4 Plants

The above experiments suggest that we must search for other factors to explain clearly differentiated correlations of abundance in C_4 types with annual precipitation (Hattersley 1982, Henderson et al. 1992). For example, it now seems that the decline in relative abundance of C_4 grasses (relative to C_3) in response to decreasing rainfall in South Africa, even though C_4 plants have higher water use efficiency when water is available, may be attributed to the greater drought sensitivity of C_4 pathway metabolism (B. Ripley and C. Osborne, personal communication). Analogous constraints may explain the correlations between growing season minimum temperatures and C_4 grass distribution along longitudinal and altitudinal gradients (Teeri and Stowe 1976). It is already clear that these are not associated with different temperature-quantum yield relationships among C_4 types, but involve complex interactions with development of the whole photosynthetic apparatus. The NAD-ME C_4 dicots may be the most cool tolerant of all (Caldwell et al. 1977, Osmond et al. 1980, 1982). There have been few studies of nitrogen use efficiency and environment in C_4 plants, even in crop plants. Wong and Osmond (1991) explored some competitive interactions between wheat and pearl

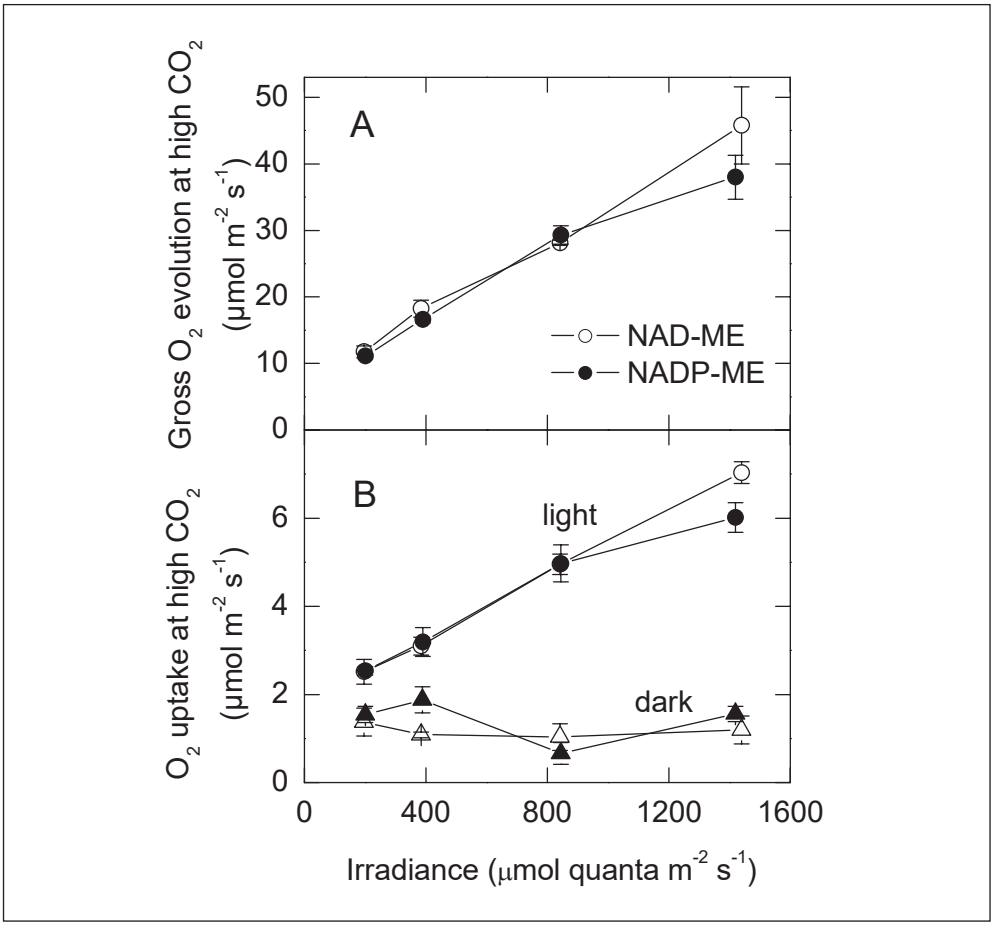

Fig. 8 Light dependence of O_2 exchange in NAD-ME (*open symbols*) and NADP-ME (*closed symbols*) grasses. (*A*) Gross O_2 evolution at 1–2 % CO_2; (*B*) Gross O_2 uptake at 1–2 % CO_2 (*circles*) and O_2 uptake in the dark (*triangles*) measured on corresponding leaf discs at 30 °C and 21 % O_2. (NAD-ME species used were *Eragrostis superba*, *Leptochloa dubia*, *Panicum coloratum*; and NADP-ME species used were *Dichanthium sericeum*, *Pennisetum alopecuroides*, *Panicum antidotale*, *Cencrus ciliaris*.) Symbols indicate average of 1–4 measurements per species and light intensity; error bars are standard errors calculated on the average of species. The Figure is adapted from Siebke et al. 2003.

millet in relation to nitrogen use efficiency and elevated atmospheric [CO_2], with emphasis on carbon partitioning belowground in relation to nutrient uptake. Overall, enormous scope remains for exploration of these relationships in common garden and competition experiments.

We should not be dissuaded from further measurement and modeling of the functional significance of heterogeneity in these systems. Some unresolved molecular and cellular issues include accumulation of starch in mesophyll cells in response to low temperature and evaluation of lateral diffusion of CO_2 in C_4 monocots and dicots. Although heterogeneity in the C_4 pathway may not matter with respect leaf-level photosynthetic performance, it may well matter in relation to environmental tolerance limits during development and senescence

as we scale up from the leaf to the landscape. At bottom, we need to remember that natural selection brings the whole environment to act upon the whole genome throughout the whole of development, survival and reproduction of the organism.

Crossing experiments with C_3 and C_4 *Atriplex* spp. at the Carnegie Department of Plant Biology in the 1970s yielded a huge array of anatomical and biochemical heterogeneity in some 300 F1-F3 hybrids. However, none showed the assembly of a functional "C_4 syndrome"; all retained CO_2 compensation points and $\delta^{13}C$ values similar to the C_3 parent (Osmond et al. 1980). Naturally occurring C_3-C_4 intermediates also show C_3-like $\delta^{13}C$ values, but a range of intermediate CO_2 compensation points, suggesting a variety of partly functional C_4-like CO_2-concentrating mechanisms (Monson and Rawsthorne 2000). Recent studies of the genus *Heliotropium* have gone one step further, making detailed assessments of the relationships between intermediate CO_2 compensation points, CO_2 fixation rates under limiting and saturating CO_2, water use efficiency and ecological niches (Vogan et al. 2007). These authors are thus closing on the mechanisms of evolution of C_4 plants, and speculate that there may be "only a few viable levels of intermediacy" (i.e., only a few viable "natural structures") and that natural selection from C_3 to C_4 proceeds in steps defined by a few functional assemblages of the elements of heterogeneity.

8. Conclusions

Spatial and functional heterogeneity is a feature of the photosynthetic apparatus at all scales, from the molecular ecology of antennae and reaction centers responsible for solar energy transduction in thylakoid membranes of chloroplasts, to the structure of leaf tissues, to the display of leaves and to canopy architecture (Osmond et al. 1999). There is a remarkable range of heterogeneity in the leaves of C_4 plants considered here, but is it reflected in functional diversity at larger scales; in selective advantage in the way different types of C_4 plants respond to gradients of water, nutrient and light availability in the environment?

- In spite of substantial differences in the anatomical and biochemical heterogeneity in different C_4 types their CO_2-concentrating mechanisms confer similar improvements in water use efficiency under comparable conditions (Ghannoum et al. 2002).
- Higher nitrogen use efficiency is also a feature of all C_4 types, and is reflected in different patterns of nitrogen allocation between thylakoid and soluble proteins in mesophyll and bundle-sheath chloroplasts in leaves of different types.
- The heterogeneity of chlorophyll and photosystem distribution in different C_4 types is integrated by chlorophyll fluorescence measurements from the thin leaves. However, the relationship between photosynthetic electron transport and CO_2 and O_2 exchange rates that emerges from these measurements is similar, in spite of the heterogeneity among components of the light and dark reactions of photosynthesis in NADP- and NAD-ME C_4 types (Siebke et al. 2003). Substantial light dependent electron flow to O_2 (Mehler reaction) is a feature of both NADP- and NAD-ME C_4 types.

The studies reviewed here confirm that the anatomical and biochemical heterogeneity among C_4 types reflects natural selection of diverse pathways that confer a similar and robust leaf-level advantage with respect to water and nutrient economy of CO_2 assimilation and light use in a low CO_2, high O_2 atmosphere. In terms of Piaget (1971) these leaf-level "natural

structures" represent the essence of "operational structuralism" within C_4 plants otherwise known as the "C_4 syndrome". In spite of having arisen multiple times in unrelated taxa, there has been remarkable functional convergence such that we cannot associate specific selective advantages with heterogeneity among C_4 types in relation to leaf-environment interactions. In scaling up to the leaf level and beyond, for most practical purposes, the C_4 pathway becomes somewhat less than the sum if its parts.

Passioura (1979) argued for better communication between molecular, organismal and ecological levels of enquiry in plant sciences to achieve more accountable outcomes. Shortly afterwards, the first steps were taken to apply integrative leaf-level methods, such as stable isotopes to scale up CO_2 and H_2O exchange (the dark reactions of photosynthesis), and chlorophyll fluorescence (the light reactions) to evaluate the significance of heterogeneity in photosynthetic systems. Today, the physiological bases of C_3 and C_4 photosynthesis (Farquhar and Richards 1984) have assisted selection of more water use efficient varieties of wheat now released to Australian farmers, and now inform "big leaf" models of regional and global carbon and water vapor fluxes using $\delta^{13}C$ and ^{18}O signatures in atmospheric CO_2 (Lloyd and Farquhar 1993, Lin et al. 1998). Although the CO_2-concentrating mechanisms of the C_4 pathway clearly mitigates O_2 uptake by Rubisco, substantial O_2 uptake involving photosynthetic electron transport in the Mehler reaction persists in these plants (Siebke et al. 2003). The $\delta^{18}O$ signature of photosynthetic electron flow to O_2 might help refine global insights into the steady state difference between the isotopic composition of atmospheric oxygen and its ultimate source in water (the "Dole effect", Guy et al. 1993, Bender et al. 1994), particularly in the face of accelerating elevated atmospheric [CO_2]. Moreover, the leaf-level advantages conferred by the heterogeneity of the C_4 pathway also need careful further evaluation in relation to rising [CO_2] (Wong and Osmond 1991, Henderson et al. 1992, Ghannoum et al. 2001). Clearly, the functional importance of photosynthetic heterogeneity in leaves may yet have much to offer in scaling from the molecule to the biosphere.

Acknowledgements

We thank Britta Förster for translation of the abstract, Rod Whitty and Brian Gunning for the micrographs in Figures 1 and 2, and are indebted to John Evans, Oula Ghannoum, Katharina Siebke and Tom Vogelmann for their stimulating inputs to the above topics over many years. In the process of preparing this review we were reminded of the outstanding early contributions to our appreciation of biochemical and cellular aspects of heterogeneity in C_4 pathway from Canadian scientists, especially the late Bruce Tregunna and John Downton, summarized in Downton (1971). We also wish to dedicate this contribution to the affectionate memory of K. C. (Casey) Woo (Woo et al. 1970) who died unexpectedly in October 2008.

References

Andrews, T. J., Lorimer, G. H., and Tolbert, N. E.: Incorporation of molecular oxygen into glycine and serine during photorespiration in spinach leaves. Biochemistry *10*, 4777–4782 (1971)

Andrews, T. J., and Lorimer, G. H. (Eds.): Rubisco: Structure, mechanisms, and prospects for improvement. In: Hatch, M. D., and Boardman, N. K.: The Biochemistry of Plants: A Comprehensive Treatise. Vol. *10*, Photosynthesis; pp. 131–218. New York: Academic Press 1981

Badger, M. R., and Price, G. D.: The CO_2 concentrating mechanism in cyanobacteria and microalgae. Physiologia Plantarum *84*, 606–615 (1992)

Bender, M., Sowers, T., and Labeyrie, L.: The dole effect and its variations during the last 130,000 years as measured in the vostok ice core. Global Biogeochem. Cycles *8*, 363–376 (1994)

Caldwell, M. M., Osmond, C. B., and Nott, D. L.: C_4 pathway photosynthesis at low temperature in cold-tolerant *Atriplex* species. Plant Physiol. *60*, 157–164 (1977)

Caemmerer, S. von, Evans, J. R., Cousins, A. B., Badger, M. R., and Furbank, R. T.: C_4 photosynthesis and CO_2 diffusion. In: Sheehy, J. E., Mitchell, P. L., and Hardy, B. (Eds.): Reconfiguring the Rice Plant's Photosynthetic Pathway. Phillipines: IRRI 2007

Caemmerer, S. von, and Furbank, R. T.: The C_4 pathway: an efficient CO_2 pump. Photosynthesis Res. *77*, 191–207 (2003)

Cousins, A. B., Badger, M. R., and Caemmerer, S. von: C_4 photosynthetic isotope exchange in NAD-ME and NADP-ME type grasses. J. Exp. Bot. (submitted 2007)

Demmig, B., and Björkman, O.: Photon yield of O_2 evolution and chlorophyll fluorescence characteristics at 77K among vascular plants of diverse origins. Planta *170*, 489–501 (1987)

Downton, W. J. S.: Adaptive and Evolutionary Aspects of C_4 Photosynthesis. In: Hatch, M. D., Osmond, C. B., and Slatyer, R. O. (Eds.): Photosynthesis and Photorespiration; pp. 3–17. New York: Wiley-Interscience 1971

Drozak, A., and Romanowska, E.: Acclimation of mesophyll and bundle sheath chloroplasts of maize to different irradiances during growth. Biochim. Biopys. Acta *1757*, 1539–1546 (2006)

Duarte, H. M., Jakovljevic, I., Kaiser, F., and Lüttge, U.: Lateral diffusion of CO_2 in leaves of the crassulacean acid metabolism plant *Kalanchoë daigremontiana* Hamet et Perrier. Planta *220*, 809–816 (2005)

Edwards, G. E., and Baker, N. R.: Can CO_2 assimilation in maize leaves be predicted accurately from chlorophyll fluorescence analysis? Photosynthesis Res. *37*, 89–102 (1993)

Edwards, G. E., Furbank, R. T., Hatch, M. D., and Osmond, C. B.: What does it take to be C_4? Lessons from the evolution of C_4 photosynthesis. Plant Physiol. *125*, 46–49 (2001)

Edwards, G. E., Franceschi, V. R., and Voznesenskaya, E. V.: Single-cell C_4 photosynthesis versus the dual-cell (Kranz) paradigm. Annu. Rev. Plant Biol. *55*, 173–196 (2004)

Edwards, G. E., Huber, S. C., Ku, S. B., Rathnam, C. K. M., Gutierrez, M., and Mayne, B. C.: Variation in photochemical activities of C_4 plants in relation to CO_2 fixation. In: Burris, R. H., and Black, C. C. (Eds.): CO_2 Metabolism and Plant Productivity; pp. 83–112. Baltimore: University Park Press 1976

Ehleringer, J. R., and Björkman, O.: Quantum yields for CO_2 uptake in C_3 and C_4 plants. Plant Physiol. *59*, 86–90 (1977)

Ellis, R. P., Vogel, J. C., and Fuls, A.: Photosynthetic pathway and the geographic distribution of grasses in South Afrika/Nambia. South African J. Science *76*, 307–314 (1980)

Evans, J. R., and Caemmerer, S. von: Carbon dioxide diffusion inside leaves. Plant Physiol. *110*, 339–346 (1996)

Evans, J. R., Terashima, I., Hanba, Y. T., and Loreto, F.: Chloroplast to leaf. In: Smith, W. K., Vogelmann, T. C., and Chritchley, C. (Eds.): Ecological Studies, Photosynthetic Adaptation, Chloroplast to Landscape. Vol. *178*. Berlin: Springer 2004

Evans, J. R., and Vogelmann, T. C.: Profiles of C-14 fixation through spinach leaves in relation to light absorption and photosynthetic capacity. Plant Cell Environ. *26*, 547–560 (2003)

Evans, J. R., Vogelmann, T. C., and Caemmerer, S. von: Balancing light capture with distributed metabolic demand during C4 photosynthesis. In: Sheehy, J. E., Mitchell, P. L., and Hardy, B. (Eds.): Reconfiguring the Rice Plant's Photosynthetic Pathway. Philippines: IRRI 2007

Farquhar, G. D.: On the nature of carbon isotope discrimination in C_4 species. Aust. J. Plant Physiol. *10*, 205–226 (1983)

Farquhar, G. D., and Richards, R. A.: Isotopic composition of plant carbon correlates with water-use efficiency of wheat genotypes. Aust. J. Plant Physiol. *11*, 539–552 (1984)

Genty, B., Goulas, Y., Dimon, B., Peltier, G., Briantais, J. M., and Moya, I.: Modulation of efficiency of primary conversion in leaves, mechanisms at PS2. In: Murata, N. (Ed.): Research in Photosynthesis. Vol. *IV*; pp. 603–610. Dordrecht: Kluwer 1992

Ghannoum, O., Caemmerer, S. von, and Conroy, J. P.: Plant water use efficiency of 17 Australian NAD-ME and NADP-ME C-4 grasses at ambient and elevated CO2 partial pressure. Aust. J. Plant Physiol. *28*, 1207–1217 (2001)

Ghannoum, O., Caemmerer, S. von, and Conroy, J. P.: The effect of drought on plant water use efficiency of nine NAD-ME and nine NADP-ME Australian C-4 grasses. Funct. Plant Biol. *29*, 1337–1348 (2002)

Ghannoum, O., Evans, J. R., Chow, W. S., Andrews, T. J., Conroy, J. P., and Caemmerer, S. von: Faster rubisco is the key to superior nitrogen-use efficiency in NADP-malic enzyme relative to NAD-malic enzyme C-4 grasses. Plant Physiol. *137*, 638–650 (2005)

Ghirardi, M. L., and Melis, A.: Photosystem electron transport capacity and light harvesting antenna size in maize chloroplasts. Plant Physiol. *74*, 993–998 (1984)

Gunning, B. E. S.: Plant Cell Biology on DVD. www.plantcellbiologyonDVD.com ISBN 978-0-9751682-1-9 (2007)

Gunning, B., Koenig, F., and Govindjee: A dedication to pioneers of research on chloroplast structure. In: Weise, R. R, and Hoober, K. J. (Eds): The Structure and Function of Plastids. Advances in Photosynthesis and Respiration. Vol. *23*; pp. xxiii-xxix. Dordrecht: Springer 2006

Guy, R. D., Fogrl, M. L., and Berry, J. A.: Photosynthetic fractionation of the stable isotopes of oxygen and carbon dioxide. Plant Physiol. *101*, 37–47 (1993)

Haberlandt, G.: Physiologische Pflanzenanatomie; 650 pp., 4. Aufl. Leipzig: Engelmann 1909

Hatch, M. D.: C_4 photosynthesis: A unique blend of modified biochemistry, anatomy and ultrastructure. Biochim. Biophys. Acta *895*, 81–106 (1987)

Hatch, M. D., Kagawa, T., and Craig, S.: Subdivision of C_4-pathway species based on differing C_4 acid decarboxylating systems and ultrastructural features. Aust. J. Plant Physiol. *2*, 111–128 (1975)

Hatch, M. D., and Osmond, C. B.: Compartmentation in C_4 photosynthesis. In: Heber, U., and Stocking, C. R. (Eds.): Encyclopedia of Plant Physiology (New Series). Vol. *3*; pp. 144–184. Heidelberg: Springer 1976

Hattersley, P.: $\delta^{13}C$ values of C_4 types in grasses. Aust. J. Plant Physiol. *9*, 139–154 (1982)

Hattersley, P. W.: The distribution of C_3 and C_4 grasses in Australia in relation to climate. Oecologia *57*, 113–128 (1983)

Hattersley, P. W.: C_4 photosynthetic pathway variation in grasses (Poaceae) its significance for arid and semi-arid lands. In: Chapman, G. P. (Ed.): Grass Evolution and Diversification; pp. 181–212. London: Academic Press 1992

Hattersley, P. W., and Watson, L.: Anatomical parameters for predicting photosynthetic pathways of grass leaves: The "maximum lateral cell count" and the "maximum cells distant count". Phytomorphology *25*, 325–333 (1975)

Henderson, S., Caemmerer, S. von, and Farquhar, G. D.: Short-term measurements of carbon isotope discrimination in several C_4 species. Aust. J. Plant Physiol. *19*, 263–285 (1992)

Henderson, S., Hattersley, P., Caemmerer, S. von, and Osmond, C. B.: Are C_4 pathway plants threatened by global climatic change? In: Schulze, E.-D., and Caldwell, M. M. (Eds.): Ecophysiology of Photosynthesis, Ecological Studies. Vol. *100*; pp. 529–549. Heidelberg: Springer 1994

Krall, J. P., and Edwards, G. E.: Quantum yields of photosystem II electron transport and carbon fixation in C_4 plants. Aust. J. Plant Physiol. *17*, 579–588 (1990)

Leegood, R. C., Caemmerer, S. von, and Osmond, C. B.: Metabolite transport and photosynthetic regulation in C_4 and CAM plants. In: Dennis, D. T., Turpin, D. H., Leferbvre, D. D., and Layzell, D. B. (Eds.): Plant Metabolism; pp. 341–369. Burnt Mill: Longman 1997

Lin, G. H., Marino, B. D. V., Wei, Y. D., Adams, J., Tubiello, F., and Berry, J. A.: An experimental and modeling study in responses of ecosystems carbon exchanges to increasing CO_2 concentrations using a tropical rainforest mesocosm. Aust. J. Plant Physiol. *25*, 547–556 (1998)

Lloyd, J., and Farquhar, G. D.: ^{13}C Discrimination during CO_2 assimilation by the terrestrial biosphere [Review]. Oecologia *99*, 201–215 (1994)

Long, S. P.: Environmental responses. In: Sage, R. F., and Monson, R. (Eds.): C_4 Plant Biology; pp. 215–250. San Diego: Academic Press 1999

Makino, A., Sakuma, H., Sudo, E., and Mae, T.: Differences between maize and rice in N-use efficiency for photosynthesis and protein allocation. Plant Cell Physiol. *44*, 952–956 (2003)

Mayne, B. C., Dee, A., and Edwards, G. E.: Distribution of photochemical activities between mesophyll protoplasts and bundle sheath cells of C_4 plants. Plant Physiol. *28* (1974)

Meierhoff, K., and Westhoff, P.: Differential biogenesis of photosystem-II in mesophyll and bundle-sheath cells of monocotyledonous NADP-malic enzyme-type C_4 plants – the non-stoichiometric abundance of the subunits of photosystem-II in the bundle-sheath chloroplasts and the translational activity of the plastome-encoded genes. Planta *191*, 23–33 (1993)

Monson, R. K., and Rawsthorne, S.: C_3-C_4 intermediate photosynthesis. In: Leegood, R. C., Sharkey, T. S. and Caemmerer, S. von (Eds.): Photosynthesis, Physiology and Metabolism; pp. 533–550. Dordrecht: Kluwer Academic Publishers 2000

Morison, J. I. L., Gallouet, E., Lawson, T., Cornic, G., Herbin, R., and Baker, N. R.: Lateral diffusion of CO_2 in leaves is not sufficient to support photosynthesis. Plant Physiol. *139*, 254–266 (2005)

Naidu, S. L., Moose, S. P., Al-Shoaibi, A. K., Raines, C. A., and Long, S. P.: Cold tolerance of C_4 photosynthesis in Miscanthus × giganteus: Adaptation in amounts and sequence of C_4 photosynthetic enzymes. Plant Physiol. *132*, 1688–1697 (2003)

Nelson, E. A., Sage, T. L., and Sage, R. F.: Functional leaf anatomy of plants with crassulacean acid metabolism. Funct. Plant Biol. *32*, 409–419 (2005)

Osmond, C. B., Anderson, J. M., Ball, M. C., and Egerton, J. J. G.: Compromising efficiency: the molecular ecology of light resource utilisation in terrestrial plants. In: Press, M. C., Scholes, J. C., and Baker, M. (Eds.): Advances in Physiological Plant Ecology; pp. 1–24, Oxford: Blackwell 1999

Osmond, C. B., Björkman, O., and Anderson, D. J.: Physiological Processes in Plant Ecology: Towards a Synthesis with Atriplex. Ecological Studies. Vol. *36*. Heidelberg: Springer 1980

Osmond, B., Schwartz, O., and Gunning, B.: Photoinhibitory printing on leaves, visualised by chlorophyll fluorescence imaging and confocal microscopy, is due to diminished fluorescence from grana. Aust. J. Plant Physiol. *26*, 717–724 (1999)

Osmond, B., Winter, K., and Ziegler, H.: Functional Significance of different pathways of CO_2 fixation in photosynthesis. In: Lange, O. L., Nobel, P. S., Osmond, B., and Ziegler, H. (Eds.): Physiological Plant Ecology II, Encyclopedia of Plant Physiology New Series. Vol. *12B*; pp. 479–549. Heidelberg: Springer 1982

Passioura, J. B.: Accountability, philosophy and plant physiology. Search *10*, 347–350 (1979)

Piaget, J.: Structuralism. London: Routledge and Kegan Paul 1971

Pieruschka, R., Schurr, U., and Jahnke, S.: Lateral gas diffusion inside leaves. J. Exp. Bot. *56*, 857–864 (2005)

Rascher, U., Huett, M. T., Siebke, K., Osmond, B., Beck, F., and Luettge, U.: Spatiotemporal variation of metabolism in a plant circadian rhythm: The biological clock as an assembly of coupled individual oscillators. Proc. Natl. Acad. Sci. USA *98*, 11801–11805 (2001)

Sage, R. F.: The evolution of C-4 photosynthesis. New Phytol. *161*, 341–370 (2004)

Seemann, J. R., Badger, M. R., and Berry, J. A.: Variations in the specific activity of ribulose-1,5-bisphosphate carboxylase between species utilizing differing photosynthetic pathways. Plant Physiol. *74*, 791–794 (1984)

Siebke, K., Ghannoum, O., Conroy, J. P., Badger, M. R., and Caemmerer, S. von: Photosynthetic oxygen exchange in C-4 grasses: the role of oxygen as electron acceptor. Plant Cell Environ. *26*, 1963–1972 (2003)

Slack, C. R., Roughan, R. G., and Bassett, H. C. M.: Selective inhibition of mespohyll chloroplast development in some C_4 pathway species by low night temperature. Planta *118*, 67–73 (1974)

Smith, W. K., Nobel, P. S., Reiners, W. A., Vogelmann, T. C., and Critchley, C.: Summary and future perspectives. In: Smith, W. K., Vogelmann, T. C., and Critchley, C. (Eds.): Photosynthetic Adaptation Chloroplast to Landscape. Ecological Studies. Vol. *178*; pp. 297–309. New York: Springer 2004

Taub, D. R.: Climate and the US distribution of C_4 grass subfamilies and decarboxylation variants of C_4 photosynthesis. Amer. J. Bot. *87*, 1211–1215 (2000)

Taylor, A. O., and Craig, S.: Plants under climatic stress. II. Low temperature, high light effects on chloroplast ultrastructure. Plant Physiol. *47*, 719–725 (1971)

Tazoe, Y., Noguchi, K., and Terashima, I.: Effect of growth light and nitrogen nutrition on the organization of the photosynthetic apparatus in leaves of a C_4 plant Amaranthus cruentis. Plant Cell Environ. *29*, 691–700 (2006)

Tcherkez, G. G. B., Farquhar, G. D., and Andrews, T. J.: Despite slow catalysis and confused substrate specificity, all ribulose bisphosphate carboxylases may be nearly perfectly optimized. Proc. Natl. Acad. Sci. USA EFIRST DATE *27* (2006)

Teeri, J. A., and Stowe, L. G.: Climatic patterns and the distribution of C_4 grasses in North America. Oecologia *23* (1976)

Terashima, I., and Inoue, N.: Palisade tissure chloroplasts and spongy tissue chloroplasts in spinach: biochemical and ultrastructure differences. Plant Cell Physiol. *26*, 63–75 (1985a)

Terashima, I., and Inoue, Y.: Vertical gradient in photosynthetic properties of spinach chloroplasts dependent on intra-leaf light environment. Plant Cell Physiol. *24*, 1493–1501 (1985b)

Terashima, I., and Saeki, T.: Light environment within a leaf. 1. Optical properties of paradermal sections of *Camellia* leaves with special reference to differences in the optical properties of palisade and spongy tissues. Plant Cell Physiol. *24*, 1493–1501 (1983)

Terashima, I., Wong, S.-C., Osmond, C. B., and Farquhar, G. D.: Characterization of non-uniform photosynthesis induced by absissic acid in leaves having different mesophyll anatomies. Plant Cell Physiol. *29*, 385–394 (1988)

Vogan, P. J., Frohlich, M. W., and Sage, R. F.: The functional significance of C_3-C_4 intermediate traits in *Heliotropium* L. (Boraginaceae): gas exchange perspectives. Plant Cell and Environment *30*, 1337–1345 (2007)

Vogel, J. C., Fuls, A., and Ellis, R. P.: The geographic distribution of Kranz grasses in South Afrika. South African J. Sci. *74*, 209–215 (1978)

Wong, S. C., and Osmond, C. B.: Elevated atmospheric partial pressure of CO_2 and plant growth. III. Interactions between *Triticum aestivum* (C_3) and *Echinochloa frumentacea* (C_4) during growth in mixed culture under different CO_2, N nutrition and irradiance treatments, with emphasis on below-ground responses estimated using the $\delta^{13}C$ value of root biomass. Aust. J. Plant Physiol. *18*, 137–152 (1991)

Woo, K. C., Anderson, J. M., Boardman, N. K., Downton, W. J. S., Osmond, C. B., and Thorne, S. W.: Deficient photosystem II in agranal bundle sheath chloroplasts of C_4 plants. Proc. Natl. Acad. Sci. USA *67*, 18–25 (1970)

Prof. Susanne von Caemmerer
Molecular Plant Physiology Group
Research School of Biology
The Australian National University
Canberra ACT 0200
Australia
Phone: 0061 2 61255053
Fax: 0061 2 61255057
E-Mail: susanne.caemmerer@anu.edu.au

Prof. Dr. Barry Osmond
School of Biochemistry and Molecular Biology
The Australian National University
Canberra ACT 0200
Australia
Phone: 0061 2 62871487
Fax: 0061 2 61250313
E-Mail: barry.osmond@anu.edu.au

Festakt zur Ernennung der Deutschen Akademie der Naturforscher Leopoldina zur Nationalen Akademie der Wissenschaften

Ceremony to Mark the Nomination of the German Academy of Sciences Leopoldina to the National Academy of Sciences

Nova Acta Leopoldina N. F., Bd. *98*, Nr. 362
Herausgegeben vom Präsidium der Deutschen Akademie
der Naturforscher Leopoldina
(2009, 76 Seiten, 50 Abbildungen, 21,95 Euro,
ISBN: 978-3-8047-2551-5)

Die Deutsche Akademie der Naturforscher Leopoldina wurde am 14. Juli 2008 im Rahmen eines Festaktes in Halle zur Nationalen Akademie der Wissenschaften ernannt. Damit erhielt Deutschland – wie andere europäische Länder oder die USA – eine Institution, die Politik und Gesellschaft wissenschaftsbasiert berät und die deutsche Wissenschaft in internationalen Gremien repräsentiert. Der Band dokumentiert den Festakt mit der Übergabe der Ernennungsurkunde durch die Vorsitzende der Gemeinsamen Wissenschaftskonferenz und Bundesministerin für Bildung und Forschung Annette SCHAVAN. Er enthält die Reden von Bundespräsident Horst KÖHLER, Sachsens-Anhalts Ministerpräsident Wolfgang BÖHMER und Leopoldina-Präsident Volker TER MEULEN sowie den Festvortrag „Rolle und Verantwortung nationaler Akademien der Wissenschaften“ von Jules A. HOFFMANN, Präsident der Académie des sciences, Paris. Der Aufbau einer Nationalen Akademie ist ein richtungsweisender Schritt für die deutsche Forschungslandschaft, da für den kontinuierlichen Dialog von Wissenschaft und Politik eine solche Einrichtung erforderlich wurde. Der Publikation ist eine DVD mit dem Mitschnitt der Festveranstaltung beigefügt.

Wissenschaftliche Verlagsgesellschaft mbH Stuttgart

Nova Acta Leopoldina NF *96*, Nr. 357, 93–100 (2009)

Lateral Gas Diffusion inside Leaves: A Long Neglected Topic in Plant Physiology

Siegfried JAHNKE[1,2] and Roland PIERUSCHKA[1,3] (Jülich)

With 3 Figures

Abstract

A requirement for lateral gas movement inside leaves is the interconnectivity of intercellular air spaces which is a striking feature of homobaric leaves. Lateral diffusion of CO_2 in leaves has been shown to affect both gas exchange measurement and leaf CO_2 uptake. In particular under conditions of low stomatal conductance, studies using chlorophyll fluorescence imaging showed that laterally diffusing CO_2 from shaded parts can contribute to photosynthesis in illuminated leaf parts. We hypothesize that homobaric leaf anatomy is an adaptation to conditions of transitory drought and light stress.

Zusammenfassung

Eine Voraussetzung für laterale Gasflüsse in Blättern ist die durchgehende Vernetzung der Interzellularräume, welches ein auffallendes Merkmal homobarer Blätter darstellt. Es konnte gezeigt werden, dass laterale Diffusion von CO_2 sowohl Gaswechselmessungen als auch den Gasaustausch selbst beeinflussen kann. Aus Untersuchungen mit Hilfe der Chlorophyll-Fluoreszenz-Bildgebung konnte geschlossen werden, dass laterale CO_2-Diffusion aus beschatteten Bereichen zur Photosynthese in beleuchteten Blattbereichen beitragen kann. Dies ist insbesondere unter Bedingungen niedriger stomatärer Leitfähigkeit der Fall. Wir stellen die Hypothese auf, dass homobare Blattanatomie eine Adaptation an Standortfaktoren mit zeitweiligem Trocken- und Lichtstress darstellt.

1. Introduction

The supply of CO_2 to the photosynthetic active leaf cells is mainly by gas diffusion from the surrounding air through the stomata into the leaf mesophyll. Due to the preferential direction this can be denoted "vertical diffusion". However, once inside a leaf, gas molecules may also move laterally depending on the size and interconnectivity of the intercellular air space systems of the respective leaves. The internal leaf structure in this respect depends on the occurrence of bundle sheath extensions a term which, according to WYLIE (1952), was suggested by Katherine ESAU. Bundle sheath extensions reach from the upper to the lower leaf epidermis and define form and size of leaf internal compartmentation and thus the maximal possible range of lateral gas movement (WEYERS and LAWSON 1997). NEGER (1912) reported

1 Forschungszentrum Jülich GmbH, Institut für Chemie und Dynamik der Geosphäre (ICG), ICG-3: Phytosphäre, 52425 Jülich, Germany.
2 Universität Duisburg-Essen, Fachbereich Biologie und Geographie, 45117 Essen, Germany.
3 Carnegie Institution of Washington, Department of Global Ecology, 260 Panama St, 94305 Stanford, CA, USA.

that as early as in the last decades of the 19th century, HABERLANDT and WESTERMAIER made first reports on leaf structures which later on were called bundle sheath extensions. Leaves having bundle sheath extensions were named "heterobarisch" (heterobaric) by NEGER (1912). The bundles sheath extensions in such leaves are more or less free of intercellular air space and therefore inhibit lateral gas movement effectively. Leaves which lack bundle sheath extensions were denoted "homobarisch" (homobaric; NEGER 1912) and provide substantially less restrictions to lateral air movement than heterobaric leaves. NEGER (1918) measured lateral sizes of "air chambers" in hetero- and homobaric leaves and classified them into several groups and, more recently, leaf lamina compartmentation has been shown by WEYERS and LAWSON (1997). NEGER (1918) reported that bundle sheath extensions were differently reflected in leaves grown under different light intensities: Fewer bundle sheath extensions were observed in shade than in sun leaves which was also supported by WYLIE's studies (WYLIE 1951). WYLIE (1952) investigated 348 plant species based on microscopic analysis of leaf anatomy and classified 40 % of the species homobaric and, in these early days, already considered that the occurrence of bundle sheath extensions might have consequences for "lateral gas movement" inside leaves. MEIDNER (1955) performed studies on homobaric leaves with an air-flow porometer and observed lateral air movement over distances of 0.5 (max. 2.5) mm. Further studies on lateral diffusion inside leaves were resumed after a long time gap in the 1990s. Lateral gas diffusion on the micrometer scale was considered to have an impact on stomatal patchiness (e.g. DOWNTON et al. 1988, TERASHIMA et al. 1988, and many others) and many aspects of gas diffusion inside leaves were broadly discussed later on in a review by PARKHURST (1994). Here we propose that lateral gas diffusion in leaves should receive more attention for various reasons. It may impair gas exchange measurements, in particular, when small clamp-on leaf chamber are used causing annoying artifacts. It might also have physiological consequences on the gas-exchange performance of homobaric leaves under certain environmental conditions or at the specific growth locations within canopies of individual plants. We are convinced that lateral gas diffusion in leaves could substantially influence plant performance which has not been adequately accounted for so far.

2. Effects on Gas Exchange Measurement

Starting in the 1990s numerous reports appeared in the literature claiming that an increase in atmospheric CO_2 concentration (c_a) has an impact on plant respiration in the dark. Most publications reported a substantial decrease in plant respiration rate when the ambient c_a of about 370 ppm was experimentally doubled to approximately 700 ppm as expected by Intergovernmental Panel on Climate Change (IPCC) scenarios at the end of the 21th century. Most of the reports were summarized in a review of AMTHOR (1997). These reports were the starting point for our interest in the so-called direct effect of CO_2 concentration on respiration in the dark. In a first series of experiments performed with heterobaric leaves of *Phaseolus vulgaris* and *Populus x deltoides* we were able to show that atmospheric CO_2 concentration had no effect on respiration up to 4000 ppm (JAHNKE 2001). These findings were obtained with a conventional gas exchange system based on the detection of CO_2 concentration. These results were confirmed by an independent method using an oxygen analyzer with high sensitivity (1 ppm resolution) showing that also the respiratory exchange of oxygen (O_2) was not affected by changes in atmospheric CO_2 concentration (AMTHOR et

al. 2001, Davey et al. 2004). Due to these observations we were convinced that a direct CO_2 effect on dark respiration does not exist.

However, apparent dark respiration rates with mature homobaric leaves of *Nicotiana tabacum* were significantly reduced due to lateral CO_2 diffusion in the mesophyll when atmospheric CO_2 concentration was increased inside the clamp-on leaf chamber (Jahnke and Krewitt 2002). This was the first report that lateral gas diffusion inside leaves may have an impact on gas-exchange measurements over the distance of leaf-chamber sealing (i.e. several millimeters), and the measured effect of elevated CO_2 on respiration was simply an artifact. When the CO_2 concentration was increased not inside but outside the leaf chamber, the measured respiration rate apparently increased, whereas, when the CO_2 concentration was similar inside and outside of the leaf chamber, the respiration rate was not altered and independent of the CO_2 concentration (Fig. 1). This apparent CO_2 dependency of measured respiration rate was only observed when homobaric leaves were investigated with clamp-on leaf chambers where only a leaf part is enclosed inside the leaf chamber; it was absent when the entire leaves were enclosed (Jahnke and Pieruschka, unpublished) and no such effect was found on heterobaric leaves (Jahnke 2001). Both observations indicate that the "direct CO_2 effect" was simply caused by lateral CO_2 movement when homobaric leaves were measured. On the other hand, most reports about the "direct CO_2 effect" on respiration (cf. Amthor 1997) were based on measurements on heterobaric leaves where the influence of lateral CO_2 diffusion can be definitely excluded. We assume that these measurement errors were based on technical problems of gas exchange systems with clamp-on leaf chambers which are simple and easy to use but prone to errors. Leakage through gaskets or at the interface between the gaskets have been discussed in that context (Rodeghiero et al. 2007, Flexas et al. 2007) but leakage between leaf surfaces and the gaskets is even more likely (Jahnke 2001). Furthermore, there is a number of other instrumental issues which may contribute to erroneous measurements such as non-linearities of infrared gas analysers (IRGA), memory effects of gas exchange systems or shortcomings in calibration of the water vapour pressure effect ("CO_2 dilution effect") on measured CO_2 concentration (Jahnke 2001). In order to minimize the effect of lateral CO_2 diffusion on gas exchange measurements with homobaric leaves when clamp-on leaf chambers are used, we applied a controlled overpressure inside the leaf chamber (Jahnke and Pieruschka 2006). Measuring respiration in the dark when stomata are mostly closed overpressure completely eliminated any measurement artefacts. However, in the light stomata are open and overpressurizing the leaf chamber led to substantial lateral net gas flux via the leaf mesophyll causing a substantial (apparent) reduction in measured photosynthetic CO_2 uptake. This effect was clearly dependent on stomatal conductance and overpressure is therefore not a suitable tool to reduce the drawbacks associated with the use of clamp-on leaf chambers (Jahnke and Pieruschka 2006).

3. Impact on Photosynthesis

When homobaric leaves of *Vicia faba* were measured with a clamp-on leaf chamber, shading or illuminating of leaf parts outside of the chamber influenced the assimilation rates measured inside the leaf chamber (Fig. 2; see also Pieruschka et al. 2006). When shaded, the internal CO_2 concentrations in the leaf parts outside the leaf chamber ($c_{i,o}$) is higher than in the clamped illuminated leaf area ($c_{i,i}$) causing a gradient and a net CO_2 flux into the clamped leaf

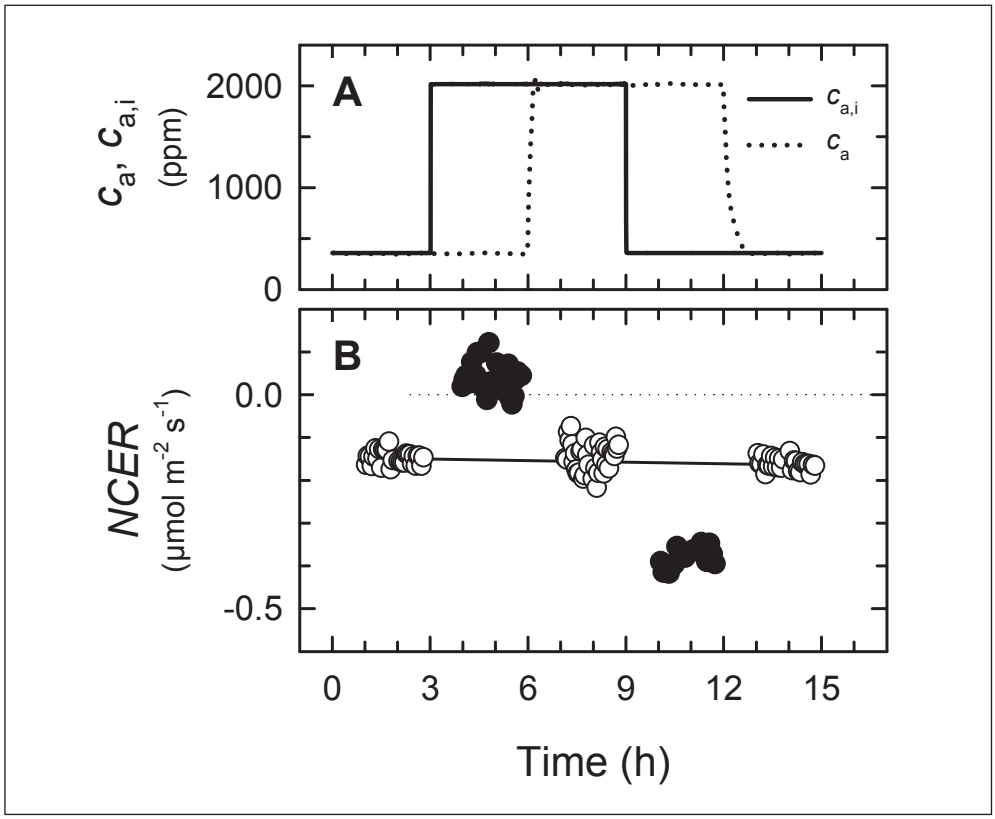

Fig. 1 Net CO_2 exchange rate (*NCER*) of a homobaric leaf of *Vicia faba* measured in the dark with a clamp-on leaf chamber. In (*A*), the experimentally manipulated atmospheric CO_2 concentration outside (c_a) and inside ($c_{a,i}$) the leaf chamber is presented. The *NCER*s obtained at the various CO_2 concentrations are shown in (*B*). Modified after Fig. 2 of Jahnke and Pieruschka 2006.

part. Such leaf internal CO_2 exchange is not detectable with conventional gas exchange measurements. Here, it was indirectly measured by a decrease in assimilation rate when the outer leaf parts were shaded as compared to measurement with illuminated outer leaf parts (Fig. 2*A*). In heterobaric leaves, lateral CO_2 exchange is hindered by the bundle sheath extensions and therefore no similar effect of shading or lightening the leaf parts outside the leaf chamber on measured assimilation rate of the clamped leaf part was observed (Fig. 2*B*).

Based on these observations it was assumed that lateral gas diffusion in leaves might be most effective under conditions when stomatal conductance is low. To evaluate the influence of lateral diffusion on photosynthetic performance of leaves with different stomatal conductances, chlorophyll fluorescence imaging studies were conducted to monitor the quantum yield of photosystem II (Φ_{PSII}) at a light/shade border (Pieruschka et al. 2006). When a *Vicia faba* plant was exposed to drought stress, Φ_{PSII} was highest near the light/shade border of a homobaric leaf and clearly decreased with increasing distance to that border; however, when the plant was re-watered, the observed gradient in Φ_{PSII} disappeared almost completely within about 25 min (Fig. 3). As long as stomatal conductance is low, c_i in the illuminated part

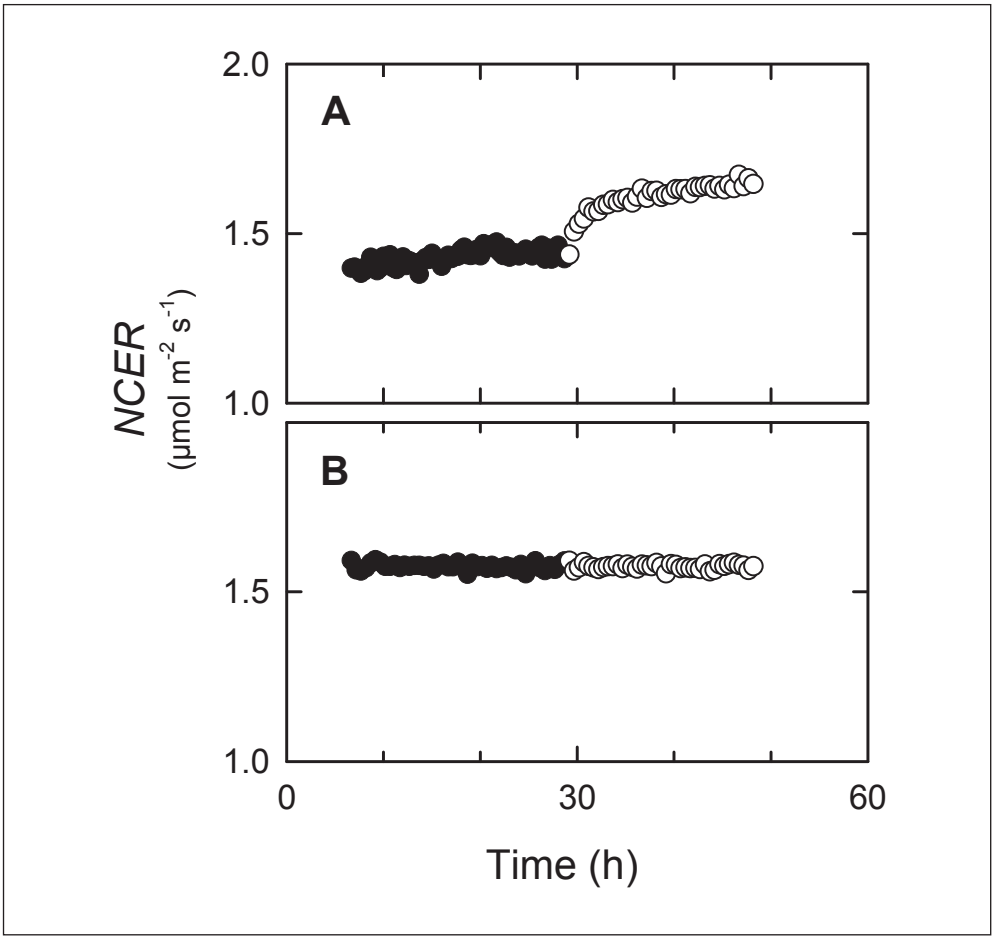

Fig. 2 *NCER*s measured with a clamp-on leaf chamber on a homobaric leaf of *Vicia faba* (*A*) or a heterobaric leaf of *Glycine max* (*B*). Light inside the clamped leaf part was not altered but outside the leaf chamber illumination was switched on or off: shade is indicated by the black circles, light by the white circles. The experiment is similar to the one shown in Fig. 1 of Pieruschka et al. 2008, but measured with an improved signal-to-noise ratio by using a LI-7000 infrared gas analyser instead of a LI-6400 instrument.

of a leaf is low but, in the vicinity of the light/shade border, c_i may be considerably higher due to leaf internal lateral CO_2 supply from the shaded parts. That means that the observed gradient in Φ_{PSII} was caused by an underlying gradient in c_i eventually limiting the apparent assimilation rate of the leaves which is measured as the CO_2 exchange between the leaf and atmosphere (Pieruschka et al. 2006).

In contrast to these findings, Morison et al. (2005) concluded from their studies with homobaric leaves of *Commelina communis* that lateral diffusion of CO_2 is not sufficient to support photosynthesis in leaf areas in which stomata were artificially closed by grease patches. However, in a following opinion paper the authors changed their opinion regarding lateral CO_2 diffusion as a potential contribution to leaf performance (Morison and Lawson 2007).

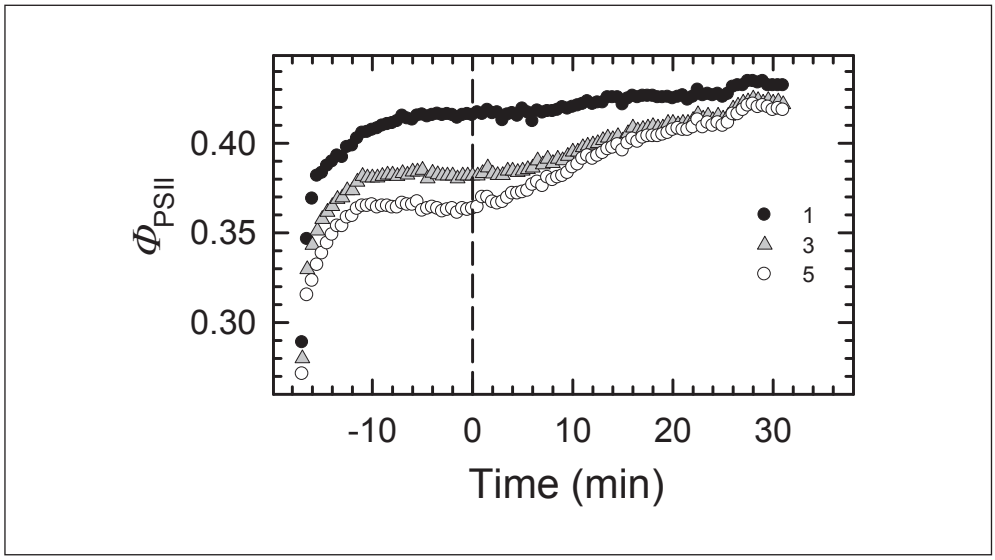

Fig. 3 Quantum yield of photosystem II (Φ_{PSII}) measured on the illuminated part of a homobaric *Vicia faba* leaf at different distances to a shade provided to that leaf. The Φ_{PSII} were pooled in regions of interests (ROI) being 1 mm wide and plotted for distances of 1 mm (black circle), 3 mm (grey triangle) and 5 mm (white circle) to the light/shade border. Modified after Fig. 6E of Pieruschka et al. 2006.

This is further confirmed by a more recent paper where they came to the conclusion that laterally diffusing CO_2 can indeed substantially influence photosynthesis (Morison et al. 2007). However, in that study the impact of lateral diffusion on photosynthesis was similar in all five investigated dicotyledoneous species with different leaf anatomies. By improving the method of sealing leaf patches with silicon grease used by the Morison group and calculating gradients of leaf internal CO_2 concentrations (c_i) from chlorophyll fluorescence image data (Φ_{PSII} mapping), we were able to show that the contribution of laterally diffusing CO_2 to photosynthesis of sealed leaf parts differs substantially between different species; it is dependent on the physical properties and mainly defined by the lateral CO_2 diffusion coefficients of the particular leaves (Pieruschka et al. 2008).

4. Lateral Gas Conductivity of Leaves and its Possible Role for Plants

The possible role of lateral diffusion of CO_2 has been already considered in literature but was mostly restricted to small distances such as between neighboring stomata (reviewed e.g. by Parkhurst 1994). This may play a role in particular when patchiness of stomata causes non-uniform photosynthesis in heterobaric but not homobaric leaves (Downton et al. 1988, Terashima et al. 1988). Leaves of the CAM plant *Kalanchoë daigremontiana* have densely packed mesophyll cells which limits CO_2 diffusion and thus contributes to the interplay of coupled individual oscillators involved in spatiotemporal variations in the metabolism of this plant (Rascher et al. 2001). Though the intercellular space in homobaric leaves of *K. daigremontiana* is small, lateral diffusion of CO_2 was demonstrated to affect PSII activity (Duarte

et al. 2005). Moreover, high concentration of CO_2 in the mesophyll of CAM species may also provide a basis for CO_2 signaling facilitated by lateral gas diffusion (Lüttge 2007).

In order to illustrate the possible magnitude of lateral porosity, an example calculation of a homobaric *Nicotiana tobacco* leaf may be helpful. With a leaf thickness of 300 µm, leaf porosity of 40 % and total length of the chamber gaskets of 100 mm, the cross-section area of such a tobacco leaf under the leaf chamber sealing possibly open for lateral air movement accounts for 12 mm^2 and is equivalent to a tubing with an inner diameter of 4 mm. It is obvious that this has to lead to considerable lateral leakage rates (gas fluxes) as observed in the already presented experiments. Gas exchange measurements and chlorophyll fluorescence imaging were used to quantify such lateral gas conductivities (or lateral diffusion coefficients) for leaves of different species. The results indicate that gas diffusion in homobaric leaves can be even larger in lateral than in vertical directions of the leaves; when homobaric leaves of different species were compared, lateral conductivities of CO_2 ranged between 67 and 255 µmol m^{-1} s^{-1} whereas the vertical conductivities were between 15 and 78 µmol $m^{-1}s^{-1}$ (Pieruschka et al. 2005, 2008).

Two major factors play a role when the possible "effectiveness" of lateral gas diffusion is considered. First, the potential for lateral gas movement inside leaves depends on the interconnectivity of the intercellular air spaces (degree of homobaricity). Second, whether lateral CO_2 diffusion from shaded leaf parts influences adjacent illuminated areas depends on stomatal conductance. Since stomatal conductance mainly reflects the (actual) water status of a plant, we hypothesize that homobaric leaf anatomy is an adaptation to environments in which transient water and light stress situations may negatively influence plants vitality. Lateral CO_2 diffusion from shaded to illuminated leaf parts may increase quantum yield, decrease light stress of the illuminated leaf part and enhance water use efficiency of the plants under certain conditions. To test the hypothesis that homobaric leaf anatomy is an advantageous trait at plant or stand level, leaf homobaricity has to be screened for a large number of species including data of the position and developmental stage of the particular leaves, the specific conditions at leaf level (light, shading, temperature, humidity etc.) and the climatic conditions at the natural stands. However, quantification of leaf homobaricity and its possible significance for plant performance is still a challenge particularly under field conditions. This may have two consequences for future research: either the "homobaric effect" is still being ignored (and its possible contribution to plant carbon gain neglected) or methods will be developed by which the hypothesized impact on plant performance can be finally verified or falsified at stand conditions.

References

Amthor, J. S.: Plant respiratory responses to elevated carbon dioxide partial pressure. In: Allen, L. H. Jr., Kirkham, M. B., Olszyk, D. M., and Whitman, C. E. (Eds.): Advances in Carbon Dioxide Effects Research; pp. 35–77. Madison, Wisconsin: ASA Special Publication Number *61* (1997)

Amthor, J. S., Koch, G. W., Willms, J. R., and Layzell, D. B.: Leaf O_2 uptake in the dark is independent of coincident CO_2 partial pressure. J. Exp. Bot. *52*, 2235–2238 (2001)

Davey, P. A., Hunt, S., Hymus, G. J., Delucia, E. H., Drake, B. G., Karnosky, D. F., and Long, S. P.: Respiratory oxygen uptake is not decreased by an instantaneous elevation of [CO_2], but is increased with long-term growth in the field at elevated [CO_2]. Plant Physiol. *134*, 520–527 (2004)

Downton, W. J. S., Loveys, B. R., and Grant, W. J. R.: Non-uniform stomatal closure induced by water stress causes putative non-stomatal inhibition of photosynthesis. New Phytol. *110*, 503–509 (1988)

Duarte, H. M., Jakovljevic, I., Kaiser, F., and Lüttge, U.: Lateral diffusion of CO_2 in leaves of the crassulacean acid metabolism plant *Kalanchoe daigremontiana* Hamet et Perrier. Planta *220*, 809–816 (2005)

Flexas, J., Diaz-Espejo, A., Berry, J. A., Cifre, J., Galmes, J., Kaldenhoff, R., Medrano, H., and Ribas-Carbo, M.: Analysis of leakage in IRGA's leaf chambers of open gas exchange systems: quantification and its effects in photosynthesis parameterization. J. Exp. Bot. *58*, 1533–1543 (2007)

Jahnke, S.: Atmospheric CO_2 concentration does not directly affect leaf respiration in bean or poplar. Plant Cell Environ. *24*, 1139–1151 (2001)

Jahnke, S., and Krewitt, M.: Atmospheric CO_2 concentration may directly affect leaf respiration measurement in tobacco, but not respiration itself. Plant Cell Environ. *25*, 641–651 (2002)

Jahnke, S., and Pieruschka, R.: Air pressure in clamp-on leaf chambers: a neglected issue in gas exchange measurements. J. Exp. Bot. *57*, 2553–2561 (2006)

Lüttge, U.: Carbon dioxide signalling in plant leaves. Compt. Rend. Biol. *330*, 375–381 (2007)

Meidner, H.: The determination of paths of air movement in leaves. Physiologia Plantarum *8*, 930–935 (1955)

Morison, J. I. L., Gallouet, E., Lawson, T., Cornic, G., Herbin, R., and Baker, N. R.: Lateral diffusion of CO_2 in leaves is not sufficient to support photosynthesis. Plant Physiol. *139*, 254–266 (2005)

Morison, J. I. L., and Lawson, T.: Does lateral gas diffusion in leaves matter? Plant Cell Environ. *30*, 1072–1085 (2007)

Morison, J. I. L., Lawson, T., and Cornic, G.: Lateral CO_2 diffusion inside dicotyledonous leaves can be substantial: quantification in different light intensities. Plant Physiol. *145*, 680–690 (2007)

Neger, F. W.: Spaltöffnungsschluß und künstliche Turgorsteigerung. Ber. Deutsch. Bot. Gesell. *30*, 179–194 (1912)

Neger, F. W.: Die Wegsamkeit der Laubblätter für Gase. Flora *111*, 152–161 (1918)

Parkhurst, D. F.: Tansley Review No. 65. Diffusion of CO_2 and other gases inside leaves. New Phytol. *126*, 449–479 (1994)

Pieruschka, R., Chavarría-Krauser, A., Cloos, K., Scharr, H., Schurr, U., and Jahnke, S.: Photosynthesis can be enhanced by lateral CO_2 diffusion inside leaves over distances of several millimeters. New Phytol. *178*, 335–347 (2008)

Pieruschka, R., Schurr, U., and Jahnke, S.: Lateral gas diffusion inside leaves. J. Exp. Bot. *56*, 857–864 (2005)

Pieruschka, R., Schurr, U., Jensen, M., Wolff, W. F., and Jahnke, S.: Lateral diffusion of CO_2 from shaded to illuminated leaf parts affects photosynthesis inside homobaric leaves. New Phytol. *56*, 857–864 (2006)

Rascher, U., Hütt, M. T., Siebke, K., Osmond, B., Beck, F., and Lüttge, U.: Spatiotemporal variation of metabolism in a plant circadian rhythm: the biological clock as an assembly of coupled individual oscillators. Proc. Natl. Acad. Sci. USA *98*, 11801–11805 (2001)

Rodeghiero, M., Niinemets, Ü., and Cescatti, A.: Major diffusion leaks of clamp-on leaf cuvettes still unaccounted: how erroneous are the estimates of Farquhar et al. model parameters? Plant Cell Environ. *30*, 1006–1022 (2007)

Terashima, I., Wong, S. C., Osmond, C. B., and Farquhar, G. D.: Characterisation of non-uniform photosynthesis induced by abscisic acid in leaves having different mesophyll anatomies. Plant Cell Physiol. *29*, 385–394 (1988)

Weyers, J. D. B., and Lawson, T.: Heterogeneitiy in stomatal characteristics. Adv. Bot. Res. *26*, 317–352 (1997)

Wylie, R. B.: Principles of foliar organization shown by sun-shade leaves from ten species of deciduous dicotyledon trees. Amer. J. Bot. *38*, 355–361 (1951)

Wylie, R. B.: The bundle sheath extensions in leaves of dicotyledons. Amer. J. Bot. *39*, 645–651 (1952)

Dr. Siegfried Jahnke
Institute of Chemistry and Dynamics
of the Geosphere (ICG), ICG-3: Phytosphere
Forschungszentrum Jülich
52425 Jülich
Germany
Phone: +49 2461 618681
Fax: +49 2461 612492
E-Mail: s.jahnke@fz-juelich.de

Dynamics and Heterogeneity of Plant Growth and Transport

Nova Acta Leopoldina NF *96*, Nr. 357, 103–122 (2009)

Intracellular Domains and Polarity in Root Apices: From Synaptic Domains to Plant Neurobiology

František Baluška, Markus Schlicht, Yinglang Wan, Christian Burbach, and Dieter Volkmann (Bonn)

With 4 Figures

Abstract

Plant cells, especially those in the root apex, resemble neuronal cells in many respects. Firstly, root apex cells assemble, already during cytokinesis, and maintain stable intracellular cell-cell adhesion domains specialized for cell-cell communication. Properties of these domains suggest that they represent plant synapses. Several other recent advances in plant cell biology, molecular biology, and ecology have accumulated a critical mass of data which are not 'digestible' within the framework of classical disciplines of plant sciences. Plants emerge as sensitive organisms equipped with robust sensory apparatus which continuously retrieve information from their environment. Root apex cells are evolutionarily optimized to translate integrated sensory information obtained from environment into animal-like motoric responses and behavior. Root apices of parasitic plants manipulate root apices of prey plants to colonize them via haustoria which extract photosynthates from prey root apices. Moreover, plants communicate extensively with other plants, and invasive plants often kill other roots (plants) via release of toxic substances from their root apices. A newly focused field of plant biology, plant neurobiology, is aimed at understanding how communicative plants process information obtained from their environment in order to develop, prosper and reproduce optimally.

Zusammenfassung

Pflanzen zeichnen sich durch ein komplexes sensorisches System aus, womit sie ihre Umwelt wahrnehmen und auf diese reagieren. Zellen, insbesondere in der Übergangszone der Wurzel, weisen Charakteristika auf, die in mehrfacher Hinsicht solchen von neuronalen Zellen ähneln. Sie bilden im Verlauf der Cytokinese Zell-Zell-Kontakte aus, die der interzellulären Kommunikation dienen und aufgrund ihrer molekularen Strukturen als pflanzliche Synapsen bezeichnet werden können. Die Zellen der Übergangszone sind damit optimal dafür ausgestattet, vielfältige Information aus ihrer Umwelt zu integrieren und in Form von Wachstum – Teilung, Streckung und Differenzierung – zu beantworten. Auch Kommunikation zwischen verschiedenen Individuen und Spezies findet in dieser Zone der Wurzel statt; z. B. bei der Erkennung von Selbst und Nichtselbst, der Freisetzung toxischer Substanzen gegenüber Konkurrenten sowie bei der Symbiose mit Bakterien und Pilzen. Neueste Ergebnisse aus den Bereichen der pflanzlichen Zellbiologie, Molekularbiologie und Ökologie sind in das bestehende Netzwerk der klassischen Disziplinen der Pflanzenbiologie kaum zu integrieren. Der neue sich rasch entwickelnde Bereich der Neurobiologie der Pflanzen hat diesen integrierenden Ansatz zum Ziel.

1. Cell Polarity in Plant Roots: Subcellular Domains as Spatial Organizers of Polarity

The geometry of polarized eukaryotic cells is defined by subcellular domains of growing and non-growing areas when the growing areas are enriched with F-actin and active in regulated secretion (Baluška et al. 2000b, 2003a). Curiously enough, most root cells do not conform to this general rule (Baluška et al. 2001c, 2003a) and our studies, using both indirect immunofluorescence and GFP technology, reveal that transcellular transport of auxin is supported

by F-actin-based vesicular trafficking and polarized secretion at the non-growing but adhesive synaptic end-poles enriched with F-actin (Baluška et al. 1997, 2000b, 2001a, b, c, 2003a, b, c, Voigt et al. 2005a, Schlicht et al. 2006, Mancuso et al. 2007).

Two fundamentally different types of cell growth co-exist in plant roots (but not in plant shoots). One type is represented by the tip-growing root hairs (closely resembling generative pollen tubes), which are growing only at well-defined and highly polarized subcellular domains enriched with F-actin (Baluška et al. 2000a). Similar to animal and yeast cells, the growing tip of root hair is enriched with F-actin (Baluška et al. 2000a, b) and recycling endosomal vesicles (Voigt et al. 2005a). The other plant cell growth type, which is common for all other roots cells, and most shoot cells, is accomplished via diffusely growing lateral flanks (side-walls) while end-poles (cross-walls) are non-growing but dynamic (Baluška et al. 2003a, b, c). Cells within one cell file are held together via the adhesive and communicative end-poles – plant synapses (Baluška et al. 2005a), and individual cell files are interconnected via gateable plasmodesmata (electric plant synapses) grouped within lateral pit-fields which are also enriched with F-actin and myosin VIII (Baluška et al. 2003a). Both cross-walls and pit-fields (plant synapses and mini-synapses) are enriched with pectins recycling via endocytosis and endosomal vesicular secretion which makes them highly dynamic and plastic (Baluška et al. 2002, 2004b, 2005a).

2. Neuronal Features of Plant Cells

Plant cells, especially those at the root apex, exhibit features which resemble neurons. Most prominent and relevant one is mobile trans-Golgi network elements which has been demasked as early endosomes (Šamaj et al. 2005, Dettmer et al. 2006, Lam et al. 2007) and act as building blocks in formation of synaptic domains (Baluška et al. 2005a, Dettmer et al. 2006, Dhonukshe et al. 2006, Hause et al. 2006, for animal neurons see McAllister 2007). At the root apex, plant synapses resemble neuronal chemical synapses in being non-growing asymmetric adhesion domains specialized for effective cell-cell communication (Baluška et al. 2003c, 2005a). Besides this, plant cells express numerous neuronal molecules, voltage-gated ion channels, vesicle trafficking molecules, and are inherently excitable initiating and running action potentials (for the first paper on *Arabidopsis* see Favre and Degli Agosti 2007, for recent reviews see Fromm and Lautner 2007, Felle and Zimmermann 2007, for a special volume see Baluška et al. 2006).

In plant cells, cytoplasmic perinuclear microtubules are depleted (Baluška et al. 1992), and almost all microtubules are organized under the plasma membrane in form of the cortical arrays. Exceptions to this rule are tips of the tip-growing cells, pit-fields and the cross-walls which are depleted of cortical microtubules but enriched with F-actin (Baluška et al 2000b). In general, cortical microtubules are essential for keeping tubular shapes of plant cells but they play only secondary role in plant cell polarity. The cytoskeletal element defining the polarity of plant cells is the actin cytoskeleton linked inherently to polar transport of auxin (Baluška et al 2001a, 2003b, Rahman et al. 2007, Dhonukshe et al. 2006, Nick 2006).

For establishing and maintaining cell polarity, all eukaryotes use dynamic F-actin and endosomal vesicle trafficking linked to assembly of diverse modular protein scaffolds (Nelson 2003). The tip-growing root hairs and pollen tubes provide very useful system to study cell polarity. Growing hair tip is enriched with abundant meshwork of F-actin and compromis-

ing integrity of this meshwork with latrunculin B stops tip-growth immediately (Baluška et al. 2000a, b, Voigt et al. 2005a). Moreover, critical actin binding proteins like profilin and myosin VIII also show the tip-focused localization (Baluška et al. 2000a, b). Studies based on the GFP-FYVE tagged endosomes as well as labelings with endocytic tracers FM1-43 and FM4-64 revealed that both endosomes and endosomal vesicles accumulate at outgrowing bulges and at actively growing tips of root hairs (Voigt et al. 2005b, Ovecka et al. 2005). On the other hand, the non-growing root hairs possess dispersed endosomes and lack the secretory vesicle-rich "clear zone" (Voigt et al. 2005b).

Besides showing polarized endosomal secretion, the plasma membrane domain at the tip of growing root hair displays additional particular properties such as high abundance of lipid rafts (Ovecka et al., submitted) which are enriched with signaling proteins, for example NADPH oxidases which sustain the tip-focused ROS gradient that is essential for the polarized tip growth of root hairs (Foreman et al. 2003, Jones et al. 2007).

3. The Root Apex as Model System to Understand Plant Polarity, Cell-Cell Communication, and Sensory Plant Biology

Root apices have a simple anatomy and morphology which makes them for a perfect system to understand complex interactions between environment and endogenous plant polarity cues. Root apices, but not shoot apices, are composed of two major parts. Central cylinder (stele) is enclosed by epithelial-like endodermis and by cortex which is further enclosed by epithelial-like epidermis. Root apices, but not shoot apices, show also simple geometry, central cylinder (stele) which approach up to the root tip, clear zonation and very regular cell files (Baluška et al. 1990, 1994, 2001c, 2003a, 2006; Verbelen et al. 2006). The significance of all these features for neuronal active behavior of roots will be discussed later.

3.1 Root Apex Tissues, Domains and Zones

Root apices represent excellent model system to understand plant polarity. The root apex is conical organ which is composed of clearly organized longitudinal cell files (Baluška et al. 2006). Individual cells within one cell file are communicating together extensively via synaptic F-actin and myosin VIII based adhesions domains. The cell files interact among each other by so-called pit fields. Both cross-walls and pit-fields are enriched with plasmodesmata (Baluška et al. 2004b).

The central (middle) part of the whole root body is known as stele or vascular cylinder domain, with xylem and phloem elements embedded in parenchymatic cells, and enclosed by developmentally flexible pericycle cells. At the stele periphery, epithelial-like endodermis protects structurally and physiologically the vascular tissues which have a crucial importance from both physiological but also from neurobiological perspectives. Between the endodermis and epidermis, the root cortex is located which is composed of one (*Arabidopsis*) or up to ten (maize) cell files. This buffering parenchymatous tissue comprizes the largest part of the maize primary root apex. The outside surface of the root apex is covered by the epithelial-like epidermis communicating with root environment. Well-defined specialized cells of root epidermis, known as trichoblasts, form and support the tip-growing root hairs (Baluška et al. 2000a).

Similarly straightforward are the developmental zones of the root apex. The outer most root tip, but not the shoot tip, is enclosed by the root cap. This sensory and protectory organ is embedded within secretory mucilage and protects the sensitive meristematic tip and serves also as a sensor region for diverse root tropisms (Barlow 2003) and communication with rhizosphere (Hawes et al. 2000). In *Arabidopsis* root apex, the root cap covers the apical root meristem (Fig. 1) which consists of small dividing isodiametric cells. In-between the root cap and the apical meristem are root stem cells which maintain in-determined root growth. In contrast to the shoot apex stem cells, the root apex stem cells show, similarly like the animal stem cells, asymmetric cell divisions (Scheres 2007). These are essential for the maintenance of stem cell nature of the smaller cell while the larger cell leaves stem cell niche (Scheres 2007).

Following the apical meristem, two post-meristematic growth zones are located (Fig. 1). The first one is the transition zone (Baluška et al. 1990, 1994, 2001c, Verbelen et al. 2006), also known as the distal elongation zone (Wolverton et al. 2002, Massa and Gilroy 2003) or the "zone of competence" (De Smet and Jürgens 2007), which is specialized for sensory and neuronal processes (Baluška et al. 2004a). This unique root apex zone, which precedes the zone of rapid cell elongation. was discovered in 1990 (Baluška et al. 1990, 1994).

Cells of the transition zone cease their mitotic divisions but still do not elongate rapidly (Baluška et al. 1990, 1994, 2001c, Verbelen et al. 2006). These early postmitotic cells show several features which place them into unique developmental context. They are still filled with dense cytoplasm, have small vacuoles, and their nuclei are centered within the cytoplasmically dense cells. Moreover, their actin cytoskeleton assembles into unique arrays when both the cross-walls (end-poles or plant synapses) are enriched with actin filaments while prominent F-actin bundles interconnect these poles and enclose the central nucleus within a spindle-like cage (Baluška et al. 1997). This arrangement of F-actin is unique and found only in these cells from the whole plant body.

High rates of exo- and endocytosis events can be monitored at the cross-walls in this root apex region (Baluška et al. 2002, 2003a,c, 2005a). It appears that cells of this root apex region are not only in transition from cell division into rapid cell elongation, but they emerge to perceive and integrate several environmental signals. For example, during root graviresponse, most sensory events occur at the root cap and motoric events are initiated in the transition zone. Moreover, also decapped roots show gravisensitivity and develop partial gravicurvature which is based on transition zone sensory events (Mancuso et al. 2006). Electric responses within the elongation zone, which accomplishes the root bending, are scored already after few seconds of gravistimulation (Ishikawa and Evans 1990). This suggests electrical communication between cells of the root cap, meristem, transition zone, and elongation region, which integrates multiple gravisensing to achieve adaptive gravibending (Baluška et al. 2007a, Stankovic 2006).

3.2 Transition Zone: Cross-Road for Polar Cell Growth in the Root Apex

The transition zone accomplishes surprisingly complex patterns of polar auxin flows which not only influence nearly all aspects of root polarity and growth processes but which are also tightly linked with sensing of physical parameters of their environment such as light, gravity, electric and magnetic fields; and translating them into biologically relevant information (Baluška et al. 2007a). The re-direction of root growth after perceptions of gravity, light or

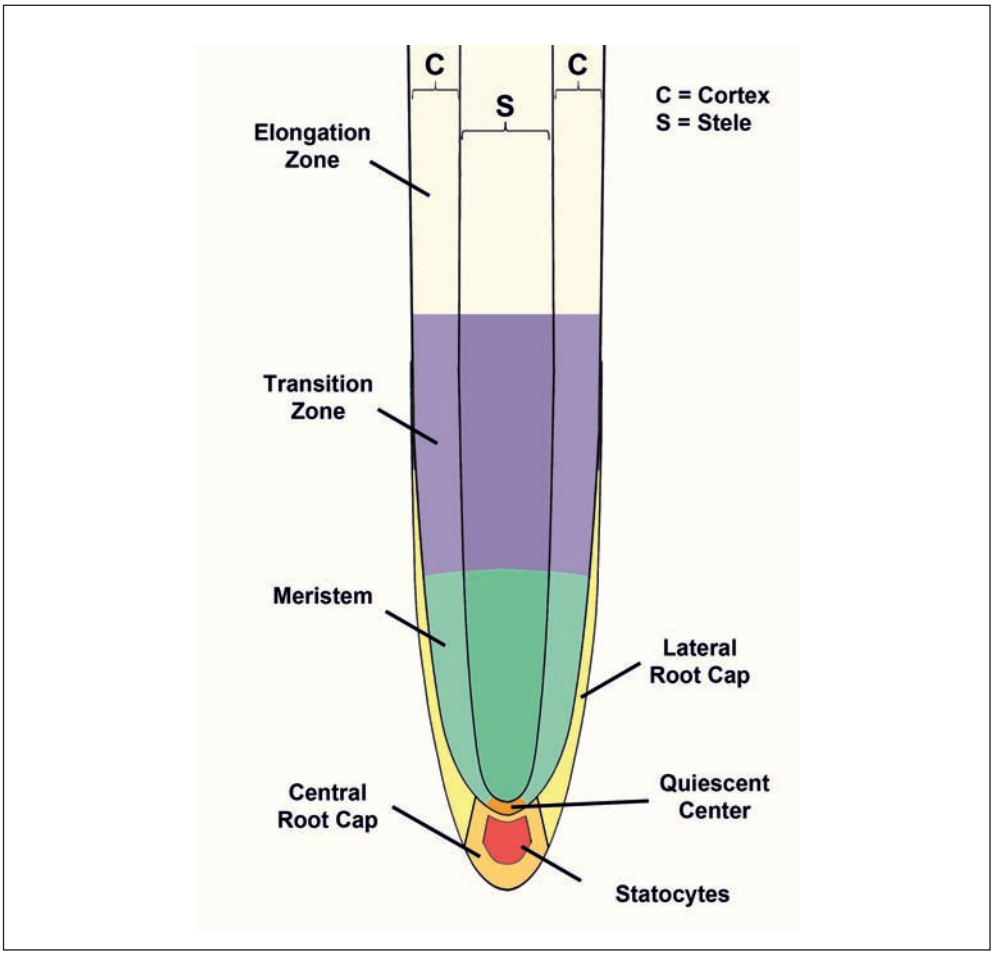

Fig. 1 Schematic view of the root apex zonation on example of *Arabidopsis*. Root apex consist of distinct zones which are depicted here in different colours. The root cap (yellow) covers the apical meristem (green), which is followed by the transition zone (blue) and the elongation zone (grey). In the root cap, centrally localized sensory statocytes (red) are embedded within the central root cap portion (brown). The lateral root cap covers the meristem and the apical portion of the transition zone. At the very tip of the root body, quiescent centre (orange) is located. Note that the stele (central cylinder) is protruding up to the very tip of the root body. For dimensions and distances from the root cap junction of individual zones in the root apex of Arabidopsis, see VERBELEN et al. (2006).

electric fields (WOLVERTON et al. 2000, 2002, DE SMET et al. 2007) starts in the transition zone. In the transition zone, some root epidermis cells gets specialized into root hair initiating trichoblasts (BALUŠKA et al. 2000a) and also some pericycle cells obtain competence for initiation of lateral root primordia which is then expressed later in their development (DE SMET et al. 2007). Moreover, transition zone cells which experience mechanical impedance due to high soil density, accomplish ethylene-mediated switch in their growth polarity and start to expand laterally (BALUŠKA et al. 1993, 1994). This allows pushing of root tips through very compact soil portions.

3.3 Transition Zone and Elongation Region: Coordination of Two Root Apex Bending Zones Allows Animal-Like Root Crawling

Plant roots exert several unique animal-like features which distinguish them clearly from plant shoots. The most prominent one is crawling-like movement of roots resembling moving worms (Fig. 2). Already Charles and Francis Darwin noted this phenomenon and concluded in their book on plant movements that the plant root apex behaves as the anterior pole of lower animals showing even brain-like features (p. 646 in Darwin 1880, Barlow 2006). Darwins also noted that roots without root cap continue in their growth but fail to show the animal-like crawling behavior. They criticized Julius Sachs who, apparently due to not careful removal of the root cap (Darwin 1880, Heslop-Harrison 1979), failed to repeat these important experiments originally performed and reported by Theophil Ciesielski (1872). Interestingly, these Ciesielski's experiments with gravistimulated root lead Charles Darwin to propose mobile signaling molecule, later discovered as auxin, mediating effects of stimulus perceived in one plant part that results in responses of other parts of the same plant (Darwin 1880, Heslop-Harrison 1979, Pennazio 2002).

In contrast to the root apices, the shoot apices do not show this animal-like behavior and can bend only slowly, in one zone far away of the shoot apex, allowing simple repositioning

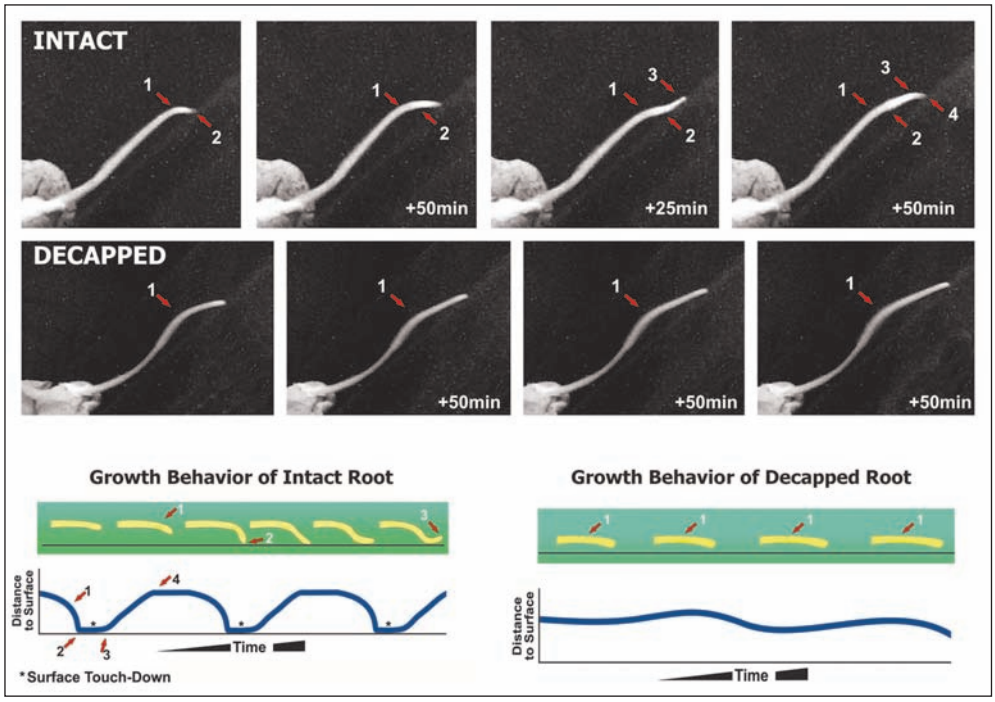

Fig. 2 *Crawling maize roots*. Images taken from a video sequence documenting crawling-like growth of maize root apices which is based on intact root apex covered with the root cap. Schematic depiction reveals that the root tip "touch-down" phases are regularly spaced between the forward-growth phases if roots are growing-up the 45° slope. Surgical removal of the root cap allows roots to accomplish the forward growth but without the 'touch-down' phases.

of growing shoot apices (Baluška et al. 2007a). What root-specific features allow growing root apices to perform this animal-like behavior? Apparently, besides the root cap, zonation of root apices is behind such worm-like movements of root apices as there are two bending zones, one in the transition zone and another one in the elongation zone (Wolverton et al. 2002, Massa and Gilroy 2003), which curve in coordinated fashion. In order to behave in such coordinated manner, these two zones must communicate together via rapid systemic signals. There are several indications that, besides slow hormonal communication, also rapid electrical communication is necessary for the coordinated bending behavior of these two root apex growth zones (Björkmann and Leopold 1987, Collings et al. 1992, Ishikawa and Evans 1994, Stankovic 2006).

3.4 Plant Synapses: Dynamic Non-Growing Domains Specialized for Neuronal Biology

An exceptional feature of plants cells are non growing end-poles, strongly enriched with F-actin and accomplishing rapid turn-over via abundant endocytosis and exocytosis events when endocytosis fully balances exocytosis preventing any new growth (Baluška et al. 1997). These cross-walls resemble neuronal synapses in animal and human brains, and we have proposed a new concept of plant synapses to explain their specific status (Baluška et al. 2005a). Similarly, the pit-fields are also cell-cell adhesive domains (Baluška et al. 2004a) resembling in many features the cross-walls, which allow communication within the individual cell files, and might represent lateral mini-synapses specialized for radial communication between individual cell files. Besides being enriched with F-actin and plant-specific myosin of the class VIII, pit-fields are active in endocytosis and endocytic vesicle recycling (Baluška et al. 2004b). Similarly like cross-walls synapses, the pit-fields are also enriched with recycling pectins and depleted in cellulose (Baluška et al. 2001b).

Importantly in this respect, RGII pectins cross-linked with boron are important for cell-cell adhesion in plants (Iwai et al. 2002, 2006) and accomplish endocytic recycling at the synaptic cross-walls (Baluška et al. 2002, 2003c, Šamaj et al. 2004). Changing of cell wall pectins via inducible expression of pectin methylesterase resulted in disintegration of cell-cell adhesion and loss of synaptic cell-cell contacts (Wen et al. 1999). So plant synapses are dynamic structures which rapidly recycle all their components via endocytosis and vesicular trafficking pathways.

3.5 Polar Transport of Auxin in Root Apices via Secretory Plant Synapses

The polar transport of auxin is a prime example for the central role cell polarity shaping the architecture of the plant body. Although each living plant cell seems to be able to produce auxin, this simple molecule having complex signaling roles is produced preferentially in young regions near the apical shoot meristems and is then transported in polar fashion from cell-to-cell along the longitudinal axis of the plant body up to the root tip (Friml 2003, Teale et al. 2006). Beside a phloem-based mass flow transport of auxin, cell-to-cell transport route is accomplished via influx-efflux carriers and ABC transporters (Petrášek et al. 2006, Bandyopadhyay et al. 2007, Zažímalová et al. 2007). Following the classical chemiosmotic model of the auxin transport, central role is played by the efflux carrier (facilitator) which provides a checkpoint of the transport process (Zažímalová et al. 2007). The pH value of the apoplastic cell wall is maintained at approximately pH 7 resulting in an uncharged form

of extracellular indole acetic acid (IAA), which can diffuse through the plasma membrane easily (Gutknecht and Walter 1980). The pH of the cellular lumen is maintained at about pH about 7 by proton pumps continuously pumping hydrogen ions (H^+) from the cytoplasm. In the cytoplasm, IAA is ionized at this pH condition and is not permeable to the cell membrane, requiring active transport of IAA by efflux carrier PIN proteins. The polar localization at distinct subcellular domains makes PIN proteins and the auxin influx transporter AUX1 for perfect tools to study the setup and maintance of polarity in plant cells. Domain-specific asymmetric localization of efflux and influx carriers requires localized targeting of vesicles and interactions with the actin cytoskeleton (Rahman et al. 2007).

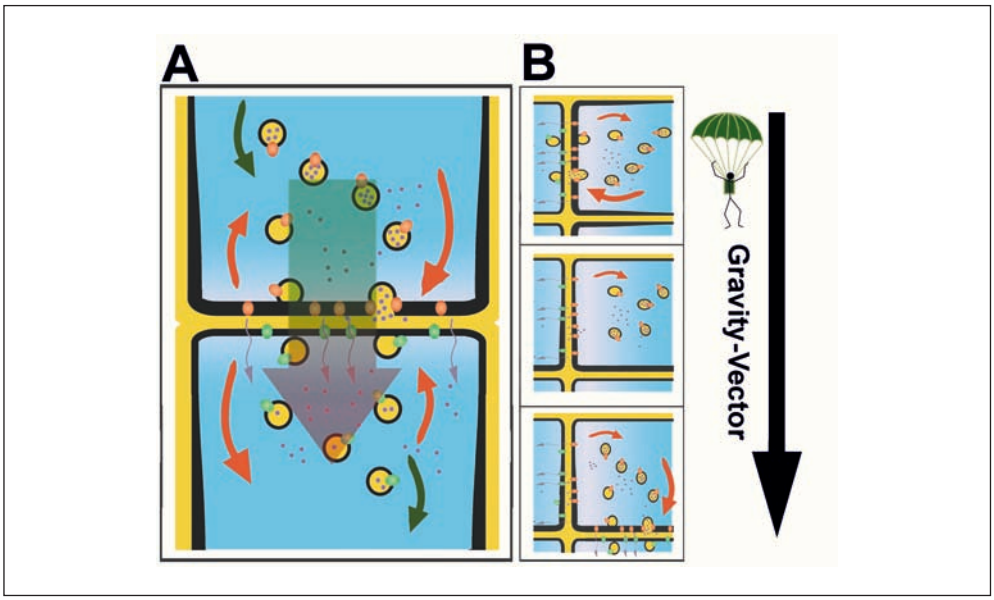

Fig. 3 Schematic view of gravisensing auxin-secreting plant synapse. (*A*) Two hypothetical root apex cells from the stele transporting auxin down the gravity vector. The above cells has greatest load, due to settling of the whole protoplast, at the cellular "bottom" (the plasma membrane is depicted here by thicker line) which is relieved by a higher rate of exocytosis (larger red arrow) while endocytosis is less active (smaller red arrow). The adjacent lower cell has the lowest load, again due to protoplast settling, at the cellular "roof" (the plasma membrane is depicted here by thinner line) which is relieved by a higher rate of endocytosis (larger red arrow) while exocytosis is less active (smaller red arrow). As vesicles are filled with auxin, the mechanical asymmetry of plant synapse determines the transport of auxin down the gravity vector (large transcellular arrow). (*B*) Reorientation of the root apex changes the load pressures within its cells immediately. The new physical "bottom" gets larger mechanical load attracting auxin-filled vesicles and changing the polarity of trancellular auxin transport again down the gravity vector (larger red arrow). In the (*A*), the root apex is down; in the (*B*), the root apex is on the left side.

Interestingly, the anatomically and morphologically simple-structured root apex shows the most complex behavior of the polar auxin transport (Blilou et al. 2005). Out of eight PIN proteins in *Arabidopsis thaliana*, five members are expressed at the root apex. They are part of a complex system which steers an auxin flow loop at the root tip (Bandyopadhyay et al. 2007). In contrast, the anatomically and morphologically much more complex shoot apices

express only PIN1 for the polar transport of auxin. Shoot derived auxin, transported in the stele by PIN1, arrives up to the most apical root cap, is then channeled to the lateral root apex sides via activities of PIN3, 4 and 7 and then transported basal back up to the basal limit of the transition zone by PIN2 till it reaches the transition zone where again PIN7 directs the auxin flow again to the apical root tip (Blilou et al. 2005). Besides PINs, also ABC transporters of the PGP (P-glycoprotein) family take part in the polar transport of auxin (Bandyopadhyay et al. 2007). This complex network of auxin transporters at the root apex controls dynamic auxin transport feedback loops, which are absent from the morphogenetically more complex shoot apex.

Importantly, there are several data which are not compatible with the original version of the chemiosmotic theory and implicate involvement of endosomes and recycling endocytic vesicles in neuronal vesicular secretion of auxin (Baluška et al. 2003b, 2005a). First of all, two inhibitors of secretion having different targets and mechanisms of action, BFA and monensin, inhibit rapidly and effectively auxin export out of plant cells (Delbarre et al. 1996, 1998, Mancuso et al. 2005). The rapidity of their action (less than ten minutes) precludes the popular interpretation of these data that these inhibitors simply prevent targeting of efflux carriers to the plasma membrane domains. Moreover, classical inhibitors of polar auxin transport, such as NPA and TIBA, turned out to be general inhibitors of endocytosis (Geldner et al. 2003) which, similarly like BFA and monensin, block secretory vesicle recycling. Furthermore, polar auxin transport is inhibited by disturbing the actin cytoskeleton or myosin motor activities (Holweg and Nick 2004, Holweg 2007a, b).

Further evidences include proper localization of PIN1 to the plasma membrane of root apex cells in maize and *Arabidopsis* mutants having inhibited auxin transport (Schlicht et al. 2006, Mancuso et al. 2007, Baluška et al. 2007b). Importantly, these auxin transport-deficient mutant root cells do not show abundant auxin at these PIN1-enriched domains (inactive plant synapses) as it is the case of the wild-type cells (active, or less active, plant synapses). In control root apices, auxin is enriched at those cross-walls which are active in vesicular auxin export, being abundant not only at cell walls but also within adjacent endosomes. Under BFA action, these auxin enriched endosomes aggregate into BFA-induced compartments enriched with auxin (Schlicht et al. 2006).

Further evidence is provided by forcing roots to grow against the gravity vector by placing them into the in glass capillaries. Such roots get progressively thinner and desperately try to turn-down despite the extremely narrow space (some even succeed in this gymnastic!). Root apices of such challenged roots get depleted of cells due to inhibited supply of auxin which cannot be transported effectively against gravity vector. Nevertheless, PIN1 in these root apices is localized properly to cross-walls even if it does not show rapid recycling as revealed by the exposure of such roots to BFA (Schlicht et al., data in preparation).

Furthermore, *Arabidopsis* PLD Zeta2, a regulator of vesicle trafficking and secretion which is expressed specifically in cells of the transition zone (Li and Xue 2007), influences strongly PAT. Knock-out of this PLD or inhibition of its activity by butanol leads to a strong reduction of IAA fluxes in root apices (Mancuso et al. 2007). In *contrast*, gain-of-function mutant or addition of PA, signal molecule produced by the PLD activity, resulted in increased auxin fluxes at the root apex. All this provides both genetic and chemical evidence that PLD Zeta2 activity drives the auxin secretion in the root apex transition zone (Mancuso et al. 2007, Baluška et al. 2007b).

3.6 Plant Synapses Active in Polar Auxin Transport as Gravisensing Domains?

Root apex synapses are active in the polar auxin transport which typically is aligned along the gravity vector. Our recent model suggests that mechanical asymmetry is behind this vectorial gravity-controlled auxin transport (Baluška et al. 2005a, 2007a). Gravity, due to the vectorial mechanical load of protoplast amplified by sedimented statoliths (amyloplasts), imposes high tensional stress on the plasma membrane of the physically lower cell pole. This mechanical stress would be then releaved by adding more membrane via shifting the endocytosis-exocytosis balance towards exocytosis (Fig. 3). Despite the fact that there is strong genetic redundancy in the PIN network (Vieten et al. 2005), reposition of roots in the gravity field easily re-distributes this auxin flux within just few minutes. For instance, PIN3 shifts to the new physical bottom of root cap statocytes within 5–10 minutes of gravistimulation (Friml 2003). So it is quite obvious that the mechanical asymmetry of plant synapses is the primary one while the molecular asymmetry is only a secondary consequence of the mechanical asymmetry (Fig. 3). This feature makes the plant synapses active in the polar auxin transport for excellent domains relevant for the plant gravisensing.

3.7 Transition Zone Plant Synapses: Integration of Gravitropic and Phototropic Responses of Root Apices via Endocytic Vesicle Recycling?

Plant organs orient their growth according to physical information from the environment, with gravity and light as the most important cues. Both gravity and light are inducing gravity- and light-oriented growth via effects on the polar auxin transport which is at least partially driven by brefeldin A-sensitive vesicle recycling. It is still unclear how gravity and light stimuli are integrated and translated into asymmetric auxin transport patterns. As suggested above, endocytosis and vesicle trafficking emerge as new players of sensing and transducing of gravity-triggered signals (Baluška et al. 2007a). The light signal can also trigger changes in endocytic vesicle recycling by mobilizing release of receptors, such as blue-light receptor phototropin 1, and other signaling molecules from the plasma membrane.

Our recent data support this new attractive concept (Wan et al. 2008, in preparation). Firstly, the site of light percetion is the root apex, the blue light receptor, phototropin 1 being enriched especially at root synapses in the root apex transition zone. Importantly, endosomal vesicle recycling of phototropin 1 is increased via blue light signals (Wan et al. 2008, in preparation), implicating that blue light signal perception and/or transduction might be accomplished at endosomes. Phototropin 1 is trapped within BFA-induced endosomal compartments (Wan et al. 2008). The endosomal recycling of putative auxin transporters PIN1 and PIN2 proteins is also affected by the blue light illumination, specifically at the root apex transition zone (Laxmi et al. 2008).

3.8 Classical Neurotransmitters Target Plant Synapses

L-Glutamate and acetylcholine (ACh) are well-known neurotransmitters in brain but have also impacts on plant root apices (Frauli et al. 2005, Walch-Liu et al. 2006). Specifically, the primary root apex is sensitive to L-Glutamate (Walch-Liu et al. 2006, Forde and Lea 2007). Plants also express glutamate-like receptor family proteins (GLRs) gated by glutamate and glycine (Chiu et al. 1999, Davenport 2002). Glutamate gated GLRs emerge to act in plants, similarly like in animals, as calcium channels that are involved in the response of plants to stimuli, like gravity, and to other stress factors from the environment (Dennison

and Spalding 2000, Demidchik et al. 2004, Qi et al. 2006). Genetic evidence suggests, that GLRs are essential for organization and functioning of primary root apices (Li et al. 2006). Acetylcholine is an abundant molecule in plants which increases under stress situations (Tretyn and Kendrick 1991). Plants express also acetylcholine esterase (AChE) which is inhibited by neostigmine bromide, a specific inhibitor of the animal AchE (Momonoki 1997, Sagane et al. 2005). Importantly, ACh-hydrolyzing activity is essential for root graviresponse (Momonoki et al. 1998). Here we have analysed effects of glutamate and ACh on the actin cytoskeleton and vesicle trafficking in primary root apices of *Arabidopsis* and maize. Our data reveal that the most sensitive subcellular domains are the cellular end-poles, which represent what we have defined as plant synapses. Particularly in a specialized area, the root transition zone, F-actin gets temporarily depleted and vesicle trafficking inhibited at the plant synapses after manipulation of L-glutamate and ACh levels (Fig. 4). Similar effects have been scored also with ethanol (Fig. 4) at concentrations even lower as those, which has been recently reported to affect F-actin at mouse brain synapses (Offenhäuser et al. 2006). In the future, we will study the behavior and performance of roots challenged with exogenous L-glutamate, ACh and ethanol, especially in relation to gravisensing and graviresponse of plant organs.

3.9 Surprising Connections Between Aluminium Toxicity in Plants and Alzheimer Disease

The toxicity of aluminium (Al) in both plant and animal cell biology is well established, although poorly understood. Al toxicity is the most important limiting factor for crop production in acid soil environments worldwide. Al is highly toxic to plant root apices, with cells of the transition zone representing the target of Al toxicity (Sivaguru and Horst 1998). Surprisingly, aluminium is not so toxic to root cells which entered the elongation regions. Similarly, the Al toxicity is not high in most other plant cells, excluding tip-growing root hairs and pollen tubes (see the discussion in Illéš et al. 2006).

Importantly, Al inhibits basipetal auxin transport selectively in the transition zone of root apices (Kollmeier et al. 2000) and affects also root cell patterning (Doncheva et al. 2005). In recent paper, we have discovered that Al is internalized into cells of the distal portion of the transition zone in *Arabidopsis* root apices, while Al also inhibits endocytosis in these cells (Illéš et al. 2006). Intriguingly in this respect, elongating root cells are not sensitive to Al, and there is no internalization of Al into elongating cells (Illéš et al. 2006). In support of the endocytosis of Al being the primary process affected in root cells, endocytosis of Al and its toxicity is lowered in the *Arabidopsis* mutant over-expressing of a DnaJ domain protein auxillin which regulates the clathrin-based endocytosis (Ezaki et al. 2006). Moreover, Al affected also nitric oxide (NO) production which is highest in cells of the distal portion of the transition zone. Plant synapses being very active in endocytosis and transporting auxin show highest activities in the transition zone, and it might turn out that the active plant synapses represent the Al target in the root apices. This scenario is strongly supported by our finding that Al causes strongest depolarization of the plasma membrane potential exactly in these root cells (Illéš et al. 2006). This effect is known to be mediated by glutamate and glutamate receptors (Sivaguru et al. 2003).

Interestingly, both in animals and humans, neuronal cells are extremely sensitive towards Al which is internalized specifically in these cells (Guy et al. 1990, Shi and Haug 1990). Al was found to be enriched in lysosomes (Schuurmans Stekhoven et al. 1990), similarly like Alzheimer's amyloid β-peptide plaque depositions. These are also internalized from cell sur-

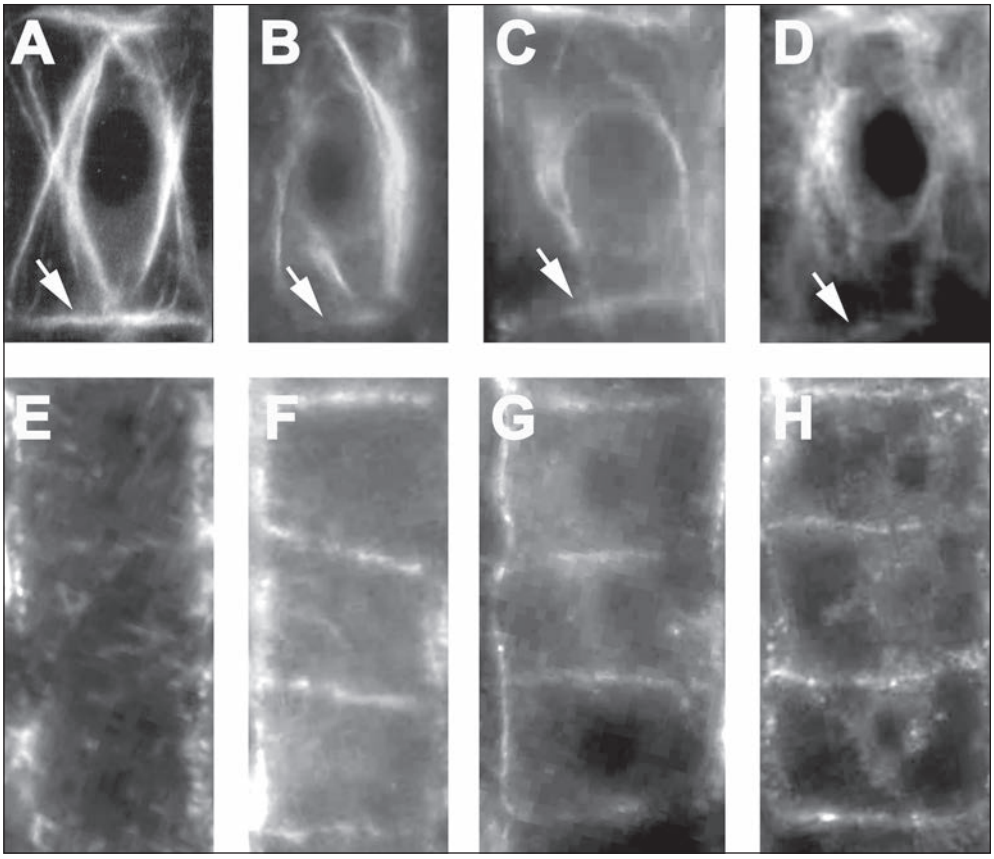

Fig. 4 Glutamate, acetylcholine, and ethanol deplete F-actin and enrich tubulin at plant synapses in the transition zone. 2 hours treatment with L-glutamate (1 mM), acetylcholine (1 mM) and ethanol (1 μM) deplete actin and increase tubulin at synapses (arrows in *A–D*) in the transition zone of maize root apices. (*A–D*): actin; (*E–H*): tubulin. (*A*) shows actin in control root apices, (*E*) shows tubulin in control root apices. For details on labelings see Baluška et al. 1992, 1997.

face, and Al was reported to inhibit their degradation (Sakamoto et al. 2006). Therefore, in both neuron-like root cells and brain neurons, endocytosis of Al is interfereing with synaptic activities and emerges to be relevant to its high toxicity. Further studies on these unique root apex cells, very active in the neuronal-like synaptic communication, might give us crucial clues not just for plant biology but also for our understanding of the Alzheimer disease.

3.10 Auxin, Retinoid Acid and Wingless: Neuronal and Synaptic Connections

Auxin has clearly several morphogen-like properties (Bhalerao and Bennett 2003, Grieneisen et al. 2007, Veit 2007). In this respect, it is intriguing that there are some similarities between auxin in plants (Benfey 2002) and retinoid acid and Wingless morphogens in animals (Ciani and Salinas 2005, Maden 2007). Morphogens are versatile signaling molecules confering positional information in organs and tissues. While retinoid acid controls the

formation and development of central nervous system of animals (Maden 2007), Wingless emerged to be important for the formation and development of synapses (Salinas 2004, Speese and Budnik 2007). In close connection to these animal morphogens, auxin as plant-specific morphogen (Veit 2007) is essential for the root apex formation and development, as well as for plant neurobiological activities (Baluška et al. 2003b, c, 2004a, 2005a). Interestingly in this respect, Wingless morphogenic gradient formation along the anterior – posterior body axis requires retromer function (Coudreuse et al. 2006), and the same have turned out recently for auxin too (Jaillais et al. 2007). Moreover, both auxin and morphogens of the Wingless family have both genomic and non-genomic signaling pathways (Paciorek et al. 2005, Lu and Van Vactor 2007). As other morphogens are also involved in patterning of nervous system (Salie et al. 2005), we are obviously just scratching the surface of this *terra incognita* and many surprises are to be revealed in future studies. It seems that our current categorization of diverse signaling molecules of multicellular eukaryotes is too naive and that we will be forced to re-define them in future.

4. Plant Neurobiology: Paradigm Shift not only in Plant Sciences

The transition zone is specialized for integration and processing of the retrieved information from especially abiotic but also biotic environment for motoric responses of growing root apices allowing effective root growth adaptation. There are striking similarities of this root apex zone to the neurobiological apparatus of animals, which translates sensory information in electrical and biological signals to induce adaptative behavior (De Weese and Zador 2006). Moreover, several anatomical aspects of transition zone cell cross-poles and neuronal synapses are in common. Both are asymmetric actin-based adhesion domains specialized for cell-to-cell communication by vesicle recycling, based on clathrin controlled endocytosis and calcium regulated secretion. For example, synaptotagmins, neuronal proteins mediating calcium regulated exocytosis and vesicle recycling at synapses, are found in plants. The *Arabidopsis* genome encodes six synaptotagmin-like genes (Craxton 2004, 2007). *Arabidopsis* synaptotagmin-like protein 1 (STL1) localizes at plant synapses in the root apex transition zone (Schapire et al. 2008). Last but not least, auxin is not only secreted out of root apex cells similarly like neurotransmitters (Baluška et al. 2003b, Schlicht et al. 2006, Mancuso et al. 2007) but is also known to induce rapid electrical responses in adjacent cells (Pickard 1984). All this leads to the new concept of plant neurobiology. The plant neurobiological apparatus at the root apex is similar to brains of lower animals (Darwin 1880, Baluška et al. 2004a, 2006, Barlow 2006). It is specialized to retrieve, process, and integrate multiple informations from environment in order to drive coordinated movements in order to achieve adaptive biological responses to abiotic and biotic stimuli (Brenner et al. 2006).

The idea to consider root apices as a decentral information processing system is not new as it was proposed already by Charles Darwin in 1880 (Darwin 1880, Baluška et al. 2004a, 2006, Barlow 2006, Trewavas 2007). This concept is comparable to a diffuse nervous net of hydra, helps to understand several aspects of plants which are not explainable with the classical view of plant sciences (Brenner et al. 2006, 2007). The role and importance of action potentials, the mechanism of root graviresponse or the complex auxin transport patterns at root apices are now all set in contex to growth behavior and adaptation with the enviroment, giving the possibility for a much better understanding of plants (Baluška et al. 2007a).

Plants communicate together extensively via a whole battery of volatile substances. In shoots, this communication allows warning of unattacked plants from their neighbor plants under attack (Dicke and Bruin 2001, Bais et al. 2003, Baldwin et al. 2006, Maffei et al. 2007). Receiving plants are not only informed but they can prime their immunity so be prepared to possible attack (Ton et al. 2006). In roots, this allelochemical communication is even more prominent as the number of organisms with which roots interact is enormous (Bais et al. 2004, 2006). Generally, roots, in contrast to shoots, often engage into symbiotic interactions with both fungi and bacteria. Especially fungi are entering into symbiotic relationships with roots of almost all plants, with few exceptions such as *Arabidopsis*. In addition, roots of invasive plants release substances which are toxic to roots of other plants, resulting in "underground wars" (Bais et al. 2003, 2004, 2006, Rudrappa et al. 2007). Roots of parasitic plants can transform into haustoria and invade roots of prey plants, and auxin is essential for this process (Tomilov et al. 2005).

5. New Neuronal View of Plants: Animal Root Pole *versus* Vegetal Shoot Pole

Root apices show several unique features distinguishing them clearly from shoot apices. Not just the mere presence of the root cap but also regular cell files, organized by active synapses (cross-walls) and mini-synapses (pit-fields), clear root apex zonation in the longitudinal axis, and existence of central cylinder and cortex in the radial axis, simple anatomy and morphology, and animal-like behavior. Moreover, root apices are fully devoted for sensory/neuronal tasks and are free of any morphogenetic activities. Just the opposite is true for shoot apices which generate new leaves and shoot branches and terminate this activity just to transform into the sexual organs known as flowers. In additon, plant roots, similarly as sexual plant cells, can discriminate self from non-self roots and also perform kin recognition (Gruntman and Novoplansky 2004, Dudley and File 2007).

All this suggests that plant root apices, represents the anterior pole of the plant body, as suggested by Charles and Francis Darwin in 1880 (Darwin 1880). This view of plants differs radically from the classical view, originating from ancient Aristotelian division of living organisms, cemented by the Linnean categorization and Sachsian physiology (Sachs 1882). It suggests that all multicellular organisms, irrespective if animals or plants, have inherent anterior-posterior body axis with the anterior pole specialized for the searching-like behavior, nutrient uptake, sensory organs, and brain-like activities. On the other hand, the posterior pole of plant body is specialized for movements and sexual reproduction. This new view of plants can replace the current controversial apical-basal polarity axis (Baluška et al. 2005b, Friml et al. 2006) and will also change dramatically our understanding of plants in their whole communicative complexity.

Acknowledgements

Financial support by grants from the Bundesministerium für Wirtschaft und Technologie (BMWi) via Deutsches Zentrum für Luft- und Raumfahrt (DLR, Cologne, Germany; project 50WB 0434), from the European Space Agency (ESA-ESTEC Noordwijk, The Netherlands; MAP project AO-99-098), and from the Ente Cassa di Risparmio di Firenze (Italy) is gratefully acknowledged. F. B. receives partial support also from the Grant Agency VEGA, Bratislava, Slovakia – project 2/5085/25; and from the Grant Agency APW, Bratislava, Slovakia – project APVV-0432-06.

References

Bais, H. P., Vepachedu, R., Gilroy, S., Callaway, R. M., and Vivanco, J. M.: Allelopathy and exotic plant invasion: from molecules and genes to species interactions. Science *301*, 1377–1380 (2003)

Bais, H. P., Park, S.-W., Weir, T. L., Callaway, R. M., and Vivanco, J. M.: How plants communicate using the underground information superhighway. Trends Plant Sci. *9*, 26–32 (2004)

Bais, H. P., Weir, T. L., Perry, L. G., Gilroy, S., and Vivanco, J. M.: The role of root exudates in rhizosphere interactions with plants and other organisms. Ann. Rev. Plant Biol. *57*, 233–266 (2006)

Baldwin, I. T., Halitschke, R., Paschold, A., Dahl, C. C. von, and Preston, C. A.: Volatile signaling in plant-plant interactions: "talking trees" in the genomics era. Science *311*, 812–815 (2006)

Baluška, F., Kubica, Š., and Hauskrecht, M.: Postmitotic 'isodiametric' cell growth in the maize root apex. Planta *181*, 269–274 (1990)

Baluška, F., Parker, J. S., and Barlow, P. W.: Specific patterns of cortical and endoplasmic microtubules associated with cell growth and tissue differentiation in roots of maize (*Zea mays* L.). J. Cell Sci. *103*, 191–201 (1992)

Baluška, F., Brailsford, R. W., Hauskrecht, M., Jackson, M. B., and Barlow, P. W.: Cellular dimorphism in the maize root cortex: involvement of microtubules, ethylene and gibberellin in the differentiation of cellular behaviour in post-mitotic growth zones. Bot. Acta *106*, 394–403 (1993)

Baluška, F., Barlow, P. W., and Kubica, Š.: Importance of the post-mitotic 'isodiametric' growth (PIG) region for growth and development of roots. Plant Soil *167*, 31–42 (1994)

Baluška, F., Vitha, S., Barlow, P. W., and Volkmann, D.: Rearrangements of F-actin arrays in growing cells of intact maize root apex tissues: a major developmental switch occurs in the postmitotic transition region. Eur. J. Cell Biol. *72*, 113–121 (1997)

Baluška, F., Salaj, J., Mathur, J., Braun, M., Jasper, F., Samaj, J., Chua, N. H., Barlow, P. W., and Volkmann, D.: Root hair formation: F-actin-dependent tip growth is initiated by local assembly of profilin-supported F-actin meshworks accumulated within expansin-enriched bulges. Dev. Biol. *227*, 618–632 (2000a)

Baluška, F., Volkmann, D., and Barlow, P. W.: Actin-based domains of the 'cell periphery complex' and their associations with polarized 'cell bodies' in higher plants. Plant Biol. *2*, 253–267 (2000b)

Baluška, F., Jasik, J., Edelmann, H. G., Salajova, T., and Volkmann, D.: Latrunculin B induced plant dwarfism: plant cell elongation is F-actin dependent. Dev. Biol. *231*, 113–124 (2001a)

Baluška, F., Cvrcková, F., Kendrick-Jones, J., and Volkmann, D.: Sink plasmodesmata as gateways for phloem unloading. Myosin VIII and calreticulin as molecular determinants of sink strength? Plant Physiol. *126*, 39–41 (2001b)

Baluška, F., Volkmann, D., and Barlow, P. W.: A polarity crossroad in the transition growth zone of maize root apices: cytoskeletal and developmental implications. J. Plant Growth Regul. *20*, 170–181 (2001c)

Baluška, F., Hlavacka, A., Samaj, J., Palme, K., Robinson, D. G., Matoh, T., McCurdy, D. W., Menzel, D., and Volkmann, D.: F-actin-dependent endocytosis of cell wall pectins in meristematic root cells: insights from brefeldin A-induced compartments. Plant Physiol. *130*, 422–431 (2002)

Baluška, F., Wojtaszek, P., Volkmann, D., and Barlow, P. W.: The architecture of polarized cell growth: the unique status of elongating plant cells. BioEssays *25*, 569–576 (2003a)

Baluška, F., Šamaj, J., and Menzel, D.: Polar transport of auxin: carrier-mediated flux across the plasma membrane or neurotransmitter-like secretion? Trends Cell Biol. *13*, 282–285 (2003b)

Baluška, F., Šamaj, J., Wojtaszek, P., Volkmann, D., and Menzel, D.: Cytoskeleton – plasma membrane – cell wall continuum in plants: emerging links revisited. Plant Physiol. *133*, 482–491 (2003c)

Baluška, F., Mancuso, S., Volkmann, D., and Barlow, P. W.: Root apices as plant command centres: the unique 'brain-like' status of the root apex transition zone. Biologia *59*, 9–17 (2004a)

Baluška, F., Šamaj, J., Hlavacka, A., Kendrick-Jones, J., and Volkmann, D.: Myosin VIII and F-actin enriched plasmodesmata in maize root inner cortex cells accomplish fluid-phase endocytosis via an actomyosin-dependent process. J. Exp. Bot. *55*, 463–473 (2004b)

Baluška, F., Volkmann, D., and Menzel, D.: Plant synapses: actin-based domains for cell-to-cell communiction. Trends Plant Sci. *10*, 106–111 (2005a)

Baluška, F., Barlow, P., Baskin, T., Chen, R., Feldman, L., Forde, B., Geisler, M., Jernstedt, J., Menzel, D., Muday, G., Murphy, A., Šamaj, J., and Volkmann, D.: What is apical and what is basal in plant root development. Trends Plant Sci. *10*, 409–411 (2005b)

Baluška, F., Hlavacka, A., Mancuso, S., and Barlow, P. W.: Neurobiological view of plants and their body plan. In: Baluška, F., Mancuso, S., and Volkmann, D. (Eds.): Communication in Plants. Neuronal Aspects of Plant Life. pp. 19–35. Berlin, Heidelberg: Springer Verlag 2006

Baluška, F., Barlow, P. W., Volkmann, D., and Mancuso, S.: Gravity related paradoxes in plants: plant neurobiology provides the means for their resolution. In: Witzany, G. (Ed.): Biosemiotics in Transdisciplinary Context, Proceedings of the Gathering in Biosemiotics 6, Salzburg; pp. 122–133. Umweb: Helsinky 2007a

Baluška, F., Schlicht, M., Volkmann, D., and Mancuso, S.: Vesicular secretion of auxin: Evidences and implications. Plant Signal. Behav. *3*, 254–256 (2007b)

Bandyopadhyay, A., Blakeslee, J. J., Lee, O. R., Mravec, J., Sauer, M., Titapiwatanakun, B., Makam, S. N., Bouchard, R., Geisler, M., Martinoia, E., Friml, J., Peer, W. A., and Murphyet, A. S.: Interactions of PIN and PGP auxin transport mechanisms. Biochem. Soc. Trans. *35*, 137–141 (2007)

Barlow, P. W.: The root cap: cell dynamics, cell differentiation and cap function. J. Plant Growth Regul. *21*, 261–386 (2003)

Barlow, P. W.: Charles Darwin and the plant root apex: closing a gap in living systems theory as applied to plants. In: Baluška, F., Mancuso, S., and Volkmann, D. (Eds.): Communication in Plants. Neuronal Aspects of Plant Life; pp. 37–51. Berlin, Heidelberg: Springer 2006

Benfey, P.: Auxin action: slogging out of the swamp. Curr. Biol. *12*, R389–390 (2002)

Bhalerao, R. P., and Bennett, M. J.: The case for morphogens in plants. Nature Cell Biol. *5*, 939–943 (2003)

Björkmann, T., and Leopold, A. C.: An electric current associated with gravity sensing in maize roots. Plant Physiol. *84*, 841–846 (1987)

Blilou, I., Xu, J., Wildwater, M., Willemsen, V., Paponov, I., Friml, J., Heidstra, R., Aida, M., Palme, K., and Scheres, B.: The PIN auxin efflux facilitator network controls growth and patterning in Arabidopsis roots. Nature *433*, 39–44 (2005)

Brenner, E., Stahlberg, R., Mancuso, S., Vivanco, J., Baluška, F., and Van Volkenburgh, E.: Plant neurobiology: an integrated view of plant signaling. Trends Plant Sci. *11*, 413–419 (2006)

Brenner, E. D., Stahlberg, R., Manusco, S., Baluška, F., and Van Volkenburgh, E.: Plant neurobiology: The gain is more than the name. Trends Plant Sci. *12*, 285–286 (2007)

Chiu, J., DeSalle, R., Lam, H. M., Meisel, L., and Coruzzi, G.: Molecular evolution of glutamate receptors: a primitive signaling mechanism that existed before plants and animals diverged. Mol. Biol. Evol. *16*, 826–838 (1999)

Ciani, L., and Salinas, P. C.: WNTs in the vertebrate nervous system: from patterning to neuronal connectivity. Nature Rev. Neurosci. *6*, 351–362 (2005)

Ciesielski, T.: Untersuchungen über die Abwärtskrümmung der Wurzel. Beitr. Biol. Pflanze *1*, 1–30 (1872)

Collings, D. A., White, R. G., and Overall, R. L.: Ionic current changes associated with the gravity-induced bending response in roots of *Zea mays* L. Plant Physiol. *100*, 1417–1426 (1992)

Coudreuse, D. Y. M., Roël, G., Betist, M. C., Destrée, O., and Korswagen, H. C.: Wnt gradient formation requires retromer function in Wnt-producing cells. Science *312*, 921–924 (2006)

Craxton, M.: Synaptotagmin gene content of the sequenced genomes. BMC Genom. *5*, 43 (2004)

Craxton, M.: Evolutionary genomics of plant genes encoding N-terminal-TM-C2 domain proteins and the similar FAM62 genes and synaptotagmin genes of metazoans. BMC Genom. *8*, 259 (2007)

Darwin, C.: The Power of Movements in Plants. London: John Murray 1880

Davenport, R.: Glutamate receptors in plants. Ann. Bot. *90*, 549–557 (2002)

Delbarre, A., Muller, P., Imhoff, V., and Guern, J.: Comparison of mechanisms controlling uptake and accumulation of 2,4-dichlorophenoxy acetic acid, naphthalene-1-acetic acid, and indole-3-acetic acid in suspension-cultured tobacco cells. Planta *198*, 532–541 (1996)

Demidchik, V., Essah, P. A., and Tester, M.: Glutamate activates cation currents in the plasma membrane of *Arabidopsis* root cells. Planta *219*, 167–175 (2004)

Dettmer, J., Hong-Hermesdorf, A., Stierhof, Y. D., and Schumacher, K.: Vacuolar H^+-ATPase activity is required for endocytic and secretory trafficking in Arabidopsis. Plant Cell *18*, 715–730 (2006)

Dennison, K. L., and Spalding, E. P.: Glutamate-gated calcium fluxes in *Arabidopsis*. Plant Physiol. *124*, 1511–1514 (2000)

De Smet, I., and Jürgens, G.: Patterning the axis in plants–auxin in control. Curr. Opin. Plant Biol. *17*, 337–343 (2007)

De Smet, I., Tetsumura, T., De Rybel, B., Frei dit Frey, N., Laplaze, L., Casimiro, I., Swarup, R., Naudts, M., Vanneste, S., Audenaert, D., Inzé, D., Bennett, M. J., and Beeckman, T.: Auxin-dependent regulation of lateral root positioning in the basal meristem of Arabidopsis. Development *134*, 681–690 (2007)

De Weese, M. R., and Zador, A.: Neurobiology: efficiency measures. Nature *439*, 920–921 (2006)

Dhonukshe, P., Baluška, F., Schlicht, M., Hlavacka, A., Šamaj, J., Friml, J., and Gadella, T. W. J. Jr.: Endocytosis of cell surface material mediates cell plate formation during plant cytokinesis. Dev. Cell *10*, 137–150 (2006)

Dicke, M., and Bruin, J.: Chemical information transfer between plants: back to the future. Biochem. Syst. Ecol. *29*, 981–994 (2001)

Doncheva, S., Amenós, M., Poschenrieder, C. H., and Barceló, J.: Root cell patterning: a primary target for aluminium toxicity in maize. J. Exp. Bot. *56*, 1213–1220 (2005)

Dudley, S. A., and File, A. L.: Kin recognition in an annual plant. Biol. Lett. *3*, 435–438 (2007)

Ezaki, B., Kiyohara, H., Matsumoto, H., and Nakashima, S.: Overexpression of an auxilin-like gene (F9E10.5) can suppress Al uptake in roots of Arabidopsis. J. Exp. Bot. *58*, 497–506 (2006)

Favre, P., and Degli Agosti, R.: Voltage-dependent action potentials in *Arabidopsis thaliana*. Physiol. Plant. *131*, 263–272 (2007)

Felle, H. H., and Zimmermann, M. R.: Systemic signalling in barley through action potentials. Planta *226*, 203–214 (2007)

Forde, B. G., and Lea, P. J.: Glutamate in plants: metabolism, regulation, and signalling. J. Exp. Bot. *57*, 2339–2358 (2007)

Foreman, J., Demidchik, V., Bothwell, J. H. F., Mylona, P., Miedema, H., Torres, M. A., Linstead, P., Costa, S., Brownlee, C., Jones, J. D. G., Davies, J. M., and Dolan, L.: Reactive oxygen species produced by NADPH oxidase regulate plant cell growth. Nature *422*, 442–446 (2003)

Frauli, M., Neuville, P., Vol, C., Pin, J.-P., and Prezeau, L.: Among the twenty classical L-amino acids, only glutamate directly activates metabotropic glutamate receptors. Neuropharmacology *50*, 245–253 (2006)

Friml, J.: Auxin transport – shaping the plant. Curr. Opin. Plant Biol. *6*, 7–12 (2003)

Friml, J., Winiewska, J., Benková, E., Mendgen, K., and Palme, K.: Lateral relocation of auxin efflux regulator PIN3 mediates tropism in Arabidopsis. Science *415*, 806–809 (2002)

Friml, J., Benfey, P., Benková, E., Bennett, M., Berleth, T., Geldner, N., Grebe, M., Heisler, M., Hejátko, M., Jürgens, G., Laux, T., Lindsey, K., Lukowitz, W., Luschnig, C., Offringa, R., Scheres, B., Swarup, R., Torres-Ruiz, R., Weijers, D., and Zažímalová, E.: Apical-basal polarity: why plant cells don't stand on their heads. Trends Plant Sci. *11*, 12–14 (2006)

Fromm, J., and Lautner, S.: Electrical signals and their physiological significance in plants. Plant Cell Environ. *30*, 249–257 (2007)

Geldner, N., Anders, N., Wolters, H., Keicher, J., Kornberger, W., Muller, P., Delbarre, A., Ueda, T., Nakano, A., and Jürgens, G.: The Arabidopsis GNOM ARF-GEF mediates endosomal recycling, auxin transport, and auxin-dependent plant growth. Nature *112*, 219–230 (2003)

Grieneisen, V. A., Xu, J., Marée, A. F. M., Hogeweg, P., and Scheres, B.: Auxin transport is sufficient to generate a maximum and gradient guiding root growth. Nature *449*, 1008–1013 (2007)

Gruntman, M., and Novoplansky, A.: Physiologically mediated self/non-self discrimination in roots. Proc. Natl. Acad. Sci. USA *101*, 3863–3867 (2004)

Guy, S. P., Seabright, P. J., Day, J. P., and Itzhaki, R. F.: Uptake of aluminum by human neuroblastoma cells. Biochem. Soc. Trans. *18*, 392–393 (1990)

Gutknecht, J., and Walter, A.: Transport of auxin (indoleacetic acid) through lipid bilayer membranes. J. Membr. Biol. *56*, 65–72 (1980)

Hahn, A., Firn, R., and Edelmann, H. G.: Interacting signal transduction chains in gravity-stimulated maize roots. Signal Transduct. *6*, 449–455 (2006)

Hause, G., Šamaj, J., Menzel, D., and Baluška, F.: Fine structural analysis of brefeldin A-induced compartment formation after high-pressure freeze fixation of maize root epidermis: Compound exocytosis resembling cell plate formation during cytokinesis. Plant Signal. Behav. *1*, 134–139 (2006)

Hawes, M. C., Gunawardena, U., Miyasaka, S., and Zhao, X.: The role of root border cells in plant defense. Trends Plant Sci. *5*, 128–133 (2000)

Heslop-Harrison, J.: Darwin and the movement of plants: a retrospect. In: Skoog, F. (Ed.): Plant Growth Substances; pp. 3–14. Berlin, Heidelberg, New York: Springer 1979

Holweg, C.: Living markers for actin block myosin-dependent motility of plant organelles and auxin. Cell Motil. Cytoskel. *64*, 69–81 (2007a)

Holweg, C.: Acto-myosin motorises the flow of auxin. Plant Signal. Behav. *2*, 247–248 (2007b)

Holweg, C., and Nick, P.: Arabidopsis myosin XI mutant is defective in organelle movement and polar auxin transport. Proc. Natl. Acad. Sci. USA *101*, 10488–10493 (2004)

Illéš, P., Schlicht, M., Pavlovkin, J., Lichtscheidl, I., Baluška, F., and Ovecka, M.: Aluminium toxicity in plants: internalisation of aluminium into cells of the transition zone in *Arabidopsis* root apices relates to changes in plasma membrane potential, endosomal behaviour, and nitric oxide production. J. Exp. Bot. *57*, 4201–4213 (2006)

Ishikawa, H., and Evans, M. L.: Gravity-induced changes in intracellular potentials in elongating cortical cells of mung bean roots. Plant Cell Physiol. *31*, 457–462 (1990)

Ishikawa, H., and Evans, M. L.: Correlations between changes in electrical parameters and changes in cell elongation rates in gravistimulated roots. Adv. Space Res. *14*, 125–133 (1994)

Iwai, H., Masaoka, N., Ishii, T., and Satoh, S.: A pectin glucuronyltransferase gene is essential for intercellular attachment in the plant meristem. Proc. Natl. Acad. Sci. USA *99*, 16319–16324 (2002)

Iwai, H., Hokura, A., Oishi, M., Chida, H., Ishii, T., Sakai, S., and Satoh, S.: The gene responsible for borate cross-linking of pectin rhamnogalacturonan-II is required for plant reproductive tissue development and fertilization. Proc. Natl. Acad. Sci. USA *103*, 16592–16597 (2006)

Jaillais, Y., Santambrogio, M., Rozier, F., Fobis-Loisy, I., Miège, C., and Gaude, T.: The retromer protein VPS29 links cell polarity and organ initiation in plants. Cell *130*, 1057–1070 (2007)

Jones, M. A., Raymond, M. J., Yang, Z., and Smirnoff, N.: NADPH oxidase-dependent reactive oxygen species formation required for root hair growth depends on ROP GTPase. J. Exp. Bot. *58*, 1261–1270 (2007)

Kollmeier, M., Felle, H. H., and Horst, W. J.: Genotypical differences in aluminum resistance of maize are expressed in the distal part of the transition zone. Is reduced basipetal auxin flow involved in inhibition of root elongation by aluminum? Plant Physiol. *122*, 945–956 (2000)

Lam, S. K., Tse, Y. C., Robinson, D. G., and Jiang, L.: Tracking down the elusive early endosomes. Trends Plant Sci. *12*, 497–505 (2007)

Laxmi, A., Pan, J., Morsy, M., and Chen, R.: Light plays an essential role in intracellular distribution of auxin efflux carrier PIN2 in *Arabidopsis thaliana*. PLoS ONE *1*, e1510 (2008)

Li, G., and Xue, H. W.: *Arabidopsis* Dζ2 regulates vesicle trafficking and is required for auxin response. Plant Cell *19*, 281–295 (2007)

Li, J., Zhua, S., Songa, X., Shena, Y., Chena, H., Yua, J., Yia, K., Liub, Y., Karplusb, V. J., Wua, P., and Deng, X. W.: A rice glutamate receptor-like gene is critical for the division and survival of individual cells in the root apical meristem. Plant Cell *18*, 340–349 (2006)

Lu, C. S. and Van Vactor, D.: Synapse specificity: Wnts keep motor axons on target. Curr. Biol. *17*, R895–R898 (2007)

Maden, M.: Retinoic acid in the development, regeneration and maintenance of the nervous system. Nature Rev. Neurosci. *8*, 755–765 (2007)

Maffei, M. E., Mithöfer, A., and Boland, W.: Insects feeding on plants: rapid signals and responses preceding the induction of phytochemical release. Phytochemistry *68*, 2946–2959 (2007)

Mancuso, S., Marras, A. M., Volker, M., and Baluška, F.: Non-invasive and continuous recordings of auxin fluxes in intact root apex with a carbon-nanotube-modified and self-referencing microelectrode. Anal. Biochem. *341*, 344–351 (2005)

Mancuso, S., Barlow, P. W., Volkmann, D., and Baluška, F.: Actin turnover-mediated gravity response in maize root apices: gravitropism of decapped roots implicates gravisensing outside of the root cap. Plant Signal. Behav. *1*, 52–58 (2006)

Mancuso, S., Marras, A. M., Mugnai, S., Schlicht, M., Zarsky, V., Li, G., Song, L., Hue, H. W., and Baluška, F.: Phospholipase Dζ2 drives vesicular secretion of auxin for its polar cell-cell transport in the transition zone of the root apex. Plant Signal. Behav. *2*, 240–244 (2007)

Massa, G. D., and Gilroy, S.: Touch modulates gravity sensing to regulate the growth of primary roots of *Arabidopsis thaliana*. Plant J. *33*, 435–445 (2003)

McAllister, A. K.: Dynamic aspects of CNS synapse formation. Annu. Rev. Neurosci. *30*, 425–450 (2007)

Momonoki, Y. S.: Asymmetric distribution of acetylcholinesterase in gravistimulated maize seedlings. Plant Physiol. *114*, 47–53 (1997)

Momonoki, Y. S., Himeno, C., and Noguchi, K.: Acetylcholine as a signaling system to environmental stimuli in plants. III. Asymmetric solute distribution controlled by ACh in gravistimulated maize seedlings. Plant Prod. Sci. *1*, 83–88 (1998)

Nelson, W. J.: Adaptation of core mechanisms to generate cell polarity. Science *422*, 766–774 (2003)

Nick, P.: Noise yields order – auxin, actin, and polar patterning. Plant Biol. *8*, 360–370 (2006)

Offenhäuser, N., Castelletti, D., Mapelli, L., Soppo, B. E., Regondi, M. C., Rossi, P., D'Angelo, E., Frassoni, C., Amadeo, A., Tocchetti, A., Pozzi, B., Disanza, A., Guarnieri, D., Betsholtz, C., Scita, G., Heberlein, U., and Di Fiore, P. P.: Increased ethanol resistance and consumption in Eps8 knockout mice correlates with altered actin dynamics. Cell 127, 213–226 (2006)

Ovecka, M., Lang, I., Baluška, F., Ismail, A., Illeš, P., and Lichtscheidl, I. K.: : Endocytosis and vesicle trafficking during tip growth of root hairs. Protoplasma *226*, 39–54 (2005)

Paciorek, T., Zažímalová, E., Ruthardt, N., Petrášek, J., Stierhof, Y.-D., Kleine-Vehn, J., Morris, D. A., Emans, N., Jürgens, G., Geldner, N., and Friml, J.: Auxin inhibits endocytosis and promotes its own efflux from cells. Nature *435*, 1251–1256 (2005)

Pennazio, S.: The discovery of the chemical nature of the plant hormone auxin. Riv. Biol. *95*, 289–308 (2002)

Petrášek, J., Mravec, J., Bouchard, R., Blakeslee, J. J., Abas, M., Seifertová, D., Wiśniewska, J., Tadele, Z., Kubes, M., Covanová, M., Dhonukshe, P., Skupa, P., Benková, E., Perry, L., Krecek, P., Lee, O. R., Fink, G. R., Geisler, M., Murphy, A. S., Luschnig, C., Zažímalová, E., and Friml, J.: PIN proteins perform a rate-limiting function in cellular auxin efflux. Science *312*, 914–918 (2006)

Pickard, B. G.: Voltage transients elicited by sudden step-up of auxin. Plant Cell Physiol. *7*, 171–178 (1984)

Rahman, A., Bannigan, A., Sulaman, W., Pechter, P., Blancaflor, E. B., and Baskin, T. I.: Auxin, actin and growth of the *Arabidopsis thaliana* primary root. Plant J. *50*, 514–528 (2007)

Rudrappa, T., Bonsall, J., Gallagher, J. L., Seliskar, D. M., and Bais, H. P.: Root-secreted allelochemical in the noxious weed *Phragmites australis* deploys a reactive oxygen species response and microtubule assembly disruption to execute rhizotoxicity. J. Chem. Ecol. *33*, 1898–1918 (2007)

Qi, Z., Stephens, N. R., and Spalding, E. P.: Calcium entry mediated by GLR3.3, an Arabidopsis glutamate receptor with a broad agonist profile. Plant Physiol. *42*, 963–971 (2006)

Sachs, J.: Lectures on the Physiology of Plants. Oxford: Clarendon Press 1882

Sagane, Y., Nakagawa, T., Yamamoto, K., Michikawa, S., Oguri, S., and Momonokiet, Y. S.: Molecular characterization of maize acetylcholinesterase. A novel enzyme family in the plant kingdom. Plant Physiol. *138*, 1359–1371 (2005)

Sakamoto, T., Saitoa, H., Ishiia, K., Takahashia, H., Tanabeb, S., and Ogasawaraet, Y.: Aluminum inhibits proteolytic degradation of amyloid β peptide by cathpsin D: a potential link between aluminum accumulation and neurotic plaque deposition. FEBS Lett. *580*, 6543–6549 (2006)

Salie, R., Niederkofler, V., and Arber, S.: Patterning molecules; multitasking in the nervous system. Neuron *45*, 189–192 (2005)

Salinas, P. C.: Signaling at the vertebrate synapse: new roles for embryonic morphogens? J. Neurobiol. *64*, 435–445 (2005)

Šamaj, J., Baluška, F., Voigt, B., Schlicht, M., Volkmann, D., and Menzel, D.: Endocytosis, actin cytoskeleton and signalling. Plant Physiol. *135*, 1150–1161 (2004)

Šamaj, J., Read, N. D., Volkmann, D., Menzel, D., and Baluška, F.: The endocytic network in plants. Trends Cell Biol. *15*, 425–433 (2005)

Schapire, A. L., Voigt, B., Jasik, J., Rosado, A., Lopez-Cobollo, R., Menzel, D., Salinas, J., Mancuso, S., Valpuesta, V., Baluška, F., and Botella, M. A.: Arabidopsis synaptotagmin-like protein 1 is essential for plasma membrane viability and survival under abiotic stress. Plant Cell *20*, 3374–3388 (2008)

Scheres, B.: Stem-cell niches: nursery rhymes across kingdoms. Nature Rev. Mol. Cell Biol. *8*, 435–354 (2007)

Schlicht, M., Strnad, M., Scanlon, M. J., Mancuso, S., Hochholdinger, F., Palme, K., Volkmann, D., Menzel, D., and Baluška, F.: Auxin immunolocalization implicates vesicular neurotransmitter like mode of polar auxin transport in root apices. Plant Signal. Behav. *1*, 122–133 (2006)

Schuurmans Stekhoven, J. H., Renkawek, K., Otte-Holler, I., and Stols, A.: Exogenous aluminium accumulates in the lysosomes of cultured rat cortical neurons. Neurosci. Lett. *119*, 71–74 (1990)

Shi, B., and Haug, A.: Aluminium uptake by neuroblastoma cells. J. Neurochem. *55*, 551–558 (1990)

Sivaguru, M., and Horst, W. J.: The distal part of the transition zone is the most aluminium-sensitive apical root zone of maize. Plant Phyiol. *116*, 155–163 (1998)

Sivaguru, M., Pike, S., Gassmann, W., and Baskin, T. I.: Aluminum rapidly depolymerizes cortical microtubules and depolarizes the plasma membrane: evidence that these responses are mediated by a glutamate receptor. Plant Cell Physiol. *44*, 667–675 (2003)

Speese, S. D., and Budnik, V.: Wnts: up-and-coming at the synapse. Trends Neurosci. *30*, 268–275 (2007)

Stankovic, B.: Electrophysiology and plant gravitropism. In: Volkov, A. G. (Ed.): Plant Electrophysiology; pp. 423–436. Berlin, Heidelberg: Springer 2006

Teale, W. D., Paponov, I. A., and Palme, K.: Auxin in action: signalling, transport and the control of plant growth and development. Nature Rev. Mol. Cell Biol. *7*, 847–859 (2006)

Tomilov, A. A., Tomilova, N. B., Abdallah, I., and Yoder, J. I.: Localized hormone fluxes and early haustorium development in the hemiparasitic plant *Triphysaria versicolor*. Plant Physiol. *138*, 1469–1480 (2005)

Ton, J., D'Alessandro, M., Jourdie, V., Jakab, G., Karlen, D., Held, M., Mauch-Mani, B., and Turlings, T. C. J.: Priming by airborne signals boosts direct and indirect resistance in maize. Plant J. *49*, 16–26 (2006)

Tretyn, A., and Kendrick, R. E.: Acetylcholine in plants: presence, metabolism, and mechanism of action. Bot. Rev. *57*, 33–73 (1991)

Trewavas, A.: Response to Alpi et al.: Plant neurobiology – all metaphors have value. Trends Plant Sci. *12*, 231–233 (2007)

Veit, B.: Plumbing the pattern of roots. Nature *449*, 991–992 (2007)

Verbelen, J.-P., Cnodder, T. de, Le, J., Vissenberg, K., and Baluška, F.: The root apex of *Arabidopsis thaliana* consists of four distinct zones of cellular activities: meristematic zone, transition zone, fast elongation zone, and growth terminating zone. Plant Signal. Behav. *1*, 296–304 (2006)

Vieten, A., Vanneste, S., Winiewska, J., Benková, E., Benjamins, R., Beeckman, T., Luschnig, C., and Friml, J.: Functional redundancy of PIN proteins is accompanied by auxin-dependent cross-regulation of PIN expression. Development *132*, 4521–4531 (2005)

Voigt, B., Timmers, A. C., Samaj, J., Müller, J., Baluška, F., and Menzel, D.: GFP-FABD2 fusion construct allows *in vivo* visualization of the dynamic actin cytoskeleton in all cells of *Arabidopsis* seedlings. Eur. J. Cell Biol. *84*, 595–608 (2005a)

Voigt, B., Timmers, A. C. J., Šamaj, J., Hlavacka, A., Ueda, T., Preuss, M., Nielsen, E., Mathurf, J., Emansg, N., Stenmark, H., Nakano, A., Baluška, F., and Menzel, D.: Actin-based motility of endosomes is linked to polar tip-growth of root hairs. Eur. J. Cell Biol. *84*, 609–621 (2005b)

Walch-Liu, P., Liu, L. H., Remans, T., Tester, M., and Forde, B. G.: Evidence that L-glutamate can act as an exogenous signal to modulate root growth and branching in *Arabidopsis thaliana*. Plant Cell Physiol. *47*, 1045–1057 (2006)

Wan, Y.-L., Eisinger, W., Ehrhardt, D., Kubitscheck, U., Baluška, F., and Briggs, W.: The subcellular localization and blue-light-induced movement of phototropin 1-GFP in etiolated seedlings of *Arabidopsis thaliana*. Mol. Plant *1*/1, 103–117 (2008)

Wen, F., Zhu, Y., and Hawes, M. C.: Effect of pectin methylesterase gene expression on pea root devlopment. Plant Cell *11*, 1129–1140 (1999)

Wolverton, C., Mullen, J. L., Ishikawa, H., and Evans, M. L.: Two distinct regions of response drive differential growth in *Vigna* root electrotropism. Plant Cell Environ. *23*, 1275–1280 (2000)

Wolverton, C., Ishikawa, H., and Evans, M. L.: The kinetics of root gravitropism: dual motors and sensors. J. Plant Growth Regul. *21*, 102–112 (2002)

Zažímalová, E., Krecek, P., Skupa, P., Hoyerova, K., and Petrasek, J.: Polar transport of the plant hormone auxin – the role of PIN-FORMED (PIN) proteins. Cell. Mol. Life Sci. *64*, 1621–1637 (2007)

PD Dr. František Baluška
Institut für Zelluläre und Molekulare Botanik
Zellbiologie der Pflanzen
Rheinische Friedrich-Wilhelms-Universität Bonn
Kirschallee 1
53115 Bonn
Germany
Phone: +49 228 734748
Fax: +49 228 739004
E-Mail: baluska@uni-bonn.de

Nova Acta Leopoldina NF *96*, Nr. 357, 123–134 (2009)

Leaf Growth Dynamics

Achim WALTER (Jülich)

With 8 Figures and 1 Table

Abstract

Leaf growth of dicot plants varies in a pronounced way throughout the diel cycle. Alterations of environmental parameters often impose dramatic and unexpected imprints in the time-series of leaf area expansion. The effect of alterations of different environmental parameters on the diel leaf growth cycle of a number of species is demonstrated. For example, if light incident on tobacco leaves is increased transiently for some hours, leaf relative growth rate (RGR) decreases rapidly and recovers more slowly. Compared to untreated leaves average RGR is not increased during the day but light pulses accelerate RGR during the night. Overall, the conclusion is drawn that the diel leaf growth cycle is driven to a major extent by the interplay between light, carbohydrate metabolism and water relations.

Zusammenfassung

Das Blattwachstum von dikotylen Pflanzen variiert in einer charakteristischen Art und Weise während eines Tagesganges. Änderungen von Umweltparametern wirken sich oft dramatisch und unerwartet auf den Verlauf des Blattwachstums aus. Die Auswirkungen der Änderungen verschiedener Umweltparameter auf den Blattwachstumstagesgang einer Reihe von Arten werden gezeigt. Wenn beispielsweise die Lichtintensität, der eine Tabakpflanze ausgesetzt ist, vorübergehend für einige Stunden erhöht wird, nimmt die relative Wuchsrate (RGR) des Blattes rasch ab und erhöht sich danach langsamer wieder. Insgesamt wird die durchschnittliche RGR während des Tages nicht erhöht; in der Nacht steigt sie jedoch im Vergleich zu den Werten von Kontrollpflanzen an. Es wird die Schlussfolgerung aufgestellt, dass der Tagesgang des Blattwachstums durch das Zusammenspiel von Licht, Kohlenhydraten und Wasserrelationen maßgeblich angetrieben wird.

1. Introduction

Human interest in plants arises from the fact that plants produce biomass which can be used for a variety of purposes. The energy needed by plants for biomass production is usually gained from sunlight via photosynthesis. Hence, photosynthesis has been a focus of intense research throughout the 20th century. As other contributions to this meeting show, many diverse research efforts are being pursued successfully on a wide range of scales, from single chloroplast investigation of photosystems to satellite imaging of ecosystem gas exchange and models have been developed to explain in detail how changes of environmental factors affect photosynthesis at all levels.

Although models connecting light interception and plant growth have been established for plant breeding purposes (GRANIER et al. 2002, CHENU et al. 2007) they only provide a resolution of days to weeks and often only relate plant growth to daily integral temperature.

Yet, environmental conditions are far from being constant throughout 24 h. In fact, temperature, light intensity and a range of other factors vary widely throughout the day. The extents to which plants acclimate to the ever-changing external set of growth-controlling parameters remain unclear.

For how long can high temperatures during midday heat events be tolerated before shoot growth declines? Are plants performing worse or better, if they are exposed to fluctuating conditions compared to constant conditions? How much of a certain stress can they bear for how long? Can a certain degree of stress be intentionally applied in an early developmental stage to harden plants for unforeseen stress events? As we find answers to those questions, how can they be explained on the basis of our regulatory understanding of the plant? Current knowledge tends to be tissue- or cell-specific, and temporally dynamic processes are often poorly integrated into whole-plant signaling networks.

A key requirement for refining these approaches is to resolve leaf growth on a scale of hours to minutes and to clarify, how single-leaf growth dynamics are interlocked with total shoot growth and with root growth. Hence, the intention of this article is to highlight some aspects of the interaction between light intensity and leaf growth, as well as some other environmental modifications that affect both photosynthesis and plant growth.

2. Environmental Effects on Leaf Growth Dynamics in Tobacco and other Species

Tobacco has been a model plant for leaf growth investigations for some time (Avery 1933, Poethig and Sussex 1985). Initially, it was used because breeding efforts focused on leaf growth, selecting for wide, flat and fast-growing leaves in a range of cultivars. More recently, the opportunity to work with mutant and transgenic lines of different tobacco species has led to an increasing use in research. Tobacco is a monopodial plant with all leaves sequentially arranged along the shoot axis. Leaf area expansion is distributed in a binomial manner along the shoot axis with increments in individual leaf area being related to increments of neighboring leaves (Fig. 1). With time, the number of leaves increases and the total leaf area of the plant increases by correlated growth of leaves at different individual positions.

Temporally, characteristic variations of leaf growth intensity have been observed throughout the last years for this species (Walter and Schurr 2005). Relative growth rates are calculated for individual leaves from time-lapse image sequences (images are taken every three minutes throughout day and night) by custom-made algorithms (Schmundt et al. 1998, Walter and Schurr 2005). When leaves are properly constrained to grow within the focal plane of a camera (Fig. 2), tobacco leaves show pronounced diel growth cycles (Fig. 3) with maxima in the late night or dawn. Strong, transient excursions are observed as an immediate reaction to switching on or off lights. This diel growth pattern is overlaid by the general decrease of RGR during post-emergent development.

The diel growth pattern described above for tobacco varies between species. For dicot C_3 plants, two main post-emergent growth patterns seem to be present: RGR is either maximal at dawn or it is maximal at dusk (Tab. 1). When environmental conditions change, excursions from this pattern occur which might be characteristic for the conditions to which the plant is exposed.

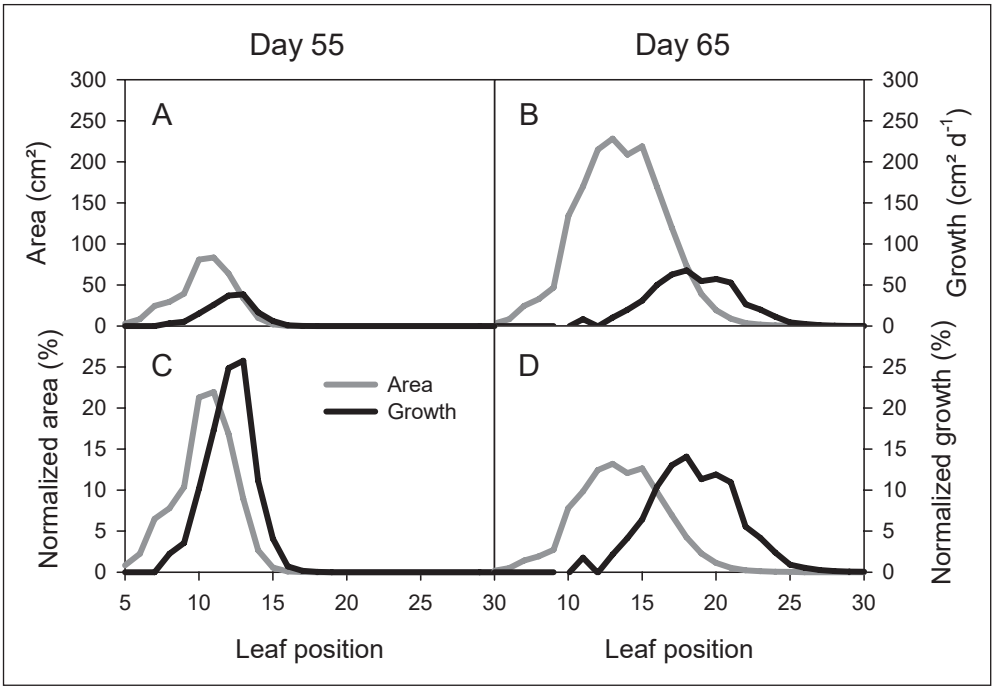

Fig. 1 Distributions of leaf area and leaf growth along the stem of tobacco plants. Average values of ten replicate plants grown in soil under standard conditions of this study (12 h/12 h day/night with 25/20 °C, respectively). (*A*) Leaf area and growth of individual leaves at day 55 after germination. (*B*) Leaf area and growth of individual leaves at day 65 after germination. (*C*) and (*D*) Normalized distributions at day 55 and day 65: Values for individual leaves are divided by total leaf area and by total increase in plant leaf area from day to day, respectively.

Tab. 1 Time of maximal leaf growth in several species, determined with digital image sequence processing.

Species	Time of maximal growth activity	Reference
Tobacco	Dawn	Walter and Schurr 2005
Arabidopsis	Dawn	Wiese et al. 2007
Castor bean	Dawn	Walter et al. 2002
Poplar	Dusk	Walter et al. 2005
Soybean	Dusk	Ainsworth et al. 2005

2.1 Light Pulses Alter the Diel Leaf Growth Cycle in Tobacco

In an experiment with seedling tobacco plants, light intensity was doubled three times during the day (light pulses were given at 11:00–14:00, 16:00–18:00, and 19:00–20:00, respectively; night: 20:00–8:00). For control plants light intensity during the day was constant at 80 µmol m^{-2} s^{-1} photosynthetically active radiation (PAR). During a 'light pulse', RGR of the leaf decreased rapidly in a first phase, increased more gradually in a second phase and reached or exceeded RGR of control plants at the end of the high light period (Figs. 4*A*, *B*). The exact

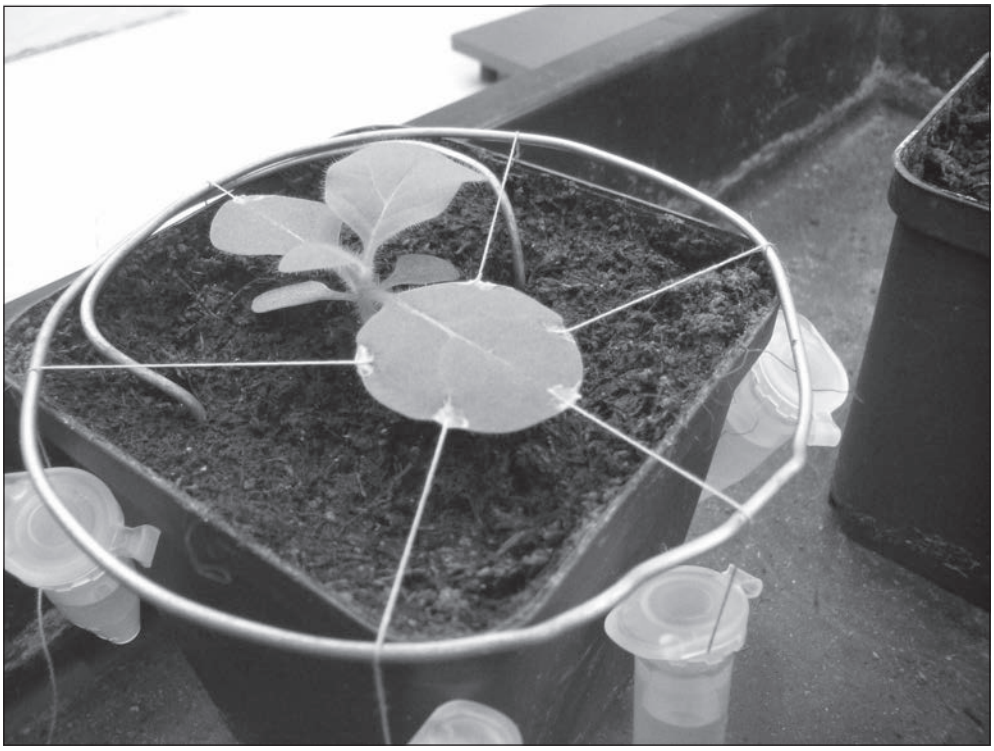

Fig. 2 Image of a tobacco seedling 20 days after germination. Leaf 4 is fixed with six strings glued to the leaf border, each carrying a weight of 2 g. Perpendicularly from the top, a camera acquires images of the growing leaf every three minutes; the leaf is illuminated with near-infrared light emitting diodes throughout day and night. Relative growth rates of the leaf are calculated from this image sequence via custom-made algorithms. For more details of the procedure see Walter and Schurr 2005.

progression of RGR during the three light pulse treatments differed, which is no surprise as also the development of RGR of control leaves differed among those three intervals. During the intervals between the light pulses, in which the treated leaves received control light intensity, RGR declined almost monotonically towards the RGR-value of control leaves. The initial decrease of RGR – or the first phase – has been described before (Hsiao et al. 1970, Walter and Schurr 2005) and is probably due to the sudden increase of transpiration which can lead to decreased turgor (Mott and Buckley 2000) or acid-induced increased cell wall extensibility (Mühling et al. 1995, Cosgrove 1999).

When average RGR values were compared among treatments for the periods between 08:00 and 20:00 (day) and between 20:00 and 08:00 (night), it became obvious, that the increase in light intensity of a factor of two during half of the day in the treated plants did not lead to a strong increase of daily RGR compared to control leaves (Fig. 4*C*). Yet, when ratios for values between the treatment day (day 2) and the day before treatment (day 1) were calculated, a much clearer picture with smaller variability within treatments emerged (Fig. 4*D*). Statistical evaluation of treated and control plants for the ratio at day showed that the difference was not significant ($p = 0.4$; t-test). When the same evaluation was performed for

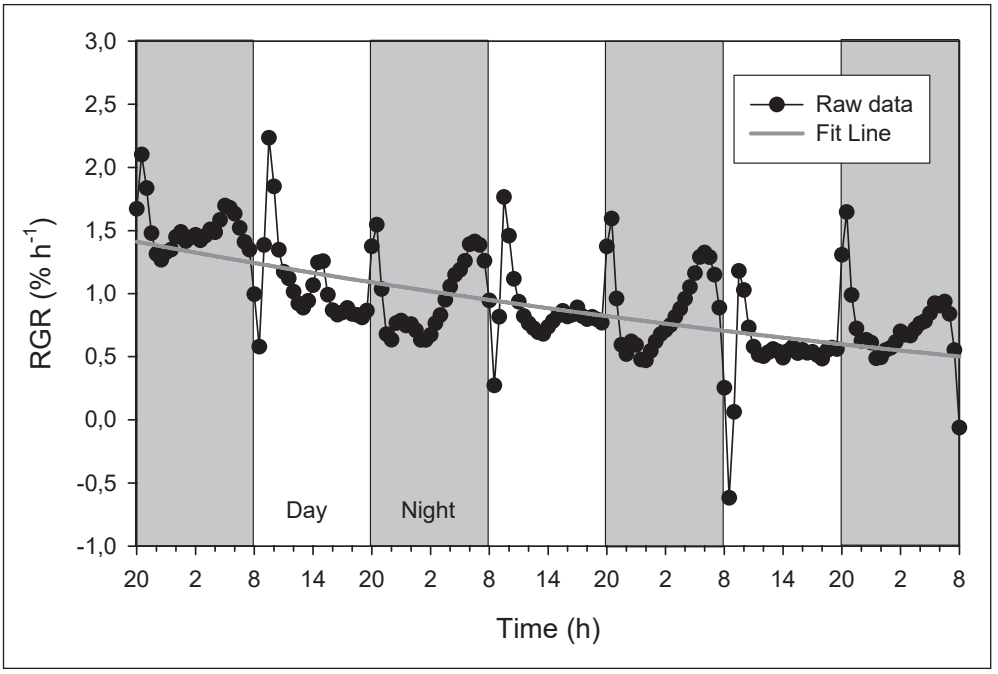

Fig. 3 Tobacco diel leaf growth cycle. Relative growth rate (RGR) was determined for a typical plant as briefly explained in Fig. 2.

the average nocturnal RGR values, a significant difference was obtained ($p = 0.002$); treated leaves grew 27 % faster than control leaves. This result matches the findings of a comparable experiment, in which growth of the total projected leaf area was monitored on a day-to-day basis (Walter et al. 2007). There, a significant increase of growth in the same order of magnitude was observed during the first 24 h, when light intensity was increased in a similar manner.

2.2 Starch Remobilization Plays a Crucial Role for the Diel Leaf Growth Cycle in Arabidopsis

Indirect evidence for the cause of this response comes from a study with *Arabidopsis* mutant plants (Wiese et al. 2007). In starch-free (stf1) mutants which cannot build up starch during the day, RGR and leaf glucose concentration increased at the end of the day compared to wild-type Landsberg erecta (Ler) plants, while at the end of the night, RGR and leaf glucose level were markedly lower than in WT plants (Fig. 5). This supports the view that growth at dusk is provided with carbohydrates necessary to increase the structural material of the tissue by recently produced photosynthates, while at the end of the night, carbohydrates for growth processes are mainly derived from starch remobilization. Hence, during the day transiently increasing light intensity leads (*i*) to stomatal opening which initially reduces RGR and (*ii*) to increased carbohydrates which increase RGR. It has to be expected that depending on the amplitude and duration of the increase in light intensity, this may or may not lead to increased

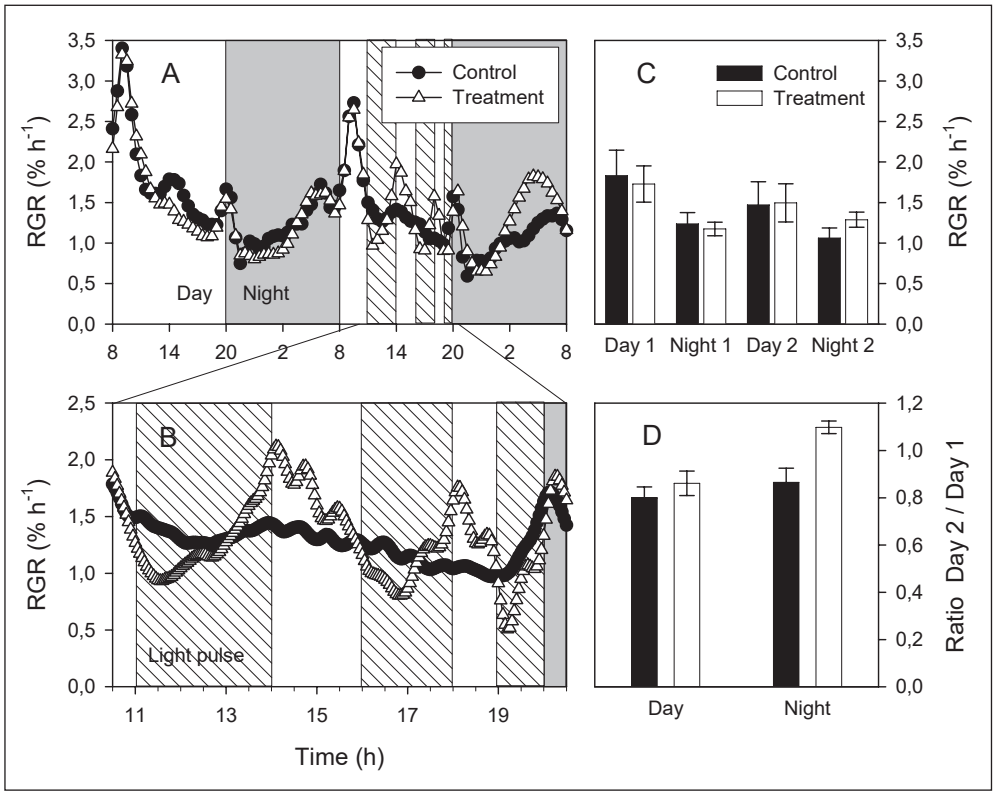

Fig. 4 Tobacco diel leaf growth behavior before and after 'light pulse' treatments (hatched bars indicate 2-times elevated light intensity in treated plants. n = 6; mean values and SE). (*A*) Average relative growth rate (RGR) of leaves from control plants and treated plants. (*B*) Enlarged depiction of RGR during 'light pulse' treatment phase. (*C*) Average RGR during day (08:00–20:00) and night (20:00–08:00) of control and treated plants, respectively at day 1 and day 2 of the experiment. (*D*) Average values of ratios of RGR for individual plants (night 2/night 1 and day 2/day 1, respectively).

integral growth during the day compared to growth of control leaves that are illuminated with a constantly lower light intensity. At night though, growth definitely increases due to the extra starch built up during the day. The above results demonstrate that mechanistic understanding of plant biomass growth in response to fluctuating light intensity requires experimental approaches that allow for a sufficient temporal resolution.

2.3 Diel Leaf Growth Cycles in Poplar are Affected by Atmospheric CO_2 Content via Altered Carbohydrate Availability

Another dramatic short-term effect of altered carbohydrate availability on the diel leaf growth cycle was observed in the leaves of rapidly growing woody poplar saplings (Walter et al. 2005). Leaves grown at ambient CO_2 were compared with leaves grown at elevated atmospheric CO_2. In elevated CO_2, increased leaf growth was observed at the end of the night, while growth was decreased compared to control leaves at ambient conditions in the late afternoon

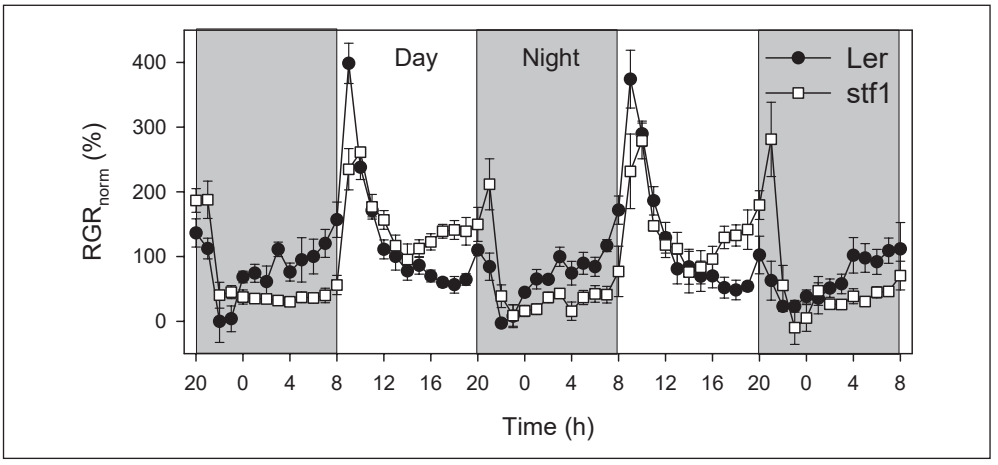

Fig. 5 *Arabidopsis* diel leaf growth cycle. Relative growth rate (RGR) of leaves of *Arabidopsis* wild type (Ler) and starch free mutant (stf1) plants (n = 6; mean values and SE; hourly means normalized on 24-h-mean values). Reproduced from WIESE et al. 2007 with kind permission of the authors.

(Fig. 6). In the late afternoon, glucose content of leaves growing at elevated CO_2 was lower than in control leaves, while the reverse was observed for starch content at this time of the day. Evidently the enzymatic machinery of the expanding leaves diverted the surplus of carbohydrates produced during increased photosynthesis at elevated CO_2, away from increased leaf growth towards increased storage and/or increased export into other plant organs or to the soil.

Overall however, leaves in elevated CO_2 treatments grew faster than leaves in ambient CO_2. The differences between treatments and the amplitude of the diel growth cycle increased during the season. A larger final leaf area was reached in the elevated CO_2 treatment by prolonging the phase in which leaves grew with an RGR of 30 to 40 % d^{-1} (WALTER et al. 2005).

2.4 Reversal of Diel Leaf Growth Cycle in Clusia due to the Switch from C_3 to CAM

A most pronounced example of the ways alterations in carbohydrate metabolism and/or transpiration dynamics can rapidly affect leaf growth behavior was recently reported in a study on *Clusia minor* (WALTER et al. 2008). This facultative CAM plant (LÜTTGE 2007) was induced to shift its mode of photosynthesis from C_3 behavior to CAM by a drought stress treatment (Fig. 7). Consequently, the phase of predominant carbohydrate assimilation was shifted from day to night, and cycling of malate as an intermediate storage form of assimilated carbon was increased. In parallel to this shift in carbohydrate metabolism, the diel leaf growth activity switched from a C_3-like behavior similar to that of poplar (maximal RGR at dusk) to a completely different temporal pattern with maximal growth activity during the day and practically no growth at all during the night. It is hypothesized that the correlated shift in growth activity is induced by the reduced availability of carbohydrates for growth at night when carbohydrates are almost entirely diverted to malate in CAM conditions. Altered transpiration behavior can also leave its imprint in the temporal pattern of the diel leaf growth cycle. During the

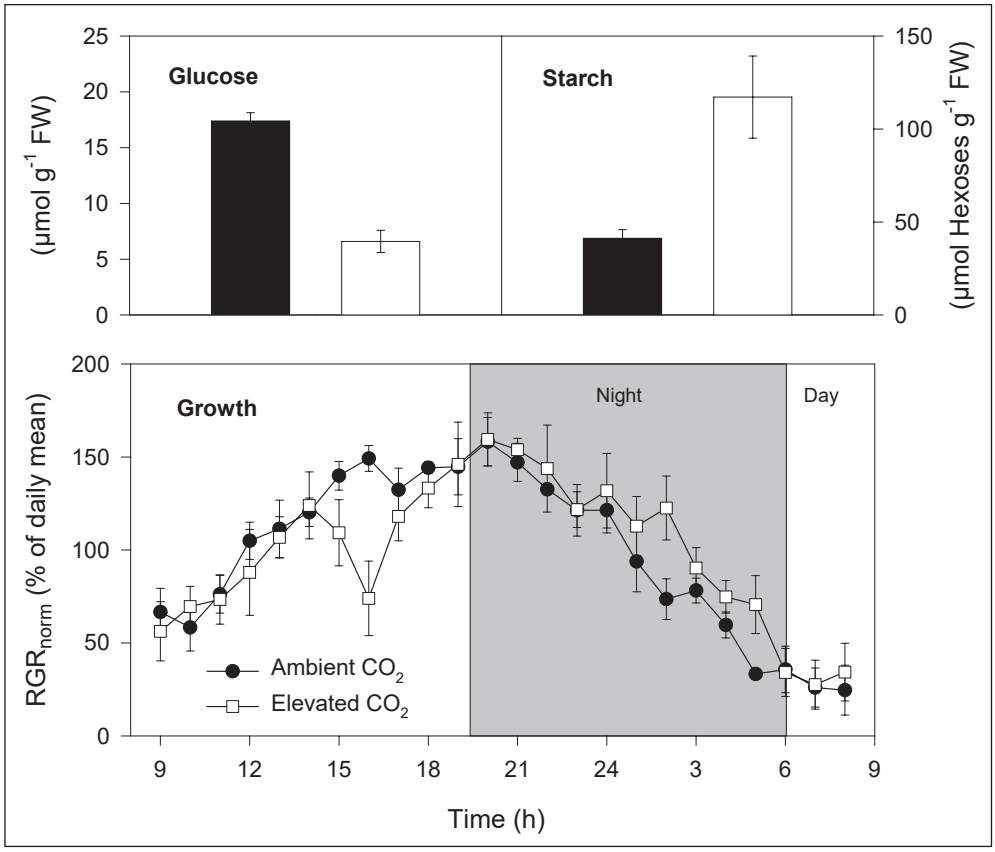

Fig. 6 Poplar diel leaf growth cycle. Relative growth rate (RGR) of poplar leaves (diel cycle; n = 17; mean values and SE; normalized values); glucose (n = 15) and starch (n = 15) content in growing leaves were determined at 16:00. Plants were grown at Biosphere 2 Center, Oracle, Arizona, under ambient and 3-times elevated CO_2, respectively. Reproduced with kind permission of Wiley-Blackwell Publishing from WALTER et al. 2005.

shift from C_3 to CAM, the phasing of transpiration is reversed from predominantly diurnal to predominantly nocturnal.

3. Towards some General Principles

Maximal growth activity is found during a period of minimal transpiration. This does not only hold true for *Clusia minor* but also for the other diel leaf growth cycles reported above. Maximal growth activity either occurs at dusk or at dawn; at times when transpiration is usually reduced compared to midday maxima. However, this is not the case for leaves of monocots, which show highest growth activity in the middle of the day, when temperatures are highest (BEN-HAJ-SALAH and TARDIEU 1995). In monocots, the growing leaf tissue itself is not engaged in transpiration, but is enclosed within the sheaths of older leaves. In the absence of competition between tissue water loss by transpiration and tissue volume increase by acquir-

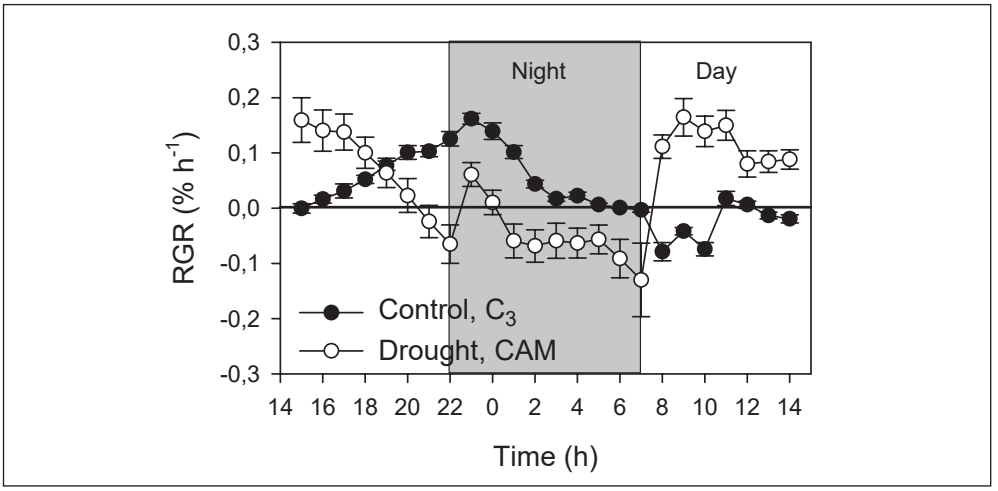

Fig. 7 *Clusia minor* diel leaf growth cycle. Relative growth rate (RGR) was determined in control plants and drought-stressed plants (n = 18; mean values and SE). Reproduced with kind permission of Wiley-Blackwell Publishing from Walter et al. 2008.

ing water might be the reason for the different timing and regulation of the diel growth pattern of monocots compared to dicots. Monocot leaf growth activity seems to be predominantly controlled by the temperature of the growth zone (Ben-Haj-Salah and Tardieu 1995) while dicot leaf growth activity seems to be primarily driven by the dynamic interplay between carbohydrate metabolism and water relations.

Biophysically, growth arises from the tension between turgor pressure an the rigidity/extensibility of plant cell walls, which is expressed in the Lockhart equation (Lockhart 1965). It will be a challenge for future studies to disentangle and precisely model how carbohydrate metabolism and water relations interact with cell wall extensibility and turgor. As the results of this articel show, sensitive analysis of the reaction of dicot leaf expansion in a range of species and environmental scenarios is a prerequisite to come to an improved understanding of the biophysical control of leaf growth dynamics which can be connected to the current molecular understanding of plant function.

4. Scaling from the Single Leaf Area to Shoot Biomass Growth

Up to now, leaf growth has been treated as a two-dimensional process, in which the leaf lamina develops a larger area. Is it appropriate to deal with this question at all and to discuss it in terms of biomass growth or is an analysis of leaf dry weight development or at least of leaf thickness a necessary prerequisite to provide serious data on plant growth? The former seems reasonable because there is no non-destructive method to date with which one could practically measure the thickness, volume or dry weight of a leaf or plant shoot. Moreover, in dicot leaves the increase in leaf area dominates greatly over the increase in thickness during post-emergent leaf development (Foster 1936); which is another marked contrast to the development of monocot leaves.

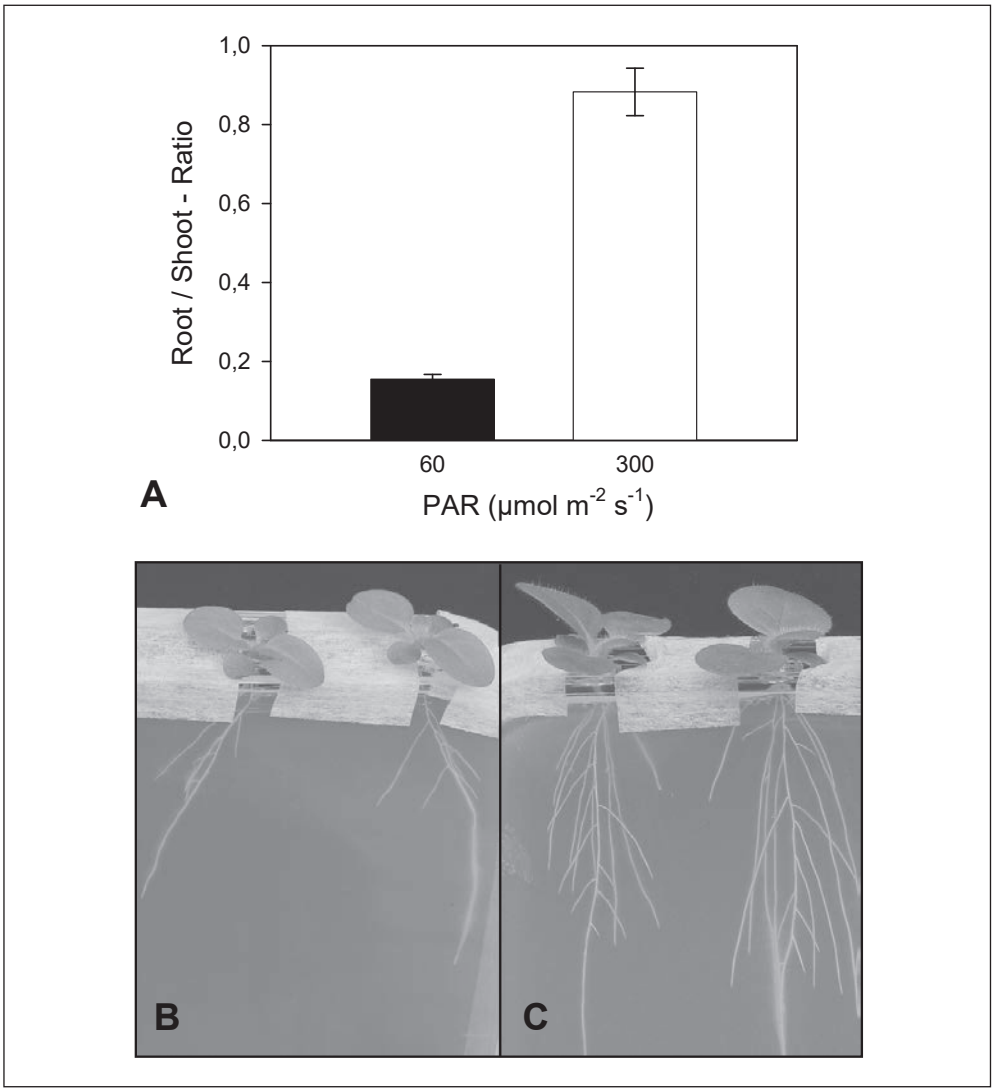

Fig. 8 Tobacco root/shoot-ratio in response to different light intensities. (*A*) Root/shoot-ratio based on fresh weight of plants grown on agar-filled Petri dishes (n = 5; mean values and SE). (*B*) and (*C*) plants grown in 60 and 300 µmol m^{-2} s^{-1} PAR, respectively, prior to harvest. Reproduced with kind permission of Landes Bioscience from WALTER and NAGEL 2006.

However, it is self-evident that the increases in leaf area and leaf biomass are not likely to be linearly correlated. In the above-mentioned study on poplar leaf growth (WALTER et al. 2005), leaves from the elevated CO_2 treatment overall had a 22 % increased leaf area compared to control leaves, but average leaf dry weight differed by 46 %. The discrepancy between area and dry weight depended on the exact positioning of the leaves to be compared between treatments. Leaf area of leaves from lower branches and leaves from the south side of trees was

comparable between treatments, while leaves from upper branches and leaves growing on the north side of the stem were larger in elevated CO_2 compared to ambient CO_2. Moreover, these differences seemed to increase during development. Nevertheless, the temporal evolution of differences that were obvious both in biomass and leaf area of the trees towards the end of the season, were reflected by non-destructively analyzed leaf area growth. Hence, leaf area analysis as described above is a valuable tool for investigation of growth differences. This conclusion is also supported by evidence from studies with much smaller tobacco and *Arabidopsis* plants: There, quasi-linear relations between the increase in leaf area and leaf biomass have been shown in several studies (Leister et al. 1999, Walter et al. 2007).

5. Connecting Leaf and Root Growth Dynamics

The increases in root and shoot biomass of a plant are connected with each other. Roots and growing leaves are competing sinks for all material substrates required for growth processes. While in some situations, root and shoot increase in parallel, there are numerous examples where investment in one organ is favored on costs of investment in the other organ. Often, it is not clear which environmental changes lead to increased (or decreased) investment in root or in the shoot. Increasing the light incident on tobacco shoots, for example, can lead to strong increase of root growth (Nagel et al. 2006, Walter and Nagel 2006) that far exceeds the increase of leaf growth (Fig. 8).

Herbivorous attacks, which might be perceived to decrease primarily leaf growth, paradoxically affect root growth stronger than leaf growth (Hummel et al. 2007). It is beyond the scope of this manuscript to explore the interaction between shoot and root growth in detail, but the few examples mentioned above are sufficient to emphasize that environmental effects on leaf growth often can be understood only if the reaction of the 'hidden half' of the plant is also taken into account.

Acknowledgements

I am grateful to Ulrich Schurr, who made this work possible by supporting me from my first scientific steps until the installation of an independent research group on leaf growth dynamics. Also, I want to express my gratitude to Barry Osmond, Wendy Silk, Uwe Rascher, Shizue Matsubara and numerous other colleagues and coworkers for their cooperation and for stimulating scientific discussions.

References

Ainsworth, E. A., Walter, A., and Schurr, U.: *Glycine max* leaflets lack a base-tip gradient in growth rate. J. Plant Res. *118*, 343–346 (2005)

Avery, G. S.: Structure and development of tobacco leaves. Amer. J. Bot. *20*, 565–592 (1933)

Ben-Haj-Salah, H., and Tardieu, F.: Temperature affects expansion rate of maize leaves without change in spatial distribution of cell length. Analysis of the coordination between cell division and cell expansion. Plant Physiol. *109*, 861–870 (1995)

Chenu, K., Franck, N., and Lecoeur, J.: Simulations of virtual plants reveal a role for SERRATE in the response of leaf development to light in *Arabidopsis thaliana*. New Phytol. *175*, 472–481 (2007)

Foster, A. S.: Leaf Differentiation in Angiosperms. Bot. Rev. *2*, 349–372 (1936)

Granier, C., Massonnet, C., Turc, O., Muller, B., Chenu, K., and Tardieu, F.: Individual leaf development in *Arabidopsis thaliana*: a stable thermal-time based programme. Ann. Bot. *89*, 595–604 (2002)

Hsiao, T. C., Acevedo, E., and Henderson, D. W.: Maize leaf elongation: Continuous measurements and close dependence on plant-water status. Science *168*, 590–591 (1970)

Hummel, G. M., Naumann, M., Schurr, U., and Walter, A.: Root growth dynamics of *Nicotiana attenuata* seedlings are affected by simulated herbivore attack. Plant Cell Environ. *30*, 1326–1336 (2007)

Leister, D., Varotto, C., Pesaresi, P., Niwergall, A., and Salamini, F.: Large-scale evaluation of plant growth in *Arabidopsis thaliana* in non-invasive image analysis. Plant Physiol. Biochem. *37*, 671–678 (1999)

Lockhart, J. A.: An analysis of irreversible plant cell elongation. J. Theor. Biol. *8*, 264–275 (1965)

Lüttge, U. (Ed.): Clusia. A Woody Neotropical Genus of Remarkable Plasticity and Diversity. Ecological Studies Vol. *194*. Heidelberg: Springer 2007

Mott, K. A., and Buckley, T. N.: Patchy stomatal conductance: emergent collective behaviour of stomata. Trends Plant Sci. *5*, 258–262 (2000)

Mühling, K. H., Plieth, C., Hansen, U. P., and Sattelmacher, B.: Apoplastic pH of intact leaves of *Vicia faba* as influenced by light. J. Exp. Bot. *46*, 377–382 (1995)

Nagel, K. A., Schurr, U., and Walter, A.: Dynamics of root growth stimulation in *Nicotiana tabacum* in increasing light intensity. Plant Cell Environ. *29*, 1936–1945 (2006)

Poethig, R. S., and Sussex, I. M.: The developmental morphology and growth dynamics of tobacco leaf. Planta *165*, 158–169 (1985)

Schmundt, D., Stitt, M., Jähne, B., and Schurr, U.: Quantitative analysis of the local rates of growth of dicot leaves at a high temporal and spatial resolution, using image sequence analysis. Plant J. *16*, 505–514 (1998)

Walter, A., Christ, M. M., Barron-Gafford, G. A., Grieve, K. A., Murthy, R., and Rascher, U.: The effect of elevated CO_2 on diel leaf growth cycle, leaf carbohydrate content and canopy growth performance of *Populus deltoides*. Global Change Biol. *11*, 1207–1219 (2005)

Walter, A., Christ, M. M., Rascher, U., Schurr, U., and Osmond, C. B.: Diel leaf growth cycles in Clusia spp. are related to changes between C_3 photosynthesis and crassulacean acid metabolism during development and during water stress. Plant Cell Environ. *31*, 484–491 (2008)

Walter, A., Feil, R., and Schurr, U.: Restriction of nyctinastic movements and application of tensile forces to leaves affects diurnal patterns of expansion growth. Funct. Plant Biol. *29*, 1247–1258 (2002)

Walter, A., Scharr, H., Gilmer, F., Zierer, R., Nagel, K. A., Ernst, M., Wiese, A., Virnich, O., Christ, M. M., Uhlig, B., Jünger, S., and Schurr, U.: The dynamics of seedling growth acclimation towards altered light conditions can be quantified via GROWSCREEN – a setup designed for rapid optical phenotyping of different plant species. New Phytol. *174*, 447–455 (2007)

Walter, A., and Schurr, U.: Dynamics of leaf and root growth – endogenous control versus environmental impact. Ann. Bot. *95*, 891–900 (2005)

Walter, A., and Nagel, K. A.: Root growth reacts rapidly and more pronounced than shoot growth towards increasing light intensity in tobacco seedlings. Plant Signal. Behav. *1*, 225–226 (2006)

Wiese, A., Christ, M. M., Virnich, O., Schurr, U., and Walter, A.: Spatio-temporal leaf growth patterns of *Arabidopsis thaliana* and evidence for sugar control of the diel leaf growth cycle. New Phytol. *174*, 752–761 (2007)

Dr. Achim Walter
Institute of Chemistry and
Dynamics of the Geosphere
ICG-3: Phytosphere
Forschungszentrum Jülich GmbH
52425 Jülich
Germany
Phone: +49 2461 618684
Fax: +49 2461 612492
E-Mail: a.walter@fz-juelich.de

Nova Acta Leopoldina NF *96*, Nr. 357, 135–141 (2009)

Shoot Heterogeneity in Trees: Consequences of Patchy N Availability and Vascular Transport

Vít Gloser[1], Pavel Sedláček[1]; and Colin M. Orians[2]

With 1 Figure and 1 Table

Abstract

We examined responses of two gymnosperms, *Picea abies* and *Thuja occidentalis*, to two nitrogen treatments, homogenous and patchy. We quantified whether the distribution and abundance of newly assimilated N would be more heterogeneous when the nitrogen supply was patchy. Plants were grown for three months in inorganic substrate fertilized with nutrient solution. Nitrogen was supplied as ^{15}N ammonium ^{15}N nitrate homogeneously to the whole root system (homogeneous treatment) or to a side root isolated in a split-root setup (patchy treatment). In the patchy treatment the rest of the root system received all nutrients except N. After 3 months of cultivation we quantified $\delta^{15}N$ content in the current year needles for each branch. We found that patchy N supply lead to significant increases in heterogeneity of N distribution within the shoots of both species. In the patchy treatment, the coefficient of variation in relative $\delta^{15}N$ was greater for lower branches than for upper branches indicating that the distribution of ^{15}N was less variable toward the top of the plant. We discuss several mechanisms that may contribute to more homogeneous N distribution in upper branches of the shoot. We conclude that seasonal N recycling of N within the plant did not result in homogeneous distribution of newly assimilated N when N supply is patchy.

Zusammenfassung

Wir haben die Reaktion zweier Gymnospermen, *Picea abies* und *Thuja occidentalis*, auf unterschiedliche Stickstoffversorgung, nämlich homogene und inhomogene N-Zufuhr, untersucht. Wir haben quantitativ geprüft, ob die Verteilung und Menge des neu assimilierten N bei inhomogener Zufuhr heterogener ist. Pflanzen wurden für drei Monate auf anorganischem Substrat mit Nährstofflösung angezogen. Stickstoff wurde als ^{15}N-Ammonium und ^{15}N-Nitrat dem ganzen Wurzelsystem homogen angeboten (homogene Behandlung) oder nur einer Nebenwurzel in einer Anordnung mit geteiltem Wurzelsystem (inhomogene Behandlung). Bei der inhomogenen Behandlung erhielt das übrige Wurzelsystem alle Nährstoffe außer Stickstoff. Nach 3 Monaten Kultivierung wurde der $\delta^{15}N$-Gehalt der Nadeln des laufenden Jahres jeden Zweiges analysiert. Wir fanden, dass inhomogene N-Zufuhr zu einem signifikanten Anstieg der Heterogenität der N-Verteilung in den Sprossen beider Arten führt. Bei der inhomogenen Behandlung war der Variationskoeffizient des relativen $\delta^{15}N$ in den unteren Zweigen größer als in den oberen Zweigen. Dies weist darauf hin, dass die Verteilung des $\delta^{15}N$ gegen die Spitze der Pflanzen hin weniger variabel war. Wir diskutieren verschiedene Mechanismen, die zu homogenerer N-Verteilung in den oberen Zweigen beitragen können. Wir schließen aus unseren Versuchen auch, dass saisonales Rezirkulieren des N innerhalb der Pflanzen nicht zu einer homogenen Verteilung des neu assimilierten N führt, wenn die N-Zufuhr inhomogen ist.

1 Masaryk University, Department of Experimental Biology, Kotlářská 2, 611 37 Brno, Czech Republic.
2 TUFTS University, Department. of Biology, Medford, MA 02155, USA.

1. Introduction

Availability of nitrogen, one of the most important nutrients for plant growth, frequently limits plant metabolic processes, and it may result not only in slower growth rate but also in altered biomass distribution and plant morphology. Nitrogen availability is often patchy (Jackson and Caldwell 1993, Stark 1994) and this can further limit the capacity of plants to acquire and to distribute N within the plant. Species differ in their capacity to respond to patches of nutrient availability (Robinson and van Vuuren 1998, Hodge 2004), and for species with high sectoriality – the restricted transport of resources along specific vascular pathways – the distribution of nitrogen may vary within the crown (Orians et al. 2004, Zanne et al. 2006). This unequal distribution of nutrients within a plant can constrain plant growth and development (Gloser et al. 2008). Gloser et al. (2008) found significant leaf-to-leaf variation in chlorophyll and leaf area in *Acer rubrum* following long-term fertilization of an isolated lateral root. In sum, the consequences of patchy nutrient availability depend upon the degree of sectoriality of each species, and upon the capacity for nutrient recycling and redistribution within the plant.

Several techniques have been used to describe differences among species in sectorialiy. Using hydraulic techniques, Orians et al. (2005b) found extensive variation in sectoriality, or vascular integration, among temperate deciduous trees. Dye transport studies have found similar differences among species (Orians et al. 2004, 2005a). Ultimately, it is the distribution of limited nutrients, such as N, that matters. Orians et al. (2004) showed that ^{15}N transport is more restricted in *Populus tremuloides*, *Acer saccharum* and *A. rubrum* than in *Betula lenta* and *B. papyrifera*, and Gloser et al. (2008) showed restricted transport can lead to differential growth and chemistry of *Acer rubrum*. Can the distribution of N in the crown be predicted? For straight grained sectored species, such as *Populus tremuloides*, the leaves above the labeled root accumulate more ^{15}N (Orians et al. 2004).

Do gymnosperms exhibit restricted nitrogen transport as well? Larson et al. (1994) showed that dye transport in *Thuja occidentalis* is highly sectored. Whether N transport is similarly restricted in *Thuja* and other gymnosperms is unknown. In the long-term, N recycling and redistribution may result in little if any heterogeneity in N distribution. Trees rely on the internal cycling of mobile nutrients to sustain their growth. Millard (1996) showed that 18–93 % of the nitrogen required for growth of young trees may come from remobilization. In *Picea sitchensis*, most of the N used for the growth of new needles at the beginning of the growing season is recycled from old needles and not dependent on external N supply (Proe and Millard 1994). Thus nitrogen transport following N recycling is likely to be quite local – from old to young needles on the same branch. Therefore we expect that recycling will not eliminate patterns of heterogeneity in gymnosperms.

Here we examined, (*i*) the distribution of ^{15}N in two gymnosperms, *Thuja occidentalis* and *Picea abies*, after 3 months of differential fertilization (homogeneous versus patchy), and (*ii*) how the variation in ^{15}N distribution changes with height along the stem. We hypothesized that both gymnosperms would exhibit heterogeneity in ^{15}N distribution, even after 3 months, and that the magnitude of heterogeneity would be the lowest higher on the stem as Zanne et al. (2006) found in tomato.

2. Materials and Methods

2.1 Plant Cultivation

Four-year old saplings of *Picea abies* (L.) Karst. and *Thuja occidentalis* (L.) were obtained from a local tree nursery and grown from seeds. Plants were 30 to 50 cm tall with approximately 10 and 20 branches of variable size for *Thuja* and *Picea* respectively. Branches were evenly distributed along the stem. Plants were cultivated in an experimental garden from May until August. When experimental treatments were started in May, *Picea* saplings had new buds that had just opened, and *Thuja* had a few new needles on the branches. Plants were grown in 6 l containers with perlite.

Nutrients were supplied every other day with 100 ml of modified Hoagland nutrient solution that contained 3 mM $CaCl_2$, 2 mM K_2SO_4, 1.9 mM KH_2PO_4, 2.7 mM $MgSO_4$, 20 µM $MnSO_4$, 8.5 µM $ZnSO_4$, 1.5 µM $CuSO_4$, 200 µM H_3BO_3, 2.5 µM Na_2MoO_4 and 405 µM FeNa-EDTA, and nitrogen as ammonium nitrate. The location of nitrogen addition depended on the treatment (patchy versus homogenous). On alternate days plants were watered with deionized water.

Plants in the patchy treatment were grown in a split-root setup – one lateral root was selected and placed separately into a smaller pot on the side of the main pot. In split-root cultivation only the pot with the lateral root received complete nutrient solution with nitrogen (5 mM). The main pot received a nutrient solution without nitrogen. Plants in the homogeneous treatment were grown in a single pot with a complete nutrient solution including N. The nitrogen supplied in the nutrient solution was enriched by ^{15}N provided as $^{15}NH_4{}^{15}NO_3$ (4 % enrichment, Sercon Ltd., UK) during the whole experimental period. This approach allowed us to quantify how plants partition newly acquired N over the entire growing season.

2.2 Plant Harvest and Biomass Analysis

At the end of the experimental period, 6 to 10 plants were harvested from each treatment. For each plant, all branches were detached and separated into current year and older growth, dried, ground and stored for subsequent isotope analysis. Since we expected that ^{15}N accumulation would be greatest in new needles, only the current-year needles of individual branches were analyzed for ^{15}N. In *Thuja* plants, all branches (n = 8–10) were analyzed whereas in *Picea* 10 to 15 branches were selected from different positions along the stem. Content of ^{15}N was analyzed using a continuous flow mass spectrometer (Europa Scientific Integra) at the University of California Stable Isotope Facility (Davis, USA). ^{15}N accumulation, expressed as $\delta^{15}N$, was determined by subtracting background levels of ^{15}N. Relative $\delta^{15}N$ content of needles on a single branch was calculated as ratio of the $\delta^{15}N$ of the respective branch and the highest $\delta^{15}N$ found within the evaluated plant.

2.3 Statistics

To determine the extent of variation in ^{15}N accumulation within each plant of each species, we calculated the coefficient variation (CV) within two branch positions along the stem: lower (branches below 0.4 relative height) and upper (branches above 0.7 relative height). CV of accumulation within each position for each plant was treated as one replicate (n = 6–10 plants

per treatment). Effects of experimental treatments as well as the effect of branch position on stem were tested in repeated measures ANOVA model with CVs from lower and upper branch positions as the repeated measure (both were from the same plant).

3. Results

After continuous supply of isotope during the growing season, $\delta^{15}N$ of needles ranged from 0 to 10000. Patterns of distribution were similar for relative $\delta^{15}N$ (to control for differential plant uptake) and absolute $\delta^{15}N$. For simplicity we report relative $\delta^{15}N$ only. The magnitude of variation in relative $\delta^{15}N$ within a plant varied by N treatment (patchy versus homogeneous), species, height along the stem, and by a branch position x N treatment interaction (Tab. 1). Variation in relative $\delta^{15}N$ was much greater in the patchy treatment in both species than in the homogeneous treatment and *Thuja* was more variable than *Picea* (Fig. 1). Within the patchy treatment, the CV of relative $\delta^{15}N$ was greater for lower branches than for upper branches (*Thuja*: mean = 0.89 and 0.43 respectively; *Picea*: mean 0.60 and 0.26 respectively) (Tab. 1). When supply was homogeneous, no significant difference between the lower and upper branches were observed for *Picea*, but they were marginally significant for *Thuja*.

Tab. 1 The results of repeated measures analysis of variance of coefficients of variation (CV) of relative ^{15}N isotopic enrichment of biomass of needles *Picea abies* and *Thuja occidentalis*. Plants were supplied with N to the whole root system or to one separated root only (N supply). Samples of needles for N analysis were taken either from lower (below 0.4 relative height) or upper (above 0.7) branches for both species in all N treatments. CV of branches on one plant and height group was treated as one replicate (6–10 plants per treatment).

	d.f.	*F*	*P*
Intercept	1	191.14	<0.001
Species	1	11.53	0.002
N supply	1	105.44	<0.001
Species x N supply	1	2.71	0.112
Branch Position	1	29.73	<0.001
Position x Species	1	2.20	0.15
Position x N supply	1	11.84	0.002
Position x Species x N supply	1	0.07	0.791

4. Discussion

Our experiments showed that when N supply is heterogeneous, distribution of ^{15}N tracer is also highly heterogeneous in shoots of both species. Similar results were obtained with angiosperms (Orians et al. 2004, Gloser et al. 2008, Zanne et al. 2006). Previous experiments, using dyes, with gymnosperms also showed vascular restrictions of xylem sap movement (Larson et al.1994, Gloser and Sedláček, unpublished data). Data presented in this paper are, to our knowledge, the first evidence that patchy N availability leads to heterogeneous N distribution in conifers and, hence, demonstrates sectorial transport of nutrients *in vivo*. We can only speculate what precisely limits tangential transport of nutrients in gymnosperms but

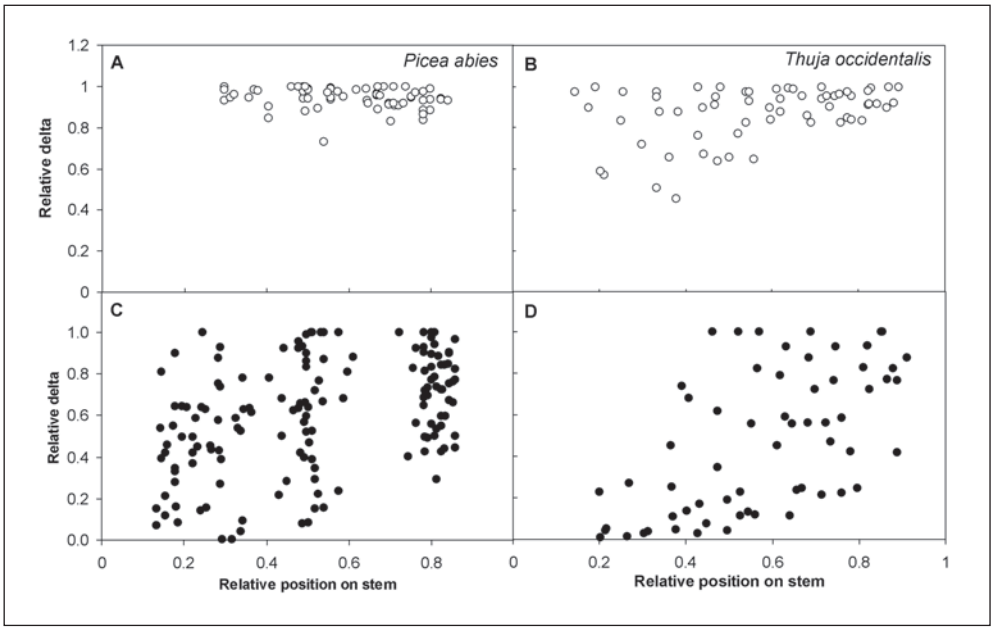

Fig. 1 The relative accumulation of isotope ^{15}N in needles of *Picea abies* and *Thuja occidentalis* as relative $\delta^{15}N$ and related to the relative height of the branch on the stem (from soil level to top of plant). Plants were supplied with N to the whole root system (homogeneous N supply *A*, *B*) or to one separated root only (patchy N supply *C*, *D*). Every point represents analysis of a single branch (6–10 plants per treatment).

most likely the number and size of interconduit pits in tracheids will be an important trait, similarly to intervessel pits in xylem of angiosperms (Orians et al. 2005a).

Long term (seasonal) cultivation in patchy treatment and recycling of N did not eliminate the heterogeneous distribution of the tracer. Continuous nitrogen recycling occurs in gymnosperms namely between growing and senescing needles (Millard and Proe 1993). For *Picea sitchensis*, the majority of N mobilized in the spring growth comes from previous year foliage (Millard and Proe 1993), and N taken up in the current season and partitioned to preexisting shoots is not remobilized later in the season to support growth of new shoots (Proe and Millard 1994). Thus, the distribution of newly assimilated N was most likely not affected by N recycling later in the season. Moreover, we assume that effects of heterogeneous distribution of N in conifers will extend beyond the current growing season because most nitrogen is stored in needles. We suggest that reduced N delivery to some parts may lead to smaller growth of needles, to smaller potential for N mobilization (sensu Chandler and Dale 1990) and to greater heterogeneity in the following growing season.

The heterogeneity in $\delta^{15}N$ distribution in both species was smaller towards the top of the plant (Fig. 1). We propose two possible mechanisms for this effect. First, tangential transfer of nutrients between tracheids may be higher further up the stem. This could occur if there is: (*i*) more active transport between adjacent tracheids higher on the stem, or (*ii*) lower resistance between conduits due to higher density of interconduit pits and a shorter transport pathway as the stem gets narrow. Second, N recycling could lead to a more homogeneous distribution of newly assimilated N. Because, recycling of N frequently occurs between old

and new needles within the same branch young upper branches with few older needles have less opportunity for recycling. These young branches rely on import of new N from roots and this could lead to more homogeneneous distribution of newly acquired N ($\delta^{15}N$).

Both species exhibited substantial heterogeneity in $\delta^{15}N$ distribution despite large differences in wood anatomy. *Picea* has spiral anatomy while *Thuja* is more straight grained (Nadezhdina and Cermak 2000, Larson et al. 1994, Gloser and Sedláček, unpublished). We suggest that the spiral pattern of sap flow in *Picea* may potentially facilitate the ability of this species to respond to spatial variation in other environmental factors (e.g. patchy light availability) as it increases the likelihood that at least one branch in that high light patch will be vascularly connected to the root in the nutrient-rich patch.

In summary, patchy nitrate availability generates aboveground heterogeneity in N distribution and abundance. This effect is likely to cause long-term consequences to the morphology and chemistry of leaves and needles (Gloser et al. 2008, Gloser and Sedláček, unpublished). This indicates that while redistribution may occur within a growing season, it is not of sufficient magnitude to eliminate aboveground heterogeneity in N distribution within a plant. This suggests that short-term experiments are indicative of long-term patterns of nutrient distribution.

Acknowledgements

This work was financially supported by the Ministry of Education, Youth and Sport of the Czech Republic project no. 1P05ME793, Grant agency of the Czech Republic project no. 522/04/0631 (to VG) and The Andrew Mellon Foundation (to CMO). We thank Amy Zanne for technical assistance and valuable comments on the presentation of results.

References

Chandler, J. W., and Dale, J. E.: Needle growth in Sitka spruce (*Picea sitchensis*) – Effects of nutrient deficiency and needle position within shoots. Tree Physiol. *6*, 41–56 (1990)

Gloser, V., Libera, K., and Orians, C. M.: Contrasting below- and aboveground responses of two deciduous trees to patchy nitrate availability. Tree Physiol. *28*, 37–44 (2008)

Hodge, A.: The Plastic plant: root responses to heterogeneous supplies of nutrients. New Phytol. *162*, 9–24 (2004)

Jackson, R. B., and Caldwell, M. M.: The Scale of nutrient heterogeneity around individual plants and its quantification with geostatistics. Ecology *74*, 612–614 (1993)

Larson, D. W., Doubt, J., and Matthessears, U.: Radially sectored hydraulic pathways in the xylem of *Thuja occidentalis* as revealed by the use of dyes. Int. J. Plant Sci. *155*, 569–582 (1994)

Millard, P.: Ecophysiology of the internal cycling of nitrogen for tree growth. J. Plant Nutr. Soil Sci. *159*, 1–10 (1996)

Millard, P., and Proe, M. F.: Nitrogen uptake, partitioning and internal cycling in *Picea sitchensis* (Bong.) Carr. as influenced by nitrogen supply. New Phytol. *125*, 113–119 (1993)

Nadezhdina, N., and Cermak, J.: Changes in sap flow rate in tree trunks and roots after mechanical damage. In: Klimo, E., Hager, H., and Kulhavý, J. (Eds.): Spruce Monocultures in Central Europe – Problems and Prospects. EFI Proceedings No. *33*, 167–175 (2000)

Orians, C. M., Babst, B., and Zanne, A. E.: Vascular constraints and long-distance transport in dicots. In: Holbrook, N. M., and Zwieniecki, M. (Eds.): Vascular Transport in Plants; pp. 355–371. Oxford: Elsevier/AP coimprint 2005a

Orians, C. M., Smith, S. D. P., and Sack, L.: How are leaves plumbed inside a branch? Differences in leaf-to-leaf hydraulic sectoriality among six temperate tree species. J. Exp. Bot. *56*, 2267–2273 (2005b)

Orians, C. M., Van Vuuren, M. M. I., Harris, N. L., Babst, B. A., and Ellmore, G. S.: Differential sectoriality in long-distance transport in temperate tree species: Evidence from dye flow, ^{15}N transport, and vessel element pitting. Trees *18*, 501–509 (2004)

Proe, M. F., and Millard, P.: Relationships between nutrient supply, nitrogen partitioning and growth in young Sitka spruce (*Picea sitchensis*). Tree Physiol. *14*, 75–88 (1994)

Robinson, D., and Van Vuuren, M. M. I.: Responses of wild plants to nutrient patches in relation to growth rate and life-form. In: Lambers, H., Poorter, H., and Van Vuuren, M. M. I., (Eds.): Inherent Variation in Plant Growth: Physiological Mechanisms and Ecological Consequences; pp. 237–257. Leiden: Backhuys 1998

Stark, J. M.: Causes of soil nutrient heterogeneity at different scales. In: Caldwell, M. M., and Pearcy, R. W. (Eds.): Exploitation of Environmental Heterogeneity by Plants: Ecophysiological Processes Above- and Belowground; pp. 255–284. San Diego: Academic Press 1994

Zanne, A. E., Lower, S. S., Cardon, Z. G., and Orians, C. M.: ^{15}N partitioning in tomato: Vascular constraints versus tissue demand. Funct. Plant Biol. *33*, 457–464 (2006)

Dr. Vít Gloser
Masaryk University
Department of Experimental Biology
Kotlářská 2
CZ-611 37 Brno
Czech Republic
Phone: +420 5 32146337
Fax: +420 5 41211214
E-Mail: vitekg@sci.muni.cz

Escherichia coli – Facets of a Versatile Pathogen

On the Occasion of the 150th Birthday of Theodor Escherich (1857–1911)

Leopoldina-Symposium
Deutsche Akademie der Naturforscher Leopoldina
in Zusammenarbeit mit der *European Molecular Biology Organization* (EMBO) und der *Federation of European Microbiological Societies* (FEMS)
vom 9. bis 12. Oktober 2007 im Bildungszentrum Kloster Banz, Bad Staffelstein

Nova Acta Leopoldina N. F., Bd. *98*, Nr. 359
Herausgegeben von Gabriele Blum-Oehler (Würzburg), Ulrich Dobrindt (Würzburg), Jörg Hacker (Würzburg – Berlin) und Volker ter Meulen (Würzburg – Halle/Saale)
(2008, 180 Seiten, 22 Abbildungen, 7 Tabellen, 22,95 Euro,
ISBN: 978-3-8047-2519-5)

Aus Anlass des 150. Geburtstages von Theodor Escherich, dem Entdecker des Bakteriums *Escherichia coli*, werden hier neue Forschungsergebnisse aus den Gebieten der Genomik, Pathogenese bakterieller Erkrankungen und Wirts-Bakterien-Interaktionen zusammengestellt.
Der Kinderarzt und Mikrobiologe Escherich beschrieb 1885 erstmals das „*Bacterium coli commune*“. Das später nach seinem Entdecker *Escherichia coli*, kurz *E. coli*, genannte Bakterium entwickelte sich zum beliebtesten „Haustier“ der Molekularbiologen. *E. coli* stellt mittlerweile molekularbiologisch den am besten untersuchten Organismus dar und wird von Wissenschaftlern weltweit als Modellorganismus genutzt. Behandelt werden außer der Bedeutung von *E. coli* in der molekularbiologischen Forschung vor allem Fragen der Genregulation, Beziehungen zwischen Kommensalismus und Pathogenität und das Problem der Virulenzfaktoren.

Wissenschaftliche Verlagsgesellschaft mbH Stuttgart

Modelling and Theory of Spatial Heterogeneity

Nova Acta Leopoldina NF *96*, Nr. 357, 145 –159 (2009)

Systematics of Spatiotemporal Heterogeneity Regulation of Large-scale Patterns by Biological Variability

Daniel Geberth[1], Christiane Hilgardt[2], and Marc-Thorsten Hütt[1]

With 7 Figures

Abstract

Spatiotemporal patterns often arise from local interactions in a self-organizing fashion. The resulting pattern, however, is shaped by the systematic differences between the system's constituents. Here we propose a new approach of studying spatiotemporal data, namely by analyzing the correlation between the spatial distribution of the constituents' properties and the features of the spatiotemporal pattern. We briefly embed this approach into a larger concept of pattern formation and then apply it to simulated patterns and experimental data for a model organism of biological pattern formation, the slime mold *Dictyostelium discoideum*. Simulations are performed with a simple *n*-state model of excitable dynamics. We show that the heterogeneous distribution of pattern characteristics has two distinct components, which correlate well with spatial distributions of highly sensitive and highly excitable cells, respectively. For the experimental system, we found systematic correlations between the spatial distribution of cellular fluctuations before pattern formation and the positions of spiral waves. Understanding this relation will be a considerable progress in uncovering the role of biological variability in complex cellular communication processes.

Zusammenfassung

Raumzeitliche Muster entstehen oft durch Selbstorganisation aus lokalen Wechselwirkungen. Das resultierende Muster ist jedoch geprägt durch systematische Unterschiede zwischen den Konstituenten des Systems. Hier schlagen wir eine neue Herangehensweise an raumzeitliche Daten vor, nämlich die Analyse der Korrelation zwischen Konstituenteneigenschaften und Mustern. Wir fügen diesen Ansatz in den allgemeinen theoretischen Rahmen der Musterbildung ein und wenden ihn dann an auf simulierte Muster und experimentelle Daten für einen Modellorganismus biologischer Musterbildung, den Schleimpilz *Dictyostelium discoideum*. Für die Simulationen wurde ein einfaches n-Zustands-Modell erregbarer Dynamiken verwendet. Wir zeigen, dass die statistische Verteilung von Mustereigenschaften aus zwei Komponenten besteht, die mit der räumlichen Verteilung der hochsensitiven beziehungsweise der hocherregbaren Elemente korrelieren.

Für die experimentellen Daten finden wir systematische Korrelationen zwischen der räumlichen Verteilung von Fluktuationen vor der Musterbildung und der Position späterer Spiralwellen. Diese Zusammenhänge in Modellen zu verstehen, kann einen erheblichen Fortschritt für ein Verständnis komplexer zellulärer Kommunikationsprozesse und ihrer Steuerung durch biologische Variabilität bedeuten.

1. Introduction

A few years ago, Peak et al. (2004) interpreted the dynamics of stomatal patchiness as the result of a distributed computation of an optimal metabolic state. Without an explicit math-

1 School of Engineering and Science, Jacobs University Bremen.
2 Biophysics Group, Otto-von-Guericke-Universität Magdeburg.

ematical model specifically designed to reproduce key features of stomatal dynamics, the authors compare the transient sizes of the spatiotemporal patterns upon a change of environmental conditions with those from a generic (cellular-automaton based) model of distributed computation (see also Mott and Peak 2007).

This approach is conceptually different from the usual framework of theoretical biology, where specific mathematical models are formulated and then, e.g., analyzed with methods from nonlinear dynamics. Here the mathematical description focuses on analogies. A quantitative analysis then relies on comparing statistical properties of the real-life data with those from the theoretical counterpart.

In spite of its intrinsic lack of quantitative comparison with a precise mathematical model from our point of view the study by Peak et al. (2004) constitutes a huge progress in conceptually understanding the spatiotemporal behavior of stomatal guard cells. By observing that stomata, basically, have to compute an opening state optimal on the global (leaf-wide) level using only local (cell-cell) communication the authors compare stomatal dynamics with a model system from complexity theory, namely cellular automata (CA).

One can view this study as an example of a new trend in theoretical biology on its way to an understanding at a system-wide level (Hütt and Lüttge 2007): Ever larger systems require models with abstract, discrete dynamics and the use of stochastic processes to implement the effect of stochasticity on this abstract level (see also Bornholdt 2005).

Beyond this basic difference of not relying on the visual agreement between observed and simulated patterns, this approach also introduces a new conceptual view on the analysis of spatiotemporal patterns in general. Often standard approaches implicitly impose a hierarchical order on the dimensions of the space-time cube. For example, the time series at a particular spatial point is analyzed and thus converted into a single number (the observable). Repeating this analysis for each spatial point yields the spatial distribution of this observable as the final result of this analysis. Conversely, one sometimes studies the spatial image at a given time point, condenses these data into a single observable (e.g., the spatial heterogeneity) and then repeats this analysis for each point in time yielding the time course of the observable (see Fig. 1 for an illustration of such a sequential treatment of space and time).

Over the last few years the range of applications of such an analogy-based statistical approach to analyzing spatiotemporal patterns has gained momentum and has contributed significantly to our understanding of pattern formation processes. The remarkable property of this approach is the bridging of scales. A regulatory principle on the cellular level is related to a statistical property of the spatiotemporal patterns. In the case of Peak et al. (2004) the regulatory principle is the distributed computation based upon neighborhood interactions with the corresponding statistical property being the transient time distributions observed in the spatiotemporal patterns. Another example is the work by Sawai et al. (2005), where the strength of a regulatory feedback loop is related to the spatial density of spiral wave patterns in cell colonies of the pattern-forming social amoebae *Dictyostelium discoideum*. By studying mutants in key components of the regulatory feedback loop, the authors can vary this intrinsic parameter systematically and study, how the spatiotemporal patterns change accordingly.

Upon nutrient deprivation, amoeboid *Dictyostelium* cells pass through a developmental program, where spatiotemporal pattern formation, coordinated cell aggregation and a morphogenetic transition from uni- to multicellular organization is involved. At the beginning of that developmental cycle single cells start to emit cAMP at random positions, which is detected by neighboring cells via highly specific surface receptors. These cells in turn pro-

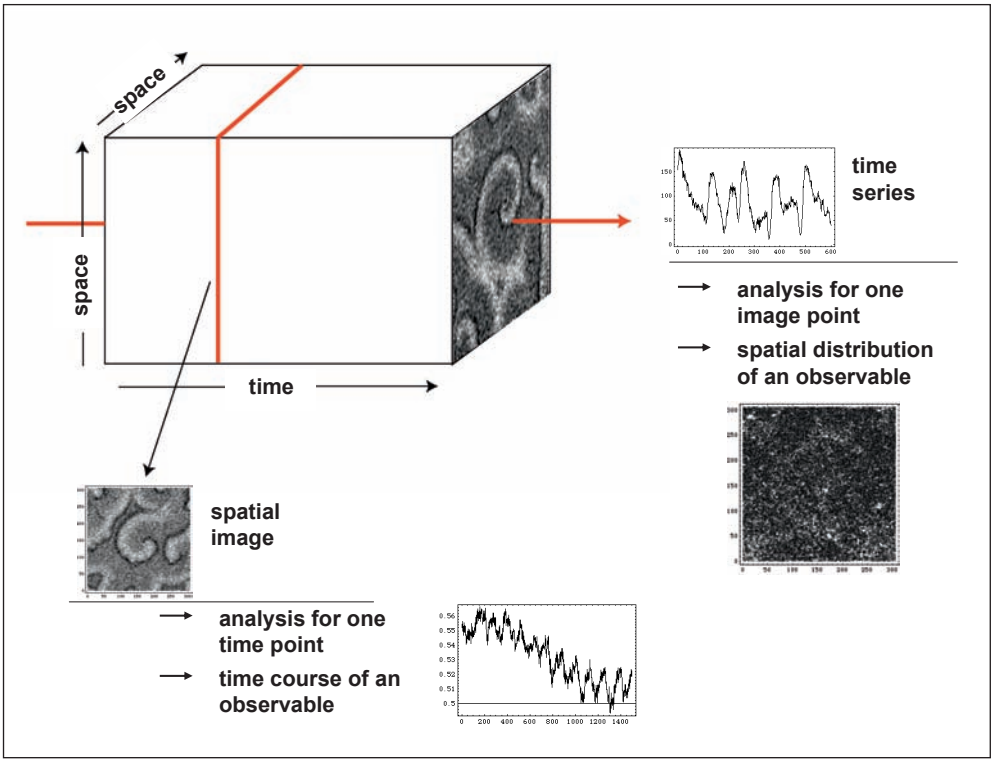

Fig. 1 Classical strategies of analyzing spatiotemporal patterns.

duce cAMP as well and secrete it to their environment. The excitation process is followed by a refractory period, where the cells are incapable of excitation. The autocatalytic reaction (cAMP-induced cAMP production) together with diffusion results in propagating excitation waves in a spatially extended cell population. Beside autocatalytic cAMP production the cells react by positive chemotaxis upon excitation, moving perpendicular to the wave front as long as the local cAMP concentration increases with time. Later on, characteristic streams of aggregating cells attracted to few geometrically well-defined aggregation centers appear. After the cells have assembled at the aggregation centers they transform into a mound state and later on into a migrating slug. The developmental cycle completes in a fruiting body, consisting of a stalk and germinable spores (see Kessin 2001 for details on the *Dictyostelium* life cycle).

In order to display the systematics of their finding more clearly, Sawai et al. (2005) simulate patterns using a simple cellular-automaton based model, where the feedback strength (i.e., the cAMP pulse-dependent increase in excitability) appears as an explicit parameter. Their observable is the spatial frequency of spiral waves, which they obtain by counting the phase singularities in their spatiotemporal patterns. Remarkably, the intermediate feedback strength found in wild type cells turns out to produce an optimal (i.e. minimal) number of phase singularities compared to higher and lower feedback strength mutants, respectively. In the extreme case, where feedback is constantly absent, no stable spiral wave pattern evolves. From that, two implications result. Firstly, aggregation territory size is optimized by the pulse-dependent

development of feedback strength. For the wild type this allows for optimally sized basins of attraction for the consecutive aggregation process of the cells leading to the multicellular organism capable of spore generation and thus completing the developmental cycle of *Dictyostelium*. Secondly, wave geometry is determined by feedback strength. Spiral waves seem to be favored by the system compared to target waves, although both wave geometries result in fruiting bodies for the experimental system. Spirals are self-sustaining continuous structures, which preserve their stability, to a certain extend outside the excitable regime. This allows for maintenance of the aggregation process under developmentally and environmentally conditioned changes. In contrast, target waves require the periodic activity of oscillatory regions (i.e., pacemakers).

In this article we would like to discuss this new view on spatiotemporal patterns both from a conceptual and from a practical (or methodological) perspective. First, we would like to address the question, why this view on patterns can work in principle, as this from our perspective highlights very interesting differences between pattern formation processes in biology and, e.g., in physics. Secondly, we would like to provide a toolbox for exploiting this new concept and for analyzing a wide range of spatiotemporal patterns from this perspective. Within this article we will discuss the application of these tools to a specific set of pattern-forming systems, namely excitable media, which are found in a wide range of biological contexts.

2. The Concept

The new view on spatiotemporal patterns described in the introduction focuses on statistical comparisons rather than on the visual layout of the patterns. From our perspective, the reason for this approach's success lies in the theory of pattern formation itself. A theoretical description of pattern formation often relies on the concept of self-organization. Patterns are emergent properties of the system, appearing in a phase-transition like manner. While in physics such a symmetry-breaking is typically triggered by random fluctuations, the corresponding process in biology contains far more deterministic features: The constituents of the system may with their individual, non-identical properties pre-determine the outcome of the symmetry breaking. Figure 2 summarizes this situation for the simple potential landscape of a second-order phase transition. Under variation of a control parameter a potential minimum (representing a stable steady state of the system and therefore a possible state of the order parameter) gradually de-stabilizes and gives rise to two co-existing minima. This transition is the decisive step in a pattern formation process, where small fluctuations can have a large effect on the system state (critical fluctuations) and can eventually determine which of the competing minima is at last selected by the system at hand.

In contrast to, e.g., many situations in physics (Fig. 2*A*), in biology (Fig. 2*B*) differences between the constituents of the system provides an additional stochastic (but stationary) modulation of the potential, which may pre-determine the outcome of the symmetry breaking and can in principle allow predicting the layout of resulting patterns. This possibility to translate cellular variability into features of patterns requires new methods of analyzing spatiotemporal data.

Why is it interesting to look at patterns from this perspective? Firstly, if indeed the spatial distribution of cellular properties substantially shapes the patterns emerging in the system, these distributions, when measured during the early phase of pattern formation, may serve as a basis for predicting later stages of the pattern formation process. In principle, this intrinsic

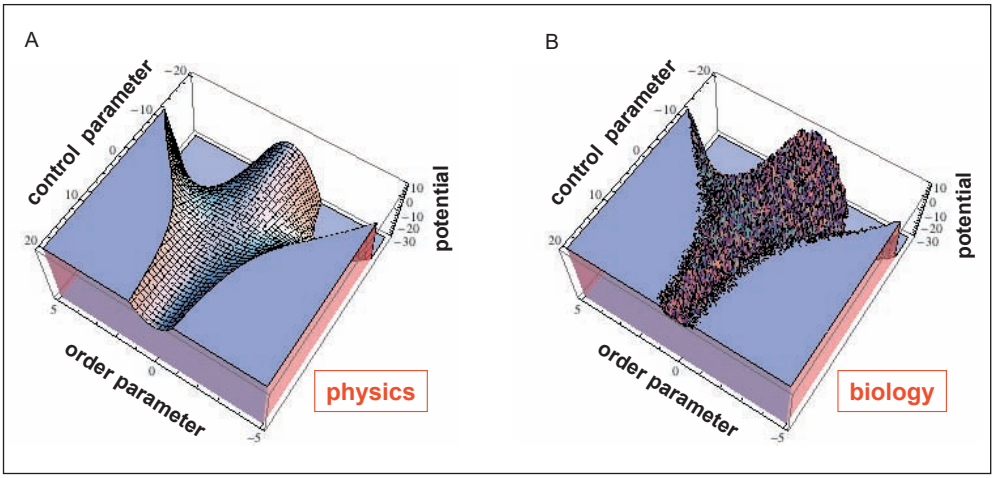

Fig. 2 Potential landscape of a second-order phase transition. Under change of a control parameter the minima (i.e. the stable states) of the order parameter (representing different types of patterns of the underlying system) change from a single minimum to two co-existing minima. In contrast to many situations in physics, where the decisive step for selecting one of the minima is due to local fluctuations (*A*), in biology the systematic differences between the system's constituents often large enough to bias the state towards one of the minima (here represented as a random modulation of the potential, which in contrast to noise does not change in time, *B*).

predictability may be exploited to avoid unintended patterns or to channel the system's self-organization into a desirable regime.

Secondly, this correlation between distributions of cellular properties and features of the spatiotemporal pattern can provide insight into the regulatory mechanisms on the cellular and intercellular levels. Just as with the examples given in the *Introduction*, the enormous power of this view lies in building a bridge between the two scales: patterns as a collective state of a very large number of cells on the one hand, and internal parameters of the single cells on the other. By analyzing patterns from this perspective we want to understand, which regulatory mechanisms are responsible for the observed correlations between cellular properties and macroscopic patterns.

3. Methods and Data

Here we briefly summarize the (simulated and measured) data on spatiotemporal patterns, as well as the tools for analyzing them.

Details on the simulation and the experimental data can be found in Hilgardt et al. (2007). The spatiotemporal filters have been discussed in detail in Hütt and Neff (2001) and applied to excitable dynamics in Hütt et al. (2002), Busch and Hütt (2004) and Hilgardt et al. (2007).

Studying *Dictyostelium* patterns with phase singularitiy methods (as a means of identifying the spatial distribution of spiral wave tips) has been pioneered by Sawai et al. (2005). The correlation between phase singularities and cell properties for a model of *Dictyostelium* pattern formation has first been analyzed in Geberth and Hütt (2008).

4. The Model

In order to study the link between intrinsic cellular properties and the local signature of these properties in the spatiotemporal patterns it is convenient to consider a simple model of an excitable medium given by a cellular automaton. An advantage of cellular automata is that the spatial discretization coincides with the discrete nature of the biological cells, and the observed states within the spatiotemporal pattern are reduced to few essential elements. In its simplest form, an excitable medium is a spatial arrangement of identical elements, for which (at least) three states exist, namely "quiescent" (excitable) (Q), "excited" (E) and "refractory" (R). A typical time sequence of states for a single cell is characterized by a switch from the quiescent state Q to the excited state E when a certain condition is fulfilled; the falling into the refractory state R after one time step and the remaining in R for a fixed period of time (called the refractory time). This sequence immediately leads to the formation of propagating wave fronts and, when disrupted, to spiral waves.

From the different cellular automaton models of excitable media (see e.g., Gaylord and Wellin 1995, Mikhailov and Calenbuhr 2006) we select a variant, which combines simple update rules involving few parameters with a quasi-continuous state space helpful in achieving similarity with experimental data (Dewdney 1988, see also Hilgardt et al. 2007 for additional details in the model). In this model we implement a simple interaction rule for the epidemic spreading of excitations from cell to cell, which allows to study the global dynamics on a quasi-continuous state space (which in an epidemic scenario would correspond to the immunization state of the elements). The state space has the form $S=\{0,1,...,n-1,n\}$, where healthy elements are represented by 0 (corresponding to the Q state of our general model introduced above), infected cells can be in states 1, ..., n–1 (the E state), and the diseased (sick) elements are given by n (the R state). The update rules, which determine the state of a cell in the next time step, are as follows:

$$0 \to \left[\frac{a}{k1}\right] + \left[\frac{b}{k2}\right] \qquad [1]$$

$$i \to \min\left(\left[\frac{s}{a+b+1}\right] + g, n\right), \quad 0 < i < n, \qquad [2]$$

$$n \to 0, \qquad [3]$$

where $[x]$ is the integer remainder of x (i.e. the remaining integer value after removing the decimal part), a denotes the number of infected cells in the neighborhood N_{ij} of a point (ij) and b represents the corresponding number of sick cells in N_{ij}. The quantity s in the update rule for infected cells is the sum over all elements in N_{ij}. The remaining quantities $k1$, $k2$ and g are model parameters, which regulate the impact of infected and sick cells on neighbors and the excitability of a cell, respectively.

5. Implementation of Biological Variability

We introduce variability in this system as distributions of g and of $k2$. In both cases we use a minority of cells with modified parameter values: a higher value $g^* > g$ corresponding to a faster traversing of the infected state and a lower value $k2^* < k2$ corresponding to a higher sensitivity. The modifications in g and $k2$ are independent; a certain (different) percentage of spatial sites is assigned the modified values. The percentage of modified sites constitutes the strength of variability, while the spatial distribution of parameter values is the matrix we aim at reconstructing (with the help of our spatiotemporal observables defined in the following section) and correlating (with the distribution of spiral waves obtained with the phase singularity method described below). The spatial matrices K_{ij} and G_{ij} for $k2$ and g distributions, respectively, constitute our model implementation of cell-cell differences (in two different cellular properties). In the following, k and g denote the respective percentage of $k2^*$ and g^* values in the parameter matrices. These quantities allow tuning the strength of variability. Indeed, the patterns produced by the model depend systematically on the two sources of variability. Figure 3 shows typical snapshots of simulations for different strengths of variability. Parameter settings are the same as in HILGARDT et al. (2008).

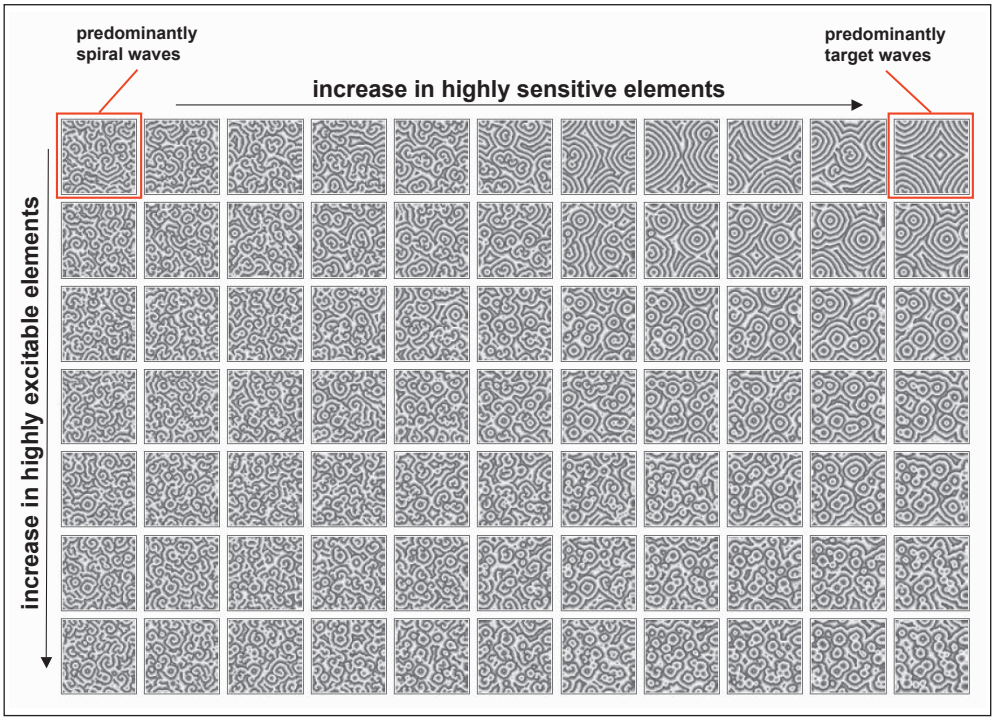

Fig. 3 Snapshots for different percentages of high-excitability and high-sensitivity cells. The percentage of high-sensitivity cells increases from 5 % (*left*) to 55 % (*right*), the percentage of high excitability cells increases from 0.1 % (*top*) to 3.1 % (*bottom*). Systematic changes in the density of active centers and in the target wave to spiral ratio can be observed.

6. The Spatiotemporal Filters

The first filter for extracting cell properties from the patterns focuses on local fluctuations. We start from a spatiotemporal data set $\{a_{ij}(t)\}$. For each spatial point (ij) and three consecutive time points t–1, t and t+1 we take the (spatial) differences to each neighbor of (ij), $(a_{ij}(t))$–$a_{ij-1}(t)$, $(a_{ij}(t))$– $a_{i-1j}(t)$, etc.; next, we take the temporal difference for each of these spatial differences; this is possible for the two time steps involved: t–1 to t and t to t+1; whenever these two values differ in sign, they are added to the overall fluctuation value at the spatial point (ij); performing this operation for all points (ij) and normalizing this value to the maximal number of contributing values yields the spatial distribution of fluctuations Ω_{ij}.

In the case of our other filter, the local mutual information, we take time differences a $a_{ij}(t-1)$–$a_{ij}(t)$ for all spatial and temporal points and map these values to 1 (if they are positive) or 0 (otherwise). From the resulting binary time series at each spatial point we estimate probabilities (as relative frequencies) $p_{rs}(ij)$ of finding r and s as consecutive symbols (r, s can be 0 or 1). Together with the single-symbol probabilities $p_{rs}(ij)$ (r = 0,1) we obtain the mutual information $I(i, j)$ for the spatial point (ij):

$$I(i,j) = \sum_{\substack{r=0,1 \\ s=0,1}} p_{rs}(i,j) \log \frac{p_{rs}(i,j)}{p_r(i,j)\, p_s(i,j)}. \qquad [4]$$

We found recently that these two spatial matrices Ω_{ij} and $I(i, j)$ correlate well with cell properties in the simulations and also show a systematic behavior when applied to experimental data (Hilgardt et al. 2007).

7. Analysis of Spiral Wave Patterns

There are two generic sustainable patterns on excitable media: target waves caused by a pacemaker element firing periodically, and self-sustained spiral waves. In both cases, the action of all single elements is basically periodic (quiescent – excited – refractory – quiescent), which can be used to map the state of an element to a circle from 0 to 2π. The phase φ of a single oscillator is defined by considering the current state s compared to the state at a later time

$$\varphi = \text{Arctan } 2(s(t+\tau)–E(s), s(t)–E(s)) \qquad [5]$$

where E(s) is the average value of s. The time delay τ needs to be chosen large enough for the variable to change significantly, but not so large as to allow the state to return to its previous value (skipping over a peak); the rise time for the ascending flank of an excitation wave has proven to be a good value in several systems. This technique is called *phase embedding*. For a linear oscillator and $\tau = T/4$, the resulting figure in the embedding plane is a circle around the average value (which is why one subtracts the average value before taking the arc tangent, in order to get a well-defined phase angle); for nonlinear oscillators and different τ, the result is a deformed curve that will nevertheless circle around the average value.

When looking at a snapshot of the phases of all oscillators in an excitable system, the phase is constant along excitation wave fronts, but all phase isolines join together in a phase

singularity at the position of the spiral tip, where the phase is undefined. Mathematically, a phase singularity can be characterized by a non-vanishing value of a closed loop path integral over the gradient of the phase around it (Bray et al. 2001)

$$n = \int_C \nabla \varphi d\vec{l}. \qquad [6]$$

For phase singularities n assumes integer multiples of 2π, and zero otherwise. The sign of n determines whether one has a left- or right-handed spiral wave. The fact that n is zero for nonsingular locations is easily understood by applying Stoke's theorem to the above integral and noting that the expression under the integral is then the curl of a gradient field, which is zero for "sufficiently smooth" φ; the only non-zero contribution can come from a singularity, where φ is not smoothly derivable. This integral operation can be rewritten as a combination of convolution kernels that implement the derivatives and the integration on discrete data (spatially and temporally). The integral is then essentially reduced to a discrete summation over adjacent pixels.

8. Experimental Data on *Dictyostelium* Pattern Formation

For the experimental data analyzed here, cells of the axenic *Dictyostelium discoideum* strain AX2 were cultivated in HL5-medium (Sussman 1987) until they reached a cell density of $6 \cdot 10^6$ cells/ml. These cells were harvested by low speed centrifugation (400·g, 4 min) and washed twice in phosphate buffer (15.7 mM KH_2PO_4/Na_2HPO_4, pH 6.4). The cells were spread homogeneously to a density of $6.2 \cdot 10^5$ cells/cm^2 onto agar plates (1 % Difco Bacto Agar, 2 mM caffeine in phosphate buffer, pH 6.14) and incubated in darkness for a few hours until first coherent structures appeared. The waves were visualized in dark field according to Gross et al. (1976) and recorded in equidistant intervals of 3 s (Hamamatsu C 3077, DT-Open Layers DT 3155 Mach Series Frame Grabber).

The principle behind dark field optics is that only light scattered by the cells is detected. The macroscopic impression of propagating excitation waves results from periodic changes in individual cell shape depending on the excitation state of the cells and concerted chemotactic response within a cell population. Moving cells are elongated and appear as bright regions within the patterns. Dark regions correspond to spherical non-moving cells.

Tomchik and Devreotes (1981) have shown that excitation dependent cell shape is reflecting directly the local cAMP concentration within a field of aggregating cells.

9. Results

9.1 Application to Simulated Data

In order to study the systematic biasing of patterns by a specific realization of cellular variability, we studied an ensemble of patterns based on a fixed cell property distribution but with 1000 random initial conditions. We calculated the time averages of spiral tip occupancy for every single random run and then averaged these to obtain the result shown in Figure 4. Furthermore, we applied a Gaussian smoothing ($\sigma = 2$ pixels) to the binary cell property

distributions to avoid discretization artifacts when calculating correlations between the distributions.

Comparing the average phase singularity occupancy (Figure 4*B*) with the distribution of modified cells shows a strong match with the high excitability cells (high *g*; Figure 4*A*). The influence of the high sensitivity cells (low *k*2) is less drastic (Figure 4*C*), but still clearly discernible. In this model, both types of modified cells favor the formation and localization of spiral tips in their close proximity. Qualitatively speaking, the average spatial distribution of phase singularities consists of two contributions: clearly pronounced, highly localized peaks and broad diffuse regions of elevated spiral occupancy. Our comparison with the distributions of cell properties reveals that the former is determined by the arrangement of highly excitable cells, while the latter correlates with the distribution of highly sensitive cells.

Note that all findings obtained in this discrete system are very sensitive to (statistical properties of) initial conditions, as well as interference between the simulation and (similarly discretized) analysis tools. For a more thorough discussion of correlations between cell properties and patterns, see the two case studies published in Geberth and Hütt (2008, 2009).

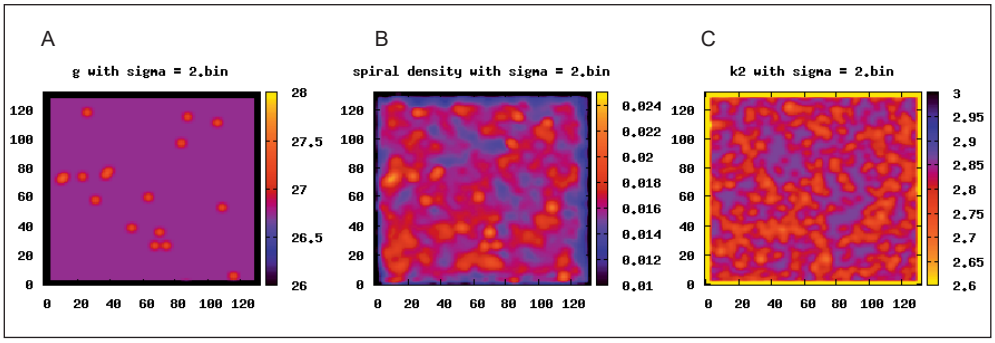

Fig. 4 Distribution of high excitability (high *g*) cells (*A*) and of high sensitivity (low *k*2) cells (*C*). Both binary distributions have been smoothed with a Gaussian filter ($\sigma = 2$ pixels). In (*B*) the average spiral tip occupancy is shown, corresponding to the probability of finding a spiral in a certain position in any given random run, gained from 1000 random initial conditions imposed on a field with the shown cell distribution. The correspondence of high spiral probability sites (*B*) to high *g* sites (*A*) is obvious. The correspondence of high sensitivity cells to raised spiral probability (*B*) is not quite as pronounced, but can still be seen in gaps in the *k*2 distribution (*C*).

9.2 Application to Experimental Data

Macroscopic propagation waves during the early phase of the *Dictyostelium* life cycle originate from intracellular communication via excitation and relay of the chemoattractant cAMP. Spatiotemporal data of these patterns offer the possibility to apply our analysis tools to extract cellular variability from a spatially extended cell population. The pixel-based approach of the tools accounts for the discrete nature of individual cells. We assume that the observables provide estimates valid as averages for the cells residing at a particular spot. Figure 5 illustrates schematically the application of our analysis tools to experimental data. Phase singularities (ps) were detected from spatiotemporal wave patterns as described (Fig. 5*A*). We have chosen a time interval of 200 images (corresponding to 10 min) possessing stable rotating spiral waves and $\tau = 15$ images (corresponding to a temporal off-set of 45 s). The data have been smoothed by Gaussian convolution $\sigma = 4$ pixels).

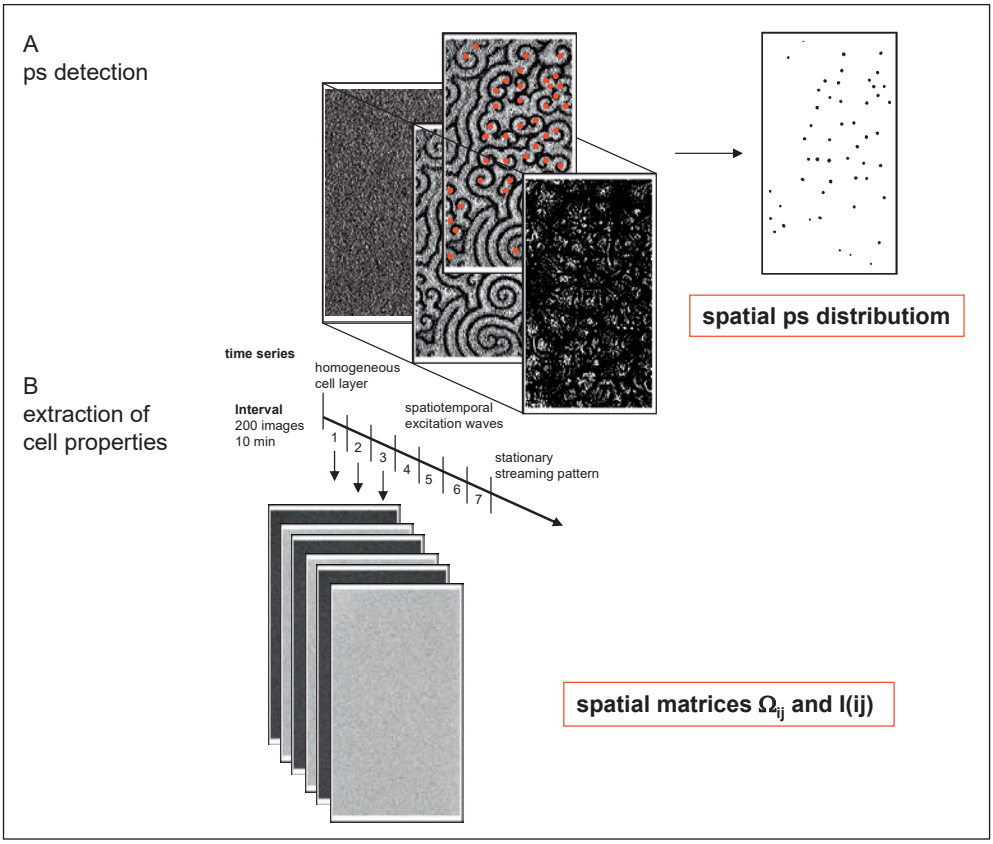

Fig. 5 Schematic representation of data treatment to determine the spatial positions of phase singularities (PS) within a field of propagating excitation waves (*A*) and to extract single cell properties represented by spatial distributions in Ω_{ij} and $I(i, j)$ (*B*).

To extract single cell properties we computed Ω_{ij} and $I(i, j)$ for several experimental data sets (Fig. 5*B*). Each data set covered the successive developmental stages from the not yet excitable homogeneous cell layer shortly after cell preparation, over propagating excitation waves after development of cellular excitation and aggregation competence, to the appearance of streaming patterns in the advanced phase of the aggregation process. Here, only the first two developmental stages have been analyzed, so that cell movement could be disregarded, as in that stage of early pattern formation chemotactic activity is small. Each data set has been divided into intervals of 200 images from which Ω_{ij} and $I(i, j)$ were determined.

Previously we found that Ω_{ij} and $I(i, j)$ show very systematic results, which suggests that each individual pixel possesses a specific dynamic response, even though the system displays a spatiotemporal pattern on a large scale. For consecutive intervals the correlation coefficients are almost identical, while they are systematically reduced with increasing temporal difference (Hilgardt et al. 2007). Figure 6 shows an example of this behavior for Ω_{ij} for one data set. Attention should be paid to the high correlation coefficients even for temporal distances of several hours.

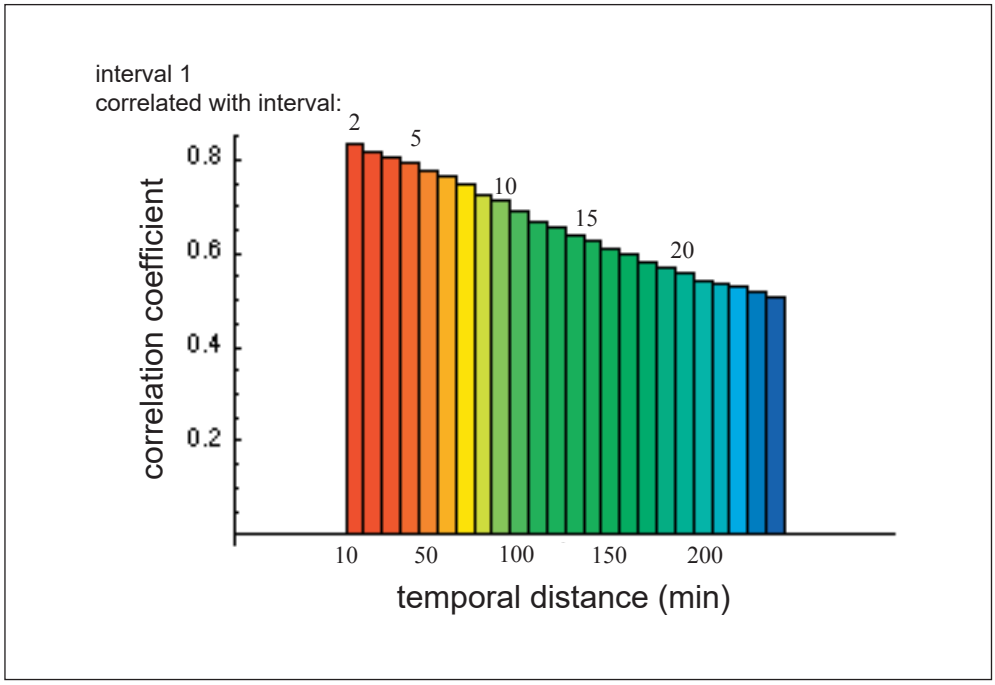

Fig. 6 Correlation coefficients between the spatial distributions of Ω_{ij} extracted from 25 intervals of one experimental data set. Each interval corresponds to 10 min of experimental observation time. The correlations between interval 1 (early developmental state, i.e., homogeneous cell layer without excitation competence) and the following intervals are plotted successively in the order of increasing temporal distance.

To approximate the impact of individual cell properties (now translated into distributions of Ω_{ij} and $I(i, j)$ on pattern formation more precisely, we analyzed the relations between Ω_{ij} and $I(i, j)$ and the spatial distribution of spiral waves by computation of the correlation coefficients between the corresponding matrices (cf. Fig. 5), similar to the analysis of the simulated data (summarized in Fig. 4). Figure 7 shows the correlation coefficients between the distributions of Ω_{ij} (Fig. 7*A*) or $I(i, j)$ (Fig. 7*B*) and the distribution of phase singularities for different time intervals. Shown in gray are correlation coefficients with randomly distributed phase singularities for comparison. While the values for Ω_{ij} show very systematic changes with increasing interval number (i.e. advancing time), the mutual information does not clearly display any relation to spiral wave distribution (or a clear deviation from the null model of randomly distributed phase singularities). The change in sign of the correlation coefficient between Ω_{ij} and the phase singularity distribution, which occurs approximately at the 11th time interval, coincides with the onset of excitation waves. It must be pointed out, however, that the course of the correlation coefficients with Ω_{ij} and $I(i, j)$ can look very differently for individual data sets depending on the spatial scale and quality. Nevertheless, quite often characteristics in pattern formation can be related to systematic changes in the amount of correlation to phase singularities.

In general, our results complement nicely the observations of Samadani et al. (2006), where the authors found individual differences in *Dictyostelium* cells under well-defined stimuli constant in time. We analyze statistically a very large ensemble of cells from a mac-

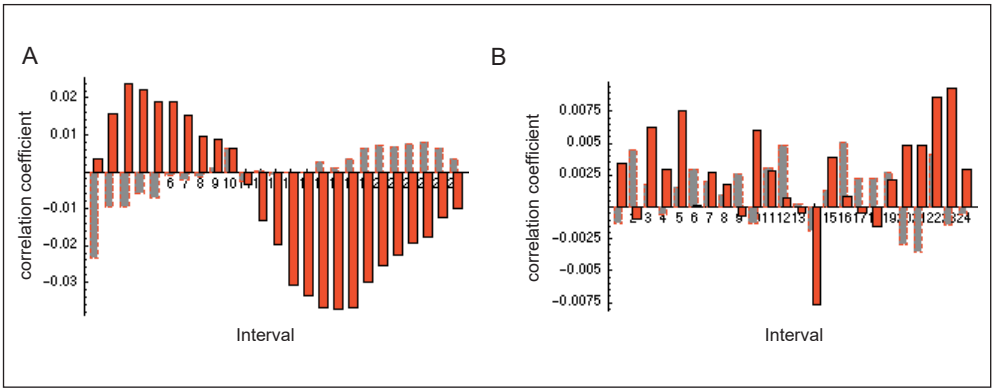

Fig. 7 Correlation coefficients between the matrices Ω_{ij} and $I(i, j)$ (B) of individual time intervals and the spatial frequency in phase singularities (red bars) compared to the results for randomly distributed phase singularities (gray bars).

roscopic view in the process of pattern formation. In this way, our result is a cell-population variant of the findings in SAMADANI et al. (2006).

10. Conclusion

In biology differences between the constituents of the system may pre-determine (or bias) the outcome of the symmetry breaking involved in spatiotemporal pattern formation. This possibility to translate cellular variability into features of patterns requires new methods for analyzing spatiotemporal data and new views on patterns. We have described this new concept of analyzing spatiotemporal patterns by comparing the spatial distribution of cell properties with features of the patterns emerging from the local interactions between the constituents. In applying this general view, our key result is that in a simple n-state model of an excitable system the distribution of both excitability and sensitivity correlate with the distribution of spiral wave tips, i.e. of phase singularities. By calibrating spatiotemporal filters to the simulated data, we have been able to formulate a scheme for extracting such cell property distributions from experimental data and, using these tools, we could identify similar correlations in experimental data on *Dictyostelium* pattern formation.

Correlating the reconstructed distributions of cell properties with the phase singularity pattern in the experimental data extends our results from HILGARDT et al. (2007), where we looked at the systematics of the reconstruction process, both for simulated patterns and experimental data.

Beyond the technical level (phase singularities, correlations with pacemaker cells; the detailed mathematical modeling of excitable systems and the specific example of *Dictyostelium* pattern formation) this approach to analyzing patterns in biological systems is fairly general, as it focuses on two general ideas: (*i*) the spatial distributions of cellular properties may serve as a basis for predicting later stages of a pattern formation process; (*ii*) for a satisfactory model description of a system, one needs to understand which regulatory mechanisms are responsible for the observed correlations between cellular properties and spatial patterns.

How can these methods be applied to a wider range of spatiotemporal patterns and, particularly, to photosynthesis studies?

On a general level, of course, it is an interesting perspective to influence the probability of certain patterns by modifying the spatial distributions characterizing the constituents. One could think of applications to vegetation patterns and the spatiotemporal competition for resources like light and nutrients.

On a more specific level, any spatiotemporal dynamics, where the involvement of a particular cellular component or the details of the underlying regulatory process are unclear or debated, could be an interesting starting point for such an investigation: A regulatory mechanism failing to account for the observed or expected correlation between constituent's properties and patterns could be discarded on these grounds. Chlorophyll fluorescence dynamics for example (Rascher et al. 2001, Rascher and Lüttge 2002, Rascher and Nedbal 2006), together with models of the underlying circadian oscillator (Hütt and Lüttge 2002) may constitute a promising starting point for such a model validation scenario. Here is from our perspective the strongest potential for applying this concept.

In the case of *Dictyostelium*, for example, several mechanisms have been proposed to establish the appropriate amount of heterogeneity in the system for spiral wave patterns to emerge. One example is the hypothesis of a desynchronized cell population along a developmental path (Lauzeral et al. 1997). An alternative concept (Pálsson et al. 1997) assumes the different kinetics for the production and spatial diffusion of a secreted protein inhibitor, namely the phosphodiesterase inhibitor, to be an essential ingredient for the route towards spiral waves.

For both cases, it can be proposed that the source of cellular individuality (and cell-cell differences) can be, among others, the different positions in cell cycle at the time point starvation is induced. So, it is interesting to turn ones attention to the degree of fluctuations and information transport capacity of the system under synchronized conditions.

References

Bornholdt, S.: Systems biology. Less is more in modeling large genetic networks. Science *310*, 449–451 (2005)

Bray, M. A, Lin, S. F., Aliev, R. R., Roth, B. J., and Wikswo, J. P. Jr.: Experimental and theoretical analysis of phase singularity dynamics in cardiac tissue. J. Cardiovasc. Electrophysiol. *12*, 716–722 (2001)

Busch, H., and Hütt, M.-T.: Scale-dependence of spatiotemporal filters inspired by cellular automata. Int. J. Bif. Chaos *14*, 1957–1974 (2004)

Dewdney, A. K.: Computer recreations: the hodgepodge machine makes waves. Sci. Amer. *225*, 104–107 (1988)

Gaylord, R. J., and Wellin, P. R.: Computer Simulations with Mathematica. Explorations in Complex Physical and Biological Systems. Santa Clara: TELOS 1995

Geberth, D., and Hütt, M.-T.: Predicting spiral wave patterns from cell properties in a model of biological self-organization. Phys. Rev. E *78*, 031917 (2008)

Geberth, D., and Hütt, M.-T.: Predicting the distribution of spiral waves from cell properties in a developmental-path model of Dictyostelium pattern formation. PLoS Computational Biology. In press 2009

Gross, J. D., Peacey, M. J., and Trevan, D. J.: Signal emission and signal propagation during early aggregation in Dictyostelium discoideum. J. Cell Sci. *22*, 645–656 (1976)

Hilgardt, C., Müller, S. C., and Hütt, M.-T.: Reconstruction of cellular variability from spatiotemporal patterns of *Dictyostelium discoideum*. Nonlinear Biomed. Phys. Aug. 30; 1(1):10 (2007)

Hütt, M.-T., and Neff, R.: Quantification of spatiotemporal phenomena by means of cellular automata techniques. Physica A *289*, 498–516 (2001)

Hütt, M.-T., and Lüttge, U.: Nonlinear dynamics as a tool for modeling in plant physiology. Plant Biol. *4*, 281–297 (2002)

HÜTT, M.-T., NEFF, R., BUSCH, H., and KAISER, F.: A method for detecting the signature of spatiotemporal stochastic resonance. Phys. Rev. E 66:026117 (2002)

HÜTT, M.-T., and LÜTTGE, U.: Noise-induced phenomena and complex rhythms: theoretical considerations, modelling and experimental evidence. In: MANCUSO, S., and SHABALA, S. (Eds.): Rhythms in Plants: Phenomenology, Mechanisms, and Adaptive Significance. Berlin, Heidelberg: Springer 2007

KESSIN, R. H.: Dictyostelium: The Evolution, Cell Biology, and Development of a Social Organism. Cambridge: University Press 2001

LAUZERAL, J., HALLOY, J., and GOLDBETER, A: Desynchronization of cells on the developmental path triggers the formation of spiral waves of cAMP during *Dictyostelium* aggregation. Proc. Natl. Acad. Sci. USA *94*, 9153–158 (1997)

MIKHAILOV, A. S., and CALENBUHR, V.: From Cells to Societies: Models of Complex Coherent Action. Springer Series in Synergetics. Berlin, Heidelberg: Springer 2006

MOTT, K. A., and PEAK, D.: Stomatal patchiness and task-performing networks. Ann. Bot. (Lond.) *99*, 219–226 (2007)

PÁLSSON, E., LEE, K. J., GOLDSTEIN, R. E., FRANKE, J., KESSIN, R. H., and COX, E. C.: Selection for spiral waves in the social amoebae Dictyostelium. Proc. Natl. Acad. Sci. USA *94*, 13719–13723 (1997)

PEAK, D., WEST, J. D., MESSINGER, S. M., and MOTT, K. A.: Evidence for complex, collective dynamics and emergent, distributed computation in plants. Proc. Natl. Acad. Sci. USA *101*, 918–1922 (2004)

RASCHER, U., HÜTT, M.-T., SIEBKE, K., OSMOND, C. B., BECK, F., and LÜTTGE, U.: Spatio-temporal variation of metabolism in a plant circadian rhythm: the biological clock as an assembly of coupled individual oscillators. Proc. Natl. Acad. Sci. USA *98*, 11801–11805 (2001)

RASCHER, U., and LÜTTGE, U.: High-resolution chlorophyll fluorescence imaging serves as a non-invasive indicator to monitor the spatio-temporal variations of metabolism during the day-night cycle and during endogenous rhythm in continuous light in the CAM-plant *Kalanchoë daigremontiana*. Plant Biol. *4*, 671–681 (2002)

RASCHER, U., and NEDBAL, L.: Dynamics of photosynthesis in fluctuating light. Curr. Opin. Plant Biol. *9*, 671–678 (2006)

SAMADANI, A., METTETAL, J., and VAN OUDENAARDEN, A.: Cellular asymmetry and individuality in directional sensing. Proc. Natl. Acad. Sci. USA *103*, 11549–11554 (2006)

SAWAI, S., THOMASON, P. A., and COX, E. C.: An autoregulatory circuit for long-range self-organization in *Dictyostelium* cell populations. Nature *433*, 323–326 (2005)

SUSSMAN, M.: Cultivation and synchronous morphogenesis of *Dictyostelium* under controlled experimental conditions. Methods Cell Biol. *28*, 9–29 (1987)

TOMCHIK, K. J., and DEVREOTES, P. N.: Adenosine 3',5'-monophosphate waves in *Dictyostelium discoideum*: a demonstration by isotope dilution-fluorography. Science *212*, 443–446 (1981)

Prof. Dr. Marc-Thorsten HÜTT
School of Engineering and Science
Jacobs University Bremen
Campus Ring 1
28759 Bremen
Germany
Phone: +49 421 2003238
Fax: +49 421 2003249
E-Mail: m.huett@jacobs-university.de

Altern in Deutschland

Die Deutsche Akademie der Naturforscher Leopoldina und die Deutsche Akademie für Technikwissenschaften acatech gründeten im Mai 2005 eine gemeinsame interdisziplinäre Akademiengruppe „Altern in Deutschland“, die auf der Grundlage der besten verfügbaren wissenschaftlichen Evidenz öffentliche Empfehlungen erarbeitete, um die Chancen der im letzten Jahrhundert erheblich gestiegenen Lebenserwartung – die „gewonnenen Jahre“ – vernünftig zu nutzen und mit den Herausforderungen des demographischen Alterns klug umzugehen.

Nova Acta Leopoldina N. F.

Bd. *99*, Nr. 363 – Altern in Deutschland Band 1
Bilder des Alterns im Wandel
Herausgegeben von Josef Ehmer und Otfried Höffe unter Mitarbeit von Dirk Brantl und Werner Lausecker
(2009, 244 Seiten, 32 Abbildungen, 1 Tabelle, 24,00 Euro, ISBN: 978-3-8047-2542-3)

Bd. *100*, Nr. 364 – Altern in Deutschland Band 2
Altern, Bildung und lebenslanges Lernen
Herausgegeben von Ursula M. Staudinger und Heike Heidemeier
(2009, 279 Seiten, 35 Abbildungen, 9 Tabellen, 24,00 Euro, ISBN: 978-3-8047-2543-0)

Bd. *101*, Nr. 365 – Altern in Deutschland Band 3
Altern, Arbeit und Betrieb
Herausgegeben von Uschi Backes-Gellner und Stephan Veen
(2009, 157 Seiten, 29 Abbildungen, 20 Tabellen, 24,00 Euro, ISBN: 978-3-8047-2544-7)

Bd. *102*, Nr. 366 – Altern in Deutschland Band 4
Produktivität in alternden Gesellschaften
Herausgegeben von Axel Börsch-Supan, Marcel Erlinghagen, Karsten Hank, Hendrik Jürges und Gert G. Wagner
(2009, 157 Seiten, 28 Abbildungen, 2 Tabellen, 24,00 Euro, ISBN: 978-3-8047-2545-4)

Bd. *103*, Nr. 367 – Altern in Deutschland Band 5
Altern in Gemeinde und Region
Stephan Beetz, Bernhard Müller, Klaus J. Beckmann und Reinhard F. Hüttl
(2009, 210 Seiten, 10 Abbildungen, 11 Tabellen, 24,00 Euro, ISBN: 978-3-8047-2546-1)

Bd. *104*, Nr. 368 – Altern in Deutschland Band 6 (in Vorbereitung)
Altern und Technik
Herausgegeben von Ulman Lindenberger, Jürgen Nehmer, Elisabeth Steinhagen-Thiessen, Julia Delius und Michael Schellenbach

Bd. *105*, Nr. 369 – Altern in Deutschland Band 7
Altern und Gesundheit
Herausgegeben von Kurt Kochsiek
(2009, 302 Seiten, 46 Abbildungen, 18 Tabellen, 24,00 Euro, ISBN: 978-3-8047-2548-5)

Bd. *106*, Nr. 370 – Altern in Deutschland Band 8
Altern: Familie, Zivilgesellschaft und Politik
Herausgegeben von Jürgen Kocka, Martin Kohli und Wolfgang Streeck unter Mitarbeit von Kai Brauer und Anna K. Skarpelis
(2009, 343 Seiten, 44 Abbildungen, 9 Tabellen, 24,00 Euro, ISBN: 978-3-8047-2549-2)

Bd. *107*, Nr. 371 (2009) – Altern in Deutschland Band 9
Gewonnene Jahre. Empfehlungen der Akademiengruppe Altern in Deutschland
(2009, 102 Seiten, 1 Abbildung, 12,00 Euro, ISBN: 978-3-8047-2550-8)

Wissenschaftliche Verlagsgesellschaft mbH Stuttgart

Nova Acta Leopoldina NF *96*, Nr. 357, 161–174 (2009)

Talking Patterns: Communication of Organisms at Different Levels of Organization – An Alternative View on Systems Biology

Ulrich Lüttge ML (Darmstadt) and Marc-Thorsten Hütt (Bremen)

With 4 Figures

Abstract

Systems biology currently is providing the focus for considering biological complexity. Comprehensive analyses of gene expression and translation (transcriptomics and proteomics) produce complex patterns inherent in large sets of data. It is a great challenge to relate these abstract patterns to basic principles of cellular organization. Processes of communication are of particular importance for establishing order. The abstraction of patterns outlines a way towards theory. Via abstraction, theory can produce generalization incorporating a large variety of patterns, which in return can also produce patterns serving as templates for comparison with data. In this review this will be illustrated at different scales reaching from molecules to ecosystems and using a range of biological objects ("models"). The correspondence of rules and patterns leads to the formulation of straightforward generative laws. This supports the move from abstraction of patterns to theory, which becomes a new approach currently discernible in systems biology.

Zusammenfassung

In den Mittelpunkt der Betrachtung biologischer Komplexität ist heute die Systembiologie gerückt. Umfassende Analysen von Genexpression und -translation (*Transcriptomics* und *Proteomics*) liefern unter anderem in großen Datensätzen komplexe Muster. Es ist ein herausfordernder Schritt, diese abstrakten Muster auf grundlegende zelluläre Organisationsprinzipien zurückzuführen. Von besonderer ordnender Bedeutung sind dabei Kommunikationsakte. Die Theorie abstrahiert die Muster. In der abstrakten Form kann sie dann so stark verallgemeinern, dass ihre Aussage eine große Vielfalt von Mustern inkorporiert. Aus dem Abstrahieren heraus kann sie dann solche Muster auch generisch wieder hervorbringen. Dies wird hier auf unterschiedlichen Skalen vom Molekül bis zum Ökosystem und mit variablen biologischen Studienobjekten („Modellen") illustriert. Die Verknüpfung von Regeln und Mustern führt zu einfachen Bildungsgesetzen und bereitet den Weg von der Abstraktion von Mustern zur Theorie, der sich aktuell in der Systembiologie abzuzeichnen beginnt.

1. Introduction

Biology is full of patterns and structures. Viewing them often creates aesthetic pleasure, and one can easily be taken away by the enjoyment of their variability. The study of biological pattern formation has always been a fascination for scientists. Quoting Ernst Haeckel, one can regard them with admiration as "*Kunstformen der Natur*" (nature's forms of art), or one can try to fathom their particular functions like the stripes of zebras interpreted as serving camouflage. In the present days comprehensive analyses of gene expression and translation (transcriptomics and proteomics) generate complex patterns at an abstract level, i.e. inherent in the huge sets of data of systems biology. It is challenging to take the step towards relating

these patterns to basic principles of cellular organization shaped by various ways of communication in biological systems.

In this article we shall approach this by first considering a classical example of biological pattern formation, namely spiral wave patterns, in order to see, how in this well studied, illustrative context the link between patterns and forms of communication is mediated by a minimal model. We shall then describe the path from abstraction of patterns towards theory. The examples we selected for this purpose shall serve as an array of templates, showing a number of rather diverse biological model systems and covering the large range of scales from molecules to ecosystem. Communication within the different model systems shall be described briefly to show that such templates make structures visible which bear out similar principles of organization at the different scales. This also addresses the rationale behind the plan of organizing and arranging the various contributions of the Leopoldina-Meeting in July 2007, from which the present volume is emerging, covering a large manifoldness of study systems lined up according to scaling. The model systems only apparently look disparate. It is the very manifoldness that will guide us the way to working out general principles.

2. Spiral Waves

Spiral waves are an example for patterns, which are particularly useful to start with. The observation that spiral waves are such a frequent form of pattern formation already leads to the assumption that there must be a simple generative law, i.e. a minimal mathematical formulation, which can be implemented biologically in different ways. Let us consider a two dimensional lattice plane with regularly arranged elements. Each element has three possible states (Q, E, R). Each element also shows a dynamical behavior which is subject to clearly defined rules and indicates the transitions from one state to another. Time is proceeding in discrete steps. The rules are: An excited element (E) changes to the refractory state (R) after one time step. After the refractory period, typically a few time steps, the refractory element (R) changes to the quiescent state (Q). The quiescent element (Q) changes to the excited state (E), when an excitation is in the immediate neighborhood. This model is also called excitable medium (see also in this volume: Geberth et al. 2009). One of the many realizations of this basic scheme in actual living systems is the collective dynamics of the amoeba *Dictyostelium discoideum.* In large populations of the amoebae under the influence of a chemotactic signal (cyclic AMP, cAMP) the cells aggregate and form a multicellular organism, which can move in the substrate. For example this aggregation is elicited by nutrient limitation. In the new aggregated condition the cells are able to leave locations of adverse environmental conditions. During aggregation one observes concentric wave fronts and spiral waves of signal propagation as a collective behavior due to the cAMP signal transferred from cell to cell. The subsequent process of aggregation itself is that of a highly complex rheological structure of streams of cells directed to the places where the cells collect, i.e. the centers of aggregation. The upper part of Figure 1 (observed data) presents snapshots of these two phases of organization. The centre part (abstraction) shows a few time steps between the states Q, E and R and simulation by a minimal mathematical model.

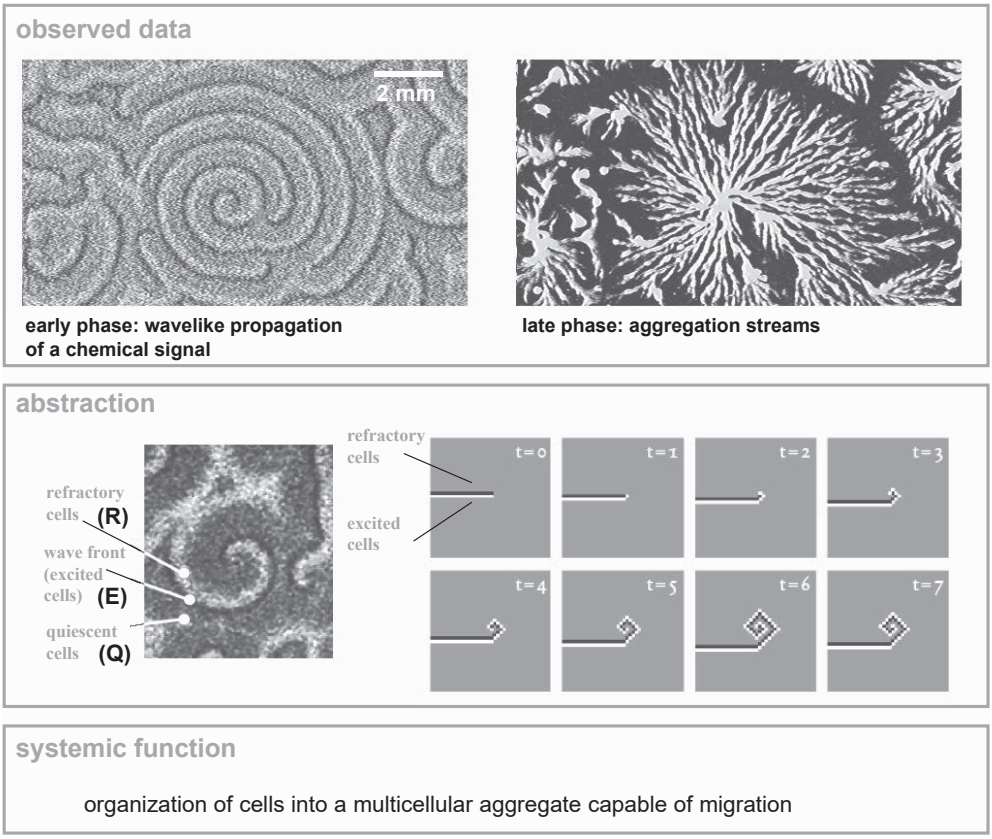

Fig. 1 *Upper part*: Snapshots of the two early phases of the organization of *Dictyostelium discoideum*. The chemotactic signal (cAMP) spreads out in the system in the form of closed wave fronts and spiral waves. In a subsequent state brought about by signal transmission the cells move in streams towards centers where the multicellular organism can be formed. (Experimental data of C. HILGARDT, Magdeburg, Germany). Note that in the middle part of the left picture one can distinguish the three states discussed in our minimal mathematical model as different, clearly discernable grayscale regimes. With this model a typical sequence in time of the three states is also clear: A cell is in state Q. When it receives the cAMP signal produced by a neighboring cell it changes to E and begins to also emit cAMP. Then it changes to R. After the refractory time it is again sensitive to cAMP and changes to Q and so forth. The letters Q, E and R in the left picture in the center of the figure, depicting some time steps of the minimal model, thus constitute a discrete encoding of the collective dynamics of *D. discoideum*. The simulation of a linear wave front (bright cells) is followed by a layer of refractory cells (dark cells) in a plane of otherwise quiescent cells. By describing the pattern as a sequence of the three states (Q, E, R) and identifying local rules of transition one obtains a minimal model in which the application of these transition rules directly leads to the formation of spiral waves (right part of the center of the figure). In order to move from one time point to the next one applies the rules of the minimal model at each point of the plane (taken from HÜTT 2006).

3. The Path from Abstraction of Patterns to Theory

Via the abstraction of patterns, like the ones described above, one finds a way towards theory. By abstraction, theory can generalize to such an extent that it incorporates a large variety of patterns. From the abstraction it can in turn reproduce such patterns in a generic manner. Therefore one must work at developing a general and unifying understanding from the large

variety of biological patterns and structures. From the biological data via abstraction we advance to systemic function (Fig. 2).

In Figure 3 we arrange different templates in the z-axis of a three dimensional block. In the other two axes (x, y) the selected pictures symbolize diversity and network hierarchies by combining differing structures with similar principles in the organization of communication. The manifoldness comprized in this may look like a collection of pictures by pure chance. However, these pictures are by far not as isolated from each other as it may appear at first glance. If one looks at them under the guidance of a leading concept like communication in biological systems on all scalar levels from molecules to the organism in its environment they are clearly connected. In fact, a graduate school of the *Deutsche Forschungsgemeinschaft* has exactly worked along these lines using a wide range of model systems. The templates of Figure 3 are actually taken from the work of this group (GRK 340: Communication in Biological Systems: from Molecule to the Organism in its Environment, 1999–2007).

4. Self-Organization from Integrating Elements

From the patterns one extracts an elementary formation law that can generate a basic form of these patterns. Then one identifies the components of the system which can contribute to this

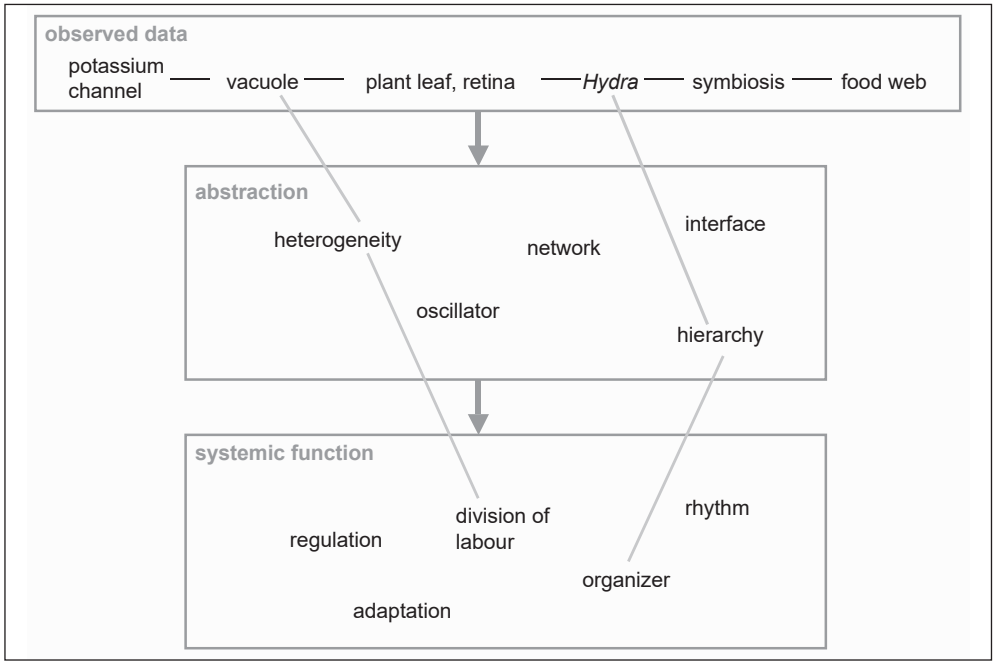

Fig. 2 The path from biological data to hypotheses on systemic function. Abstraction is the link between these different levels, i.e. the transformation of patterns (inherent in the data) into a mathematical description. Two such paths through these levels ((*i*) vacuole – heterogeneity – division of labor, and (*ii*) *Hydra* – hierarchy – organizer) are explicitly labeled in the figure. They are further explained in the text. (The other examples of biological data are illustrated and arranged in Fig. 3 along their spatial order of magnitude [scale].)

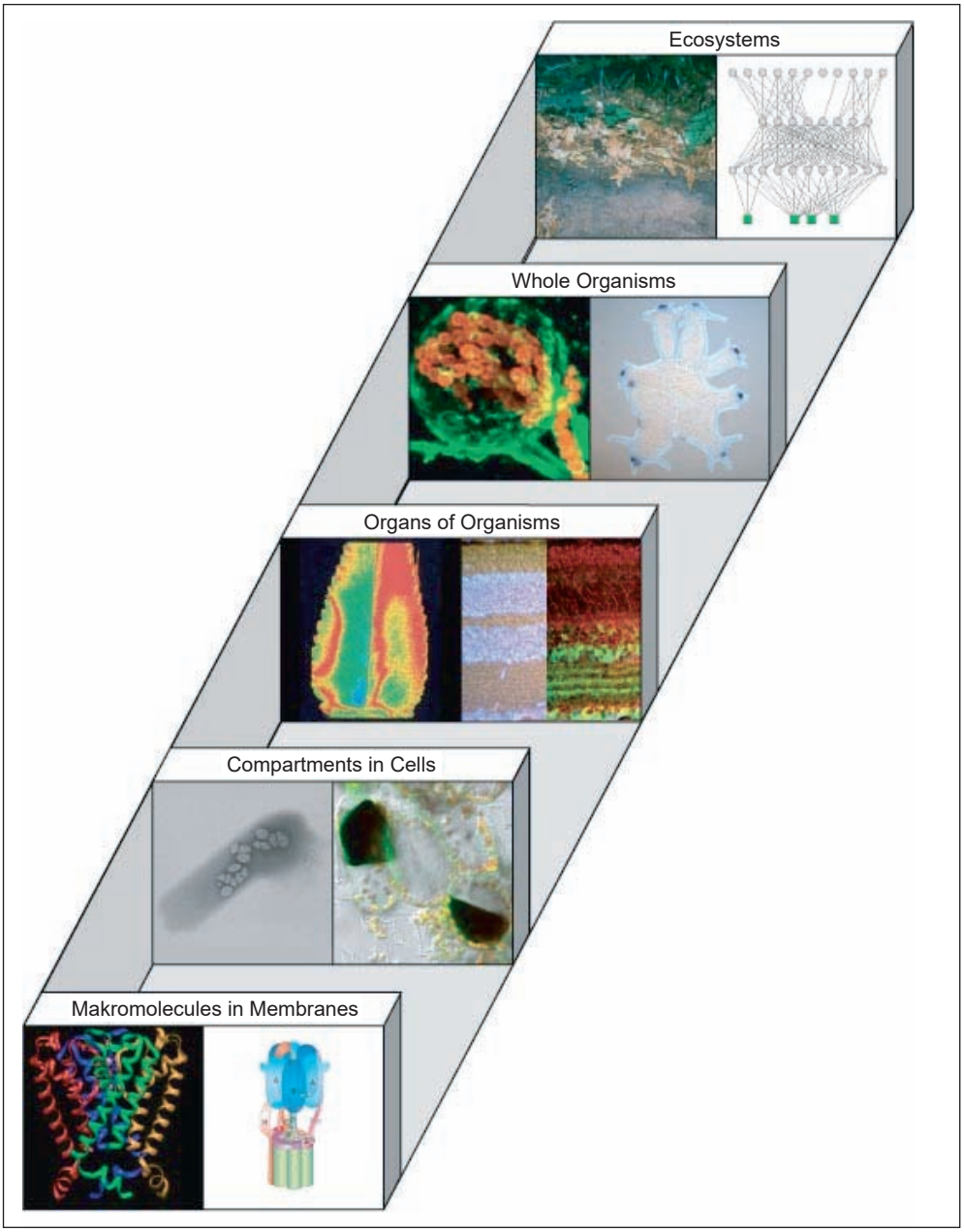

Fig. 3 Hierarchy of descriptions arranged according to levels of scaling. From lower left to upper right: Level of macromolecules, K^+-channel (*left*) and proton transporting ATPase (*right*); level of compartments, gas vesicles in an archae bacterium (*left*), two vacuoles with different function within one plant cell (*right*); level of organs in organisms, leaf of *Kalanchoë daigremontiana* with patterns of photosynthetic activity (*left*), retina of the chicken eye (*right*); level of whole organisms, *Geosiphon pyriformis* (*left*), *Hydra*: self-organizing aggregation five days after re-aggregation of a suspension of individual cells with Wnt expression (violet) at the tip of signal centers in newly developed polyps (*right*); level of ecosystems, soil (*left*), food web (*right*).

formation law of the patterns. The theory of complex systems provides methods suitable to unravel the formation laws behind patterns. Together with the field of theoretical biology it is attempted to develop mathematical descriptions of biological processes. A typical procedure of theoretical biology is the translation of the processes known or assumed in a biological system into mathematical expressions. This creates minimal mathematical models, where observations of nature can be interpreted using the language of interacting elements. One calls this form of pattern formation self-organization (see, e.g., HÜTT 2006 for more details and further references). Self-organization means that a set of elements under the influence of local interactions creates long-range and frequently very complex structures, which cannot be described any more by the degrees of freedom of the individual elements but need to be assessed on the scale of the entire system. Qualitatively speaking, self-organization describes the formation of structures and patterns close to a phase transition.

Based on scientific theory, what is the legitimation of a model based on the concept of self-organization? One needs to consider this in relation to a reductionist argument. The foundation of reductionist models lies in the hierarchy of nested descriptions translating between scales as for example in Figure 3. The aim is to deduce properties of systems from first principles, i.e. to relate them back to properties of the underlying components, the properties of which again are deduced in a similar way.

In contrast to this, the foundation of models based on self-organization is exclusively given by the meta-theory of self-organization. Patterns and structures are emergent properties of the system components and their interactions. The structures cannot be deduced from first principles in a reductionist fashion, but they can be directly produced (e.g. by numerical simulation) from minimal rules. Precisely by this strategy of explanation self organization is becoming a general principle in nature, unifying a large manifoldness of observations.

5. Templates Reveal Structures

This ideal path towards understanding a system is actually only accessible in rare cases. In a similar but more general approach one does not attempt to find the precise formation laws of the patterns. Abstraction is rather used like a template, which can make visible the structures (or dependencies, hierarchies and correlations) inherent in the experimental data. Nevertheless, we must note a basic difference between theory and experiment: In simple models, complex structures (or patterns) result from the interaction of many identical elements. This step from simplicity to complexity is characteristic of theory. The units building up a biological system are in themselves already extremely complex. Each unit often has a multitude of different functions and rarely two units resemble each other. Here we encounter a relation between local complexity (i.e., individual elements, constituents) and global complexity (i.e., system).

A good concrete example for such a relation between signal cascades and biological complexity is the interesting and important protein p53, which is often termed the “guardian of the genome”. It can suppress cancer in humans and many other multi-cellular organisms because it is centrally placed in various signal transduction pathways. In this way it can translate information on the state of cells into activations and deactivations of various signal transduction pathways. For instance, it can activate DNA repair mechanisms when DNA is damaged. It can stop the cell cycle, and in the case of damage, which cannot be repaired, it can trigger

apoptosis, i.e. programmed cell death. The formation of p53 is regulated by more than 20 transcription factors. A large number of additional components modify the protein und thus determine further functions. Due to this complexity it is not possible to reduce the property as a tumor repressor to the level of the single component p53. The system and its reactions on external effectors thus become nearly unpredictable (KITANO 2002).

6. Similar Principles of Organization at Different Scales

In proceeding from collecting data towards a systemic understanding, the biological manifoldness needs to rely on structuring principles. Notwithstanding the overwhelming variety, similar principles of organization become evident on many different organismic scales. The basic idea of the theory of complex systems, namely the capability of self-organization of an ensemble of interacting individual elements as a prerequisite for the generation of patterns, provides the theoretical methods for identifying such principles. It leads the way from specific biological data to an abstract model, which as a template can be compared with totally different actually occurring real biological phenomena. This formal view of biological observations is based on acts of communication between the units or elements of a system.

In this modern view of biological complexity, in the center of which is systems biology, the step from pure collecting of facts towards flow of information is completed. Thus, patterns and structures in biology are also intimately linked with formal languages. This is given in two ways. First, it is the aim of this level of understanding systems to decipher the acts of communication or the generalized language in which the elements or units exchange information. This is the system immanent language. Second, the observed structures provide an analytical and experimental access to the local interactions, which often is the only rigorously checkable one. Thus, the patterns communicate their laws of generation to the experimenter. This is the analytical language. The language – or rather the multitude of forms of communication – which is at issue here, is a formal generalized language. It lastly aims at understanding the biological function, the processes of exchange of information and the biochemical implementation of the acts of communication. The patterns of biology speak the language of mathematics. In a certain way, the acts of communication, which underlie the biological structures, are not individual acts of dialogue but networks of communication.

How then can such a template look for an abstract system which is compared to a concrete observed structure? In all cases the way leads via a small number of abstract basic types which can be extracted from the biological data. Examples for such basic types are oscillator, network, and interface (see Fig. 2). Abstraction then facilitates the step towards systemic function.

One concrete example of far reaching developments that arises from a very simple basic principle is the *Wnt* gene path of signal transduction governing the organization of body axes and organs of animals (GUDER et al. 2006, HOBMAYER et al. 2000, KUSSEROV et al. 2005). Centers of signaling ("organizers") play an important role because they emit growth factors which function as short or far reaching morphogenes in regulation of the formation of body axes and cell differentiation. Wnt/Wg proteins are a family of highly conserved glyco-proteins. (The name comes from the segment polarity gene *wingless* [wg] of the fruit fly *Drosophila* and the homolog *integrated-1* [int-1] of vertebrates which is induced by the mouse mammary tumor virus [MMTV]). The *Wnt* gene family belongs to a mechanism of pattern formation which

is extremely old in evolution. It has arisen 650 million years ago, i.e. before the conspicuous explosion of the formation of species in the Cambrian. *Wnt* genes must have been involved in the evolution of multi cellular animals from protozoan ancestors. Starting from considering the freshwater polyp *Hydra* (Cnidaria) with its most simple body organization one can advance at understanding the organization of higher animals. The head organizer of *Hydra* and neuronal differentiation can be homologized with an organizer of vertebrates so that one can consider the body axis of *Hydra* as a counterpart of the vertebrate brain. The oral pole of the Cnidarians corresponds to the posterior and the aboral pole of Cnidarians corresponds to the anterior end of vertebrates. In aggregates of *Hydra* cells head organizers are formed by chance and are stabilized by a community effect. Clusters consisting of 5–15 cells expressing Wnt act as local sources instructing their environment and creating at the same time a lateral field of inhibition extending up to 1000 µm. The pattern-formation systems of higher animals may well have arisen from such a robust and flexible molecular self-organized system.

7. Biological Scales in Time and Space

Referring to theoretical and abstract template-like types of patterns on the one hand and considering the concrete example of bridging the gap from the simple head organizer of *Hydra* to the complex body plan of highly developed vertebrates on the other hand, we have already implicitly revisited the scheme of templates in the scaling levels of Figure 3. These templates represent the very broad range of the model systems studied in the graduate school mentioned above. Similarly we could have chosen examples from the manifoldness of systems used in the various contributions of the Leopoldina Meeting covered in this volume. Such a variety of concrete examples, when looked at superficially, appears quite disparate. However, it now readily allows qualitative demonstration of how the use of theoretical starting points and templates, or, conversely, the way from a concrete biological system towards an abstract structure, leads to information about the functions of systems exploiting precisely the very manifoldness given. It is a very important aspect of this step towards an abstract structure that observations on many very different scales can be unified and described with the same formal methods.

With this we cover many spatial and temporal scales. If one considers all relevant levels of life from the photons in the excitation of the light reactions of photosynthesis or the processes of vision in the eye up to the large biological regions, the zonobiomes of the earth and finally the entire biosphere of our planet this covers 32 orders of magnitude in time and 16 orders of magnitude in space (Fig. 4). The examples of Figure 3 only cover a very small section of that. In the following we want to briefly consider them individually.

8. Concrete Examples of Communication in very Different Biological Model Systems at Different Scales

8.1 Molecules

At the level of macromolecules transporters in membranes, such as ion channels and ATP-ases, are both essential parts of cascades of transmission of communication and themselves subject to regulation by communication.

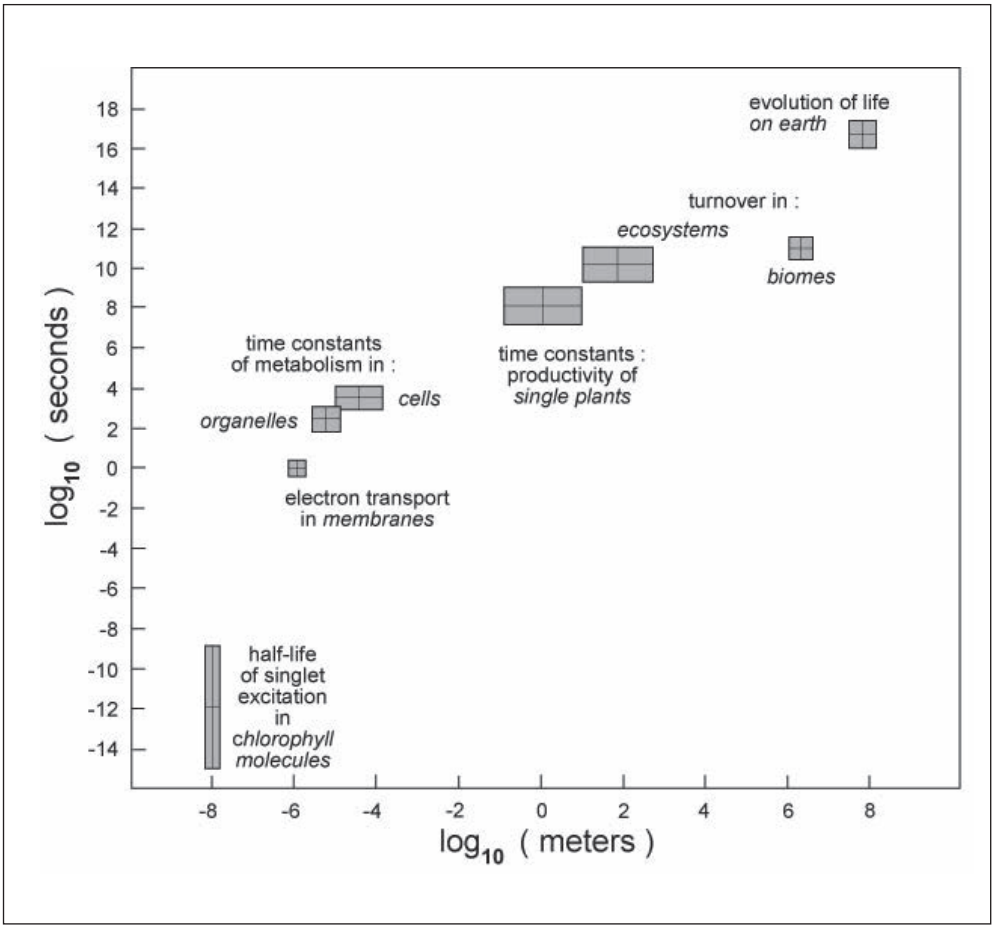

Fig. 4 Orders of magnitude of the scales in space (y-axis) and time (x-axis) where biological processes are occurring

The transport molecules in a membrane normally form small networks which via interaction among each other regulate the transport of molecules into the cell or out of the cell. The basis of such networks is a connection of the different transporters via common factors of regulation. For example, these may be the electrical membrane potential or regulatory ligands, such as Ca^{2+} or H^{+}. When in such a network a transporter is affected in its activity by a signal that triggers kind of a quantified chain reaction: the change of activity of the first element changes the factor of coupling, which in turn affects the activity of all other transporters. As a result the coupling factor itself is changed again and therefore the properties of the entire system. A system operating according to such rules is the action potential of nerve cells. A depolarization of the membrane activates Na^{+} channels. The resulting depolarization stimulates the activation of further Na^{+} channels until the electric membrane potential is so positive that also K^{+} channels become active and the membrane is re-polarized again, which has a further negative effect on the activity of the Na^{+} channels.

Depending on cell type and physiological function such systems can be infinitely complex and therefore generate a large scope of temporal patterns. An interesting example is the autonomous oscillation of sinus node in the heart. In these cells the connection of several transporters via the membrane potential leads to autonomous oscillations of the membrane potential which in turn determines the beat frequency of the heart. This temporally encoded pattern of heartbeat can be influenced by different factors such as neuro-transmitters and hormones. As by input signals the properties of a single K^+ channel, the so-called pace maker channel, can be varied, the physiologically relevant heart rhythm can be regulated (DiFrancesco et al. 1993).

Moreover, in plants as well we find very similar systems. The guard cells of stomata in leaves, which regulate gas exchange via stomatal pores, also possess a network system of membrane transporters. This allows keeping the membrane potential of the cells at a stationary level, either depolarized or hyperpolarized. The membrane potential, however, may also oscillate continuously between these two states. This temporal pattern of changes of membrane potential allows the cells to fine tune exactly their K^+ flows and with them their turgor pressure.

In order for such networks to function the participating macromolecules must have an appropriate structure. In the simplest case the autonomous oscillations on the guard cells can be explained when all participating transporters depend on the membrane potential in very individual ways (Gradmann et al. 1993).

8.2 Cell Compartments and Communication with the Environment

Compartments involved in the communication system at the level of cells can be exemplified by vesicles or vacuoles. Halophilic archaea of the genera *Halobacterium* and *Haloferax* produce gas vesicles (Scheuch and Pfeifer 2007). These are hollow protein bodies which support the floating of the organisms and allow them to move into and stay in favorable zones within the water. When conditions in the external medium of saline ponds become inadequate, by communication with the medium the formation of gas vesicles is induced via a complex path of regulation. In essence at the end of the regulatory network there is the interaction of two regulator proteins which eventually stimulates or deactivates gene expression.

Although of quite a different nature than the gas vesicles of halobacteria, the two different vacuoles within a given leaf cell of the Aizoaceae *Mesembryanthemum crystallinum* also have something to do with halophilic performance (Epimashko et al. 2004). They are surrounded by biomembranes. *M. crystallinum* is an annual higher plant which under salinity stress accumulates much NaCl in its cells and then switches from normal C_3 photosynthesis to the water saving crassulacean acid metabolism (CAM). In CAM, atmospheric CO_2 is first fixed during the night and stored in the form of malate in the vacuoles before the malate is remobilized during the subsequent day, decarboxylated, and the resulting CO_2 made available for fixation by RubisCO. This requires two different types of vacuoles because the dynamic acid metabolism with day/night oscillations of malate content in the vacuoles and NaCl accumulation require the operation of different physiological mechanisms. High concentrations of Na^+ are toxic in the cytoplasm. It needs to be accumulated in the vacuoles and to remain to be stored there. The membrane needs to have a Na^+/H^+ exchanger for vacuolar Na^+ accumulation and the proton pump at the membrane needed for energizing the transport (H^+-ATPase) must be permanently active to be able to retrieve any Na^+ leaking out into the cytoplasm. In the other type of vacuoles malate must be accumulated and remobilized in the night/day-rhythm. The

membrane must have a malate transporter, and the H^+-ATPase must be up and down regulated in the night/day-rhythm. For osmotic adjustment both vacuoles must communicate in the night/day-rhythm.

8.3 Functional Self-Organization and Cell-to-Cell Communication in Organs

For the communication level in organs of organisms we take the liberty to consider side by side such different systems as a photosynthesizing plant leaf and a sensory epithelium, the retina in the organ of the eye.

In a plant leaf the imaging technique of chlorophyll fluorescence photography can demonstrate the spatiotemporal dynamics of patches of different photosynthetic activity (Rascher et al. 2001, see Lüttge, this volume, 2009). In this way spatiotemporal time sequence data can be obtained which can be subject to a theoretical correlation analysis of the mechanisms of synchronization/desynchronization of different areas on the leaves (see Bohn, this volume, 2009). This is particularly important in transitions between rhythmic and arrhythmic performance of the free running endogenous rhythmicity of photosynthesis where the communication of oscillators, of which each leaf cell has its own copy, is regulated. It works like the functional self-organization of individual leaf cells in space and time. The decisive signal may be the lateral diffusion of CO_2 in the leaf (Lüttge 2007, see Jahnke and Pieruschka, this volume, 2009).

In a principally similar way we can consider the spatiotemporal development of the retina from isolated cells of the chicken eye as a self-organization governed by the chemical signal of the neuro-transmitter actylcholine. In this case it is a structural self-organization leading to the regeneration of completely functional mini eyes *in vitro* (Layer et al. 2005). The arrangement of different cell types in cell layers is a characteristic feature of many parts of the vertebrate brain as a basic prerequisite for successful network formation. The formation of the cell layers is largely dependent on cell-to-cell communication. One can produce separated single retina cells mechanically or enzymatically and suspend them in an appropriate medium. Experimentally dissociated cells reaggregate under continuous rotation and form spheres of cells, retino-spheroids, with a complete layering of cells as required for the neuronal order in the eye. Acetylcholine is the decisive signal for the development from the neuro-epithelium to a completely synaptically wired retina.

8.4 Pathways of Molecular Signaling in Communication within Multi Cellular Organisms

Communication at the level of whole organisms in Figure 3 is symbolized by *Geosiphon pyriformis* and the freshwater polyp *Hydra*. *G. pyriformis* (Schüssler 2002) is a unique endosymbiosis between a eukaryotic organism, a fungus, and a prokaryotic organism, the cyanobacterium *Nostoc*. In the cooperation between both partners *Nostoc* provides autotrophy of carbon and nitrogen acquisition by photosynthesis and atmospheric di-nitrogen fixation and the fungus mediates mineral nutrition. The major problem of communication is the mutual recognition of the partners for forming the symbiosis. The understanding of the molecular basis of the establishment of the symbiosis is not yet very advanced. One knows that a galactose specific lectin mediates recognition. Lectins are proteins which bind carbohydrates, and thus form glycoproteins and fulfill tasks of cell recognition at the cell surface. For two reasons *G. pyriformis* is of broad and general biological interest. First, as it is an endosymbiosis which is

currently and observably established, it is important for supporting the endosymbiosis theory of the evolution of eukaryotic cells. Second, it is relevant for the understanding of mykorrhiza because the fungus belongs to the *Glomus*-group which generally forms arbuscular mykorrhiza. In *Hydra* – as we have seen above (Section 6) – the simple body axis between an oral pole with a "head"-region bearing the tentacles and an opposite aboral pole is determined by the *Wnt* gene family (Guder et al. 2006, Hobmayer et al. 2000, Kusserov et al. 2005). The Wnt signal transduction way starts at an organizer center, and the signals are Wnt glycoproteins. Thereby neuronal differentiation is activated. This casts a bridge towards understanding of vertebrate organization and makes *Hydra* – like *Geosiphon* – a biological model which generically bears out far reaching conclusions. Obviously very complex differences in organization are based on a simple and common molecular ground.

8.5 Communication in Ecosystems – Nutrition as a Signal

At the level of ecosystems, food webs in the soil can serve as an example for pattern formation by signaling systems and by communication (Scheu 2002). The micro flora in the soil is dominated by saprophytic fungi decomposing organic material in the soil. The soil fauna is characterized by locally high species diversity. Saprophytic fungi constitute the nutritional basis for a large variety of micro arthropods in the soil, especially collembola and oribatida. A high degree of specialization is considered to be an important mechanism for the establishment of large species diversity. Therefore, one might expect that species feeding on fungi, such as the collembola and oribatida, are specialized on feeding on particular soil fungi. The analysis of the flow of stable carbon and nitrogen isotopes as well as patterns of fatty acids in the food web and methods of molecular biology of species recognition allow collecting experimental data on the nutrients actually taken up by the animals and the participating organisms. It turns out that the animals, especially the collembola are not at all so specialized but rather generalist consumers, which feed on fungi, soil algae, litter and debris of plants and animals. The mixed nourishment and sustenance has experimentally supported advantages, such as improved growth and increased reproduction. The different kinds of prey complement each other with respect to their nutritional value. In kind of a signaling-regulated communication between consumer and prey the animals prove to be able to recognize fungi and to assess their physiological state and nutritional value, and thus, selectively feed on particular species of fungi. The structure of such populations of decomposers and the pattern formation of food webs influence the processes of decomposition and mineralization of nutrients, and thus, can even affect the growth of plants. The degree of coupling of individual components is decisive. It must be subject to theoretical network analysis and accessible to model simulations (Drossel et al. 2001). Since most species in fact are nutritional generalists, a particularly high degree of coupling is given. Realistic mathematical formulations must strive to incorporate the most important paths of coupling and the non-linear population dynamics with the effects of availability of nutrients, saturation, competition and communication between the participating species.

9. Outlook: the Future

Recently the development of systems biology based on molecular information has been compared with the historical development of astronomy (Alter 2006). The way from designing

instrumentation (GALILEO) and accumulation of data (BRAHE) towards an understanding of natural laws (NEWTON) went via an interpretation of patterns in the data (KEPLER). If this analogy holds, biology at present is at a most exciting point of this path: the move from the patterns towards the natural laws and fundamental principles. The path is paved by understanding the language of patterns.

Acknowledgements

We thank the project directors of the graduate school 340 of the *Deutsche Forschungsgemeinschaft*, "Kommunikation in biologischen Systemen: Vom Molekül zum Organismus in seiner Umwelt" for their cooperation in arranging Figure 3 and describing the various templates. Both authors were project directors in the graduate school and thank the *Deutsche Forschungsgemeinschaft* for the support.

References

ALTER, O.: Discovery of principles of nature from mathematical modeling of DNA microarray data. Proc. Natl. Acad. Sci. USA *103*, 16063–16064 (2006)

BOHN, A.: Integrative computational approaches to complex ecophysiological systems. Nova Acta Leopoldina NF *96*/357, 175–192 (2009)

DIFRANCESO, D.: Pacemaker mechanisms in cardiac tissue. Annu. Rev. Physiol. *55*, 455–472 (1993)

DROSSEL, B., HIGGS, P., and MCKANE, A.: The influence of predator-prey population dynamics on the long-term evolution of food web strucutre. J. Theoret. Biol. *208*, 91–107 (2001)

EPIMASHKO, S., MECKEL, T., FISCHER-SCHLIEBS, E., LÜTTGE, U., and THIEL, G.: Two functionally different vacuoles for static and dynamic purposes in one plant mesophyll leaf cell. Plant J. *37*, 294–300 (2004)

GEBERT, D., HILGARDT, C., and HÜTT, M.-T.: Systematics of spatiotemporal heterogeneity. Regulation of large-scale patterns by biological variability. Nova Acta Leopoldina NF *96*/357, 145–159 (2009)

GUDER, C., PHILLIP, I., LENGFELD, T., WATANABE, H., HOBMAYER, B., and HOLSTEIN, T. W.: The Wnt code: cnidarians signal the way. Oncogene *25*, 7450–7460 (2006)

GRADMANN, D., BLATT, M. R., and THIEL, G.: Electrocoupling of ion transporters in plants. J. Membr. Biol. *136*, 327–332 (1993)

HOBMAYER, B., RENTZSCH, F., KUHN, K., HAPPEL, C. M., LAUE, C. C. VON, SNYDER, P., ROTHBACHER, U., and HOLSTEIN, T. W.: Wnt signalling molecules act in axis formation in the diploblastic metazoan hydra. Nature *407*, 186–189 (2000)

HÜTT, M.-T.: Was ist Selbstorganisation und was nützt sie zum Naturverständnis? In: VEC, M., HÜTT, M.-T., und FREUND, A. M. (Eds.): Selbstorganisation – Ein Denksystem für Natur und Gesellschaft. Köln, Weimar, Wien: Böhlau 2006

JAHNKE, S., and PIERUSCHKA, R.: Lateral gas diffusion inside leaves: a long neglected topic in plant physiology. Nova Acta Leopoldina NF *96*/357, 93–100 (2009)

KITANO, H.: Computational Systems Biology. Nature *420*, 206–210 (2002)

KUSSEROW, A., PANG, K., STURM, C., HROUDA, M., LENTFER, J., SCHMIDT, H. A., TECHNAU, U., HAESELER, A. VON, HOBMAYER, B., MARTINDALE, M. Q., and HOLSTEIN, T. W.: Unexpected complexity of the *Wnt* gene family in a sea anemone. Nature *433*, 156–160 (2005)

LAYER, P. G., ROBITZKI, A., ROTHERMEL, A., and WILLBOLD, W.: Of layers and spheres: the reaggregate approach in tissue engineering. Trends Neurosci. *25*, 131–134 (2002)

LÜTTGE, U.: Carbon dioxide signalling in plant leaves. Comptes Rendus Biologies *330*, 375–381 (2007)

LÜTTGE, U.: Crassulacean acid metabolism a natural tool to study photosynthetic heterogeneity in leaves. Nova Acta Leopoldina NF *96*/357, 65–72 (2009)

RASCHER, U., HÜTT, M.-T., SIEBKE, K., OSMOND, B., BECK, F., and LÜTTGE, U.: Spatio-temporal variation of metabolism in a plant circadian rhythm: the biological clock as an assembly of coupled individual oscillators. Proc. Natl. Acad. Sci. USA *98*, 11801–11805 (2001)

SCHEU, S.: The soil food web: structure and perspectives. Eur. J. Soil Biol. *38*, 11–20 (2002)

SCHEUCH, S., and PFEIFER, F.: GvpD-induced breakdown of the transcriptional activator GvpE of halophilic archaea requires a functional p-loop and an arginine-rich region of GvpD. Microbiology *153*, 947–958 (2007)

SCHÜSSLER, A.: Molecular phylogeny, taxonomy, and evolution of *Geosiphon pyriformis* and arbuscular mycorrhizal fungi. Plant Soil *244*, 75–83 (2002)

Prof. Dr. Ulrich LÜTTGE
Institut für Botanik
Technische Universität Darmstadt
Schnittspahnstraße 3–5
64287 Darmstadt
Germany
Phone: +49 6151 163700
Fax: +49 6151 164630
E-Mail: luettge@bio.tu-darmstadt.de

Prof. Dr. Marc-Thorsten HÜTT
School of Engineering and Science
Jacobs University Bremen
Campus Ring 1
28759 Bremen
Germany
Phone: +49 421 2003238
Fax: +49 421 2003249
E-Mail: m.huett@jacobs-university.de

Nova Acta Leopoldina NF *96*, Nr. 357, 175–192 (2009)

Integrative Computational Approaches to Complex Ecophysiological Systems

Andreas Bohn (Oeiras, Portugal)

With 6 Figures

Abstract

The present work highlights the application of integrative computational tools in ecophysiological studies. With the example of circadian rhythms in Crassulacean acid metabolism, modeling approaches for the integration of diverse levels of biological organization, as well as different time- and space scales are assessed. The integration of heterogeneous data sources is discussed with the case of a web-based computational infrastructure in a multinational, multidisciplinary project on phototrophic biofilms. Both examples underline the importance of aligning the respective scientific cultures and communication forms of the project partners for the successful application of computational techniques in the research on complex biological systems.

Zusammenfassung

Die vorliegende Arbeit behandelt die Anwendung integrativer Computerwerkzeuge in ökophysiologischen Studien. Am Beispiel circadianer Rhythmen im Crassulaceen-Säurestoffwechsel werden Modellierungsansätze zur Integration verschiedener Ebenen biologischer Organisation sowie verschiedener Zeit- und Längenskalen erörtert. Die Integration heterogener Datenquellen wird anhand der Fallstudie einer internetbasierten Dateninfrastruktur im Rahmen eines multinationalen, multidisziplinären Projekts über phototrophe Biofilme diskutiert. Beide Beispiele unterstreichen die Bedeutung der wechselseitigen Abstimmung der wissenschaftlichen Kulturen und Kommunikationsformen der Projektpartner für die erfolgreiche Anwendung von computerbasierten Techniken in der Erforschung komplexer biologischer Systeme.

1. Introduction

In the second half of the 20th century, technological breakthroughs in biochemistry, imaging and information processing have triggered a tremendous increase in the generation of information about the constituent parts of living organisms. Until the full sequencing of the human genome, the predominant approach to understanding the complex nature of biological systems followed a reductionist paradigm, relating organismal functionality and dynamics to the activity of individual molecules (Keller 2005, Hütt and Lüttge 2005). The evidence that the functionality or disease of entire biological systems could not be explained by deciphering solely the letters of the 'Book of Life' (Noble 2003), lead to a massive paradigmatic change in life sciences and the emergence of a large number of novel research approaches, attempting to unravel how whole-organismic function surges from the interactions between the parts of the system (Busch and Eils 2005). One of the most prominent approaches taking a systemwide perspective on life has been entitled systems biology (Ideker et al. 2001, Kitano

2001). Since its beginnings, this field has attracted scientists of many different disciplines, from experimental biology over engineering to computer sciences and physics (Keller 2005). Despite the existing lack of a clear definition of what exactly constitutes systems biology, common elements to most suggestions for a definition include the quantitative modeling of biological systems across different levels of organization, the integration of heterogeneous data sets, and the interdisciplinary networking of experimental biologists and quantitatively trained scientists (Morris et al. 2005).

The inherently quantitative character of systems biology, together with the traditionally strong connection between molecular high-throughput studies and bioinformatics, has founded an implicit tendency to understand systems biology as the genome-wide, or generally 'ome-wide', study of cellular and organismal function emerging from the interactions of its molecular parts (Westerhoff and Palsson 2004). Yet, it has been suggested that in studies of multicellular organisms and their environmental interactions, e.g., in crop development, a dialectic between bottom-up and top-down approaches provides a more efficient approach to biocomplexity and biotechnological developments, than hierarchical, unidirectional advances, working from the molecular level up to higher levels of organization (Hammer et al. 2004). These arguments gain even more weight if one understands systems biology as a truly holistic attempt to integrate all space-scales of the biosphere from molecules to ecosystems.

Bridging the entire spectrum of scales will also increase the spectrum of computational tools to be applied. While molecular studies are mainly challenged by the large volumes of information to be processed, quantitative ecological studies also face a bewildering variety of data types, sources and logical structures which need to be integrated (Jones et al. 2006). Situated between the molecular and the ecological scale, computational ecophysiology is about to become an interesting meeting point of bottom-up and top-down approaches in full-scale systems biology.

By means of two case studies, the present work discusses the implementation of the basic elements of systems biology in ecophysiological studies. Section 2 discusses multilevel modeling with the example of circadian rhythms of whole-leaf gas exchange in a Crassulacean acid metabolism (CAM) plant. It is demonstrated how the development of logically connected models with differing degrees of abstraction can elucidate the connection of dynamical processes at the cellular and organismal level, and enhance related experimental studies. Section 2.3 draws some general conclusions on multilevel modeling approaches in environmental physiology. The second example, presented in Section 3, highlights the integration and analysis of heterogeneous data sources in ecophysiology, generated in the context of a multinational, multidisciplinary project on phototrophic biofilms. It stresses the importance of metadata management to balance flexibility with consistence in data integration, and the importance of matching the applied analysis tools with the size and structure of the given data pool. Section 3.4 discusses general aspects in the creation of effective scientific data workflows and underlines the importance of the interdisciplinary communication between the involved partners. The conclusions on both examples are integrated in Section 4, discussing the necessity to complement new technologies for knowledge discovery and hypothesis testing with cultural and sociological advances in networked team science, to promote successful interdisciplinary research in biocomplexity.

2. Circadian Rhythms in Crassulacean Acid Metabolism: Integrating Data and Hypotheses on Different Levels of Organization

2.1 Chronobiology of CAM

Cyclic, oscillatory dynamics are deeply entrenched into the temporal organization of living organisms. An elusive example is the adaptation to geophysical cycles, in particular the 24 h-cycle of day and night (Pittendrigh 1993). These co-called circadian rhythms are ubiquitously observed in plants, animals and microorganisms, and there is increasing evidence that the coordinated timing driven by endogenous, circadian clocks enhances organismal fitness (Paranjpe and Sharma 2005, Dodd et al. 2005). A prominent example for how the temporal organization of metabolic processes by a circadian system can provide ecological advantages to plants is Crassulacean acid metabolism (CAM), an adaptation of plants to drought stress (Black and Osmond 2003, Lüttge 2004, and references therein): Governed by an endogenous circadian system, the uptake of CO_2 from the environment is shifted to occur predominantly at nighttime. The temporal separation of CO_2 uptake from its fixation and storage as starch via the light-dependent C_3 pathway, allows the use of the internal CO_2 store accumulated during the night. Diurnal photosynthesis can then take place behind closed stomata during the hottest and driest phase of the day, yielding an overall improvement of water-use efficiency.

Over the last two decades, two principal hypotheses about the origin of the endogenous oscillations in the carbon metabolism of CAM plants have been proposed. One is based on a molecular feedback system which hierarchically drives metabolic rhythmicity by modulating the activity of key enzymes in CAM carbon metabolism (Hartwell 2005, and references therein). The second approach features a biophysical pacemaker localized at the the vacuolar membrane, the tonoplast. The principal feedback mechanism is based on the nonlinear interdependence of the efflux rate of vacuolar malic acid, the principal store for nocturnally acquired CO_2 and the order of the vacuolar membrane (Lüttge 2000). While the former hypothesis to date has not been modeled in a quantitative fashion, the latter mechanism was subject to an ongoing iteration of experimental studies and quantitative multi-level modeling.

2.2 Modeling CAM Rhythmicity: From Single- to Multi-Oscillator Systems and Back

The first quantitative model of CAM, based on the experimental knowledge available at that time was presented by Nungesser et al. (1984). By interdisciplinary collaboration between engineers and botanists, a computational model was developed, featuring 6 ordinary differential equations (ODEs), representing 6 metabolic pools, interacting by first order reaction and regulation terms. Already in that model, the principal point of impact for environmental parameters like light intensity was the transport of malic acid at the tonoplast. As described in detail by Lüttge (2000), this model evolved in several steps in alignment with surging experimental evidences. The hitherto final point in the evolution of cellular CAM models was reached with the model by Blasius et al. (1999), quantifying the mentioned nonlinear interdependency of the efflux of vacuolar malic acid and its level of accumulation.

A principal merit of this model is the representation of the conditionality of the CAM cycle in continuous light: here, the circadian cycle is arrested in steady states with a filled vacuole at low temperatures, and an empty vacuole when the plant is exposed to high temper-

atures (Grams et al. 1997). Starting to lower the temperature from the latter arrested state, the model predicts the onset of circadian oscillations once the temperature crosses the bifurcation threshold, independent on the rate of temperature change. This prediction was contradicted by experiments by Rascher et al. (1998): rhythm re-initiation could only be observed experimentally in response to fast temperature changes, while a slow transition between the two temperature regimes maintained the gas-exchange cycle arrested in the arrhythmic state.

This finding induced a fundamental change in the modeling approach to CAM rhythms. The experimental results by Rascher et al. (1998) became interpretable by considering populations of several copies of the CAM model (Blasius et al. 1999) with an additional noise term (Beck et al. 2001). Taking into account the multi-cellular nature of the measured whole-leaf gas exchange, and the stochastic dynamics of the oscillations emerging from omnipresent noise in real systems, rhythm re-initiation after a fast temperature transition could be understood as the synchronization of a population of noisy oscillators by a quick common transition of all oscillators from a fixed-point to a limit-cycle regime. Slow temperature transitions would yield an onset of oscillations in each individual oscillator, however, phase desynchronization of the population would maintain the arrhythmic global signal. In addition to that, this multi-level approach gave rise to interpret macroscopic arrhythmicity and rhythm damping as a noise-induced loss of phase coherence among the microscopic oscillating elements of the system. The success of this multi-oscillator model, introducing the "clockshop" hypothesis (Winfree 1975) to CAM rhythms, lead to a new experimental approach to whole-leaf rhythmicity. By implementing a chlorophyll fluorescence imaging facility, image sequences of photosynthetic efficiency could be recorded to assess the spatio-temporal metabolic dynamics in CAM leaves in day-night cycles and in continuous light (Rascher et al. 2001). This new technique unraveled a significant amount of spatio-temporal heterogeneity in the CAM leaves in day-night cycles and continuous light conditions, which was a new and unexpected result for a physiologically and anatomically homogeneous leaf.

By taking a pixelwise time-series approach, Bohn (2003) analyzed the spatio-temporal data quantitatively and compared them with numerical simulations of populations of uncoupled oscillators. As the hypotheses about whole-leaf rhythm generation to be tested were concerned with purely dynamical processes, not involving biophysical details of rhythm generation, the CAM model by Blasius could be further reduced in complexity and degrees of freedom. For the given purposes it can be substituted by the FitzHugh-Nagumo (FHN) model, a generic, phenomenological model for excitatory behavior and limit cycle oscillations, consisting of two differential equations (Keener and Sneyd 1998), whose dynamical properties fully represent the CAM model. Arrested circadian cycles in continuous conditions had been modeled earlier for rhythms observed in insects (Peterson 1980) and fungi (Gooch et al. 1994), using the so-called displaced limit-cycle (DLC) model. As this model also incorporates rhythm damping at the level of a single oscillator, it was suited to create an alternative hypothesis to the suggested loss of phase coherence in the population exhibited in the FHN model, whose single elements show either oscillations with unattenuated amplitude, or no oscillation at all. Figure 1 exhibits simulations of the spatiotemporal dynamics of uncoupled ensembles of both FHN (left panels) and DLC (right panels) systems. Underneath the space-time plots in the top row, the temporal development of the spatial average of each population and a representative time-series of a single oscillator is given. The middle panels of Figure 1 show the corresponding time-series from a data set derived from the chlorophyll image sequences by Rascher et al. (2001). From visual inspection, one may conclude that

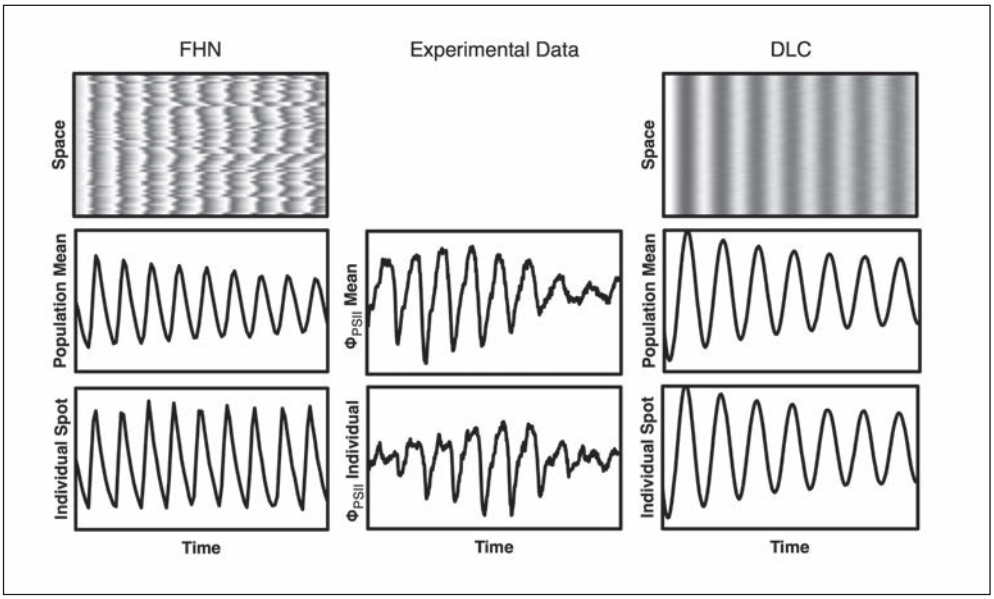

Fig. 1 Comparison of two hypotheses on the amplitude attenuation of overt circadian rhythmicity in the CAM plant *Kalanchoë daigremontiana*. *Top row*: Spatiotemporal dynamics of 100 uncoupled oscillators. *Middle row*: Temporal dynamics of the spatial average of the population. *Bottom row*: typical temporal dynamics of a single oscillator. *Left column*: FitzHugh-Nagumo (FHN) model (KEENER and SNEYD 1998). *Middle column*: Quantum efficiency of photosystem II, data from RASCHER et al. (2001). *Right column*: Simulations of the Displaced Limit-Cycle (DLC) model by PETERSON (1980)

the global dynamics of leaf metabolism is correlated to the local dynamics, which favors the hypothesis represented by the DLC model. This has been further substantiated by quantitative statistical analyses (BOHN 2003), suggesting that the origins of amplitude attenuation and arrhythmicity should emerge from the interactions of the biophysical and chemical entities at the cellular level.

The pixelwise time-series analysis applied to the mentioned image sequence of photosynthetic efficiency furthermore revealed synchronized patches in the leaf, which could be related to a slight 24h-modulation of light intensity (BOHN 2003). This observation pointed to a dynamical phenomenon which had not been studied in depth in fundamental nonlinear dynamics: the spatio-temporal dynamics of a population of spatially arranged oscillators under the influence of an external periodic driver, which acts with a spatially heterogeneous amplitude on the oscillators (BOHN and GARCÍA-OJALVO 2008). The central question of biological interest in this system is if and which type of inter-oscillator coupling could bring the entire array into synchronization with itself and the environmental driver, in spite of the heterogeneous impact of the latter on the array. As synchronization of non-chaotic oscillators is characterized by phase differences between oscillators, rather than amplitude deviations (PIKOVSKY et al. 2001), the additional complexity introduced by coupling was balanced by considering phase oscillators, a minimal model for oscillatory processes, which consists of one single differential equation describing the evolution of the phase of the system (ACEBRÓN et al. 2005). The spatio-temporal plots in Figure 2 show the principal effects of two different

types of coupling on a heterogeneously driven array. The left panel shows the dynamics of an uncoupled array under a driver which has its peak amplitude in the center of the array: this leads to the synchronization of the oscillators in a center strip, while at the margin, where the external driver strength drops below the critical entrainment strength, oscillators show independent free-running dynamics, resulting from their individual period mismatch with the external force (see Bohn and García-Ojalvo 2008 for details). Applying global coupling, i.e. each oscillator adjusting its own phase in dependence on its difference to the average of all phases in the array (Fig. 2, top right panel), the entire array becomes synchronized both internally, as well as to the external driver. Applying local, next-neighbor coupling (Fig. 2, lower right panel), global synchronization is replaced by running phase waves in the non-synchronized zone in the uncoupled state. Hence, under heterogeneous external driving, local coupling provides order in the array, however it is less efficient in comparison to global coupling. This is in general compliance with the theory of coupled phase oscillators (Acebrón et al. 2005).

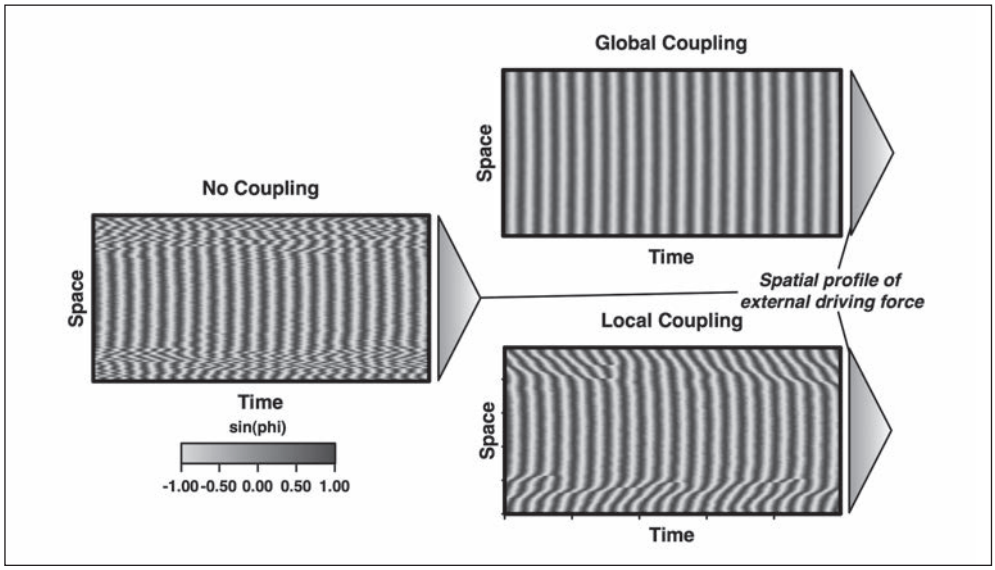

Fig. 2 The effect of different coupling types on the synchronization of 100 phase oscillators (Bohn and García-Ojalvo 2008). *Left*: Spatiotemporal dynamics of 100 uncoupled oscillators. *Top right*: 100 globally coupled oscillators. *Bottom right*: 100 locally coupled oscillators.

An advantage of the generic nature of the used model is the ease of comparison of rhythmic phenomena in various organisms. Besides the present case of spatio-temporal CAM rhythmicity, global coupling by the medium surrounding the cell population has also been indicated as the main synchronization mechanism between circadian rhythms in populations of unicellular algae (Broda et al. 1985) and neurons in the suprachiasmatic nucleus, the central mammalian pacemakes (Gonze et al. 2005). This suggests that if circadian oscillators are indeed coupled across cell boundaries, the coupling agent must be quickly diffusing throughout the entire system on time-scale much faster than the 24h-period of the oscillation. Taking

this hypothesis into account in future research on intercellular coupling agents of circadian rhythms could catalyze the screening of possible molecular candidates and hence guide the design of future experiments.

In the concrete case of circadian CAM oscillations, this hypothesis might inspire the design of prospective experiments. Assuming CO_2 to be the intercellular coupling agent as proposed by Duarte et al. (2005), suggest that fully synchronized leaves in the presence of heterogeneous environmental signals could be easier achieved in plants with low internal CO_2 diffusion resistance. The succulence of CAM leaves and the resulting low internal CO_2 conductivity could thus be an important factor for the emergence of running phase waves, as phase adjustments by CO_2 signaling might be limited to cells in close vicinity, corresponding to the numerical scenario of local next-neighbor coupling (Fig. 2). This hypothesis could be tested by exposing CAM plants with different internal CO_2 conductivities to a light source with controlled temporal modulation of its intensity and a controlled spatial geometry of light incidence on the leaf.

Returning from the organismal to the cellular scale, the results of the presented numerical studies using phenomenological models could also trigger novel modeling approaches to the biochemical bases of CAM rhythmicity. The present mechanistic model should be extended in order to include rhythm attenuation in continuous conditions at the cellular level, to provide a mechanistic background to the phenomenological DLC model. As the comparison of simulations exposing the model by Blasius et al. (1999) to CO_2-free epochs with corresponding experiments suggest, a second oscillator robust to severe metabolic perturbations must be involved in the generation of overt CAM rhythm generation (Wyka et al. 2004). Hence, a new model at the cellular level is likely to be a multi-level model also, integrating the metabolic dynamics with circadian gene expression cycles. Given the similarity of the molecular CAM clock with the molecular *Arabidopsis* oscillator (Hartwell 2005), the gene expression cycles might be represented by a model similar to the one developed by Locke et al. (2006) for *Arabidopsis.* As this class of model gives a very detailed description of the involved molecular feedback loops, it might contain an excess of complexity to the study of the interaction between gene expression and metabolism, which should be a bidirectional connection, as in some cases, metabolic signals have been shown to override periodic gene expression cycles in CAM plants (Borland et al. 1999). It is thus suggested that future numerical studies of the multi-level nature of cellular CAM rhythms might – at least initially – rely on models with a reduced number of variables. The complexities at both levels could be reduced in analogy to Forger and Kronauer (2002), who explicitly showed the mathematical equivalence of the two-dimensional van-der-Pol oscillator, a phenomenological model for nonlinear oscillations, with the five-dimensional model of circadian gene expression by Goldbeter (1995).

2.3 Modeling in Systems Biology: Integration across Organisms and Levels of Organization

Integrated understanding of the behavior of living organisms in their natural environments requires the integration of diverse levels of organization. Successful system models of entire organisms, e.g. the human heart, suggest that the most efficient way to achieve multilevel understanding is not by a hierarchical, unidirectional modeling attempt, be it bottom-up or top-down, but by starting at those intermediate levels where sufficient data are available (middle-out approach, Noble 2003). Hybrid multilevel models, relying on the flexible handling of the model granularity in function of the data availability, might reconcile inductive and deductive

concepts in systems biology (Coveney and Fowler 2005). In practice, it is both the failure as well as the success of a given model that can advance the knowledge on a given system, as long as modeling activity remains logically connected to experimental work (Noble 2002). It is in this sense, that the modeling of CAM rhythms, using an entire spectrum of models with different levels of detailedness has guided and inspired corresponding experimental endeavors for more than two decades.

Perceiving quantitative models as navigation tools in tackling the multilevel complexity of living organisms (Hammer et al. 2006), and as being "no more, but no less, than a way of thinking clearly" (May 2004), could be a promising stance to foster the acceptance of a heterogeneous landscape of coexisting models of a given organism. In the same fashion that complex functions of living organism emerge from the interaction of many diverse parts on different levels, the knowledge of this complexity might rather emerge from a heterogeneous network of models, than form one single, optimally designed model. The success of such a "modelomics" approach requires new technologies to facilitate the connection of diverse models. Modeling meta-languages such as the Systems Biology Markup Language SBML (http://www.sbml.org), which serve as common descriptor for a large spectrum of models, are one example. However, as will be further discussed in the concluding Section 4 of this work, to be fully efficient, these technological advances need to be accompanied by an increasing awareness of the socio-psychological challenges to interdisciplinary team research in life sciences.

3. Phototrophic Biofilms: Integrating Data Sources, Analysis Tools and Scientific Activity

3.1 The PHOBIA Project: Diverse Perspectives on Phototrophic Biofilms

Most hard substrates in nature are covered with biofilms, aggregations of microorganisms encapsulated in a protective and adhesive matrix. They are increasingly recognized as the preferred mode of growth of microbes in a wide range of habitats (Costerton et al. 1987, Stoodley et al. 2002). Research on biofilms has increased to a great amount over the last decades. They play a central role in many pathogenic processes in biomedicine (Parsek and Singh 2003), and cause significant damage to technical processes and transportation through biocorrosion and biofouling (Coetser and Cloete 2005). On the other hand, biofilms bear a large potential for the development of novel biotechnologies, e.g. for wastewater treatment (Rittmann 2006).

Phototrophic biofilms, mixed cultures of hetero- and autotrophic organisms (Fig. 3), are crucial elements of aquatic ecosystems and are prospective points of departure for novel environmental biotechnologies (e.g. Sansone et al. 1998, van Dam et al. 2002, Nagarkar et al. 2004). Here, phototrophic organisms, e.g. microalgae and cyanobacteria, fuel heterotrophic bacteria and fungi, which in return provide nutrients for the phototrophs. Both groups exude extracellular polymeric substances (EPS), which provide surface adhesion of the biofilm and contribute to its protection.

The project PHOBIA was a first large-scale integrative approach to phototrophic biofilms, joining 6 laboratories in 5 European countries (Fig. 4, and http:// www.photobiofilms.org). All partners used identical freshwater and marine inocula gained from the same sampling

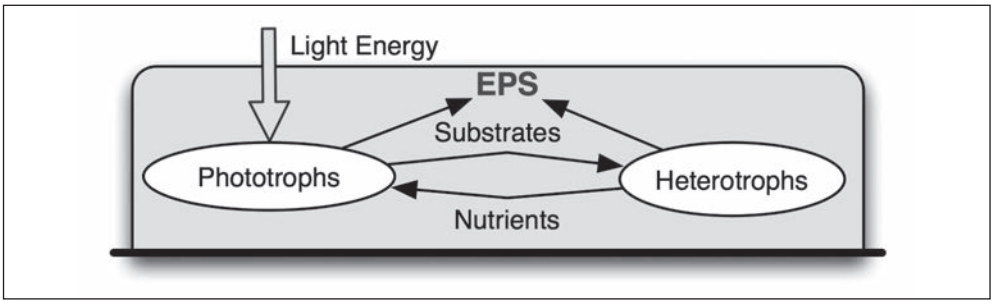

Fig. 3 Scheme of interactions between autotrophic and heterotropic organisms in phototrophic biofilms. EPS stands for "Extracellular Polymeric Substances" (see text)

sites, as well as the same incubator and protocols to assess the effects of temperature, light intensity and water flow velocity (Zippel et al. 2007). Each partner then analyzed the biofilms in different developmental stages with the specific tools of their expertise (Fig. 4). As is depicted in the following, the quantitative approach to integrate these heterogeneous and geographically dispersed data sources was based on a web-based computational infrastructure, WebPHOBIA, incorporating a data warehouse for the reposition of the data generated in the diverse laboratories, connected to a computational module based on Artificial Neural Networks for data modeling and variable selection.

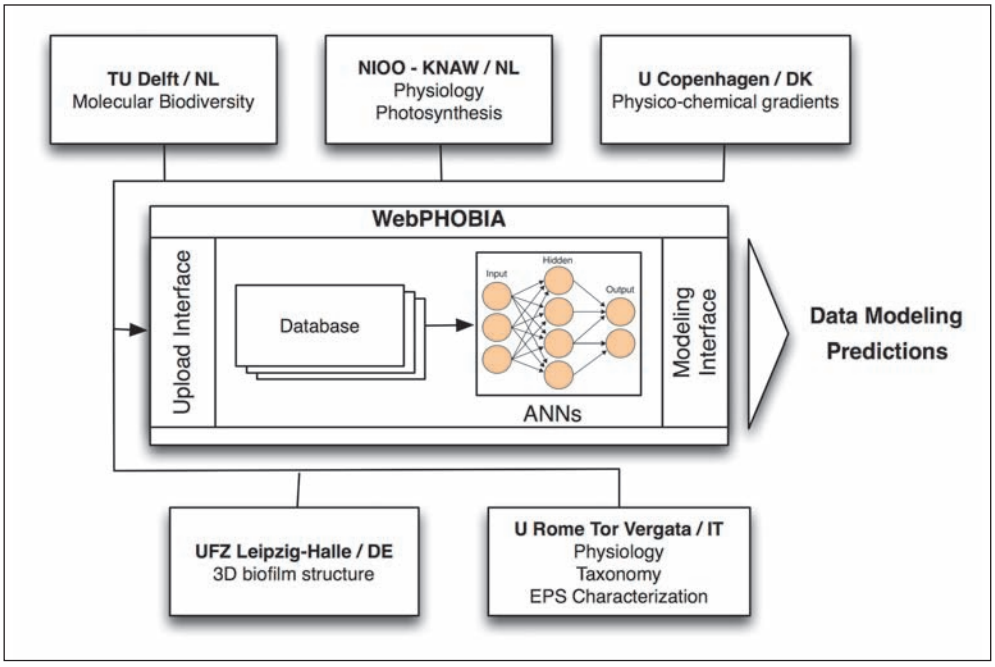

Fig. 4 Scheme of the data flux in the PHOBIA project and the composition of the WebPHOBIA data management facility.

3.2 Integration of Heterogeneous Data Sources by Data Warehousing

One approach to integrate heterogeneous data sources is data warehousing (Schönbach et al. 2000). It involves the translation of the data from the diverse sources to a central repository, on which the querying and data mining is performed. Like for other models as well, the data model on which a data warehouse is based can be developed in either a bottom-up or a top-down fashion: the former consists in integrating diverse local data repositories (data marts) into a single facility, i.e. queries submitted to the central data warehouse are translated and conveyed to the local repositories. In the top-down approach, the structure of the warehouse is designed beforehand, and all generated data in the laboratories are submitted directly to the warehouse, which also serves as the site to which further processing modules are deployed.

Inspired by an earlier web-based infrastructure developed for another European-wide research project in microbiology (Silva et al. 2003), the data warehouse in WebPHOBIA followed the top-down approach. Each PHOBIA partner communicated the structure of their data in the startup meeting of the project. Based on this knowledge, a database was designed and implemented using the relational database management system (RDBMS) PostgreSQL. A software engine was programmed in PHP to provide the user interface for data upload and querying, and to connect the database with the analysis module.

While the top-down approach based on a relational database provides a high level of consistency in the integration of the diverse sources, two of its disadvantages became prominent in the course of PHOBIA. First, changes to the data structure, due to additional experimental endeavors, cannot be accomplished without exporting the already submitted data and resubmitting them to the rebuild structure. The second drawback involves the dependence of a data warehouse relying on a complex relational database model on the knowledge of the domain expert, i.e. the database creator and programmer. A career change of the WebPHOBIA domain expert before the completion of data submission and the end of the project made a significant amount of the contextual information needed to understand and use the data repository unavailable, which significantly hampered the implementation of the necessary changes to the data structure and the completion of the database.

Both these issues relate to the importance of metadata, i.e. data about data, in integrative computational approaches in ecology and life sciences (Michener et al. 1997). Managing metadata is thus considered a key strategy in the development of data integration tools, which allow incremental modifications of the structure of the base, without compromising the already uploaded data, and grant transparency to its users without having to unravel complex data structures at the level of RDBMS. For the implementation of metadata management, and to create controlled vocabularies and ontologies for data integration in life sciences in the long run, the use of semantic web technologies has been proposed (Cheung et al. 2005, Jones et al. 2006).

A prototype software for data integration using semantic concepts is S3DB, the Simple Sloppy Semantic Database (Almeida et al. 2006). This framework refrains from pre-defining a fixed database structure, in which the data model is coded in the relationships between the tables of the database. Data are rather considered as resources with given properties, and are labeled with a Uniform Resource Identifier (URI). In analogy with the Resource Description Framework (RDF), the data are related and organized as triples [Resource][Property][Property Attribute]. The backbone of S3DB is a relational database, however, its tables contain the resources, the URIs, properties and values, and the data structure is not implicitly mapped

in the entity relationships. The S3DB engine (built in PHP) checks for the consistency of the semantic data structure. The resulting data model, i.e. the network of relations between the different resources and their properties, are visualized by the S3DB interface, and can be easily modified (Fig. 5).

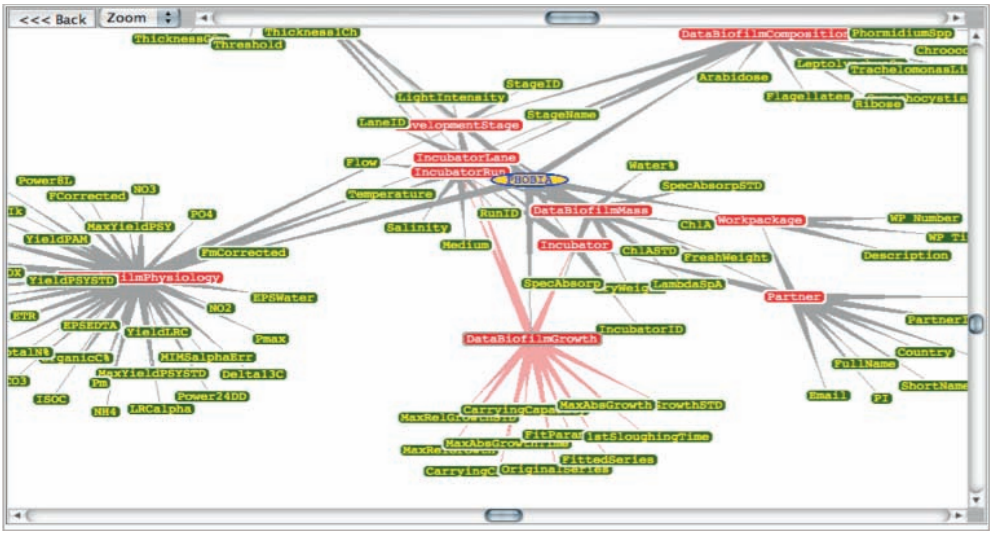

Fig. 5 Screenshot of the graphical interface to the S3DB database in the PHOBIA project, showing the semantic network.

Apart from the theoretical aspects of data integration using ontologies and controlled vocabularies, the practical advantages of applying the semantic approach mainly consist in the transparency of the metadata, and the fact that – once deployed to the webserver – no coding at the level of the RDBMS is needed to adjust the database to changes in the data model. Semantic approaches like S3DB represent thus a step towards providing data integrity across the sources to be integrated (like the top-down approach), yet maintaining some of the flexibility of the bottom-up approaches. The tradeoff for these advantages is the reduced computational efficiency and speed in query processing as compared to a taylor-made relational database.

3.3 Data Analysis and Modeling with Artificial Neural Networks

The second module of the web-based PHOBIA platform contained a modeling and analysis infrastructure relying on Artificial Neural Networks (ANNs, Basheer and Hajmeer 2000, Fig. 4). The application of this non-linear data analysis tool was inspired by its prior successful and widespread application in environmental biotechnology and biochemical engineering (Almeida 2002). They represent a machine learning tool which can establish a functional relation between a set of independent (input) variables and a set of dependent (output) variables. In analogy to the neural learning process, consisting in adjusting synapsis strength in the network of neurons, the learning process determines the number of neurons in the hidden layer, and adjusts the weights of the connections between the neurons in the diverse layers,

such that for empirically determined input values x, the prediction error of the ANN output with respect to the measured output variables is minimized. For the training process, the full data set is divided into a training part, used to adjust the weights, a testing part, from which the prediction error is tested, and a validation part to avoid overfitting (Almeida 2002). This completely data-driven approach bears the advantage of not needing any beforehand mechanistic assumption for data modeling and prediction.

In WebPHOBIA, ANNs were deployed to perform two tasks. First, through a special interface for predictive modeling in the website, users could select any pairs of input and output variables among the quantities contained in the database. By computations based on algorithms programmed in Matlab, ANNs would then be trained with the data available in the base and then serve as predictor of the output values resulting from the combination of input values chosen by the user. The objective of the second task was to detect the most important relations between the variables in the different repositories, in order generate mechanistic knowledge on biofilm development and structure. Therefore the sensitivity of an given output variable to a certain input can be estimated via the relation

$$S_{ij} = \frac{\Delta Y_j}{Y_j} \Big/ \frac{\Delta X_i}{X_i} \qquad [1]$$

The resulting sensitivity patterns can then be integrated with mechanistic knowledge in order to create testable hypotheses on the relations between the observed biofilm variables. Given the above issues of the database, ANN analyses were carried out manually using data from spreadsheets as input form. An example spreadsheet containing a predictive model for biofilm growth can be downloaded at (http://phobia.itqb.unl.pt/ann.php).

Unfortunately, the quality of the data used for the analysis indicated a loss of robustness of the obtained results. As the example of the dependence of a growth parameter (days needed to reach 50 % of the carrying capacity) on temperature shown in Figure 6 indicates, the data used to train the ANN do not share equal variances and contain outliers. Furthermore, the division of the total data set into a training, test and validation subsets in ANN training, requires a large number of cases to produce reliable results. The number of available data in PHOBIA was close to the lower limit where the application of ANNs can be considered to be reliable. Hence, in analogy to the S3DB database, the ANN analysis was developed to the stage of a proof-of-concept only. Given the issues with the scarcity and the variation of the data, obtaining robust results suggests the application of classical statistical tools in parallel to the ANNs. Furthermore, the ANN approach needs to be preceded with additional tools for data normalization and outlier removal, in order to obtain more robust and reliable results (Basheer and Hajmeer 2000).

3.4 Integration and Analysis of Small-scale Data Sets in Ecophysiological Studies

The use of web-based computational tools for data reposition, sharing and analysis is likely to become more widespread in future international interdisciplinary research projects in ecophysiology. Compared to the currently common practice of data sharing, i.e. using e-mail to exchange spreadsheets based on diverse local data models, integrated data repositories with a clear metadata structure provide a more transparent and consistent platform for discussion, interpretation and further analysis among project partners and the rest of the scientific community. Also in terms of maintaining and curating the data beyond the end of a project, inte-

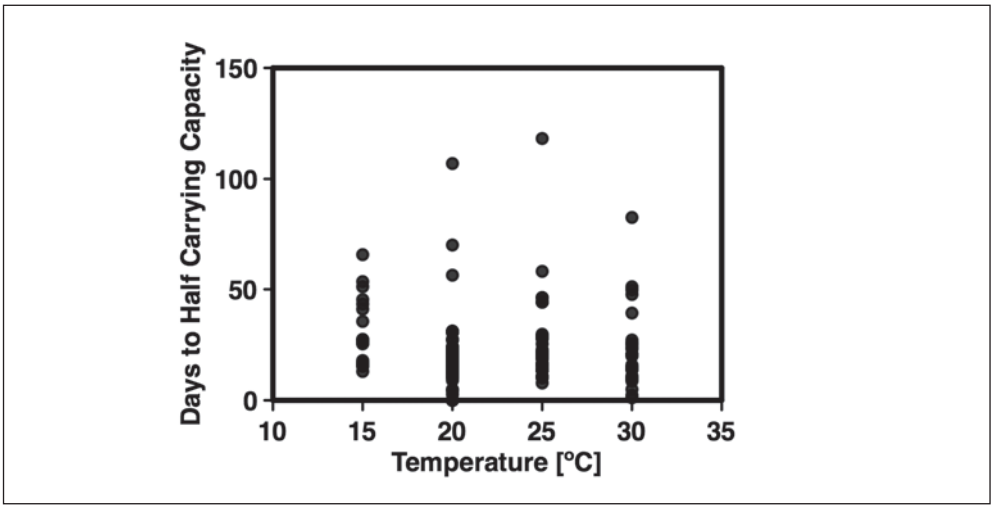

Fig. 6 Example of biofilm growth data from the PHOBIA project. The number of days to reach half the carrying capacity is plotted against the temperature of the corresponding incubator run.

grative platforms present a significant number of advantages. Finally, integrated data repositories are the basis for significant improvements of scientific data workflows by combined tools for data reposition and quantitative analysis (Jones et al. 2006).

The experience from the PHOBIA project highlights two technological challenges involved in the development of integrative data management tools. The first one consists in finding the optimal balance between flexibility and consistency in the definition of the data model: interdisciplinary, multiyear projects on complex biological systems are highly dynamical systems by themselves, hence the corresponding computational tools are required to allow modifications to the data model at a reasonable cost during the life time of the project and beyond. As was shown by the application of the prototype software S3DB, managing metadata using concepts from the semantic web is at the forefront of potential solutions to this challenge (Almeida et al. 2006). The second theme is the adaptation of the analysis tools to the data volume and the quality of the data sources. In general, the data-driven, exploratory, approach chosen here to detect patterns hidden in the data, and proceed with statistically testing concrete hypotheses only after this initial screening, is reasonable, given the situation of having many different variables from diverse sources in the repository. However, for data sets that correspond to a wide table, i.e. have a small number of cases and repetitions compared to a large number of trials, and in addition contain influential and outlying data points, machine learning tools like ANNs are likely to provide unreliable results. Tools using visual exploration (Cleveland 1993), could provide a more efficient first approach to the data structure. With high speed computers being commonly available today, the numerical exploration for the featured type of data set should give preference to modern methods of robust statistics, providing more statistical power (Wilcox 2005).

Just like there is no single "golden model" describing a biological system in a comprehensive manner across all levels of organization, there apparently is no "golden hammer" for data analysis. So far, there is no tool being optimally suited for any type of data set, ranging

from high-throughput molecular data, where the sheer amount of data to be processed poses a challenge, to ecophysiogical studies, performed *in vivo* under controlled laboratory conditions or even in the original habitat, where the objective is to obtain the maximum amount of reliable quantitative information from a given set of (unrepeatable) measurements. In the latter scenario, comparing notes on data analysis with astrophysicists, psychologists or social scientists, who experience similar sets of challenges and inherent experimental constraints, might be more fruitful than importing quantitative solutions from computational biosciences, which are optimized for other levels of organization and data volumes.

While integrative computational tools on one hand are necessary to improve the communication and interdisciplinary interaction, their successful application depends on their integration and the overall quality of the communicational network between the members of the research team (Morris et al. 2005). As the PHOBIA example shows, the earlier in the project there is clarity about the data structure and quality, the closer one can get to obtain a seamless chain of knowledge generation, featuring computational tools that are optimally matched to the experimental design and the resulting data structure. This calls for a change of a widespread pattern of communication dynamics between biologists and quantitative scientists: hitherto there is usually a surge of interaction between experimental and computational scientists towards the end of the project, when the data are available. The presented example suggests that a dominant peak of interdisciplinary communication should occur in the very initial stage of each project, in the design phase of the experiments. By eliminating potential bottlenecks in the scientific information workflow at the beginning of a project, the return of knowledge on the investment of time and material resources could be optimized. As discussed in the following concluding discussion, this appeals to a larger awareness of the existing socio-psychological roadblocks and challenges involved in the development of interdisciplinary team science.

4. Summary and Conclusions

The present work features two cases of quantitative ecophysiological studies of phototrophic systems. The example of modeling circadian rhythms in Crassulacean acid metabolism at different levels of organization, from the cell to the whole leaf, demonstrates how quantitative models with diverse levels of abstraction can serve to conduct research on the complex nature of organismal function, and thus contribute to integrate similar phenomena across a variety of organisms. It suggests that a crucial asset of models proving to be successful in advancing knowledge about systems behavior is the potential to be connected with, and to influence other model activities and experimental endeavors. In this perspective, models take the role of navigation tools in complexity (Hammer et al. 2006), rather than the representation of a universal law, or an exact *in silico* map of experimentally observable items. Knowledge discovery itself might turn out be an emergent phenomenon of complex networks of logically connected multilevel models.

The second example, demonstrating the development of a web-based computational infrastructure to integrate heterogeneous datasets on phototrophic biofilms, demonstrates the potential benefits of this type of integrative tool to enhance scientific information- and workflows. It also demonstrates the necessity for intensive interdisciplinary communication between the team members from the very start of a project, as the efficiency of the applied

computational tools is crucially depend on their adaptation to the specific character of the project. The central challenge in the development of integrative tools is to achieve an optimal balance between sufficient flexibility for local adaptation to the experimental realities and sufficient structure to provide global description patterns across different species and levels of organization.

Both cases underline the fact that integrative systems biology not only deals with networks of diverse entities in biological systems, but is itself increasingly comprised of dense networks of scientists and resources (Morris et al. 2005). From this point of view, the organization and traditions of conducting sciences have so far followed a reductionist approach: from ancient times until the 20th century, from Aristotle to Einstein, milestones of scientific progress were marked by outstanding individual accomplishments (Humphrey et al. 2005). While specialized expertise in a given experimental or computational method and in a determined area of life sciences continues to be a necessary condition to achieve a better understanding of the complexity of living organisms, it is increasingly clear that it is not sufficient, in analogy to individual molecules which are necessary but by themselves alone not sufficient to provide organismal function.

Significant breakthroughs in modern biology might most likely emerge from collaborations in which the involved partners are committed to the solution of a scientific problem of common interest, for which they hold themselves mutually accountable. This commitment generally involves changes in the attitudes and perspectives on both sides of the disciplinary spectrum (Humphrey et al. 2005). On the side of experimental biologists, it requires the commitment to produce quantitative data of the highest quality possible within a given technical frame, and the disposition to embrace quantitative tools as a vital part of their own scientific endeavor as of the beginning of the project. This requires extra effort to obtain the mathematical knowledge needed to communicate with quantitatively trained scientists, and to gain insight into the chances and limitations that arise from moving from qualitative to quantitative descriptions. This insight might then provide the willingness to put an extra amount of energy in the execution of the experiments, e.g., to perform apparently dull repetitions of measurements to obtain an optimum of statistical power to prove or disprove a given hypothesis. Computational scientists on the other side must increase their appreciation for the technical limitations and the temporal and material investments undertaken by their experimental partners, i.e. appreciate the effort behind each data point. This should be reflected in the optimization of the computational tools for the given data structure, even if that implies the application of already established algorithms, models and software, which do not warrant publication in biocomputational journals. The extra effort consists thus in the intent to satisfy and combine both the team requirements and the individual need to produce novel tools and models which make a difference in the theoretical or computational community. Designing projects that promise a win-win-situation among the project partners could be a strategy to provide a maximum return of quantitative, connectable systems knowledge on a given investment of time and resources.

The required extra investment of time and effort will make these behavioral changes unlikely, unless they are encouraged and facilitated by new modes of organization of the scientific research and its corresponding reward systems. While the importance of interdisciplinary research has become widely recognized by the scientific community, its recognition in scientific practice is still lagging behind (Payton and Zobak 2007). Practical improvements might consist, e.g., in composing committees for any type of scientific reviewing, such that

the multidisciplinary spectrum of a given project is adequately mirrored. This could foster the judgment of the integrated contribution to the given biological problem, instead of isolated appreciations of the novelty brought to the diverse disciplines of origin of the partners. As institutional and cultural changes naturally occur on a slow time-scale, short-term measures to promote interdisciplinary research could consist in highlighting success cases in order to develop best-practice standard procedures, and in exposing students of both experimental and math-based disciplines to the world of their respective partners as early as possible in their careers (Morris et al. 2005, Humphrey et al. 2005).

Two of the most prominent examples of team sciences, the Manhattan project leading to the harnessing of nuclear energy, and the Apollo project, leading to man's landing on the moon, were motivated by perceived external threats during World War II and the Cold War. It might also be up to future challenges to mankind, arising from, e.g., the uncertainties of climate change, or the evolution of novel pathogens, to ultimately catalyze the establishment of integrative, team-based approaches as a widespread or even standard protocol in life and social sciences. Promoting interdisciplinary team research out of insight into the high productivity and intellectual inspiration it provides, rather than out of mere practical necessities caused by external pressures, would not only provide novel and powerful approaches to extend human perception and understanding of the complex organization of life, but could also catalyze the development of a general culture of collaboration between people with heterogeneous skills, perspectives and backgrounds.

Acknowledgement

The author acknowledges support by the *Fundação para a Ciência e a Tecnologia*, Portuguese Ministry for Science, Technology and Higher Education, through grant SFRH/BPD/25967/2005.

References

Acebrón, J. A., Bonilla, L. L., Pérez Vicente, C. J., Ritort, F., and Spigler, R.: The Kuramoto model: a simple paradigm for synchronization. Rev. Mod. Phys. *77*, 137–185 (2005)

Almeida, J. S.: Predictive non-linear modeling of complex data by artificial neural networks. Curr. Opin. Biotechnol. *13*, 72–76 (2002)

Almeida, J. S., Chen, C., Gorlitsky, R., Stanislaus, R., Aires de Sousa, M., Eleutério, P., Carriço, J., Maretzek, A., Bohn, A., Chang, A., Zhang, F., Mitra, R., Mills, G. B., Wang, X., and Deus, H. F.: Data integration gets sloppy. Nature Biotechnol. *24*, 1070–1071 (2006)

Basheer, I. A., and Hajmeer, M.: Artificial neural networks: fundamentals, computing, design, and application. J. Microbiol. Meth. *43*, 3–31 (2000)

Beck, F., Blasius, B., Lüttge, U., Neff, R., and Rascher, U.: Stochastic noise interferes coherently with a model biological clock and produces specific dynamic behaviour. Proc. Roy. Soc. Lond. B Biol. *268*, 1307–1313 (2001)

Black, C. C., and Osmond, C. B.: Crassulacean acid metabolism photosynthesis; "working the night shift". Photosynthesis Res. *76,* 329–341 (2003)

Blasius, B., Neff, R., Beck, F., and Lüttge, U.: Oscillatory model of Crassulacean acid metabolism with a dynamic hysteresis switch. Proc. Roy. Soc. Lond. B Biol. *266*, 93–101 (1999)

Bohn, A.: Analysis and simulation of multi-oscillator systems in a Crassulacean acid metabolism plant. Ph.D. Thesis, Physics Dept., Darmstadt University of Technology, Germany (2003)

Bohn, A., and García-Ojalvo, J.: Synchronization of coupled biological oscillators under spatially heterogeneous environmental forcing. J. Theor. Biol. *250*, 37–47 (2008)

Borland, A. M., Hartwell, J., Jenkins, G. I., Wilkins, M. B., and Nimmo, H. G.: Metabolite control overrides circadian regulation of phosphoenolpyruvate carboxylase kinase and CO_2 fixation in Crassulacean acid metabolism. Plant Physiol. *121*, 889–896 (1999)

Broda, H., Brugge, D., Honma, K., and Hastings, J. W.: Cellular communication between unicells? Cell Biophys. *8*, 47–67 (1985)

Busch, H., and Eils, R.: Systems Biology. In: Meyers, R. A. (Ed.): Encyclopedia of Molecular Cell Biology and Molecular Medicine *14*; pp. 123–159. Berlin: Wiley-VCH 2005

Cheung, K. H., Smith, A. K., Yip, K. Y. L., Baker, C. J. O., and Gerstein, M. B.: Semantic web approach to database integration in the life sciences. In: Baker, C. J. O., and Cheung, K. H. (Eds.): Semanic Web. Revolutionizing Knowledge Discovery in the Life Sciences; pp. 11–30. New York: Springer 2007

Cleveland, W. S.: Visualizing data. Summit (NJ, USA): Hobart Press 1993

Coetser, S. E., and Cloete, T. E.: Biofouling and biocorrosion in industrial water systems. Crit. Rev. Microbiol. *31*, 213–232 (2005)

Costerton, J. W., Cheng, K. J., Geesey, G. G., Ladd, T. I., Nickel, J. C., Dasgupta, M., and Marrie, T. J.: Bacterial biofilms in nature and disease. Annu. Rev. Microbiol. *41*, 435–464 (1987)

Coveney, P. V., and Fowler, P. W.: Modelling biological complexity: a physical scientist's perspective. J. R. Soc. Interface *2*, 267–280 (2005)

Dodd, A. N., Salathia, N., Hall, A., Kével, E., Tóth, R., Nagy, F., Hibberd, J. M., Millar, A. J., and Webb, A. A. R.: Plant circadian clocks increase photosynthesis, growth, survival, and competitive advantage. Science *309*, 603–633 (2005)

Duarte, H. M., Jakovljevic, I., Kaiser, F., and Lüttge, U.: Lateral diffusion of CO_2 in leaves of the Crassulacean acid metabolism plant *Kalanchoë daigremontiana* Hamet et Perrier. Planta *220*, 809–816 (2005)

Forger, D. B., and Kronauer, R. E.: Reconciling mathematical models of biological clocks by averaging on approximate manifolds. SIAM J. Appl. Math. *62*, 1281–1296 (2002)

Goldbeter, A.: A model for circadian oscillations in the Drosophila period protein (PER). Proc. Roy. Soc. Lond. B *261*, 319–324 (1995)

Gonze, D., Bernard, S., Waltermann, C., Kramer, A., and Herzel, H.: Spontaneous synchronization of coupled circadian oscillators. Biophys. J. *89*, 120–129 (2005)

Gooch, V. D., Wehseler, R. A., and Gross, C. G.: Temperature effects on the resetting of the phase of the *Neurospora* circadian rhythm. J. Biol. Rhythms *9*, 83–94 (1994)

Grams, T. E. E., Borland, A. M., Roberts, A., Griffiths, H., Beck, F., and Lüttge, U.: On the mechanism of reinitiation of endogenous Crassulacean acid metabolism rhythm by temperature changes. Plant Physiol. *113*, 1309–1317 (1997)

Hammer, G. L., Sinclar, T. R., Chapman, S. C., and van Oosterom, E.: On systems thinking, systems biology, and the in silico plant. Plant Physiol. *134*, 909–911 (2004)

Hammer, G. L., Cooper, M., Tardieu, F., Welch, S., Walsh, B., van Eeuwijk, F., Chapman, S. C., and Podlich, D.: Models for navigating biological complexity in breeding improved crop plants. Trends Plant Sci. *11*, 587–593 (2006)

Hartwell, J.: The co-ordination of central plant metabolism by the circadian clock. Biochem. Soc. Trans. *33*, 945–948 (2005)

Humphrey, J. D., Coté, G. L., Walton, J. R., Meininger, G. A., and Laine, G. A.: A new paradigm for graduate research and training in the biomedical sciences and engineering. Adv. Physiol. Educ. *29*, 98–102 (2005)

Hütt, M. T., and Lüttge, U.: Network dynamics in plant biology: current progress in historical perspective. Prog. Bot. *66*, 277–309 (2005)

Ideker, T., Galitski, T., and Hood, L.: A new approach to decoding life: systems biology. Annu. Rev. Genom. Hum. Genet. *2,* 343–372 (2001)

Jones, M. B., Schildhauer, M. P., Reichman, O. J., and Bowers, S.: The new bioinformatics: Integrating ecological data from the gene to the biosphere. Annu. Rev. Ecol. Evol. Syst. *37*, 519–544 (2006)

Keener, J., and Sneyd, J.: Mathematical Physiology. New York (NY, USA): Springer 1998

Keller, E. F.: The century beyond the gene. J. Biosci. *30*, 3–10 (2005)

Kitano, H. (Ed.): Foundations of Systems Biology. Cambridge (MA, USA): MIT Press 2001

Locke, J. C. W., Kozma-Bognar, L., Gould, P. D., Fehér, B., Kevei, E., Nagy, F., Turner, M. S., Hall, A., and Millar, A. J.: Experimental validation of a predicted feedback loop in the multi-oscillator clock of *Arabidopsis thaliana*. Mol. Syst. Biol. *2*, 53 (2006)

Lüttge, U.: The tonoplast functioning as the master switch for circadian regulation of crassulacean acid metabolism. Planta *211*, 761–769 (2000)

Lüttge, U.: Ecophysiology of Crassulacean acid metabolism (CAM). Ann. Bot. *93*, 629–652 (2004)

May, R. M.: Uses and abuses of mathematics in biology. Science *303*, 790–793 (2004)

Michener, W. K., Brunt, J. W., Helly, J. J., Kirchner, T. B., and Stafford, S. G.: Non-geospatial metadata for the ecological sciences. Ecol. Appl. *7*, 330–342 (1997)

Morris, R. W., Bean, C. A., Farber, G. K., Gallahan, D., Jakobsson, E., Liu, Y., Lyster, P. M., Peng, G. C. Y., Roberts, F. S., Twery, M., Whitmarsh, J., and Skinner, K.: Digital biology: an emerging and promising discipline. Trends Biotechnol. *23*, 113–117 (2005)

Nagarkar, S., Williams, G. A., Subramanian, G., and Saha, S. K.: Cyanobacteria-dominated biofilms: a high quality food source for intertidal grazers. Hydrobiologia *512*, 89–95 (2004)

Noble, D.: Modelling the heart: insights, failures and progress. BioEssays *24*, 1155–1163 (2002)

Noble, D.: The future: putting Humpty-Dumpty together again. Biochem. Soc. Trans. *31*, 156–158 (2003)

Nungesser, D., Kluge, M., Tolle, H., and Oppelt, W.: A dynamic computer model of the metabolic and regulatory processes in Crassulacean acid metabolism. Planta *162*, 204–214 (1984)

Paranjpe, D. A., and Sharma, V. K.: Evolution of temporal order in living organisms. J. Circad. Rhythms *3*, 7 (2005)

Parsek, M. R., and Singh, P. K.: Bacterial biofilms: an emerging link to disease pathogenesis. Annu. Rev. Microbiol. *57*, 677–701 (2003)

Payton, A., and Zoback, M. L.: Crossing boundaries, hitting barriers. Nature *445*, 950 (2007)

Peterson, E. L.: A limit cycle interpretation of a mosquito circadian oscillator. J. Theor. Biol. *84*, 281–310 (1980)

Pikovsky, A., Rosenblum, M., and Kurths, J.: Synchronization. A Universal Concept in Nonlinear Sciences. Cambridge (UK): Cambridge University Press 2001

Pittendrigh, C. S.: Temporal organization. Reflections of a Darwinian Clock-Watcher. Annu. Rev. Physiol. *55*, 17–54 (1993)

Rascher, U., Blasius, B., Beck, F., and Lüttge, U.: Temperature profiles for the expression of endogenous rhythmicity and arrhythmicity of CO_2 exchange in the CAM plant *Kalanchoë daigremontiana* can be shifted by slow temperature changes. Planta *207*, 76–82 (1998)

Rascher, U., Hütt, M. T., Siebke, K., Osmond, B., Beck, F., and Lüttge, U.: Spatiotemporal variation of metabolism in a plant circadian rhythm: the biological clock as an assembly of coupled individual oscillators. Proc. Natl. Acad. Sci. USA *98*, 11801–11805 (2001)

Rittmann, B. E.: Microbial ecology to manage processes in environmental biotechnology. Trends Biotechnol. *24*, 261–266 (2006)

Sansone, U., Belli, M., Riccardi, M., Alonzi, A., Jeran, Z., Radojko, J., Smodis, B., Montanari, M., and Cavolo, F.: Adhesion of water-borne particulates on freshwater biota. Sci. Total Environ. *219*, 21–28 (1998)

Schönbach, C., Kowalski-Saunders, P., and Brusic, V.: Data warehousing in molecular biology. Brief. Bioinform. *1*, 190–198 (2000)

Silva, S., Gouveia-Oliveira, R., Maretzek, A., Carriço, J., Gudnason, T., Kristinssion, K. G., Ekdahl, K., Brito-Avô, A., Tomasz, A., Santos Sanches, I., de Lencastre, H., and Almeida, J.: EURISWEB – Web-based epidemiological surveillance of antibiotic-resistant pneumococci in Day Care Centers. BMC Med. Inform. Dec. Mak. *3*, 9 (2003)

Stoodley, P., Sauer, K., Davies, D. G., and Costerton, J. W.: Biofilms as complex differentiated communities. Annu. Rev. Microbiol. *56*, 187–209 (2002)

van Dam, A. A., Beveridge, M. C. M., Ekram Azim, M., and Verdegem, M. C. J.: The potential of fish production based on periphyton. Rev. Fish Biol. Fish. *12*, 1–31 (2002)

Westerhoff, H. V., and Palsson, B. O.: The evolution of molecular biology into systems biology. Nature Biotechnol. *22*, 1249–1252 (2004)

Wilcox, R.: Introduction to robust estimation and hypothesis testing. San Diego (CA, USA): Academic Press 2005

Winfree, A. T.: Unclocklike behaviour of biological clocks. Nature *253*, 315–319 (1975)

Wyka, T. P., Bohn, A., Duarte, H. M., Kaiser, F., and Lüttge, U.: Pertubations of malate accumulation and the endogenous rhythms of gas exchange in the Crassulacean acid metabolism plant *Kalanchoë daigremontiana*: testing the tonoplast-as-oscillator model. Planta *219*, 705–713 (2004)

Zippel, B., Rijstenbil, J., and Neu, T. R.: A flow-lane incubator for studying freshwater and marine phototrophic biofilms. J. Microbiol. Meth. *70*, 336–345 (2007)

Dr. Andreas Bohn
Instituto de Tecnologia Química e Biológica
Universidade Nova de Lisboa
Avenida da República – EAN
2780-157 Oeiras
Portugal

Phone: 351 214 469 852
Fax: 351 214 428 766
E-Mail: abohn@itqb.unl.pt

ISSN: 0369-5034
ISBN: 978-3-8047-2603-1